FUNCTIONAL ANALYSIS OF TRF1 PHOSPORYLATION IN TELOMERE MAINTENANCE

FUNCTIONAL ANALYSIS OF THE ROLE OF TRF1 PHOSPHORYLATION ON THREONINE 271 AND THREONINE 371 IN TELOMERE MAINTENANCE

By ANGUS HO, B.Sc (Hon)

A Thesis Submitted to the School of Graduate Studies in Partial Fulfillment of the Requirements for the Degree Master of Science

McMaster University MASTER OF SCIENCE (2016) Hamilton, Ontario (Biology)

TITLE: Functional Analysis of the Role of TRF1 Phosphorylation on threonine 271 and threonine 371 in Telomere Maintenance

AUTHOR: Angus Ho, B.Sc (Hon)

SUPERVISOR: Dr. Xu-Dong Zhu

NUMBER OF PAGES: cxcvii; 197 (excluding publication)

ABSTRACT

TRF1, telomeric-repeat binding factor 1, is a component of the six-subunit protein complex, referred to as shelterin, which is essential for not only regulating telomere length maintenance but also protecting mammalian telomeres from being recognized as damaged DNA. TRF1 acts as a negative mediator of telomerase-dependent telomere elongation in telomerase-expressing cells, whereas it promotes alternative lengthening of telomeres (ALT) activity by regulating ALT features including the production of extrachromosomal telomere-repeat (ECTR) DNA such as C-circles, and ALT-associated promyelocytic leukemia bodies, or APBs. The activity of TRF1 is tightly regulated by post-translational modification such as phosphorylation. This thesis sets out to investigate the function of TRF1 phosphorylation on threonine-271 (T271) and threonine-371 in telomere maintenance. The results presented in this thesis demonstrate that TRF1 phosphorylation on T271 positively regulates the association of TRF1 to telomeric DNA in telomerase-expressing cells. In ALT cells, TRF1 phosphorylation on both T271 and T371 is shown to be important for the formation of APBs. Furthermore, the work presented here suggests that transcription-associated DNA damage mediates the association of phosphorylated (pT371)TRF1 with APBs.

ACKNOWLEDGEMENTS

I entered the Zhu lab in September of 2013 as an undergraduate thesis student and have since then been motivated to strive to become an effective researcher. Dr. Xu-Dong Zhu has been a very effective and motivating supervisor throughout my undergraduate and graduate studies. Her critical evaluations and feedbacks have been tough but, at the same time, very rewarding. Without her constant support throughout my graduate work, I would not have been able to succeed in my project. To this end, I am grateful and appreciative of her guidance in my growth as a scientist. I would also like to extend my gratitude to Dr. Jon Draper and Dr. Bhagwati Gupta for their assistance as my supervisory committee members, both of whom have provided with great advice and criticisms in helping me to succeed and grow as a scientist.

Moreover, members of the Zhu lab have also been an integral part of my graduate life at McMaster University. I would like to give a HUGE thank you to Nicole L. Batenburg, who has been a constant support in helping me out with all kinds of lab techniques. She was a great mentor and a great friend. I would like to give special thanks to past member, Florence R. Wilson, who has also mentored me when I first entered the lab. Who would have known we ended up becoming great friends and co-authors on my first publication! I would also like to thank past member, Kyle. R. Lindsay, who has also provided me with constant moral support when things aren't going well. Whether it is in the lab, coffee breaks in the hallway, or at the pub, memories with these unique individuals will be cherished. I wish them all the best and success in their current and future endeavors.

Finally, there are two very important individuals whom I must thank: Bosco and Cherly, my parents, for their unconditional support and love throughout my life.

TABLE OF CONTENTS

LIST OF FIGURES

LIST OF ABBREIVATIONS

53BP1	Tumor suppressor p53-binding protein 1
9-1-1	Rad9/Hus1/Rad1 complex
Akt	Protein kinase B
ALT	Alternative lengthening of telomeres
APB	ALT-associated promyelocytic leukemia body
ASF1	Anti-silencing function protein 1/Histone chaperone ASF1
AT	Ataxia telangiectasia
ATM	Ataxia telangiectasia mutated
ATP	Adenosine triphosphate
ATR	Ataxia telangiectasia and Rad3 related
BRCA1	Breast cancer type 1 susceptibility protein
BRCA2	Breast cancer type 2 susceptibility protein
BRCT	BRCA1 C Terminus
BrdU	Bromodeoxyuridine
BSA	Bovine serum albumin
Cdk	Cyclin B-dependent kinase
CDK	Cyclin dependent kinase
Cdk1	Cyclin dependent kinase
ChIP	Chromatin immunoprecipitation
CK2	Casein kinase 2
COUP-TF2	Chicken ovalbumin upstream promoter transcription factor 2
CPT	Camptothecin
CtIP	CtBP-interacting protein
DAPI	4',6-diamidino-2-phenylindole
DDR	DNA damage response
DEPC	Diethylpyrocarbonate
DMEM	Dulbecco's Modified Eagle's Medium

DMSO	Dimethyl sulfoxide
DNA	Deoxyribonucleic acid
DNA-PKcs	DNA-dependent protein kinase
DRB	D-ribofuranosylbenzimidazole
DSB	Double strand break
DTT	Dithiothreitol
ECL	Enhanced chemiluminescence
ECTR	Extra-chromosomal telomere repeat
EDTA	Ethylenediaminetetraacetic acid
EMSA	Electrophoretic mobility shift assay
FBS	Fetal bovine serum
FISH	Fluorescence in situ hybridization
FITC	Fluorescein isothiocyanate
GAPDH	Glyceraldehyde 3-phosphate dehydrogenase
GTP	Guanosine triphosphate
HDAC	Histone deacetylase
HEPES	4-(2-hydroxyethyl)-1-piperazineethanesulfonic acid
HP1	Heterochromatin protein 1
HR	Homologous recombination
IF	Indirect immunofluorescence
IP	Immunoprecipitation
IR	Ionizing radiation
MDC1	Mediator of DNA damage checkpoint protein 1
MEF	Mouse embryonic fibroblasts
MOPS	3-(N-morpholino)propanesulfonic acid
MRE11	Meiotic recombination 11/ Double-strand break repair protein MRE11
MRN	MRN complex (Mre11, Rad50 and Nbs1)
NB	Nuclear body

NBS1	Nijmegen breakage syndrome protein 1/Nibrin
NHEJ	Non-homologous end joining
NIMA	Never in Mitosis Gene A
NR2F2	Nuclear receptor subfamily 2, group F, member 2
NTD	N-terminal domain
OBD	Oligonucleotide binding fold domain
OLB	Oligo labelling buffer
PAGE	Polyacrylamide gel electrophoresis
PBD	POT1-binding domain
PBG	Phosphate buffered gelatine
PBS	Phosphate buffered saline
PCI	Phenol/chloroform/isoamylalcohol
PCNA	Proliferating cell nuclear antigen
PD	Population doubling
PFA	Paraformaldehyde
PIKK	Phosphatidylinositol 3-kinase-related protein kinase
Pin1	Peptidylprolyl Cis/Trans Isomerase, NIMA-Interacting 1
Pin2	Proteinase Inhibitor 2
Plk1	Pololike kinase 1
PML	Promyelocytic leukemia protein
PMSF	Phenylmethylsulfonyl fluoride
PMT	Photomultiplier tube
PNA	Peptide nucleic acid
PNK	Polynucleotide Kinase
POT1	Protection of Telomeres 1
Q-FISH	Quantitative fluorescent in-situ hybridization
RAD17	RAD17 checkpoint clamp loader component
RAD51D	DNA repair protein RAD51 homolog 4

RAP1	TERF2-interacting telomeric protein 1
RCM	Rolling-circle mechanism
RNA	Ribonucleic acid
RNF168	E3 ubiquitin-protein ligase ring finger protein (RNF) 168
RNF8	E3 ubiquitin-protein ligase ring finger protein (RNF) 8
ROI	Region of interest
RPA	Replication protein A
RPA2	Replication protein A2
RPM	Revolution per minute
SDS	Sodium dodecyl sulfate
SIM	SUMO interacting motif
SP100	Speckled 100 kDa/ Nuclear autoantigen Sp-100
SSC	Saline-sodium citrate
SUMO	Small ubiquitin-related modifier
TBE	Tris/Borate/EDTA
TC-NER	Transcription-coupled nucleotide excision repair
TERC	Telomerase RNA component/hTR
TERRA	Telomeric Repeat-containing RNA
TERT	Telomerase reverse transcriptase
TIF	Telomere Dysfunction-Induced Focus
TIN2	TERF1-interacting nuclear factor 2
T-loop	Telomere loop
TNE	Tris-HCl/NaCl/EDTA
TNES	Tris-HCl/NaCl/EDTA/SDS
TPP1	TINT1/PTOP1/PIP1
TR2	Testicular receptor 2
TRF1	Telomeric-repeat binding factor 1
TRF2	Telomeric-repeat binding factor 1

TRFH	TRF homology
TRITC	Fluorescein isothiocyan
T-SCE	Telomere-sister chromatid exchange
XLF	XRCC4-like factor
XRCC4	X-ray cross-complementation group 4

CHAPTER 1 INTRODUCTION

1.1 TELOMERES AND THE MAINTENANCE OF TELOMERE LENGTH

1.1.1 Telomeres and the end-replication problem in human cells

The linear chromosomes in humans present a serious dilemma during DNA replication. Due to the semi-conservative mechanism of DNA replication, complete replication of telomeres is impossible and as such, telomeres shorten with each cell division (Meselson & Stahl, 1958; Olovnikov, 1996). This is referred to as the end-replication problem, in which after the removal of the RNA primer at the lagging strand from the terminal Okazaki fragments, each new daughter molecule will contain a shortened 5' end (Figure 1.1) (Okazaki et al., 1968; Olovnikov, 1996). In somatic cells, telomeres shorten with each division and this limits the number of times a normal human cell population can divide. With the gradual loss of telomeres, cells have limited capacity to divide until telomeres shorten to a critical length, after which they become senescent. This phenomenon is referred to as the 'Hayflick limit' (Hayflick & Moorhead, 1961; Olovnikov, 1996). Shortened chromosome ends can be recognized as DNA damage sites, and as a result, a DNA damage response (DDR) will be initiated to permanently arrest the cell from further growth (d'Adda di Fagagna et al., 2003). During DDR, DNA-damage sensing proteins will localize at damaged sites in an attempt to repair any aberrations or to signal growth arrest (i.e. cellular senescence) (Cesare & Reddel, 2010). However, it is also possible that the cell can bypass cellular checkpoints and continue to proliferate, but telomere shortening

will eventually kill the cell at crisis (Greenberg, 2005), unless telomere lengthening mechanism is activated to sustain continuous growth.

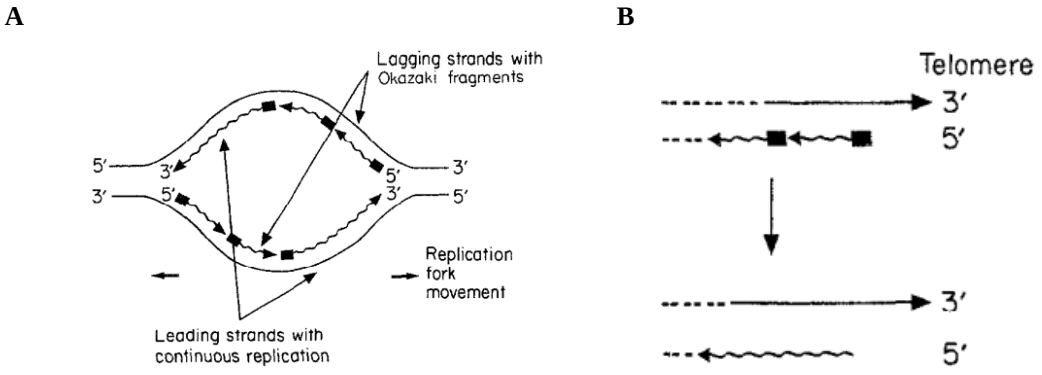

Figure 1.1. The end replication problem. A) Schematic representations of DNA replication in both the leading and lagging strands. **B)** Removal of RNA primer at the lagging strand results in a 3' overhang. Since DNA polymerase cannot initiate replication at the end of the DNA strand, linear DNA molecules shorten with each round of replication. (Taken from Olovnikov, 1996)

Activation of a telomere maintenance mechanism is an essential step for cells to escape replicative senescence due to telomere shortening (Olovnikov, 1996). Telomerase, a specialized reverse transcriptase composed of a reverse transcriptase catalytic subunit (referred to as hTERT) and a RNA subunit (referred to as hTR or TERC), can add telomeric DNA sequence repeats (TTAGGG) *de novo* to chromosome ends. Telomerase is activated in most human cancer cells to counter telomere shortening associated with the DNA end-replication problem (Cesare & Reddel, 2010; Morin, 1989; Plantinga et al., 2013). In humans, at the ends of chromosomes, DNA is double-stranded but also terminates with a G-rich 3' single-stranded overhang (Figure 1.2A) (Makarov, Hirose, & Langmore, 1997). During telomere lengthening, telomerase binds the 3' overhang that is complementary to its RNA subunit and catalyzes the extension of the G-rich sequence via reverse

transcription (Blackburn, Greider, & Szostak, 2006; Theimer & Feigon, 2006). As a result, after the removal of the terminal RNA primer at the lagging strand, telomerase is able to extend and restore telomere lengths at the 3' end of the lagging strand (Figure 1.3).

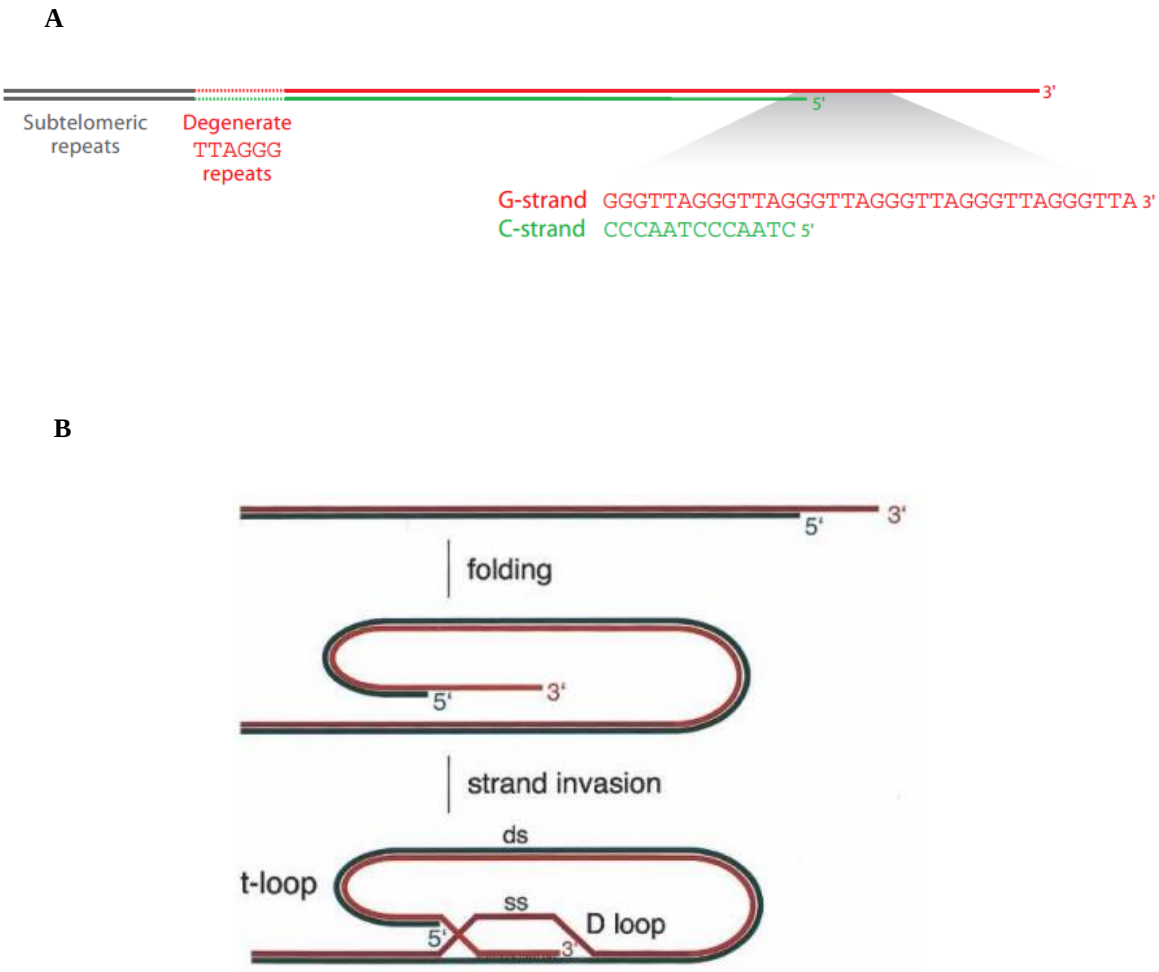

Figure 1.2. Telomere structure. A) Schematic representation of the G- and C-rich sequences of telomeres, and **B)** the formation of the t-loop via strand invasion by the G-rich 3' overhang are shown. (Taken from de Lange, 2005; Palm & de Lange, 2008)

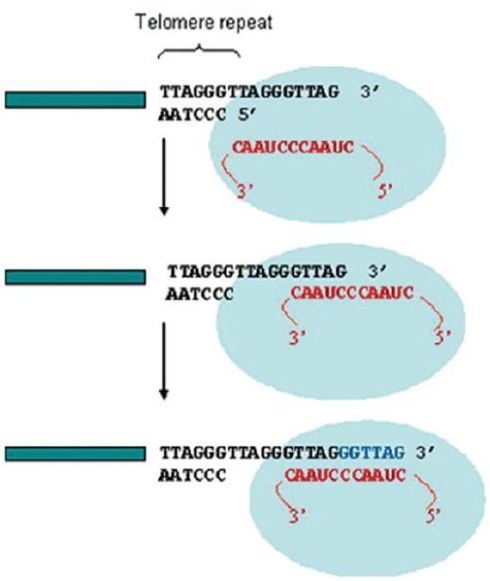

Figure 1.3. Telomere extension by telomerase. Telomerase (light blue) binds to the G-rich 3' overhang (G-overhangs) of a telomere that is complimentary to the telomerase RNA component (hTR, red). Upon proper base pairing, nucleotides are added extending the ends of chromosomes with the addition of TTAGGG telomeric sequences (dark blue). Upon completion, telomerase relocates and repeats the process while the lagging strand (i.e. C-rich telomere strand) is replicated by traditional DNA replication machinery (Taken from Sekhri, 2014).

1.1.2 The shelterin complex and telomeres

The G-rich sequences at the 3' ends of telomeres can physically fold back and invade into adjacent duplex sequences forming a telomere loop (t-loop) structure. The t-loop is formed via the association between the invading G-rich sequence and the C-rich sequence in the complementary strand (Figure 1.2B) (Griffith et al., 1999; Palm & de Lange, 2008). The t-loop structure is thought to protect chromosome ends from being recognized as DNA damaged sites, which can otherwise trigger DDR (Griffith et al., 1999).

The formation of the t-loop is believed to be catalyzed by the shelterin protein complex (de Lange, 2005), and as such telomere protection is dependent on shelterin. The shelterin complex refers to a set of telomere-associated proteins composed of six different subunits: TRF1, TRF2, TIN2, Rap1, TPP1, and POT1 (Chong et al., 1995; Colgin et al., 2003; Houghtaling et al., 2004; Sahn-ho H Kim et al., 1999; Palm & de Lange, 2008; Z. Zhong, Shiue, Kaplan, & de Lange, 1992; Zhu et al., 2003). The shelterin subunits associate with telomeres via the tandem telomeric TTAGGG repeats. The TRF1 and TRF2 subunits bind duplex telomeres while POT1 binds to the single-stranded TTAGGG repeats at the 3' overhangs of chromosome ends (Figure 1.4A) (Palm & de Lange, 2008). TRF1 and TRF2 also promote the localization of TIN2, Rap1, TPP1, and POT1 to telomeres. Together, the six-subunit shelterin complex enables cells to differentiate natural chromosome ends from actual DNA damaged sites, likely in part by inducing the t-loop formation (Figure 1.2B, 1.4B).

In mammals, telomere maintenance is achieved by a negative feedback loop that regulates telomerase activity at telomeres. If telomeres are too long, telomerase's access to the ends of telomeres is inhibited; and if too short, repression by shelterin is relaxed and telomerase is allowed to act (Figure 1.5) (de Lange, 2005). Since the amount of telomere-bound shelterin is directly proportional to TTAGGG repeats, short telomeres will present less space for shelterin, and in particular POT1, to bind at 3' overhangs and thus increase the ability for telomerase to bind to the 3' terminus to extend telomeres (Figure 1.5) (Kelleher, Kurth, & Lingner, 2005; Lei, Zaug, Podell, & Cech, 2005). Consequently,

shelterin effectively promotes telomere end protection by repressing DDR at telomeres, stabilizing the t-loop structure, and regulating 3' extension at telomeres.

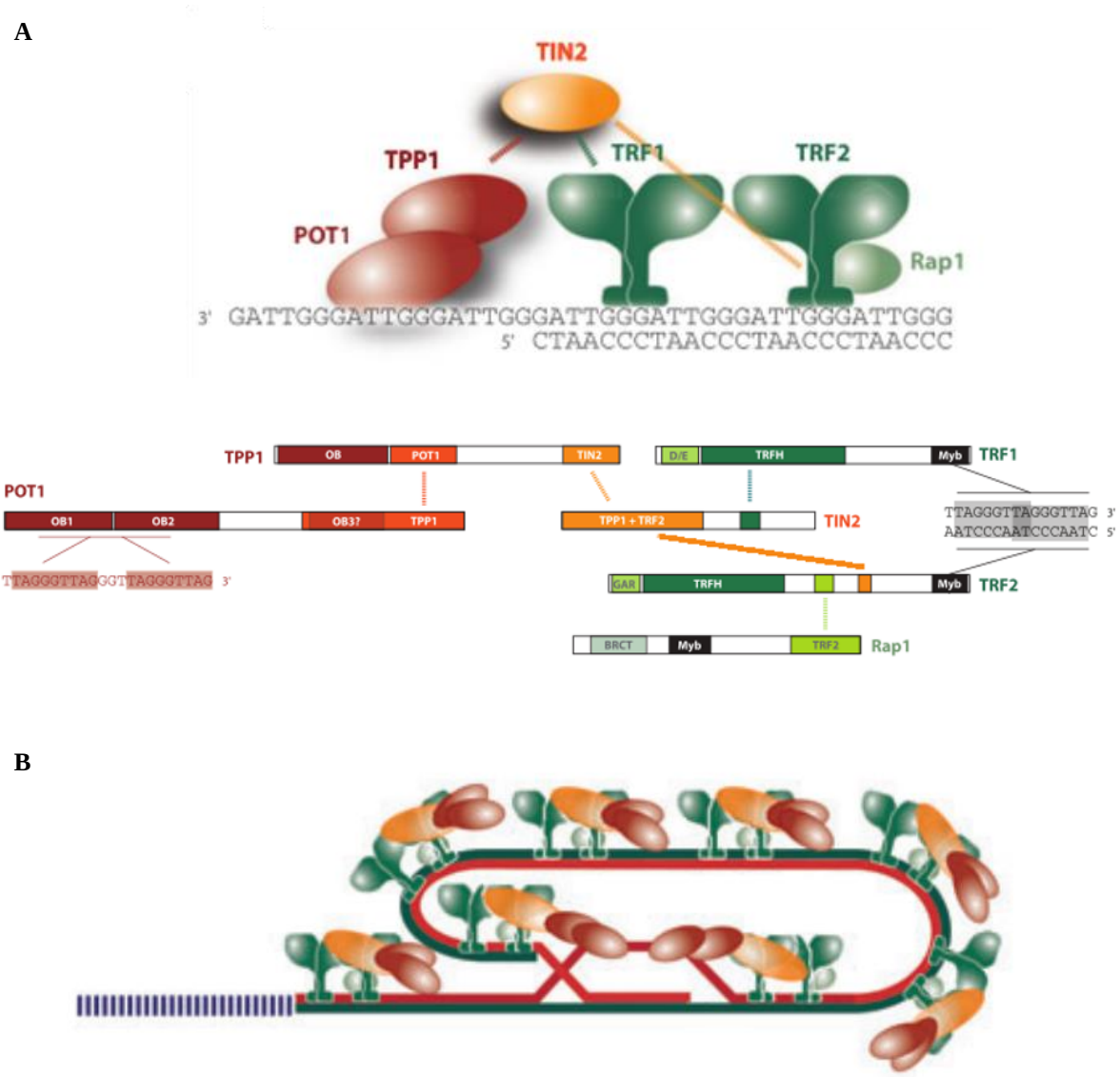

Figure 1.4. Shelterin at telomeres. A) Cartoon schematic representation of shelterin subunits at telomeres. Interactions between different shelterin subunits are shown in terms of interactions between domains (orange and green lines). Interaction between shelterin subunits and single/duplex telomeric DNA sequences are also displayed (red and black lines). **B)** The structure of human

telomeres with shelterin in a closed t-loop conformation. The colors of protein interaction correspond to one another between A and B. (Modified from Palm & de Lange, 2008)

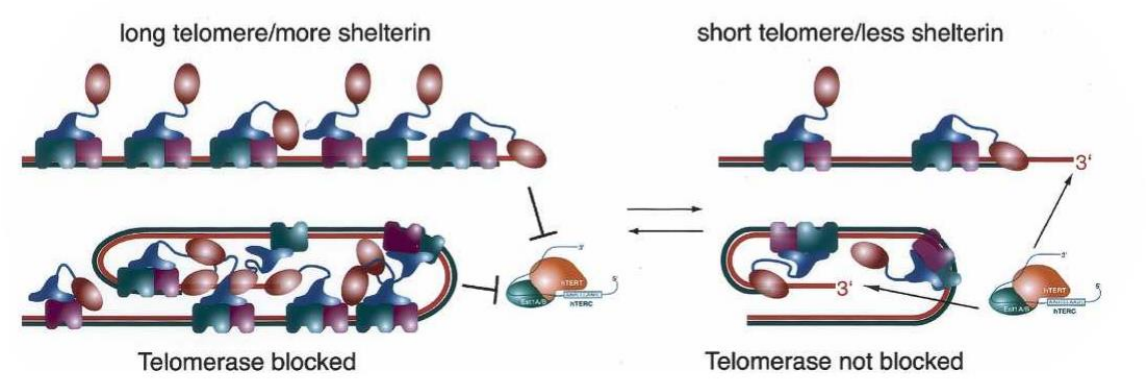

Figure 1.5. Telomere length regulation by shelterin. (Taken from de Lange, 2005)

1.2 THE ROLE OF SHELTERIN SUBUNITS IN TELOMERE LENGTH MAINTENANCE

1.2.1 Telomere Repeat Binding Factor 1 (TRF1)

TRF1, telomere repeat binding factor 1, was the first identified mammalian factor to have a DNA-binding activity with specificity for the telomeric TTAGGG repeat arrays (Z. Zhong et al., 1992). TRF1 is encoded by the *TERF1* gene which is localized to human chromosome 8 band q13 (Broccoli, Chong, et al., 1997). The domain organization of TRF1 contains an acidic N-terminus, a dimerization domain near the N-terminus, a linker or hinge domain near the C-terminus, and a C-terminal Myb-like DNA binding motif (Figure 1.6) (Arnoult & Karlseder, 2015; Broccoli, Smogorzewska, Chong, & de Lange, 1997; Fairall, Chapman, Moss, de Lange, & Rhodes, 2001; Hanaoka, Nagadoi, & Nishimura, 2005). Based on *in-vitro* protein translation of the TRF1 cDNA, the molecular weight of TRF1 has been identified to be approximately 56kDa (Broccoli, Chong, et al., 1997). As part of the shelterin complex, and as one of the two main duplex telomeric DNA binding proteins, TRF1 binds to telomeres as a homodimer and is mediated by both its dimerization TRF homology (TRFH) domain as well as the Myb-like DNA binding motif (Fairall et al., 2001; A. Smogorzewska et al., 2000).

TRF1 has been reported to be ubiquitously expressed throughout the cell cycle and demonstrated to be localized to all human telomeres in metaphase chromosomes (Broccoli, Smogorzewska, et al., 1997; Broccoli, Chong, et al., 1997; A. Smogorzewska et al., 2000). Interestingly, via alternative splicing of the *TERF1* gene, an isoform of TRF1, Pin2 is

encoded with identical sequences with the exception of an internal 20 amino acids deletion (Chong et al., 1995; Lu, Hanes, & Hunter, 1996; M. Shen, Haggblom, Vogt, Hunter, & Lu, 1997). Based on experimental evidence searching for interacting factors with the mitotic kinase NIMA (never-in-mitosis A), as well as experiments involving the progression of cells through mitosis, Pin2 was identified as part of three proteins, Pin1-3 (Lu et al., 1996). It has been reported that Pin2 is capable of forming a homodimer and a heterodimer with TRF1, and that both dimer forms are capable of localizing to telomeres. Furthermore, biochemical analysis of mRNA level suggests that the expression level of Pin2 is much higher than TRF1, peaking at G2/M phase (M. Shen et al., 1997). Beyond the well-studied role of TRF1 in telomere length maintenance, an increasing amount of evidence has suggested that TRF1 plays a non-telomeric role in cell cycle progression, namely mitotic progression in cells (J. Lee & Gollahon, 2013; Muñoz et al., 2009; Ohishi, Hirota, Tsuruo, & Seimiya, 2010; M. Shen et al., 1997). Collectively, these findings suggest for a potential connection for TRF1/Pin2 in bridging the gap in mitotic control and telomere length regulation, both of which are important in ensuring genome stability in cells.

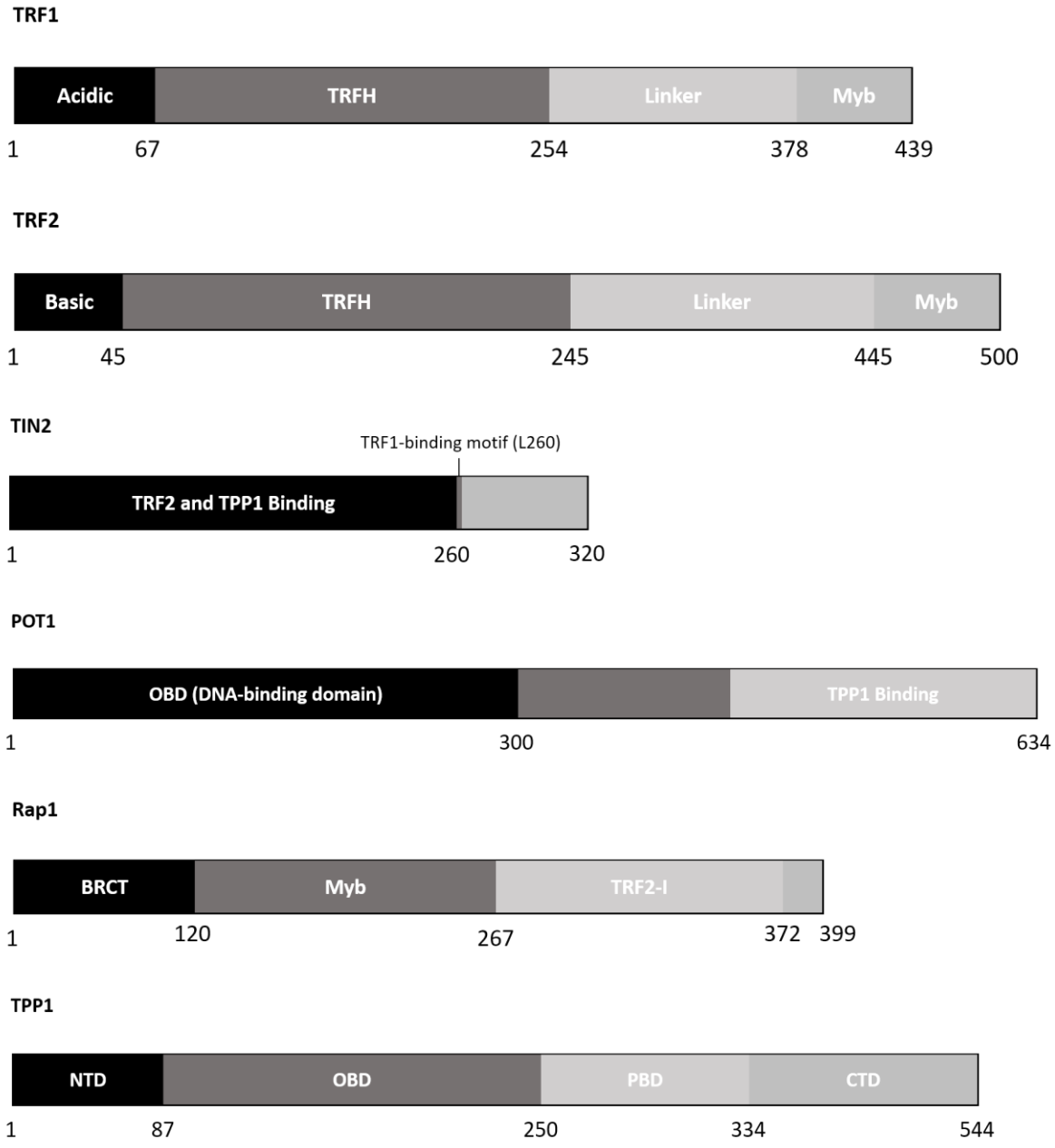

Figure 1.6. Domain organization of the shelterin components. A) Cartoon schematic depicting the individual domains of the six shelterin subunits (from top to bottom): TRF1, TRF2, TIN2, Rap1, POT1, and TPP1. Numbers below each schematic indicate residues position. See text for details.

1.2.2 The role of TRF1 in telomere length maintenance

TRF1 directly binds to mammalian telomeric DNA and participates in the regulation of telomere length. TRF1 functions as a negative regulator of telomerase-dependent telomere extension, which may be due to its ability to bind to telomeres and to restrict access of telomerase to telomeres (A. Smogorzewska et al., 2000; van Steensel & de Lange, 1997). It has been demonstrated that overexpression of a dominant negative allele of TRF1, which removes TRF1 from telomeres, can result in the elongation of telomeres in telomerase-positive cells. Conversely, the overexpression of TRF1 in telomerase-positive cells results in telomere shortening. Moreover, neither overexpression nor depletion of TRF1 affects the activity of telomerase (van Steensel & de Lange, 1997). As such, a proposed model, otherwise referred to as the protein-counting model (Marcand, Gilson, & Shore, 1997), suggests that long telomeres with an increased level of bound TRF1 would prevent the access of telomerase to telomeres, resulting in gradual telomere shortening (Figure 1.7) (A. Smogorzewska et al., 2000).

The function of TRF1 in the regulation of telomere length maintenance is controlled by various post-translational modification, one of which is phosphorylation (Walker & Zhu, 2012). In fact, TRF1 phosphorylation can occur on multiple serine and threonine residues and such modifications regulate the functions of TRF1 in telomere binding, protein stability, and its cellular localization. It has been demonstrated that Cdk1 (cyclin B-dependent kinase 1) phosphorylates threonine-371 (T371) TRF1 of TRF1 (McKerlie & Zhu, 2011), referred to as (pT371)TRF1 and that it is important for the maintenance of telomere integrity (McKerlie, Lin, & Zhu, 2012; McKerlie & Zhu, 2011).

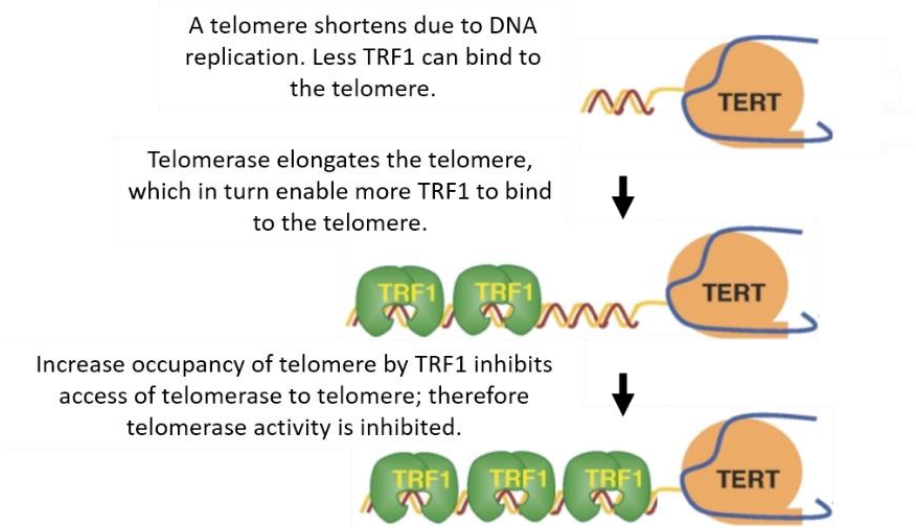

Figure 1.7. Control of human telomere length by TRF1. In humans, telomerase-dependent telomere maintenance is modeled by the protein-counting mechanism. The counting model is a traditional view for telomere length regulation, in which TRF1 functions as a negative regulator of telomere length maintenance by inhibiting the access of telomerase to telomeres for telomere elongation.

1.2.3 Telomere Repeat Binding Factor 2 (TRF2)

TRF2, telomere repeat binding factor 2, a homolog of TRF1, is also involved in the regulation of telomere length control (A. Smogorzewska et al., 2000). TRF2 is the other main duplex telomeric DNA binding protein. TRF2 contains a basic N-terminus, a TRFH domain near the N-terminus, a linker or hinge domain near the C-terminus, and a Myb-like DNA binding motif, which is structurally similar to TRF1 (Figure 1.6) (Arnoult & Karlseder, 2015; Bianchi et al., 1999). Based on *in-vitro* protein translation of the human TRF2 cDNA, the molecular weight of TRF2 has been identified to be approximately 66kDa (Broccoli, Chong, et al., 1997; Z. Zhong et al., 1992). Like TRF1, TRF2 also binds

telomeres as a homodimer, which is mediated by the TRFH domain and the Myb-like DNA binding motif. Its hinge/linker domain mediates TRF2's binding with two other shelterin subunits, Rap1 and TIN2 (Arnoult & Karlseder, 2015). Although both TRF proteins contain a similar TRFH domain that is responsible for the formation of homodimers, neither of them are capable to heterodimerize with each other. The closest relatedness in TRF1 and TRF2's domain structure is the Myb-like DNA binding motif with 56% identity (A. Smogorzewska et al., 2000). Despite their similar domain organization and cellular localization at the telomeres, TRF1 and TRF2 are structurally independent in their telomeric binding, and functionally unique in their role to regulate the protection and maintenance of telomeres.

1.2.4 The role of TRF2 in telomere length maintenance

Although structurally similar to its shelterin partner, unlike TRF1's acidic nature of the N-terminus, which inhibits TRF1's ability to condense telomeric DNA, the basic nature of TRF2's N-terminus is essential for its ability to condense telomeric DNA (Poulet et al., 2012). Yet, together, the N-termini of TRF1 and TRF2 function collectively to fine tune and regulate telomeric DNA condensation, which is important for the heterochromatic state of telomeres, the folding of telomeres into t-loop structures, and ultimately protecting chromosome ends from being erroneously recognized as damaged DNA (de Lange, 2005; Palm & de Lange, 2008). To this end, the formation of t-loops at telomeres is crucial to the control of telomerase's access to chromosome ends and therefore telomere elongation. Biochemical analyses reveal that both TRF1 and TRF2 function together in the formation of t-loops. TRF1 is required to induce the pairing of telomeric duplex DNA via bending

and looping of DNA, while TRF2 facilitates the invasion of the 3' single-stranded TTAGGG repeat strand into the duplex telomeric DNA (Poulet et al., 2012; A. Smogorzewska et al., 2000) (Figure 1.2B, 1.4B). Unlike TRF1, TRF2's negative regulatory role in telomere lengthening is its unique role in telomere end capping. Though functionally distinct, both TRF1 and TRF2 are required to ensure regulated telomere length maintenance, and thus to act as the negative regulators in telomere lengthening.

1.2.5 TERF1-interacting nuclear factor 2 (TIN2)

Using a yeast two-hybrid cDNA library screening with TRF1 as a bait, TIN2 (TERF1-interacting nuclear factor 2) was identified as the interacting partner of TRF1 and thus a component of the shelterin complex (Sahn-ho H Kim et al., 1999). *In-vitro* translation of TIN2 cDNAs demonstrated that TIN2 has a molecular weight of approximately 40kDa. TIN2 contains a large binding region for TRF2 and TPP1, and a TRF1-binding motif located near its C-terminus, which requires leucine 260 (L260) (Figure 1.6) (Y. Chen et al., 2008; Frescas & de Lange, 2014). Using fluorescence microscopy techniques, the subcellular localization of TIN2 have been demonstrated to overlap with TRF1 at telomere ends on metaphase chromosome, as well as forming punctate staining with TRF1 in interphase nuclei (Sahn-ho H Kim et al., 1999). Interestingly, in a more recent study, evidence from mass spectrometry and co-immunoprecipitation reveals that TRF1, TIN2, and POT1 are associated with the TRF2-Rap1 complex (Figure 1.4A) (J. Z. S. Ye et al., 2004). However, further analysis using a combination of gel filtration study, co-immunoprecipitation, far-western assays and two-hybrid assays has revealed that TIN2 is a direct interactor with TRF2, and thus the

TRF2-Rap1 complex, and that TRF1 is dispensable for this interaction (J. Z. S. Ye et al., 2004). Nevertheless, TIN2 is an essential component of the shelterin complex that tethers TPP1/POT1 to TRF1 and TRF2, thus contributing TRF1's indirect link to TRF2, which is important for telomere end protection.

1.2.6 The role of TIN2 in telomere length maintenance

While both TRF1 and TRF2 are key regulators in telomere length maintenance, TIN2 serves as an essential mediator to garner the functions of TRF1 and TRF2 at telomeres. Overexpression of TIN2 induces telomere shortening in telomerase-positive cells, whereas overexpression of a TIN2 mutant lacking its N-terminus but capable of binding TRF1 results in telomere shortening (Sahn-ho H Kim et al., 1999). Moreover, electrophoretic mobility shift assays (EMSA) also revealed that TIN2, TRF1, and a double stranded TTAGGG telomeric DNA probe are capable of forming large DNA-protein complexes (Sahn-ho H Kim et al., 1999). Thus, experimental evidence suggests that the role of TIN2 in mediating telomere length is partly due to its ability in controlling the activity of TRF1 binding to telomeres. Conversely, when a TIN2 mutant defective in TRF1 binding is overexpressed in telomerase-positive cells, the interaction between TRF2 and TIN2 is also drastically impaired. These results suggest that a stable interaction between TRF1 and TIN2 is important for enhancing or stabilizing TRF2-TIN2 interaction (Sahn Ho Kim et al., 2004). To further understand TIN2's importance in stabilizing TRF1 and TRF2 at telomeres to maintain functional telomeres, cells expressing a TIN2 mutant defective in TRF1/TRF2 binding were immunostained for the DNA damage markers 53BP1 or γH2AX. It was found that cells with 53BP1 or γH2AX foci were devoid of focal TRF2 staining.

TRF1 foci were also affected but to a lesser extent with reduced TRF1 staining in γH2AX-positive cells (Sahn Ho Kim et al., 2004). Evidence from western blotting also reveals that cells overexpressing the TIN2 mutant have reduced levels of TRF1 and TRF2 when compared to cells expressing wild type TIN2 (Sahn Ho Kim et al., 2004). Collectively, TIN2 is important to stabilize and localize TRF1 and TRF2 at telomeres, and therefore to promote regulated telomere length and proper telomere capping to maintain functional telomeres.

1.2.7 Telomeric repeat-binding factor 2-interacting protein 1 (Rap1)

Rap1 was first identified in a yeast two-hybrid screen of HeLa cDNAs with TRF2 protein as a bait (B. Li, Oestreich, & de Lange, 2000). The molecular weight of Rap1 is approximately 50kDa and contains various domains including an N-terminal BRCT domain, a central Myb domain, and an acidic C-terminus (Figure 1.6). Evidence from deletion mapping revealed that Rap1 associates with a central domain of TRF2 via a TRF2-interacting domain (TRF2-I), which is mapped to the C-terminus of Rap1 from amino acids 267 to 372. Despite sequence similarity in the N-termini of TRF1 and TRF2, which is responsible for TIN2 interaction, Rap1 does not interact with TRF1 in the yeast-two hybrid system (B. Li et al., 2000). Through immunofluorescence (IF) analysis, Rap1 staining showed punctate nuclear foci pattern, which also colocalized with TRF1 and TRF2 in interphase nuclei. Further analysis of metaphase chromosomes also demonstrate that Rap1 is found to show terminal signals at the ends of chromosomes (de Lange, 2005; B. Li et al., 2000). Experimental evidence from a yeast two-hybrid assay and co-immunoprecipitation suggests that the localization of Rap1 to telomeres may be dependent

on the interaction with TRF2 (B. Li et al., 2000). To this end, when a TRF2 mutant defective in forming a heterodimer with endogenous TRF2 is overexpressed in telomerase-positive HeLa cells, immunofluorescence analysis reveals that a percentage of cells shows a marked reduction on punctate TRF2 foci, which is also correlated with the lack of Rap1 foci (B. Li et al., 2000). It has also been reported that in a gel shift assay using a double stranded telomeric probe $(TTAGGG)_{12}$, a ternary DNA-protein is only detected when Rap1 is incubated with TRF2 and the telomeric probe. Thus, experimental evidence strongly suggests that Rap1's recruitment to telomeres occurs in a TRF2-dependent manner (B. Li et al., 2000). Collectively, these results demonstrate that Rap1 interacts with TRF2 and localizes to telomeres, and therefore is considered a part of the shelterin complex.

1.2.8 The role of Rap1 in telomere length maintenance

According to the protein counting model for telomere length, long telomeres are capable of recruiting a greater number of Rap1 molecules and as a result inhibit the access of telomerase-mediated lengthening (Marcand et al., 1997). When Rap1 is overexpressed in a human fibrosarcoma cell line, HTC75, in which telomerase is expressed at high levels with telomeres maintained at a stable length, gradual elongation in the mean telomere length was observed over many population doublings (PD) with a maximum rate of 40-50 base pairs increase per PD (B. Li et al., 2000). Interestingly, when cells are overexpressing Rap1 mutants that either maintained or lacked TRF2 binding activity and therefore telomere localization, telomere elongation was observed, which suggests that the elongation phenotype is independent of Rap1's ability to bind TRF2 and to localize to telomeres. These Rap1 mutants contained deletions of C-terminus, or the Myb and BRCT

domains at the N-terminus. The proposed explanation is that Rap1 is a *cis*-acting negative regulator of telomere length, in which overexpression of Rap1 can result in a high level of nucleoplasmic Rap1. It is believed that the amount of available interacting TRF2 binding sites can become saturated. Thus, it is speculated that the excess amount of nucleoplasmic Rap1 competes with telomeric Rap1 for the binding of a putative interacting partner, which is important for telomere length control. Taken together, it is proposed that the C terminus of Rap1 functions to recruit the protein to telomeres, and its cis-acting telomere length regulation is dependent on the Myb-like DNA binding motif and the N-terminal BRCT domain (B. Li & de Lange, 2003; Agata Smogorzewska & de Lange, 2004).

1.2.9 Protection of Telomeres 1 (POT1) and TINT1/PTOP1/PIP1 (TPP1)

The *POT1* gene encodes for the protein protection of telomeres 1, POT1, which is a member of the shelterin complex involved in telomere length maintenance. According to ENSEMBL and Entrez Gene databases, the genomic location of *POT1* maps to chromosome 7 band q31. The molecular weight of POT1 is approximately 72kDa (Loayza & Lange, 2003). Structurally, POT1 contains an N-terminal oligonucleotide binding fold domain (OBD), and a C-terminal TPP1 binding domain (Figure 1.6). It has been reported that human POT1 is a single-stranded telomeric DNA binding protein that binds specifically to the G-rich telomeric strand (P Baumann & Cech, 2001; Peter Baumann, Podell, & Cech, 2002). It has been previously described that the *POT1* gene produces five splice variants of POT1, all of which have been described to vary in their ability to bind to

single-stranded telomeric DNA *in-vitro* (Peter Baumann et al., 2002). POT1 is the only shelterin subunit that binds single-stranded telomeric DNA (Figure 1.4A).

TPP1, is a 60kD protein encoded by the *TPP1* gene located on chromosome 11 band p15 (Gene Card). The terms TPP1 originated from the combination of the first letter of each of the names, TINT1, PTOP1, and PIP1, which were names given by three groups that initially characterized the protein (Houghtaling et al., 2004; Liu et al., 2004; J. Z.-S. Ye et al., 2004). It is the binding partner of TIN2, which together bridges the duplex telomeric DNA binding proteins TRF1 and TRF2 to the single-stranded telomeric G-overhang binding protein POT1 (Figure 1.4A) (de Lange, 2005). The domain organization of TPP1 contains an N-terminal domain (NTD), an oligonucleotide/oligosaccharide binding fold domain (OB-fold) domain, the POT1-binding domain (PBD) and a C-terminal domain (CTD) containing multiple serine/threonine phosphorylation sites, with the last 22 residues being critical for TIN2 interaction (Figure 1.6) (Malligarjunan Rajavel, 2014). Interestingly, TPP1 also has a telomere protective role, but in conjunction with POT1. It has been demonstrated that POT1's localization to telomeres is greatly enhanced by its interaction with TPP1. Together, POT1 and TPP1 are stabilized at telomeres and elicit a protective function by preventing telomere fusions and by suppressing telomere-associated DNA damage, which can be detected as TIFs (Telomere Dysfunction-Induced Focus) (Hockemeyer et al., 2007).

1.2.10 The role of POT1 and TPP1 in telomere length maintenance

It has been reported that overexpression of POT1 results in telomere lengthening in telomerase-positive cells (Colgin et al., 2003). Further analysis of POT1's role in telomere lengthening reveals that when it is overexpressed in telomerase-negative cells, such as GM847, no detectable changes in mean telomere length was observed. These results imply that POT1 may regulate telomere length in a telomerase-dependent manner. Consistent with this view, when hTERT and POT1 are co-expressed in GM847 cells, POT1 is able to induce telomere elongation. Thus, experimental evidence suggests that POT1's telomere length regulation is likely to be a telomerase-dependent process (Colgin et al., 2003). Interestingly, studies involving POT1 knockdown in cells can also result in telomere elongation, and *in-vitro* biochemical analyses with yeast and human POT1 indicated that the protein is capable of inhibiting extension of a telomeric primer by telomerase (Colgin et al., 2003; Kelleher et al., 2005; Veldman, Etheridge, & Counter, 2004). However, the presented paradox here is that, both reducing and increasing the level of POT1 in cells can result in telomere elongation. This dilemma requires a closer analysis on the interplay between POT1 and other shelterin components, which is discussed below.

As part of the shelterin complex, TPP1-TIN2 serve as the interaction link between the single-stranded DNA binding protein POT1 and the double-stranded DNA binding components TRF1 and TRF2 (Figure 1.4A) (de Lange, 2005). When telomeres are long, the shelterin complex forms a complete bridging complex linking the duplex and single-stranded DNA at telomeres. Conversely, when telomeres are short, the shelterin complex is unable to form a complete bridging and thus leaving the TTAGGG-3' single-stranded

G-overhangs free of protein, and thus render chromosome ends open to access by telomerase (Figure 1.5) (Palm & de Lange, 2008). As such, it is hypothesized that when POT1 is overexpressed, the closed bridging conformation of the shelterin complex is impaired with excess binding of POT1 to TPP1-TIN2 (Loayza & Lange, 2003; Palm & de Lange, 2008). In the context of telomerase activity, it has been reported that the DNA binding activity of POT1 is necessary for telomerase inhibition, and that *in-vitro*, POT1 is unable to suppress telomerase's enzymatic activity to add telomeric repeats to substrates that cannot bind POT1 (Kelleher et al., 2005). These results suggest that POT1's role in telomerase-dependent elongation is likely due to some sort of substrate access regulation for telomerase at telomeres, especially at G-overhangs.

A unique molecular interaction of G-overhangs at telomeres is their ability to form stable secondary structures known as G-quadruplexes (Ambrus et al., 2006). Biochemical analysis revealed that upon loading of POT1-TPP1 on to ssDNA oligonucleotides containing wild type telomeric DNA sequences, the DNA was more susceptible to DNaseI digestion. Conversely, mutant oligonucleotides containing mutant telomeric sequences that are defective in forming G-quadruplexes were much more susceptible to nuclease digestion with or without POT1-TPP1 binding (Corriveau, Mullins, Baus, Harris, & Taylor, 2013). These experimental results indicate that POT-TPP1 binding is important to facilitate telomerase-dependent elongation by promoting telomerase binding, and the unfolding of G-quadruplexes at telomeres. As a result, the observed POT1 paradox in telomerase-dependent elongation may be explained in the context of G-overhang binding, whereby

POT1-TPP1 modulates the opened/closed conformation of telomeres, which is important for telomerase access to telomeres.

The seemingly contradictory results of increased or reduced levels of POT1 correlating with telomere elongation can be further understood by evaluating the interplay between TPP1, POT1, TIN2, and telomerase. TPP1 is necessary for POT1's nuclear import and telomere localization; it has been shown that, through immunofluorescence analysis, TPP1 regulates the recruitment of POT1 to telomeres (Hockemeyer et al., 2007; Liu et al., 2004). TPP1 contains a nuclear export signal and if disrupted, this can result in telomeric DNA damage response and telomere length dysregulation, as well as the nuclear import of POT1 in the nucleus (L.-Y. Chen, Liu, & Songyang, 2007). In agreement, southern blot analysis of telomeric restriction fragments in HT1080 cells overexpressing a TPP1 mutant defective in POT1 binding revealed that telomere elongation is promoted over time (Liu et al., 2004). Interestingly, when assessed by FISH (fluorescence *in-situ* hybridization) and IF, TPP1 and TIN2 depletion in HeLa cells can lead to a loss of telomerase localization to telomeres (as observed by hTR and telomere probes or shelterin subunits localization), but not due to POT1 depletion. Along the lines of telomerase recruitment to telomeres, when the oligonucleotide binding fold domain (OB-fold) of TPP1 is deleted, telomerase recruitment to telomeres is completely impaired and can be rescued when a shRNA-resistant form of TPP1 is expressed, suggesting that the OB-fold domain of TPP1 is essential for telomerase's recruitment to telomeres (Abreu et al., 2010; F. L. Zhong et al., 2012). Recent studies have further pinpointed the molecular interaction between TPP1, POT1, and telomerase. Residue glycine 100 (G100), which resides in the N-terminus of

telomerase have been identified to be essential for eliciting telomerase processivity mediated by POT1-TPP1 (Zaug, Podell, Nandakumar, & Cech, 2010). Moreover, mutational studies of TPP1 have identified a specific patch of highly conserved glutamate and leucine residues in the OB-fold domain of TPP1, termed "TEL" patch (**T**PP1 glutamate (**E**) and leucine (**L**) rich region), which is responsible for telomerase recruitment to telomeres (Nandakumar et al., 2012). In addition to telomerase recruitment, the binding of the POT1-TPP1 heterodimer at telomeres has also been shown to promote telomerase's processivity by adding multiple telomeric repeats to an oligonucleotide following a single binding event. This has been further supported with work demonstrating that POT1-TPP1 contributes to telomerase activity by reducing dissociation of telomerase from the DNA template (Latrick & Cech, 2010). Collectively, the apparent POT1 dilemma presented earlier may be explained by a three step model: 1) Consistent with the negative regulatory role of shelterin, POT1-TPP1 would normally bind and cover G-overhangs at telomeres, and therefore inhibit access of telomerase to telomeres. 2) Upon telomere shortening, POT1-TPP1 may be displaced from short 3' terminus by an unknown mechanism, perhaps via post-translational modification disrupting binding of the shelterin complex or POT1-TPP1 at telomeres. 3) During telomere elongation, POT1-TPP1 now function as a positive regulator by promoting telomerase recruitment and processivity until telomeres are lengthened to a certain threshold. The nascent telomeric repeats then become bound by shelterin complexes, the extended 3' G-overhangs is re-bound by POT1-TPP1, which then re-establish its function to inhibit telomerase's access, and thus return back to state 1 (Latrick & Cech, 2010; F. Wang et al., 2007).

Collectively, experimental evidence suggests a model in which POT1 and TPP1 are crucial in regulating telomerase access to telomeres and protecting telomeres from DNA damage. Nevertheless, whether POT1-TPP1's function in telomerase-dependent elongation may be further regulated by TIN2, TRF1, TRF2, and Rap1 would require further research.

1.3 TELOMERES AND THE DNA DAMAGE RESPONSE

1.3.1 Telomeres and the DNA Damage Response

DNA double-strand break (DSB) is an extremely deleterious type of DNA damage, whereby inaccurate or lack of repair of a DSB can lead to mutations, loss of genetic information or even large scale genome instability such as the generation of dicentric or acentric chromosomal fragments (Jackson, 2002). To protect the genome from the deleterious effects of lesions such as DSBs, cells have evolved mechanisms to detect and repair DNA damage, which altogether is referred to as the DNA damage response (DDR) (Brandsma & Gent, 2012) (See Figure 1.8 to accompany text that follows). In mammalian cells, repair of DNA lesions such as DSBs are regulated by members of the phosphatidylinositol 3-kinase-related protein kinases (PIKKs) family, including ATM (Ataxia telangiectasia mutated), ATR (Ataxia telangiectasia and Rad3 related), and DNA-PKcs (DNA-dependent protein kinase catalytic subunit) (Shiloh, 2003; Shiotani & Zou, 2009; Shrivastav et al., 2009). While ATM responds to DSBs, ATR activation requires formation of ssDNA at the sites of damage. Both ATM and ATR phosphorylate serine 139 (S139) of histone H2AX, referred to as γH2AX, around the site of damage, which then

serves as a signaling marker to promote the local recruitment of downstream DDR factors (Kinner, Wu, Staudt, & Iliakis, 2008; Kuo & Yang; Rogakou, Pilch, Orr, Ivanova, & Bonner, 1998). ATM, MDC1 (Mediator of DNA damage checkpoint protein 1), the MRN (MRE11-RAD50-NBS1) complex, and the RING finger E3 ubiquitin ligase RNF8 and RNF168 are some of the earliest factors found to be recruited to sites of DNA damage upon DSB induction (Daley & Sung, 2014).

The recruitment of two tumor suppressor proteins, 53BP1 (Tumor suppressor p53-binding protein 1) and BRCA1 (Breast cancer type 1 susceptibility protein) are important regulators to determine the DSB repair pathway choice between non-homologous end enjoining (NHEJ) and homologous-recombination (HR) (See 1.3.2 for details). The antagonistic interplay between 53BP1 and BRCA1 plays a crucial role in the choice of repair pathways. Recruitment and binding of 53BP1 protects DNA broken ends from resection by recruiting RIF1 (RAP1-interacting factor 1) and PTIP (Pax transactivation domain-interacting protein) to DSBs in an ATM-mediated 53BP1 phosphorylation manner in order to compete with BRCA1-mediated HR repair in G1 phase. Conversely, in S/G2 phases when DNA replication has occurred, BRCA1 antagonizes 53BP1-mediated NHEJ repair of DSBs by promoting DNA end-resection, which is crucial for the HR repair process (Callen et al., 2013; Cruz-García, López-Saavedra, & Huertas, 2014; Feng et al., 2015).

It has been demonstrated that TRF2 represses ATM, whereas POT1 prevents activation of ATR (Denchi & de Lange, 2007). Indeed, inappropriate activation of the ATM/ATR signaling pathway at deprotected telomeres has been demonstrated to result in

the formation of DNA damage signals at telomeres, or TIFs, as well as telomere fusions through NHEJ (Denchi & de Lange, 2007). One model suggests that TRF2's interaction with ATM may be a way in which it blocks the activation of ATM at telomeres (Jan Karlseder et al., 2004). Another proposal is that TRF2 is required to maintain the closed t-loop structure of telomeres (Griffith et al., 1999; A. Smogorzewska et al., 2000). The t-loop structure is thought to conceal the ends of telomeres from being recognized as broken DNA ends. Meanwhile, POT1's ability to inhibit the ATR pathway is speculated to be the result of POT1 blocking the binding of RPA (Replication protein A) to single-stranded telomeric DNA. It is suggested that POT1's ability to repress ATR signaling pathway is also dependent on its association with TPP1, which is important for POT1's ability to bind to single-stranded DNA at telomeres (Denchi & de Lange, 2007). In fact, inhibition of TPP1 elicits a DDR at telomeres that is indistinguishable from that of POT1 deletion, indicating a concerted effort for POT1/TPP1 to repress the ATR signaling pathway (Hockemeyer et al., 2007). Accordingly then, the bridging factor, TIN2, which connects POT1/TPP1 to TRF1/TRF2, should also be crucial for repressing DDR at telomeres. Indeed, it has been demonstrated that upon TIN2 depletion, cells exhibit a DDR (Sahn Ho Kim et al., 2004). Taken together, experimental evidence involving analysis of shelterin components and the DDR provides insights into how the deregulation of shelterin at telomeres, or short telomeres can trigger ATM- or ATR-mediated DNA repair at telomeres.

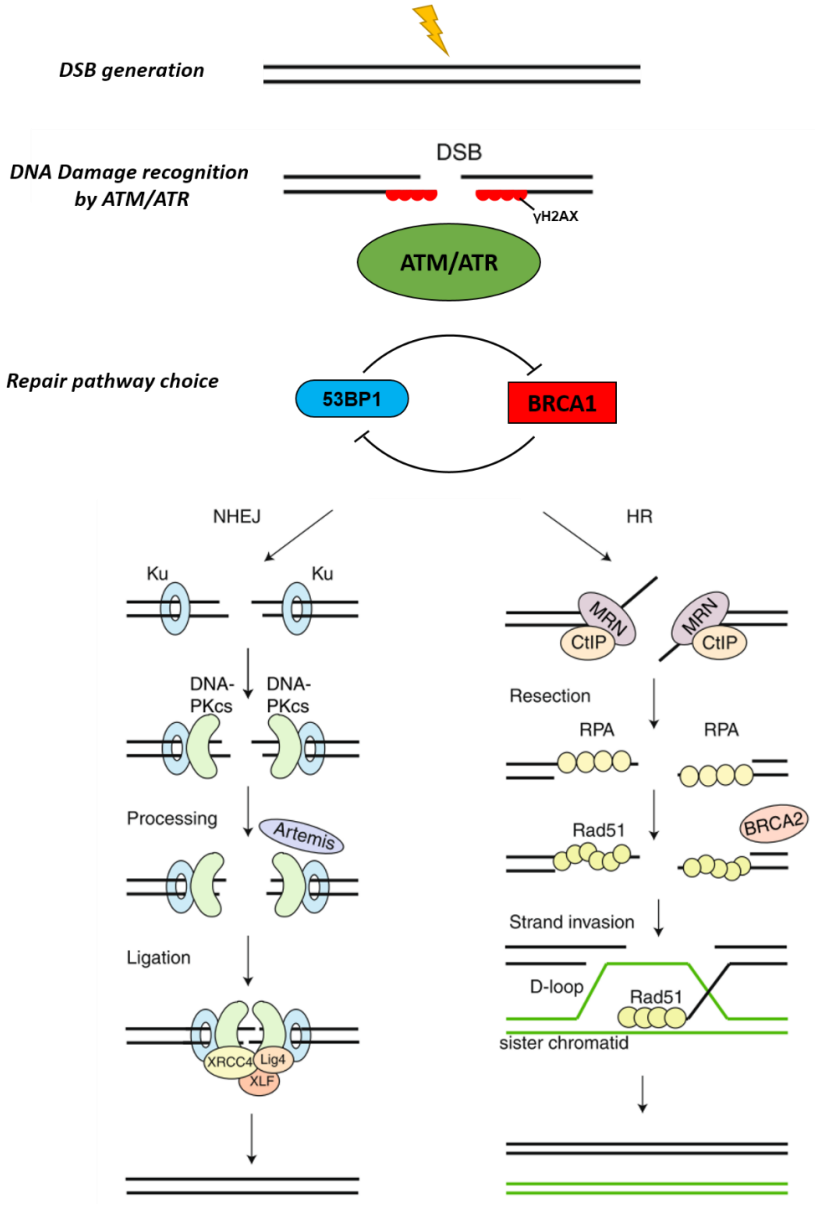

Figure 1.8. The DNA Damage Response. A cartoon diagram of the DNA damage response depicting the events that occur upon a double strand break (DSB) induction. The homologous recombination (HR) and non-homologous end joining (NHEJ) pathways are shown. Refer to text for a description of the pathways shown. Interactions are representations only. Damaged DNA is shown in black and homologous DNA is shown in green (Modified from Brandsma & Gent, 2012).

1.3.2 The DNA double-strand break repair pathways

In eukaryotes, DSBs are repaired by two major pathways: i) NHEJ (Non-homologous end joining) which is active throughout the cell cycle and involves the direct ligation of two broken ends; and ii) HR (Homologous-recombination) which is primarily active during S/G2 phases as it utilizes an undamaged homologous DNA template for the repair of the broken strands (Symington & Gautier, 2011). Thus, the pathway choice for either NHEJ or HR is dependent on cell cycle and also on the structure of the DSB ends (See Figure 1.8 to accompany text that follows).

Compared to HR, NHEJ is a relatively simple DSB repair pathway that involves two broken ends to first be bound by Ku70/Ku80 heterodimer due to its high affinity binding capacity and its high abundance in cells. The binding of the Ku heterodimers not only promotes NHEJ but also protects the DNA ends from nuclease digestion without impeding on the activation of the ATM signaling pathway (Liang & Jasin, 1996). Ku70/Ku80-bound DNA then triggers the recruitment of the DNA dependent protein kinase catalytic subunit, DNA-PKcs, to the damaged site. Together, the kinase activity of the DNA-PK complex becomes active to regulate end-processing and to facilitate the recruitment of a downstream ligation complex (Gottlieb et al., 1993). The nuclease Artermis is then recruited to the DSB site and phosphorylation by DNA-PK activates its 5' to 3' endonuclease activity, which enables a trimming process of DNA ends to create compatible ends for subsequent ligation steps (Lieber, 2010; Riballo et al., 2004). If a gap is formed during resection, a gap-filling process by DNA polymerases (Polμ or Polλ) will occur, after which the recruitment of the ligation complex (DNA ligase IV, XRCC4 (X-ray

cross-complementation group 4), XLF (XRCC4-like factor)) rejoins the DNA ends (Ahnesorg, Smith, & Jackson, 2006; Gottlieb et al., 1993) .

While NHEJ repairs DSB by ligation of broken ends, HR offers an accurate repair of DSB by using a homologous sequence from a sister chromatid as a template in S/G2 phases. Repair by HR begins with the 5' to 3' end resection of the broken ends by CtIP (CtBP-interacting protein) and the MRN (MRE11-RAD50-NBS1) complex generating 3' ssDNA (Xuan Li & Heyer, 2008; Limbo et al., 2007; Sartori et al., 2007; Stracker & Petrini, 2011). The exposed ssDNA tail is then coated by RPA to prevent the formation of secondary structures and to protect the DNA from nuclease. Subsequently, BRCA2 (Breast cancer type 2 susceptibility protein) mediates the displacement of RPA by RAD51 to form a nucleofilament that searches for homologous sequences on the sister chromatid (Pellegrini et al., 2002; Sugiyama, Zaitseva, & Kowalczykowski, 1997). The RAD51 nucleofilament promotes 3' strand invasion from the damaged template into the undamaged template, causing strand displacements of the sister chromatid, and then forming a D-loop structure. DNA synthesis occurs through the action of DNA polymerase δ and the processivity factor PCNA (Proliferating cell nuclear antigen), extending the 3' end of the invading strand using the undamaged DNA strand as a template (Xuan Li, Stith, Burgers, & Heyer, 2009; Sebesta et al., 2013). Repair is then followed by ligation of the DNA ends and resolution of the Holliday junctions, which complete the process, generating either cross-over or non–cross-over products (Maher, Branagan, & Morrical, 2011).

1.4 ALTERNATIVE LENGTHENING OF TELOMERES (ALT) CELLS

1.4.1 Telomere maintenance in telomerase-negative cells

While the majority (85-95%) of cancer cells use a telomerase-dependent mechanism to maintain their telomeres, up to 15% of human cancers maintain their telomeres through a telomerase-independent mechanism known as alternative lengthening of telomeres (ALT) (Bryan, Marusic, Bacchetti, Namba, & Reddel, 1997; Cesare & Reddel, 2010). Beyond DSB repair, HR has also been implicated to play a role in ALT cells. It is hypothesized that ALT cells use a homologous recombination (HR) dependent exchange and/or HR dependent synthesis to maintain telomere length (Dunham, Neumann, Fasching, & Reddel, 2000). Several models of how telomeres of ALT cells can become lengthened have been proposed: i) inter-molecular copying of telomeric DNA between homologous chromosomes (Figure 1.9) (Bailey, Brenneman, & Goodwin, 2004; Dunham et al., 2000); ii) intra-molecular telomeric DNA replication by copying its own sequence (Figure 1.10) (Muntoni, Neumann, Hills, & Reddel, 2009); iii) rolling circle amplification of linear or circular extrachromosomal TTAGGG DNA fragments found in ALT cells (Figure 1.11) (Henson, Neumann, Yeager, & Reddel, 2002; Natarajan & McEachern, 2002); and iv) the use of free DNA ends generated at damage repair sites or from collapsed replication forks within telomeric DNA (O'Sullivan & Almouzni, 2014). All four models of HR-mediated telomere elongation involve telomeric strand invasion of telomeric 3' overhangs, followed by the DNA synthesis of TTAGGG repeats or some variant telomeric repeats of a telomere sequence template, which in the end yield a net gain in telomere length (Bailey et al., 2004; Dunham et al., 2000; Henson et al., 2002).

In the inter-molecular replication model (Figure 1.9), HR-mediated telomeric replication can occur in two ways: i) copying of the TTAGGG repeats in the telomeric region of a chromosome or ii) copying of the variant telomeric repeats in the subtelomeric region of a chromosome. In the intra-molecular telomeric DNA replication model (Figure 1.10), ALT cells constructed to contain telomere tags display successful amplification of a telomere tag in the absence of other telomeres. These findings suggest that in addition to copying telomeric DNA of another chromosome, ALT telomeres can be lengthened by intra-telomeric DNA copying (Muntoni et al., 2009). In the extrachromosomal replication model (Figure 1.11), it is posited that the 3' telomeric overhang of a chromosome invades a circle of ECTR DNA, and then replicates via a rolling circle method. Similarly, telomere elongation may also occur between telomeres and linear or circular ECTR DNA by HR or by end-joining (Henson et al., 2002). Similar to telomerase-positive cells, telomeres in ALT cells are arranged into t-loops. In addition, the nuclei of ALT cells also contain high amounts of free DNA circles containing double-stranded telomeric repeats, referred to as t-circles. It is suggested that the t-circles are produced as a result of cleavage and resolution of t-loops at chromosome ends. Due to the low abundance of t-circles in telomerase-positive cells, it is believed that the presence of t-circles serves as a marker of ALT status in cells (Cesare & Griffith, 2004; Fasching, Neumann, Muntoni, Yeager, & Reddel, 2007; R. C. Wang, Smogorzewska, & de Lange, 2004). It has also been suggested that t-circles can serve as templates for telomere elongation in a rolling-circle mechanism (RCM) (Figure 1.11). Another form of ECTR DNA in ALT cells is partially single-stranded telomeric $(CCCTAA)_n$ DNA circles, or c-circles (Henson et al., 2009). It has been

suggested that c-circles are one of the most reliable marker for ALT cells, as they are unique and their levels tend to correlate with the level of ALT activity in cells (Henson et al., 2009). Like t-circles, c-circles are also believed to serve as DNA templates for telomere elongation by RCM, which has been demonstrated to be an effective method of amplifying telomeric DNA *in-vitro* (Henson et al., 2009), providing further support for the role of ECTR DNA in supporting ALT telomere lengthening.

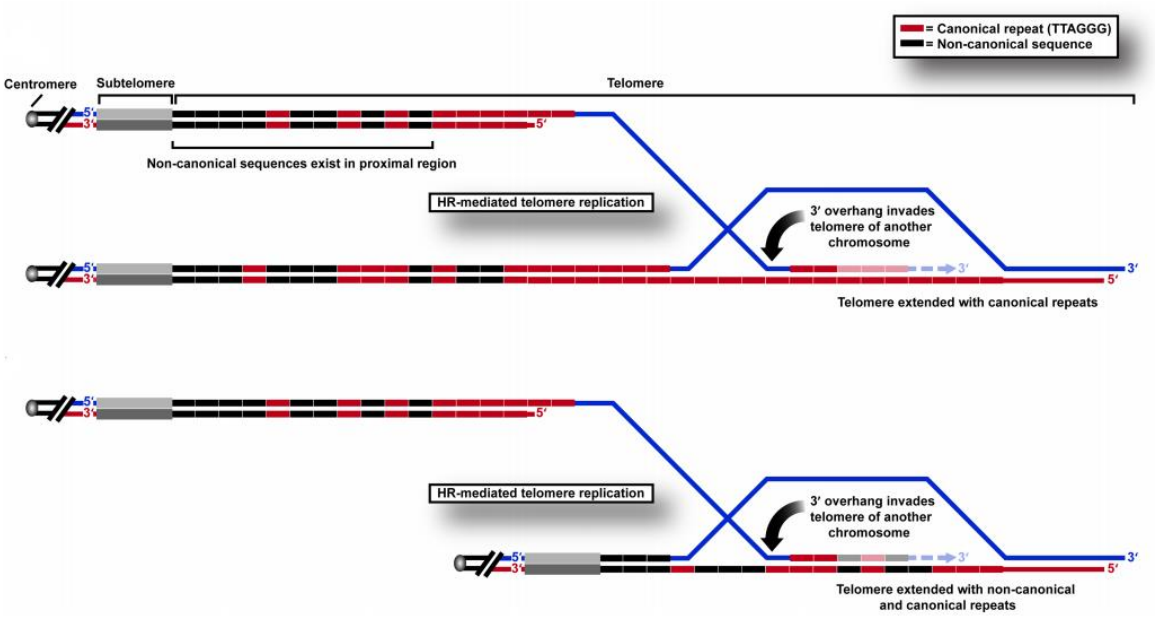

Figure 1.9. Homologous-recombination (HR) mediated telomeric replication in ALT cells. HR-mediated telomeric replication of canonical repeats in telomeric region (top). HR-mediated telomeric replication of variant repeats in telomeric region (bottom). (Taken from Conomos, Pickett, & Reddel, 2013)

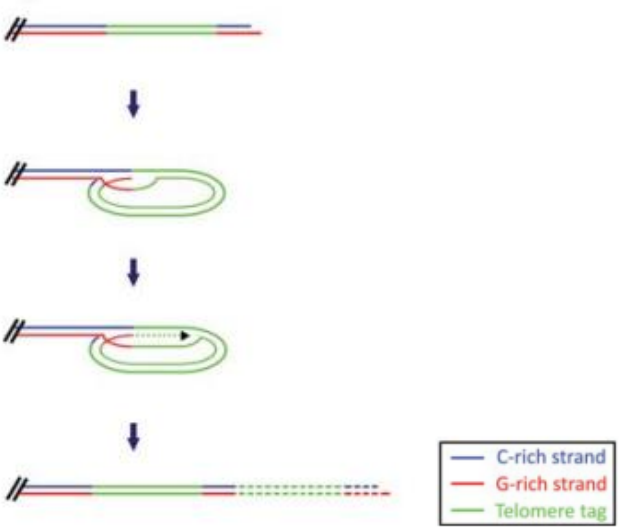

Figure 1.10. Proposed mechanism of intra-molecular telomere replication. Tagged telomere (green) folds back and forms a loop structure via strand invasion. If the loop configuration primes new DNA synthesis, this results in duplication of the telomere tag. (Taken from Muntoni, Neumann, Hills, & Reddel, 2009)

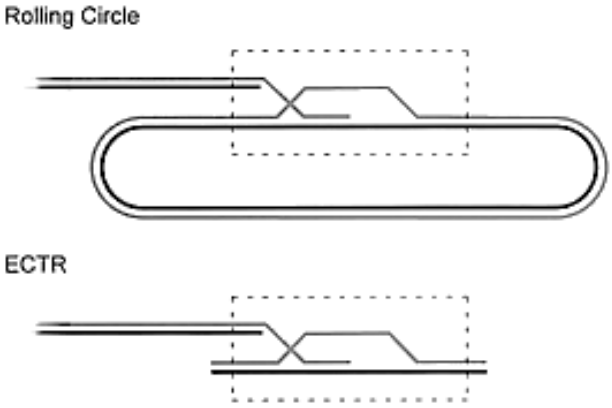

Figure 1.11. Proposed mechanism of telomere replication involving extrachromosomal telomeric repeat (ECTR) DNA. Telomere replication involving: circular ECTR DNA via rolling circle method (top) or linear ECTR DNA via strand invasion (bottom). (Taken from Henson, Neumann, Yeager, & Reddel, 2002)

1.4.2 Molecular hallmarks of ALT Cells

Although the exact mechanism by which ALT cells elongate their telomeres is not fully understood, cells that utilize ALT display several other unique features in addition to ECTRA DNA. As a result of their telomerase-independent telomere maintenance, a key feature of ALT cells is telomere length heterogeneity. Unlike primary and telomerase-positive cells in which telomeres either progressively shorten or remain at relatively fixed lengths, respectively, in ALT cells, pulsed field gel electrophoresis and southern blotting revealed that telomeric DNA can range from 2kb to 50kb in length, with an average of about 20kb (Bryan, Englezou, Gupta, Bacchetti, & Reddel, 1995; O'Sullivan & Almouzni, 2014). In support, quantitative fluorescent in-situ hybridization (q-FISH) using telomere-specific probes in metaphase ALT cells also confirms telomere length heterogeneity. Telomere signals observed by FISH in ALT cells are highly variable from no discernable signals to very large signals at chromosome ends in metaphase spreads (Figure 1.12) (Henson et al., 2002).

Consistent with the proposed mechanism of telomeric recombination activity in ALT cells, FISH or chromosome-orientation FISH (CO-FISH) analysis of metaphase spreads reveals that telomere-sister chromatid exchange (T-SCE) events are frequently observed in ALT cells (Bailey et al., 2004; Londoño-vallejo, Der-sarkissian, Cazes, & London, 2004; O'Sullivan et al., 2014). An interesting consequence of T-SCEs is that these events could result in the unequal exchange of telomeres. Since telomeres contain repetitive DNA sequences, the search for homologous sequences can occur anywhere along the telomeric region. Thus, an unequal exchange would cause one sister telomere to grow

longer at the expense of the other. In this scenario, the "winning" cell of the exchange process would maintain longer telomeres and thus proliferate to escape senescence (Bailey et al., 2004). To this end, the "losing" cells with short telomeres may eventually reach the Hayflick limit and senesce or die (Blagoev, Goodwin, & Bailey, 2010; Hemann, Strong, Hao, & Greider, 2001).

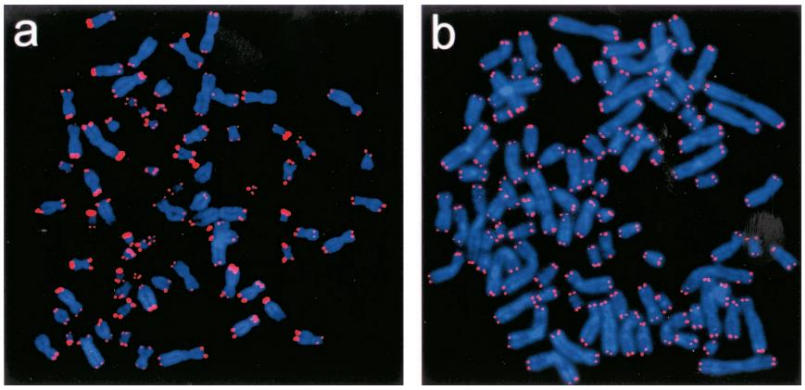

Figure 1.12. Visualizations of telomere by FISH. A) ALT cells display highly variable telomere signals when compared to **B)** telomerase-positive cells. (Taken from Henson et al., 2002)

Another unique marker of ALT status in a cell is the presence of ALT-associated promyelocytic leukemia (PML) bodies (APBs). APBs are defined as large donut-shaped nuclear bodies containing PML protein, telomeric DNA, and shelterin proteins clustered together (Yeager et al., 1999). Under fluorescence microscopy, APBs appear as large foci in which telomeric DNA is embedded within a larger PML focus (Lang et al., 2010) (Figure 1.13). High-resolution two-color laser scanning 4Pi-miscroscopy technique has revealed that the main structural components of PML nuclear bodies (PML-NBs) are the PML and SP100 proteins (Lang et al., 2010). Together PML and SP100 assemble into a shell-like structure ranging in size from 0.25 to 1µm in diameter, with PML protein forming an

envelope-like outer layer at a thickness of about 50 to 100nm (Lang et al., 2010). Both PML and SP100 can be post-translationally modified by small ubiquitin-related modifier (SUMO), and contain SUMO interacting motifs (SIM) (Chung, Leonhardt, & Rippe, 2011; Hecker, Rabiller, Haglund, Bayer, & Dikic, 2006). PML-NBs are involved in a myriad of cellular functions including transcription, apoptosis, senescence, response to DNA-damage, and stress response against micro-organisms in cells. While the exact mechanisms by which PML-NBs achieve these cellular processes is not fully understood, it is believed that PML acts as a molecular scaffold to recruit and concentrate the necessary factors in the form of a nuclear body. To this end, it is proposed that PML-NBs serve as functional reaction hubs to enable post-translational modifications of proteins, yielding activation, sequestration, or degradation of protein factors, which are all important regulatory activities for biological processes (Lallemand-Breitenbach & de The, 2010).

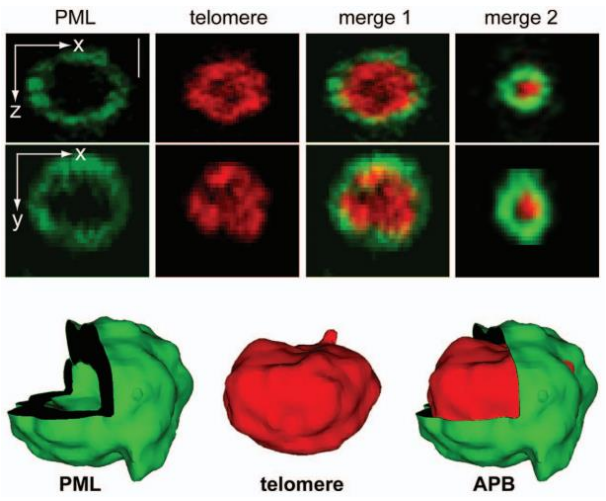

Figure 1.13. High-resolution two-color 4Pi-miscroscopy image of an APB. The PML body is shown in green, and the telomeric repeat sequence, which is hybridized to a telomere-specific peptide nucleic acid (PNA) probe, in red. The corresponding merged images (merge 1 and 2) and

the 3D image reconstruction (bottom) reveal that PML protein forms a spherical shell around telomeric DNA. Axes orientation are indicated in the PML images. (Taken from Lang et al., 2010)

In ALT cells, APBs are enriched during S/G2 phase of the cell cycle when HR activity and DNA synthesis are most active in a cell (G Wu, Lee, & Chen, 2000)(Grobelny et al., 2000), suggesting for a temporal and spatial regulation of APBs. Consistent with this view, it has been reported that during mitosis, PML proteins are found to undergo de-SUMOylation, leading to the subsequent disassembly of PML-NBs (Everett, Lomonte, Sternsdorf, van Driel, & Orr, 1999). Accordingly, in interphase, PML becomes SUMOylated and can mediate nucleation of nearby SUMOylated PML molecules to form PML-NBs through non-covalent binding of SIMs, which then elicit the recruitment of other SUMOylated proteins and/or SIM-containing proteins to the PML NBs (T. H. Shen, Lin, Scaglioni, Yung, & Pandolfi, 2006). Thus, APBs are not present in mitotic cells and are only visible from early G1 to late G2 phase (Draskovic et al., 2009). To this end, a proposed model (Figure 1.14) for APB assembly in ALT cells suggests that SUMOylation of telomeric proteins by SUMO E3 ligase MMS21 triggers the accumulation of the structural scaffold proteins PML and SP100 at telomeres via SUMO-SIM-interactions with TRF1 and TRF2 (Potts & Yu, 2007). Subsequently, nucleation events of SUMOylated factors trigger a feedback mechanism leading to additional recruitment of PML and SP100 through SUMO-SIM-interactions. The assembly of an APB is then completed with the recruitment of DNA repair factors and recombination factors such as the MRN complex, Rad17/9-1-1 (hRad9-hRad1-hHus1) complex, RAD51, RPA2, and BRCA1 (Chung et al., 2011; Draskovic et al., 2009; Nabetani, Yokoyama, & Ishikawa, 2004; Guikai Wu, Jiang, Lee, &

Chen, 2003; Z.-H. Zhong et al., 2007). Consistent with the model, functional data involving APBs suggest that telomere extension occurs in a DNA repair process manner involving non-replicative DNA synthesis, as evidenced by detection of BrdU incorporation, the presence of DSB repair marker γH2AX, and by an increase in telomeric DNA signals at APBs (Chung et al., 2011). Upon completion of telomere elongation, it is believed that APBs are disassembled by dissociation from telomeres through de-sumoylation of PML (Brouwer et al., 2009). Collectively, these results suggest that APBs serve a functional role in regulating telomere lengthening in ALT cells, and that telomeric elongations occurs at APBs.

In support of the functional role of APBs, it has been demonstrated that association of NBS1 with APBs is necessary for the downstream recruitment of RAD50, MRE11, and BRCA1, but not TRF1 or RAD51, to APBs. In addition to impaired localization of various factors at APBs, deletion of the N-terminal BRCT domain of NBS1, but not the CR2 MRE11/RAD50 interacting domain, abolished NBS1's association with APBs, indicating that NBS1's association with APBs is independent of association with MRE11/RAD50 (Guikai Wu et al., 2003). These results suggest that NBS1 and the MRN complex are important for the formation of APBs, perhaps by promoting DNA synthesis at APBs. It has also been observed that the DNA repair factors Rad17 and the 9-1-1 complex are constitutive components of APBs, which are also found to colocalize with γH2AX, NBS1, and telomeric DNA at APBs (Nabetani et al., 2004). In addition, upon treatment with caffeine, an ATM/ATR inhibitor, the percentage of APB-positive cells with BrdU/hRad9/telomeric foci was markedly reduced (Nabetani et al., 2004). Taken together,

these experimental evidence suggests that telomeric DNAs at APBs may be recognized and processed as DSBs, which can lead to telomeric DNA synthesis and thereby contributing to telomere maintenance in ALT cells.

Although many studies suggest that APBs are sites of active DNA synthesis and therefore promoting ALT activity, a direct causality between APBs and telomere maintenance in ALT cells cannot be definitely drawn. Many experimental evidence suggest that APBs could actively promote telomere elongation by promoting telomere clustering, or by recruiting proteins necessary for DNA elongation and recombination (Cesare & Griffith, 2004; Draskovic et al., 2009; Fasching et al., 2007; Molenaar et al., 2003; Tokutake et al., 1998). However, it has also been suggested that APBs could function as a sequestering complex for ECTRs, which could otherwise be recognized as damaged DNA and activate a DDR leading to senescence (Fasching et al., 2007). Therefore, it may also be the case that APBs function indirectly in the ALT pathway as a protective factor to promote cell proliferation. Furthermore, despite being a prominent marker for ALT status in cells, ALT-positive cell lines lacking APBs but still exhibiting telomere length heterogeneity have been identified (Cerone, Autexier, Londoño-Vallejo, & Bacchetti, 2005; Fasching, Bower, & Reddel, 2005). Thus, whether APBs have a direct or indirect involvement in the ALT mechanism of telomere maintenance and telomere elongation is still an ongoing investigation.

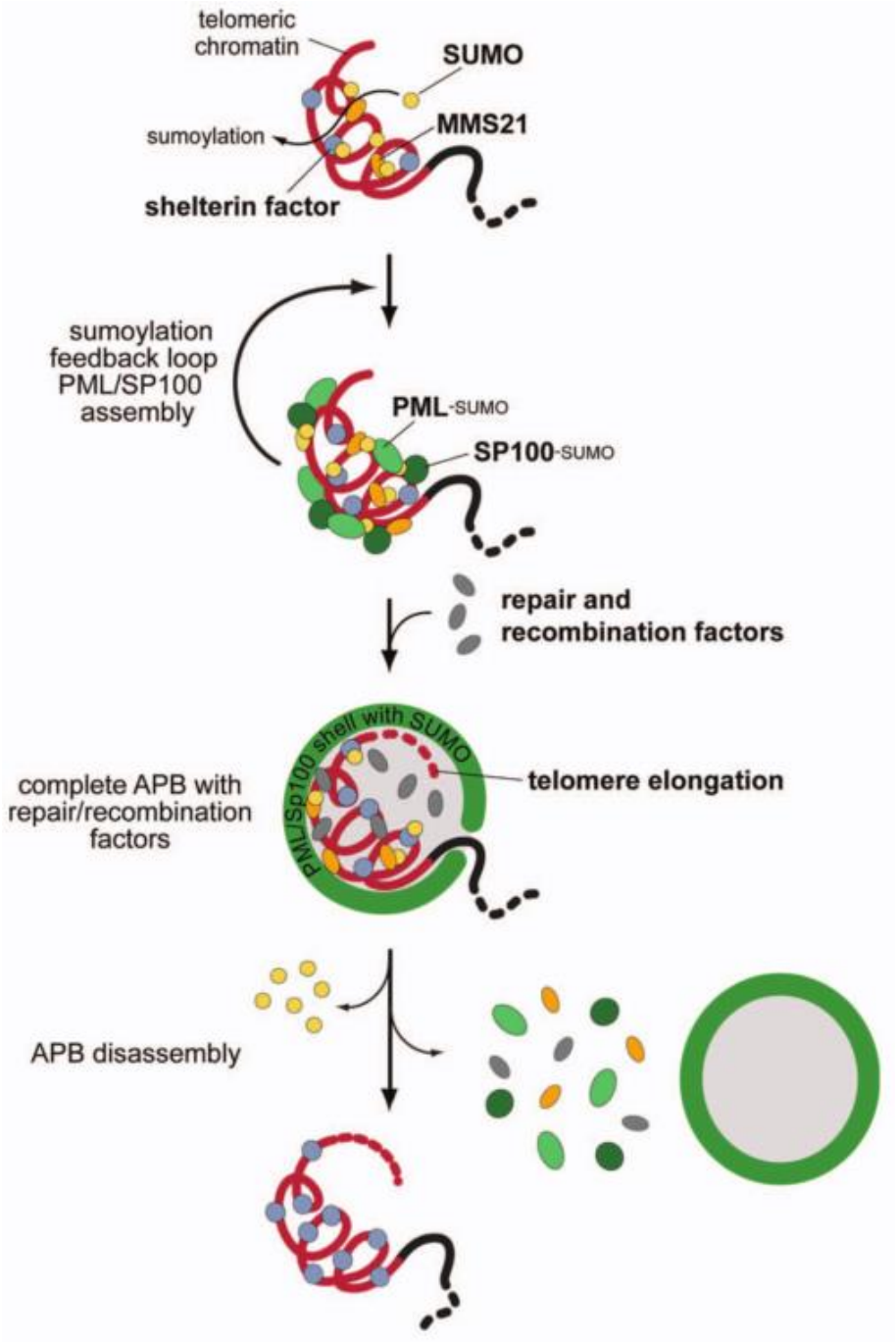

Figure 1.14. A model for APB assembly in ALT cells. See text for details. (Taken from Chung, Osterwald, Deeg, & Rippe, 2012)

1.4.3 Chromatin landscape of telomeres is important for ALT activity

In telomerase-positive cells, due to the enrichment of H3K9m3, H4K20me3, and low levels of histone acetylation, telomeres are often regarded as heterochromatic structures. The enrichment of trimethylation on lysines 9 and 20 of histone 3 and 4, respectively, also promotes the association of heterochromatin protein 1 (HP1) to telomeric chromatin, which is correlated with greater telomere lengths in human cells (Arnoult, Van Beneden, & Decottignies, 2012; Benetti, García-Cao, & Blasco, 2007). In addition, subtelomeric regions in telomerase-positive cells also show denser methylation than normal cells (Galati, Micheli, & Cacchione, 2013; Ng, Cropley, Pickett, Reddel, & Suter, 2009). Cells with heavily methylated subtelomeric regions also exhibit reduced transcription of the telomeric repeat-containing-RNA (TERRA). These observations are also consistent with notion that TERRA inhibits telomerase activity, which of course is crucial for facilitating telomerase activity at telomeres in telomerase-positive cells (Redon, Reichenbach, & Lingner, 2010; C. Wang, Zhao, & Lu, 2015). Conversely, the chromatin landscape and correlation of greater telomere length and increased heterochromatization of telomeres appear to be deregulated in ALT cells. It has been reported that in ALT human cell lines, chromatin compaction at ALT telomeres is reduced and is associated with a global decrease in telomeric H3K9me3 markers. The observed reduction in heterochromatin state also resulted in an upregulation of TERRA transcription (Episkopou et al., 2014). In contrast, overexpression of hTERT and hTR in ALT cells resulted in elongation of short telomeres, an increase in H3K9me3 density, as well as reduction in TERRA transcription (Episkopou et al., 2014). These results are also in agreement with

findings in mouse cells, in which deficiency in DNA methyltransferases display increased telomeric recombination, as evidenced by elevated rates of T-SCE events and the presence of APBs, which are all hallmarks of ALT (Gonzalo et al., 2006). Interestingly, inhibition of histone deacetylases (HDACs) by trichostatin A (TSA) in human ALT cells also resulted in an increase in APBs and T-SCE events (Jung et al., 2013). Taken together, these results suggest that ALT telomeres with a more relaxed and accessible chromatin structure and reduced nucleosome density may be preferentially recruited to APBs, which may then facilitate telomeric recombination.

In addition to the canonical TTAGGG telomeric repeats, ALT telomeres have also been reported to contain variant TCAGGG and TGAGGG telomeric repeats (Conomos et al., 2012; M. Lee et al., 2014). It has been demonstrated that TRF2 has reduced affinity for these variant telomeric sequences in ALT cells. To this end, TRF2's function in chromosome end protection and telomere length regulation is likely compromised in ALT cells, which would provide partial explanation to the atypical chromatin configuration of ALT telomeres (Conomos et al., 2012). Interestingly, the TCAGGG variant sequences provide a high affinity platform for the binding of orphan nuclear receptor proteins such as COUP-TF2 (also referred to as NR2F2) and TR2, which recruit the nucleosome remodeling deaceteylase complex, NuRD-ZNF827, resulting in decreased shelterin binding, hypoacetylation of telomeric chromatin, and recruitment of HR proteins (Conomos et al., 2012; Conomos, Reddel, & Pickett, 2014). It is proposed that the recruitment of NuRD-ZNF827 complex to telomeres promotes ALT activity by remodeling the chromatin landscape and creates a relaxed environment to support telomere-telomere recombination

events, which is a mechanistic element of ALT activity (Conomos et al., 2014). Along the lines of histone modification, the histone chaperone anti-silencing factor 1 (ASF1), which is important for DNA unwinding and replication fork progression (Groth et al., 2007), has also been implicated in ALT activity. Upon co-depletion of the ASF1a and ASF1b paralogs in telomerase-positive cells, an induction of ALT was observed, as evidenced by the upregulation of APBs, ECTR DNA, and T-SCE events (O'Sullivan et al., 2014). Consistent with the notion that changes in chromatin organization is important for the regulation of ALT, it has been reported that TIP60-dependent acetylation on histone 4 impairs the binding of 53BP1 to H4K20m3, leading to the promotion of HR repair of DSB (Tang et al., 2013). This is reminiscent of observations in ALT whereby disruption in heterochromatin and histone acetylation landscape can predispose ALT telomeres to an HR-based mechanisms for telomere lengthening. Taken together, these results further suggest that the deregulated chromatin state of ALT telomeres may be an underlying factor that give rise to the HR-based mechanism of telomere length maintenance in ALT cells.

1.4.4 Dysfunctional chromatin promotes ALT activity

ALT cells are often characterized by elevated levels of genome instability, as evidenced by complex karyotype arrangements, extensive micronucleation, and impaired DNA repair capacity (Lovejoy et al., 2012). In ALT cells, colocalization of telomeric DNA, DNA damage markers, and DNA damage repair factors are often visualized under fluorescence microscopy as foci, which are also present in APBs (Cesare et al., 2009; Jiang, Zhong, Henson, & Reddel, 2007). DNA damage inducing agents can also promote the formation ECTR DNA and increase the proportion of cells containing APBs (Fasching et

al., 2007). A form of DNA damage that can arise in ALT cells is R-loop-induced DNA damage as a result of TERRA transcription at telomeres. It is proposed that R-loops can trigger the formation of H3S10P mark, which in turn could cause replication fork stalling, transcription–replication collisions, and, ultimately the generation of DSBs in the newly synthesized DNA at telomeres (Castellano-Pozo et al., 2013). Furthermore, it has also been reported that R-loops can be actively processed into DSBs by the transcription-coupled nucleotide excision repair (TC-NER) pathway (Sollier et al., 2014). Accordingly, accumulation of TERRA at ALT telomeres can cause excessive chromatin decondensation, leading to stalling of the transcriptional machinery at telomeres, and result in R-loop-induced DNA damage (Arora et al., 2014). In support of the notion that R-loop processing can serve as a source of DNA damage to induce HR activity, a recent study proposes a model in which transcription-associated DNA damage, perhaps arising from the processing of RNA–DNA hybrids at telomeres, could trigger TRF1 recruitment to APBs to facilitate ALT activity (Wilson, Ho, Walker, & Zhu, 2016). Indeed, reduction of TERRA and R-loops have been shown to diminish rates of recombination-mediated telomere elongation in ALT cells (Arora et al., 2014; Balk et al., 2013; Griffith et al., 1999; Skourti-Stathaki & Proudfoot, 2014). Moreover, TERRA has also been implicated to function in the negative regulation of telomerase activity, which would be consistent with the notion of telomerase-independent telomere elongation in the ALT pathway (Redon et al., 2010). Collectively, the underlying mechanism of the ALT pathway appears to be an intricate network involving chromatin dysfunction, changes in heterochromatic states, and histone

modifications, which ultimately contributes to the recombination-mediated telomere elongation model of ALT.

1.5 TRF1 FUNCTIONS AND POST-TRANSLATIONAL MODIFICATIONS

1.5.1 The functional role of TRF1 in genome integrity

As part of the shelterin complex, the role TRF1 in telomere biology has been well characterized and this includes telomere protection and telomere length regulation, both of which are important for genome integrity (Muñoz et al., 2009; Palm & de Lange, 2008; van Steensel & de Lange, 1997). TRF1 is known to be important for efficient DNA replication at telomeres, and that loss of TRF1 causes increased telomere fragility and activates DNA damage responses at telomeres (Sfeir et al., 2009). In addition, cell cycle regulation studies of TRF1 has revealed that the levels of Pin2, the highly expressed isoform of TRF1, are tightly regulated during the cell cycle, being the highest in G2/M phase in cells. Moreover, overexpression of Pin2 in HeLa cells resulted in an accumulation of cells in G2/M phase (M. Shen et al., 1997). These results suggest a potential role of TRF1 in mitosis, perhaps by acting as a bridging factor in mitotic control to telomere regulatory machinery. Consistent with this view, the loss of TRF1 in cells have been shown to compromise sister centromere cohesion, resulting in the induction of merotelic kinetochore attachments, lagging chromosomes, and micronuclei, which are all consequences of impaired mitotic progression (Ohishi et al., 2010; Ohishi, Muramatsu, Yoshida, & Seimiya, 2014). In addition, depletion of TRF1 in mouse embryonic fibroblasts (MEFs) also result in rapid induction of senescence, which is associated with abundant

telomeric γH2AX foci and the upregulation of the ATM/ATR damage signaling pathways. Furthermore, it has been reported that depletion of TRF1 in both MEFs and human foreskin fibroblasts results in telomere abnormalities such as doublets and broken telomere signals, or complete loss of telomere signals on metaphase chromosomes (Martínez et al., 2009). Taken together, these results highlight the importance of TRF1 in telomere protection and the maintenance of genomic integrity, as well as the functional involvement beyond telomere length maintenance.

1.5.2 Phosphorylation of TRF1

The activity of TRF1 in a cell is highly regulated by post-translational modifications, including phosphorylation, ubiquitination, SUMOylation, and PARsylation (Walker & Zhu, 2012). TRF1 contains multiple serine and threonine phosphorylation, which can be targeted by various kinases to elicit a variety of cellular functions. A number of threonine and serine phosphorylation sites have been characterized for regulating TRF1 function in cells. Several threonine sites in TRF1 have been identified to match the consensus sequence of cyclin dependent kinases (CDKs) of S/T*-P (Serine/Threonine-Proline; asterisk indicates the site of phosphorylation) (Holt et al., 2009), including T149. Phosphorylation of TRF1 at T149 has been reported to mediate its association with Pin1 during mitosis, but this interaction was abrogated following CDK inhibition or upon disruption of the T-P motif following a T149A point mutation on TRF1 (T. H. Lee et al., 2009). Functionally, it has been suggested that Pin1 regulates telomere maintenance in a TRF1-dependent mechanism, by which knockout of Pin1 in mice resulted in elevated levels of TRF1, leading to rapid telomere loss and premature aging phenotypes (T. H. Lee et al.,

2009). These results suggest that CDK-dependent phosphorylation of TRF1 on T149 is important for Pin1's regulation on TRF1 stability and telomere length control.

In addition, T344 and T371 have been shown to be phosphorylated by Cdk1 *in-vitro* (Z.-Q. Wu, Yang, Weber, & Liu, 2008). *In-vitro* analysis indicates that phosphorylation of T344 and T371 by Cdk1 is an important priming step to promote the recruitment of Pololike kinase 1 (Plk1) to TRF1, which is believed to elicit subsequent phosphorylation of S435 on TRF1 *in-vivo*. To this end, it has been shown that TRF1 phosphorylation at S435 is important for increased telomeric association by TRF1 (Z.-Q. Wu et al., 2008). Taken together, *in-vitro* and *in-vivo* data suggest that phosphorylation of T344 and T371 may serve as a priming step to allow the binding of Plk1 to TRF1, which subsequently regulate TRF1's telomeric DNA binding activity, and thus modulate telomere length (Z.-Q. Wu et al., 2008). Interestingly, a recent study involving the phosphorylation of T371 by Cdk1 *in-vivo* argues against the proposed model that phosphorylation of T371 by Cdk1 primes TRF1 for Plk1's interaction to promote increased TRF1's binding with telomeric DNA (McKerlie & Zhu, 2011). Indeed, when TRF1 is phosphorylated at T371 by Cdk1, TRF1 becomes free of telomere association, creating a pool of unbound-TRF1 referred to as (pT371)TRF1. While dissociation of TRF1 from telomeres has been reported to result in the ubiquitination and degradation of TRF1 (Chang, 2003), T371 phosphorylation also appears to protect this unbound pool of TRF1 from being targeted for degradation (McKerlie & Zhu, 2011). Moreover, *in-vitro* analysis was unable to detect TRF1 phosphorylation at T371 by Plk1 (McKerlie & Zhu, 2011) . Taken together, these results argues against the notion that Cdk1 phosphorylation of T371 primes TRF1 for

phosphorylation by Plk1, which instead actually promotes the dissociation of TRF1 from telomeric DNA (McKerlie & Zhu, 2011; Z.-Q. Wu et al., 2008). In addition, when a TRF1 phosphothreonine-mimicking mutant (i.e. T371D) is overexpressed in cells, chromosomal abnormalities including sister telomere fusions, anaphase bridges, and lagging chromosomes are observed, which are all phenotypes of deregulated mitotic progression (McKerlie & Zhu, 2011). On the other hand, overexpression of a TRF1 non-phosphorylatable alanine mutant (i.e. T371A) results in a complete blockage of sister telomere resolution (McKerlie & Zhu, 2011). Collectively, these results suggest that Cdk1 phosphorylation on T371 of TRF1 is also important to facilitate telomere de-protection that is essential for sister telomere resolution, which may further imply a role for TRF1 in regulating cell cycle progression through mitosis.

Protein kinase B, also known as Akt, is another Serine/Threonine kinase, which requires a phosphorylation motif of RXRXX-S/T* (R-arginine, X-any amino acid; asterisk indicates the site of phosphorylation). Akt has been reported to play a key role in various cellular processes including glucose metabolism, apoptosis, cell proliferation, transcription, and cell migration, all of which are pertinent to genomic instability and tumorigenesis (Luo, Manning, & Cantley, 2003; Testa & Bellacosa, 2001). Results from *in-vitro* Akt kinase assays have demonstrated that Akt phosphorylates TRF1 on T273 (Y.-C. Chen, Teng, & Wu, 2009). Further functional analysis have also shown that overexpression of Akt in cells induced telomere shortening. These findings implicate that Akt interacts with TRF1, and perhaps via phosphorylation of TRF1 at T273, to cause telomere shortening *in-vivo* (Y.-C. Chen et al., 2009). Nevertheless, a clear mechanistic

pathway has yet to be established to fully substantiate the functional relevance of TRF1 phosphorylation on T273 *in-vivo.* Another phosphorylation site that has been implicated to regulate TRF1's control in telomere length is T122, which has been mapped to be the target site of Casein kinase 2 (CK2) (M. K. Kim et al., 2008). It has been shown that phosphorylation of TRF1 at T122 by CK2 enhances the telomere binding ability of TRF1 (M. K. Kim et al., 2008). Furthermore, inhibition of CK2 led to the ubiquitination and degradation of TRF1 (M. K. Kim et al., 2008). A lack of phosphorylation at T122 on TRF1 also led to reduced dimerization of TRF1, and this was correlated with an increase in telomere length. Taken together, these observations indicate that phosphorylation of T122 may negatively regulates telomere length by enhancing the ability of TRF1 to bind telomeric DNA (M. K. Kim et al., 2008). Consistent with the notion that phosphorylation can regulate telomeric association of TRF1, it has been suggested that upon phosphorylation on S367 by ATM, TRF1 becomes free of telomere and may be targeted to nuclear proteolytic sites for degradation (McKerlie et al., 2012). A closer analysis on protein half-life also revealed that a non-phosphorylatable S367A TRF1 mutant was much more stable compared to wild type or a phosphoserine-mimicking S367D mutant (McKerlie et al., 2012). Functionally, expression of the phosphoserine-mimicking mutant (i.e. S367D) was unable to suppress telomerase-dependent telomere elongation following TRF1-depletion, nor the formation of dysfunctional telomeres (McKerlie et al., 2012). Collectively, these results suggest that TRF1 phosphorylation on S367 is crucial for the regulation of telomere length and telomere stability.

Phosphorylation has been reported to regulate TRF1 activity in DNA damage response. Ataxia telangiectasia mutated (ATM) kinase, which requires a minimal sequence of a S/T*-Q (Serine/Threonine-Glutamine; asterisk indicates the site of phosphorylation) motif (S.-T. Kim, Lim, Canman, & Kastan, 1999), has been reported to phosphorylate S219 of Pin2, the major isoform of TRF1, following ionizing DNA damage. Mutational experiment involving substitution of S219 with either non-phosphorylatable alanine or phosphomimic glutamic acid/aspartic acid was used to address the biological significance of this site (Kishi et al., 2001). Phosphoserine-mimicking mutants of S219 completely abolished the ability of Pin2 to induce mitotic entry and apoptosis. Cells expressing the phosphoserine-mimicking mutants also exhibited reduced radiation hypersensitivity (Kishi et al., 2001). These results provide evidence to suggest that upon DSBs, ATM phosphorylates Pin2/TRF1 on S219 to regulate cell cycle progression and DDR by preventing cells entering mitosis and apoptosis after DNA damage (Kishi et al., 2001). Consistent with this view, it has been shown that the inhibition of Pin2/TRF1 in AT (Ataxia telangiectasia) cells was able to promote telomere elongation, restore G2/M checkpoints, and promote cell proliferation after ionizing radiation (Kishi & Lu, 2002). TRF1 phosphorylation of T371 has been reported to be involved in the DNA damage response (McKerlie, Walker, Mitchell, Wilson, & Zhu, 2013). Upon IR treatment, (pT371)TRF1 is found to preferentially associate with damaged chromatin, as evidenced by colocalization with the DSB damage markers 53BP1 and γH2AX (McKerlie et al., 2013). Moreover, DNA recombinational repair assays showed that T371 phosphorylation is essential to promote HR activity (McKerlie et al., 2013). Consistent with (pT371)TRF1's role in HR

activity, IR-induced (pT371)TRF1's localization to sites of DNA damage were markedly increased following a knockdown in the NHEJ-promoting factors 53BP1 and Rif1, but impaired upon depletion of the HR-promoting factor BRCA1 (Chapman et al., 2013; McKerlie et al., 2013). Taken together, these results suggest that (pT371)TRF1 facilitates DSB repair by promoting HR at sites of damage (McKerlie et al., 2013). Collectively, experimental evidence have demonstrated a critical role for TRF1 in the ATM-dependent regulation of DNA damage response.

1.5.3 The role of TRF1 in ALT activity

It is clear that post-translational modifications, such as phosphorylation, are important for controlling TRF1's function as a telomere length regulator, and this is also the case in ALT cells. As described earlier in this chapter (See section 1.3.2), TRF1 has been shown to become sumoylated and sumoylation has been implicated to regulate telomere maintenance in telomerase-negative cells, or the ALT pathway (Potts & Yu, 2007). Furthermore, it has been demonstrated that TRF1 is found to be localized to APBs in ALT cells, predominately in S/G2 phases, in which it also associates with telomeric DNA and DNA repair factors involved in HR such as NBS1 and BRCA1 (Chung et al., 2011, 2012; G Wu et al., 2000). Although the presence of the APBs is an indirect marker for ALT activity in cells, a clear role between TRF1 and APBs, and thus ALT activity has yet to be fully understood. It is hypothesized that cells which rely on the ALT pathway use a homologous recombination (HR) based mechanism to maintain telomere length (Bailey et al., 2004; Dunham et al., 2000; Henson et al., 2002; Muntoni et al., 2009). Interestingly, it has been reported that when TRF1 is phosphorylated at threonine 371, it is recruited to

sites of DNA damage in telomerase-positive cells to facilitate DNA DSB repair by promoting HR and that this recruitment is dependent on an ATM, MRN-mediated DNA damage response (See section 1.3.3) (McKerlie et al., 2013). Consequently, phosphorylated (pT371)TRF1 may also be involved HR-based mechanism of ALT activity. Accordingly, whether TRF1 phosphorylation could regulate ALT activity is an interesting avenue to explore.

1.6 OBJECTIVES AND SIGNIFICANCE

The role of TRF1 in telomerase-dependent telomere elongation and maintenance has been extensively studied and characterized. Furthermore, it has also been well documented that post-translational modifications of TRF1 is crucial to regulate the molecular function of TRF1, including telomere binding, telomere maintenance, protein stability, cellular localization, regulation of DNA damage response, and overall genome stability (McKerlie et al., 2012, 2013; Walker & Zhu, 2012). Previous work from our lab has reported a key role in the involvement of TRF1 phosphorylation in homologous-recombination activity (McKerlie et al., 2013). Whether TRF1 phosphorylation plays an important regulatory in telomere length maintenance in telomerase-positive cells or ALT cells has yet to be fully understood. It has been previously proposed that TRF1 phosphorylation on T371, referred to as (pT371)TRF1, may play a role in ALT activity (Wilson, 2014). Moreover, mass spectrometry analysis of TRF1 have showed that threonine 271 (T271) is a candidate phosphorylation site (X.-D. Zhu, unpublished data). Thus, whether TRF1 phosphorylation on T271 might influence telomerase-dependent telomere lengthening or ALT activity remain uncharacterized. This thesis sets out to

investigate the role of TRF1 phosphorylation in telomere length maintenance by addressing two aims:

1. To investigate and dissect the mechanism of TRF1 phosphorylation on threonine 271 (T271) in telomere length maintenance in telomerase-positive and –negative (ALT) cells.
2. To provide further understanding on the role of TRF1 phosphorylation on threonine 371 (T371) in telomere maintenance in telomerase-negative (ALT) cells.

To investigate the function of TRF1 phosphorylation on T271 and T371 in telomere length maintenance, genetic approaches involving the use of cell lines expressing phosphomimic or unphosphorylatable T271 and T371 TRF1 mutants were used in addition to wild type TRF1. Another unique approach in addressing the aims also includes the use of antibodies raised to recognize phosphorylated TRF1 at T271 and T371. Other major approaches include the use of molecular techniques to analyze protein stability, protein-telomeric DNA binding, as well as direct analysis of ALT activity by the means of assessing APB formation and C-circles production. While this thesis sets out to explore the functional role of TRF1 phosphorylation in telomere length maintenance, it also aims at elucidating the underlying mechanism behind APB formations and C-circle productions, both of which are indicators of ALT activity.

Cancer cells are dependent on a mechanism of telomere elongation, whether it is through telomerase-dependent telomere elongation (i.e. activation of telomerase) or through the alternative lengthening of telomeres (ALT) pathway, in order to achieve

replicative immortality. Understanding the functional role of TRF1, which is crucial for telomere length regulation, will provide further insight into our understanding in potential cancer therapeutic options. This thesis will present how TRF1 phosphorylation has an important functional role in regulating the shelterin complex at telomeres, as well as in ALT activity.

CHAPTER 2 MATERIALS AND METHODS

2.1 Plasmids and Antibodies

Expression constructs for shTRF1 and the TRF1 mutant alleles T371A, and T371D have been previously described (McKerlie et al., 2013; McKerlie & Zhu, 2011; Wilson et al., 2016). The TRF1 constructs were generated by John R. Walker using the QuickChange site-directed mutagenesis kit (Stratgene). Wild type TRF1 constructs were generated with a silent mutation (TRF1sm) that renders it resistant against shTRF1. Wild-type TRF1 and TRF1 mutants (T271A, T271D, T371A, & T371D) were subcloned into the retroviral vector pWZL-Hygro-N-myc (pWZL) (Y. Wu, Zacal, Rainbow, & Zhu, 2007). The annealed oligonucleotides encoding shTRF1 (5′-GAATATTTGGTGATCCAAA-3′) were ligated into pRetroSuper vector (pRS) (Mitchell, Glenfield, Jeyanthan, & Zhu, 2009). Primer sequences for all alleles will be made available upon request by contacting Xu-Dong Zhu (McMaster University).

The phospho-specific anti-pT371 antibody has been previously described (McKerlie et al., 2013; McKerlie & Zhu, 2011; Wilson et al., 2016). The phospho-specific anti-pT271 antibody is a rabbit polyclonal antibody developed by Biosynthesis against a TRF1 peptide containing phosphorylated threonine-271 (VESKRTR-pT-ITSQDKP). Antibodies against TRF1, TRF2, TIN2, POT1, and RAP1 were gifts from Titia de Lange (Rockefeller University). Commercially available antibodies include anti-PML (sc-966, Santa Cruz), anti-c-Myc (9E10, Calbiochem), anti-γ-tubulin (GTU88, Sigma), anti-cyclin A (6E6, Abcam), and anti-histone H2AX (Upstate).

2.2 Cell Culture and Stable Cell Lines Generation

All parental cell lines, including Phoenix A, HeLaII, HT1080, and GM847 were grown in Dulbecco's Modified Eagle Medium (DMEM) media containing 10% FBS (Fetal Bovine Serum), 20 mM L-glutamine, 100 U/ml penicillin, 0.1 mg/ml streptomycin, and 1% non-essential amino acids. Cells stably expressing the pRS constructs were grown in the presence of 2 μg/ml puromycin and cells stably expressing pWZL constructs were grown in 90 μg/ml hygromycin. Cells expressing both pRS and pWZL constructs were maintained in selection medium containing either puromycin (2 μg/ml) or hygromycin (90 μg/ml) alternating every 2 weeks for the entirety of the experiments. All cells were grown in incubators at 37°C with 5% CO_2 and 100% humidity.

The generation of cell lines generation was done by retroviral infections as previously described (Jan Karlseder, Smogorzewska, & de Lange, 2002; Wilson et al., 2016; Zhu et al., 2003). Transfection was done using Lipofectamine 2000 (Invitrogen) according to the manufacture's protocol. On day 1, $2x10^6$ Phoenix A cells were seeded onto a 6-cm plate with 5 mL of growth media. On day 2, 8 μg of DNA of each retroviral construct was diluted in 250 μL Opti-MEM (Thermofisher) mixed with 20 μL of Lipofectamine 2000. The DNA-lipid complex mixture was incubated for 5 minutes at RT and subsequently, it was added to the Phoenix A cells dropwise and incubated at 37°C. On the same day, recipient cells were seeded in 10cm plates such that they would be about 30-40% confluent the next day. On day 3, the transfected Phoenix A cells were replaced with 4 mL of fresh growth media. Ten to twelve hours later, the media containing the retrovirus

were collected into a 15 mL tube. Subsequently, the Phoenix cells from each of 6 cm plates were trypsinized with 500 μL of trypsin and re-plated onto a 10cm plate. Following being filtered through a 0.45 μm syringe filter disc into a new 15 mL tube containing 4 μL of polybrene (4 mg/mL) and 400 μL of FBS, the media containing retrovirus were used to infect respective recipient cells. On day 4, this infection process was repeated for a total of three times every 6 hours. Twelve hours post last infection, the retrovirus-containing media were replaced with 9 mL of fresh media containing either puromycin or hygromycin.

TRF1-depleted HeLaII cell lines stably expressing various TRF1 alleles (TRF1, T271A, and T271D), along with the control cell lines were generated by Angus Ho using HeLaII-pRS and HeLaII-pRS-shTRF1 generated by Sichun Li. TRF1 depleted GM847 cells overexpressing various TRF1 alleles (TRF1, T271A, and T271D), along with the control cell lines were made by Florence R. Wilson.

2.3 Inhibitor Treatments

Inhibitor treatments were performed essentially as described (Wilson et al., 2016). Inhibitors used include: KU55933 (Sigma), a specific inhibitor for ATM; camptothecin (Sigma); DRB (Cayman Chemical) and actinomycin D (Sigma), and transcription inhibitors. KU55933 was used at 20 μM. CPT was used at 5 μM. DRB was used at 100 μM. Actinomycin D was used at 2 μg/ml. All drugs were dissolved at their respective concentration in fresh media and then added to cell culture.

2.4 Cycloheximide Chase Analysis of TRF1 protein stability

Cells were treated with cycloheximide (100 µg/mL) in non-selective fresh media for indicated times and protein extracts were collected as described below. Immunoblotting was performed as described below.

2.5 Cell synchronization of ALT cells

Cell synchronization at G1/S boundary in GM847 and U2OS cells was performed as described (Wilson et al., 2016). Cells were first arrested with thymidine (2.5 mM) for 17 hours, followed by washing in 1X PBS pH 7.4 (136 mmol/L NaCl, 2.7 mmol/L KCl, 10 mmol/L Na_2HPO_4, 1.8 mmol/L KH_2PO_4) for three times and then released into fresh media for 14 hours. Subsequently, cells were arrested again with 2.5 mM thymidine for 17 hours and washed in 1X PBS for three times before their release into fresh media for 0-16 hours. Following the second arrest (48 hours later), cells were either fixed for indirect immunofluorescence analysis (see below) or harvested for total protein lysates (see below) at indicated time points.

2.6 Protein Extracts and Differential Salt Extraction of Chromatin

Protein extracts and differential salt extraction of chromatin were performed as described (McKerlie et al., 2013; McKerlie & Zhu, 2011). For total protein extracts, cells were trypsinized, washed with media containing 10% FBS and counted using Beckman Coulter Z Series Counter. Cells were spun down and washed with 1mL cold 1X PBS at 4ºC. Following washing, cells were spun at 3000rpm for 2 minutes at 4°C and the pellet was resuspended in buffer C-420 (20 mM HEPES buffer (pH 7.9), 25% glycerol, 5 mM

MgCl, 0.2% Nonidet P-40, 1 mM DTT, 1 mM PMSF (phenylmethylsulfonyl fluoride), 1 µg/ml of aprotinin, 10 µg/ml of pepstatin, 1 µg/ml of leupeptin and 420 mM KCl) to obtain 20,000 cells/µl and incubated on ice for 30 minutes. Cells were spun at 13,200 rpm for 10 minutes at 4°C and the supernatant was resuspended in an equal volume of 2X Laemmli buffer (25mM Tris-HCl pH 6.8, 5% Glycerol, 1% SDS, 0.005% bromophenol blue, 5% β-mercaptoethanol) to obtain 10000 cells/µl.

For differential salt extraction of chromatin, cells were trypsinized, washed with media containing 10% FBS and counted. Cells were spun down at 1000 rpm for 5 minutes at 4°C and the pellet was washed with 1 mL cold 1X PBS. Extraction of the soluble cytoplasmic and nucleoplasmic proteins was performed by resuspending the pellet in buffer C-150 (20 mM HEPES buffer (pH 7.9), 25% glycerol, 5 mM MgCl, 0.2% Nonidet P-40, 1 mM DTT, 1 mM phenylmethylsulfonyl fluoride, 1 µg/ml of aprotinin, 10 µg/ml of pepstatin, 1 µg/ml of leupeptin and 150 mM KCl) to obtain 20,000 cells/µl and incubated on ice for 15 minutes. Cells were spun at 3000 rpm for 5 minutes at 4°C and the supernatants (150 mM KCl fraction) were collected. Subsequently, the chromatin-bound proteins were collected by resuspending the buffer C-150-treated pellets in buffer C-420 for 20 minutes. Cells were spun at 14,000 rpm for 10 minutes at 4°C and the supernatants were collected (420mM KCl fractions). Both 150 mM and 420mM KCl fractions were resuspended in 2x Laemmli buffer to obtain a final concentration of 10000 cells/µl. The final pellets were sonicated in 2X Laemmli buffer to obtain 10000 cells/µl.

2.7 Western Blotting (Immunoblotting)

Immunoblotting was performed as previously described (McKerlie et al., 2013; McKerlie & Zhu, 2011). For immunoblotting, protein samples were heated at 95ºC for 5 minutes and loaded at a concentration of 100,000 or 200,000 cells/µl (i.e. 10 µl or 20 µl). Unless otherwise stated, samples were resolved on 8% SDS-PAGE gels for 1.5-2 hours at 105V. Transfer of protein samples from SDS-PAGE gels to nitrocellulose membranes was performed with transfer buffer (25 mM Tris, 125 mM glycine, 20% methanol, 0.02% SDS) for 1.5 hours at 90V. As a quality control evaluation of transfer efficiency, membranes were stained and visualized with Ponceau red stain (0.1% w/v Ponceau S, 1% v/v acetic acid). Membranes were then rinsed with 1X PBS to wash away excess stain and then incubated with blocking buffer (10% milk powder, 0.5% TWEEN-20 in 1X PBS) for 30 to 40 minute at room temperature (RT), washed in 1X PBS three times, and then immunoblotted with primary antibodies diluted in incubation buffer (0.1% TWEEN-20 in 1X PBS) for 2 hours at RT or for 12-14 hours at 4ºC. Following immunoblotting with primary antibodies, membranes were rinsed in incubation buffer twice and then incubated in with ECL rabbit or mouse Igg HRP-conjugated secondary antibodies (GE Healthcare) at 1:20000 dilution in incubation buffer for 45 minutes at RT. The membranes were then washed with 1X PBS twice for 5 minutes each. After washing, the membranes were treated with Amsherham ECL Western Blotting detection reagent (GE Healthcare) according to the manufacturer protocol, followed by exposure to Amersham Hyperfilm ECL (GE Healthcare).

2.8 Indirect Immunofluorescence (IF)

Indirect immunofluorescence (IF) was performed as previously described (Wilson et al., 2016; Zhu et al., 2003). Cells, grown on coverslips, were fixed with 3% PFA (Paraformaldehyde [Sigma P-6148], in 1X PBS), washed with 1X PBS twice (5 minutes each), and permeabilized with PBS-buffered 0.5% Triton X-100 buffer for 10 minutes at RT. Cells were then washed twice with 1X PBS for 5 minutes each and stored in 1X PBS with 0.02% sodium azide at 4°C. Fixed cells were blocked with 1X PBG (0.2% fish gelatin, 0.5% BSA in 1X PBS) for at least 30 minutes and incubated with primary antibody diluted in 1X PBG for 12-16hr at 4ºC. Coverslips were washed three times in 1X PBG (5 minutes each), then incubated with FITC-/TRITC-conjugated secondary antibody diluted in 1X PBG (1:250, Jackson Laboratories) for 45 minutes at RT, protected from light. After three washes with 1X PBG (5 minutes each), coverslips were incubated with DAPI diluted in 1X PBG (100 ng/ml) for 2 minutes at RT, followed by three washes in 1XPBS (5 minutes each). Coverslips were placed cell-side down on embedding media (90% glycerol, 10% PBS, 1 mg/ml p-phenylene diamine) on microscope slides and sealed with nail polish. A Zeiss Axioplan 2 microscope was used to record all cell images. Pictures were captured with a Hamamatsu C4742-95 camera and processed in Open Lab.

2.9 Quantifying cells positive for APBs using IF microscopy

Scoring method for APBs in ALT cells was performed as described (Wilson et al., 2016). Cells were identified to be positive for APB (APB+) if they contained at least one or more APBs. APBs are defined as sub-nuclear structures containing PML protein,

telomeric DNA, and factors associated with telomeric DNA or DNA repair proteins (Yeager et al., 1999). In this study, APB+ cells were identified based on the colocalization of telomere-associated proteins and PML bodies. A cell was only considered as APB+ if a telomere marker focus is contained within, and therefore overlapping, a similar or larger PML focus. Both the telomere and PML foci must appear to be bright and prominent above background fluorescence levels as well as other dimmer foci in the cell. When determining colocalization of foci, the user should not be over-adjusting the optical focus of the field of view in order to colocalize or overlap foci in between viewing channels. Cells that did not satisfy the criteria for APB+ were deemed to be negative for APB (APB-) and were not scored.

2.10 Genomic DNA Isolation and Digestion

Cells, grown to about 90% confluency, were collected by scraping and spun down at 1000 rpm for 5 minutes at 4ºC. Cell pellets were then washed in 1 mL of cold 1X PBS and spun down at 3000 rpm for 2 minutes at 4ºC. Phenol-chloroform extraction method was used to isolate for genomic DNA. Cell pellets were resuspended in 1 mL 1X TNE (10 mM Tris-HCl pH 7.4, 10 mM EDTA, and 100 mM NaCl), mixed with 1mL 1X TNES/proteinase K (10 mM Tris, 10 mM EDTA, 100mM NaCl, pH 7.4, 1% SDS, 100 µg/mL Proteinase K), and incubated in 15ml phase lock gel heavy tubes overnight at 37ºC. Next day, an equal volume (2 mL) of phenol/chloroform/isoamylalcohol (25:24:1) was added to the pellet mixture and mixed gently at RT for 5 minutes to completely mix the phases. Following a spin down at 3000 rpm for 10 minutes at 4°C, the aqueous phase was transferred to a new phase lock gel heavy tube and an equal volume of

phenol/chloroform/isoamylalcohol was added. Samples were mixed and spun down again at 3000 rpm for 10 minutes at 4°C. The aqueous phase was mixed with 2 mL iso-propanol and 220 µL 2 M sodium acetate (pH 5.5) to precipitate a bundle of genomic DNA. The precipitated DNA was then collected and incubated in 300 µL 1xTNE with 100 µg/ml RNase A for 30 minutes at 37°C. DNA was resuspended using cut tip and incubated for another 2 hours at 37°C. Then, 300 µL 1X TNES/proteinase K was added to the DNA, solutions were mixed and incubated at 37°C for 1 hour. An equal volume (600 µL) of phenol/chloroform/isoamylalcohol was added and mixed by shaking. Mixed samples were then spun down at 13000 rpm at 4°C for 10 minutes. The upper phase was transferred with cut tip to a new tube containing 600 µL of iso-propanol and 66 µL of 2 M NaOAc (pH 5.5). Samples were inverted several times to precipitate the DNA, which was then collected and dissolved in $T_{10}E_{0.1}$ buffer (10mM Tris-Cl, 0.1mM EDTA pH 8.0). Genomic DNA was digested with *Rsa*I and *Hinf*I for 12 to 16 hours at 37°C and DNA concentrations were measured using Hoechst dye (100 µg/mL, Thermofisher) fluorimetry. Digested DNA samples were stored at -20 °C.

2.11 Ethanol precipitation of DNA

Desired amount of DNA samples is transferred to fresh tubes and topped up to 100 µL using ddH_2O. Ten microliters of 3 M NaOAc pH 5.2, and 300 µL of cold 95% ethanol were then added and mixed with the DNA samples. DNA was precipitated overnight at -20°C. Next day, DNA was spun down at 13,000 rpm for 30 minutes at 4°C. Supernatant was then removed and DNA pellet was washed once with cold 70% ethanol. DNA pellet was then spun down again at 10,000rpm for 5 minutes at 4°C. Ethanol was

then decanted and then the pellet was air-dried. DNA samples was then resuspended in 10mM Tris-HCl pH 7.6. DNA can be stored in -20^{o}C.

2.12 C-circle Amplification Assays

C-circle amplification assays were performed as described (Henson et al., 2009; Wilson et al., 2016). At least 300 ng of DNA was precipitated and 50 ng of each DNA sample was incubated with or without 7.5 U ϕ29 DNA polymerase (NEB) in a 20 µL reaction containing 9.25 µL of reaction premix (0.2 mg/ml BSA, 0.1% Tween 20, 1 mM ATP, 1 mM dTTP, 1 mM dGTP, 1X ϕ29 buffer) at 30^{o}C for 8 hours. Following heat inactivation of ϕ29 at 65^{o}C for 20 minutes, samples were separated on a 0.6% agarose gel in 0.5X Tris-borate-EDTA (TBE) buffer (45 mM Tris-borate, 1 mM EDTA pH 8.0) at 1.75V/cm for 12-16 hours. Following electrophoresis, the gel was dried at 50^{o}C and then hybridized with a radioactively end-labeled single strand $(CCCTAA)_3$ probe (for details, see Radioactive probe preparation for detecting C-circles) under native conditions. Gels were exposed to PhosphorImager screens (GE Healthcare) for at least 16 hours. All screens were scanned using a Typhoon FLA9500 biomolecular imager (GE Healthcare) at 100 microns and 500V PMT settings with the IP (Phosphorimaging) filter.

2.13 Northern analysis of TERRA

Northern analysis was carried out as described (Batenburg, Mitchell, Leach, Rainbow, & Zhu, 2012; Wilson et al., 2016). Cells, grown to about 90% confluency on a 10cm plate, were washed with cold 1X PBS (made with DEPC-treated ddH_2O) twice. Cells were then lysed using 1 mL of TRIzol® reagent directly on the plate by scrapping the cells

and incubated for 5 minutes at RT. The sample was mixed with 200 µL of chloroform for 12 seconds. Following incubation for 3 minutes, the samples were spun down at 13200 rpm for 15 minutes at 4ºC. The upper aqueous phase was collected and mixed with 500 µL of isopropanol for 10 minutes at RT. RNA pellet was collected by centrifugation at 13200 rpm for 10 minutes at 4ºC. Following washing with 1mL of cold 75% ethanol twice, the RNA pellet was air-dried, resuspended in 20uL of DEPC-treated ddH_2O and incubated at 60ºC for 10 minutes. RNA concentration was quantified using a spectrophotometer by measuring the A260 and A280 readings.

For northern analysis of TERRA, 20 µg of RNA samples (5 µL) were prepared in 19 µL of loading pre-mix (1X MOPS, 7% Formaldehyde, 40% Formamide, 4 µg/mL Ethidium bromide), mixed and heated for 30 minutes at 60ºC. Prior to loading, 2.5 µL10X formamide loading buffer (50% glycerol, 10 mM EDTA pH 8.0, 0.25% bromophenol blue, 0.25% xylene cyanol FF) was added to each sample to a 1X concentration. RNA samples were separated on a 1.2% agarose gel (3% formaldehyde, 1x MOPS buffered) in 1X MOPS buffer for 6-7 hour at 4-5 V/cm. Following electrophoresis, the gel was imaged and inspected for the presence of the 28S and 18S ribosomal RNA, as indicators of RNA quality. Subsequently, the gel was hydrolyzed with 0.05 M NaOH for 20 minutes, soaked in 20X SSC (3 M NaCl, 0.3 M sodium citrate) for 40 minutes and RNA was transferred onto Hybond-N nylon membrane (GE Healthcare) for at least 14-16 hours. Following transfer, the membrane was cross linked using a Stratagene UV Stratalinker, rinsed in ddH_2O twice, and blocked in Churchmix (0.5 M NaPi pH 7.2, 1 mM EDTA pH 8.0, 7% SDS, 1% BSA) for 1 hour at 65ºC. TERRA was detected by hybridizing the membrane

with an 800-bp Klenow-labelled ^{32}P-α-dCTP TTAGGG repeat-containing probe (Loayza & Lange, 2003) for 12-16 hours at 65^{o}C. The membrane was then washed in 1X SSC (0.1% SDS) for 10 minutes at RT, then in 0.5X SSC (0.1% SDS) for 10 minutes at 65^{o}C, and exposed to PhosphorImager screens (GE Healthcare) for at least 16h.

For GAPH loading control, the membrane was stripped with stripping buffer (10mM Tris-Cl pH 7.4, 0.2% SDS) for 1.5 hours at 70^{o}C. Subsequently, the membrane was blocked and hybridized as described above with the exception that a Klenow-labelled ^{32}P-α-dCTP probe containing GAPDH specific sequence was used (For details, see Radioactive probe preparation for detecting TERRA or telomeric DNA sequences**)**.

2.14 Chromatin Immunoprecipitation (ChIP)

Chromatin immunoprecipitations were carried out as described (McKerlie & Zhu, 2011). Briefly, cells were trypsinized, washed with media containing 10% FBS and counted. Cells were directly crosslinked with 1% formaldehyde (made from 37% solution) in 1X PBS for 1 hour on a nutator. Samples were then spun down at 1000 rpm for 5 minutes at 4^{o}C. Cell pellets were then washed in cold 1X PBS twice and resuspended in lysis buffer (1% SDS, 10 mM EDTA pH 8.0, 50 mM Tris-Cl pH 8.0, 1 mM PMSF, 1 µg/mL leupeptin, 1 µg/mL aprotinin, 1 µg/mL pepstatin) to a concentration of 1x10^{7} cells/mL. The lysis buffer without protease inhibitors was kept at RT and protease inhibitors were added to the lysis buffer immediately prior to use. The resulting lysates were kept on ice all the time. Following incubation on ice for 15 minutes, the lysates were sonicated on ice (10 cycles of 20 seconds each, 50% duty and 5 output). Avoid making bubbles while sonicating.

Following sonication, the lysates, which should appear clear, were spun down at 3000 rpm for 5 minutes at 4ºC, and the supernatants were transferred to microfuge tubes. Samples were spun down again at 10000 rpm for 5 minutes at 4ºC and the supernatants were collected for immunoprecipitations.

For each ChIP, 200 µL of cell lysate was used. On ice, 1 mL of ChIP dilution buffer (0.01% SDS, 1.1% Triton X-100, 1.2 mM EDTA, 16.7 mM Tris-Cl pH 8.0, 150 mM NaCl, 1 mM PMSF, 1 µg/mL leupeptin, 1 µg/mL aprotinin, 1 µg/mL pepstatin) was added to each lysate and allowed to sit on ice for 10 minutes. Following incubation with the dilution buffer, the lysates were incubated with respective primary antibody and incubated for 12-16 hours at 4ºC on a rotator. On the next day, 30 µL of pre-blocked Protein-G sepharose beads were added to each IP sample and incubated for 30 minutes at 4ºC on a rotator. Beads were then washed with 1 mL of each of the following wash buffers: buffer A (0.1% SDS, 1% Triton X-100, 2 mM EDTA pH 8.0, 20 mM Tris-Cl pH 8.0, 150 mM NaCl, 1 mM PMSF, 1 µg/mL leupeptin, 1 µg/mL aprotinin, 1 µg/mL pepstatin), buffer B (0.1% SDS, 1% Triton X-100, 2 mM EDTA pH 8.0, 20 mM Tris-Cl pH 8.0, 500 mM NaCl), buffer C (0.25 M LiCl, 1% NP-40, 1% Na-Deoxycholate, 1 mM EDTA pH 8.0, 10 mM Tris-Cl pH 8.0), and TE (10 mM Tris-HCl pH 8.0, 1 mM EDTA pH 8.0). Samples were mixed by vortexing and kept on ice between washes. Following the last wash, the beads were resuspended in 250 µL of SDS-carbonate (1% SDS, 0.1M $NaHCO_3$) through vortexing and then incubated at RT for 10 minutes. Beads were then pelleted and the supernatant was collected and transferred to a fresh tube. Repeat the prior step and pool the supernatant with the previous eluate to collect a total of 500 µL of eluate. For the total telomeric DNA

inputs, two aliquots of 50 μL supernatant (corresponding to one-quarter of the amount of lysate used for IP) were processed along with the IP samples by voluming up to 500 μL with SDS-carbonate. At this point, the input samples were with the IP samples with the addition of 20 μL of 5 M NaCl, and then incubated at 65ºC for 4-6 hours to reverse crosslinks. After 4-6 hours, each sample was mixed with 10 μL of 0.5 M EDTA pH 8.0 and 20 μL of Tris-HCl pH 6.5, followed by the treatment with 20 μg of RNaseA at 37ºC for 40 minutes. Subsequently, the samples were each mixed with 40 μg of proteinase K, incubated for another hour at 37ºC, and then extracted with 500 μL of phenol/chloroform/isoamylalcohol. The aqueous phase containing DNA was then precipitated with 1 mL of cold 95% ethanol overnight at -20ºC in the presence of 20 μg of glycogen, which allowed visualization of the DNA pellet following precipitation. DNA was spun down at max speed for 20 minutes at 4ºC. The DNA pellet was air-dried and resuspend in 10 mM Tris-HCl pH 7.5.

Detection of telomeric DNA was done with a 800-bp Klenow-labelled ^{32}P-α-dCTP TTAGGG repeat-containing probe, as previously described (Loayza & Lange, 2003). DNA samples were boiled for 5 minutes, cooled on ice and then quickly spun to bring down condensation. Prior to loading, two 3MM Whatman papers and Hybond-N membrane (GE Healthcare) were saturated with 2X SSC. The membrane must be prewet with ddH_2O prior to being soaked in 2X SSC. The membrane was laid down on the top of the saturated Whatman papers, which was placed in the dot blot apparatus (Bio-Dot® microfiltration apparatus [BioRad]). The buffer 2X SSC was added into several wells to ensure that the

vacuum was working properly. For loading samples, 200 μL of 2X SSC were loaded into the desired wells. DNA samples were then loaded into each well, and mixed. Four-fifths of immunoprecipitated DNA was loaded onto the Hybond-N nylon membrane, whereas two inputs each containing 5% of total DNA were included to assess the consistency of loading.

After loading, the membrane was denatured on a 3MM Whatman paper saturated with denaturing solution (1.5M NaCl, 0.5M NaOH) for 10 minutes at RT. Then, the membrane was neutralized on a 3MM Whatman paper saturated with neutralizing solution (3 M NaCl, 0.5 M Tris-HCl pH 7.0) for 10 minutes at RT. Then, DNA was crosslinked onto the membrane using a Stragene UV stratalinker (Auto crosslink setting) with the DNA side up. The membrane was then prehybridized with Churchmix at 65ºC for 30-40 minutes. After prehybridization, the membrane was incubated with a radioactively-labeled probe (for details, see Radioactive probe preparation for detecting TERRA or telomeric DNA sequences) overnight on a shaker at 65ºC. The next day, the membrane was washed in 2X SSC at RT for 10 minutes each, and then once in 2X SSC (0.1% SDS) for 10 minutes at 65ºC. The membrane was then sealed in plastic wrap and exposed onto a phosphorimager screen for 5-12 hours depending on the signal intensity.

The average of the two input signals was used for quantification of telomeric DNA recovered. The ratio of the signal from each ChIP relative to the average signal from the two input lanes was multiplied by 5% (5% represents 5% of total DNA) and by a factor of 1.25 (because four-fifths of the precipitated DNA was loaded for each ChIP), giving rise to the percentage of total telomeric DNA recovered from each ChIP. For Alu control, the

membrane was stripped using 10mM Tris-Cl pH 7.4 (0.2% SDS) for 1.5 hours at 70ºC. Subsequently, the membrane was blocked and hybridized as described above with the use of Klenow-labelled ^{32}P-α-dCTP probe containing Alu specific sequence (For details, see Radioactive probe preparation for GAPDH and Alu sequences).

2.15 Radioactive probe preparation for detecting TERRA or telomeric DNA sequences

The labeling reaction was performed in a 50 µL reaction mixture containing: 3 µL of an 800-bp $[TTAGGG]_n$ Sty11 insert (220 ng/µL), 5 µL of a $[CCCTAA]_3$ oligonucleotide (1ng/µL), 5 µL of 10X OLB (oligo nucleotide labeling buffer; 0.5 M Tris-HCl pH 6.8, 0.1 M MgOAc, 1mM DTT, 0.5 mg/mL BSA, 0.6 mM each of dGTP, dATP, dTTP), 5 µL of ^{32}P-α-dCTP (3000 Ci/mmol), and 1 µL of Klenow polymerase (NEB). The reaction mixture was mixed with radioactive isotope and Klenow polymerase and then boiled for 5 minutes. The mixture was quickly spun for 5 seconds and then cooled on ice. Following the addition of 10X OLB buffer, the total reaction mixture is mixed and incubated for 90-120 minutes at RT. After the reaction, 50 µL 1X TNES was added to the reaction mixture and heated to 65ºC for 10 minutes. The radioactively labelled probe was then loaded onto a 3 mL G-50 column (3cc syringe filled with Sephadex G-50 fine beads (GE Healthcare) to the top containing glasswool at the bottom to prevent leakage of beads). The column was first equilibrated with 3 mL of 1X TNES, and then the probe was eluted with 1 mL of 1X TNES, followed by 800 µL of 1X TNES which was collected as the final eluate. Before using, the probe was heated for 5 minutes at 100ºC and filtered through a 0.2 µm syringe

filter in an appropriate volume of Churchmix depending on the size of membrane. The eluted probe may be stored at -20ºC for later use.

2.16 Radioactive probe preparation for detecting C-circles

The labeling reaction was performed in a 10 µL reaction mixture containing 1 µL $TelC_4$ oligo (50ng/µL, $[CCCTAA]_4$), 1 µL 10X T4 Polynucleotide Kinase (PNK) buffer (NEB), 1 µL T4 PNK (NEB), 5 µL ^{32}P-γ-dATP (3000 Ci/mmol), and 2 µL ddH_2O. The reaction mixture was incubated for 45 minute-1 hour at 37ºC. Following the reaction, 80 µL of 1X TNES was added to the reaction mixture and loaded onto a pre-made column (equilibrated with 10 mL of 1X TNES prior to elution). The probe was eluted with 500 µL of 1X TNES, followed by 1 mL of 1X TNES which was collected as the final eluate. Before using, the probe was heated for 5 minutes at 100ºC and filtered through a 0.2 µm syringe filter in an appropriate volume of Churchmix depending on the size of membrane. The eluted probe may be stored at -20ºC for later use.

2.17 Radioactive probe preparation for GAPDH and Alu sequences.

For Alu probe, 2.5µL of human Alu template sequence (25.2ng/µL), and 1µL of random primer (15µM, NEB) were used. For GAPDH probe, 2µL of human GAPDH template sequence (30ng/µL) and 1µL of random primer (15µM, NEB) were used. Both labelling reactions and elution process were performed as described in section 2.16. The eluted probe may be stored at -20ºC for later use.

2.18 Image analysis of IF staining of anti-(pT271)TRF1 antibody

All cell images were recorded on a Zeiss Axioplan 2 microscope with a Hammamatsu C4742-95 camera and processed in Open Lab. For image analysis, images were imported into ImageJ software (https://imagej.nih.gov/ij/index.html) as .TIFF format (RGB mode). Statistical analysis was performed using GraphPad Prism 5.0a software.

For nuclear staining of anti-(pT271)TRF1, DAPI stained images were imported into ImageJ software, and converted to 16-bit format images. Subsequently, threshold selection was performed to select nuclear regions with the following settings: "Yen" threshold method/"Red" selection/"Dark Background". The top slider in the 'Threshold window' was adjusted to optimize threshold selection of nuclear regions. After threshold selection, the region of interests (ROIs; in this case, nuclear regions) were defined using the following settings: "0.00-0.95" Circularity/Show "Overlay Outlines"/Check "Add to Manager", "Exclude on edges", "Display Results". After ROIs have been defined, the 16-bit modified images were closed, and the original anti-(pT271)TRF1 stained nuclear images were imported into ImageJ software as .TIFF format (RGB mode). Using the ROI manager, the previously defined ROIs were selected and measured using the "Measure" function. The resulting "Mean" values were used to determine pixel intensities (i.e. fluorescence intensities) of the defined nuclear regions. The measured values were then imported into GraphPad Prism 5.0a for further analysis.

For midbody-like staining, anti-(pT271)TRF1 stained mid-body images were imported into ImageJ software, and converted to 16-bit format images. Subsequently,

threshold selection was performed to select mid-body like regions with the following settings: "Yen" threshold method/"Red" selection/"Dark Background". The top slider in the 'Threshold window' was adjusted to optimize threshold selection of mid-body like regions. After threshold selection, the region of interests (ROIs; in this case, mid-body like regions) were defined using the following settings: "0.00-0.95" Circularity/Show "Overlay Outlines"/Check "Add to Manager", "Exclude on edges", and "Display Results". After ROIs have been defined, the 16-bit modified images were closed, and the original anti-(pT271)TRF1 stained mid-body images were imported into ImageJ software as .TIFF format (RGB mode). Using the ROI manager, the previously defined ROIs were selected and measured using the "Measure" function. The resulting "Mean" values were used to determine pixel intensities (i.e. fluorescence intensities) of the defined mid-body like regions. The measured values were then imported into GraphPad Prism 5.0a for further analysis.

2.19 Statistical Analysis

One-way ANOVA and Tukey HSD test (multiple comparison test of means with 95% confidence interval), and Student's t-test were performed using the statistical software GraphPad Prism 5.0a. One-way ANOVA was performed to determine whether there were significance differences between the means of 3 or more groups. Tukey's multiple comparison test was used to test for significance between all combinations of pairs when 3 or more groups of data were present. Student's t-test was used to test for the significance for each pair of individual comparisons (i.e. comparing data set to a normalized data). Significant differences ($P<0.05$) are displayed on the graphs as asterisks as follow: 'ns'

$P>0.05$, '*' $P\leq0.05$, '**' $P\leq0.01$, '***' $P\leq0.001$. Details of statistical tests and results for data presented in Chapters 3 and 4 can be found in Appendix A2 Statistical Results. The statistical test used to derive *P* values are indicated in figure legends.

CHAPTER 3 TRF1 PHOSPHORYLATION ON T271 MODULATES TRF1 BINDING TO TELOMERIC DNA AND ALT-ASSOCIATED PML BODIES

Preface

The rational on the work presented in this chapter regarding the role of TRF1 phosphorylation on threonine 271 (T271) was based on observations made by previous members of the lab. First, mass spectrometry analysis of TRF1 revealed that T271 was a candidate phosphorylation site *in-vivo*, and this was confirmed by Western analysis with an antibody raised to recognized phosphorylated TRF1 on T271, also referred to as (pT271)TRF1 (K. Jeyanthan, T.R.H., Mitchell, X-.D., Zhu, unpublished data). Second, through Southern blotting analysis in TRF1-depleted HeLaII cells that stably express a TRF1 with a non-phosphorylatable mutation T271A, telomere elongation was observed (K. Jeyanthan, F.R. Wilson, unpublished data), similar to cells TRF1-depleted cells, which is in agreement with previous findings whereby TRF1-depletion can induce telomere elongation in cells (McKerlie et al., 2012; Soohoo et al., 2011). Similar to wild type TRF1, a phosphomimic T271D mutant was able to rescue and suppress telomere elongation (K. Jeyanthan, F.R. Wilson, unpublished data). For simplicity, TRF1 will be used to denote the wild type protein, while the mutants will be referred to as the point mutations (i.e. T271A, T271D). With strong evidence supporting a role for (pT271)TRF1 in telomere length regulation, this chapter will present experimental evidence to characterize the role of (pT271)TRF1 in telomerase-dependent telomere maintenance and in ALT activity. Unless otherwise specified, all figures and experimental data were generated by Angus Ho.

3.1 Analysis of cellular staining of phosphorylated TRF1 at T271 using indirect immunofluorescence microscopy

Using an antibody that has been raised against phosphorylated (pT271)TRF1, we assessed the staining pattern of (pT271)TRF1 in cells using indirect immunofluorescence (IF). IF analysis revealed a unique cytoplasmic staining pattern of (pT271)TRF1, aside from the expected telomere-like punctate staining in the nuclei, which was unexpected for a telomeric protein such as TRF1 (Figure 3.1). Further analysis suggested that this cytoplasmic staining of (pT271)TRF1 resembled mid-body (F. R. Wilson, unpublished data), a cellular structure involved in cytokinesis during mitosis (Hu, Coughlin, & Mitchison, 2012).

To investigate whether the nuclear and midbody-like stainings of the anti-(pT271)TRF1 antibody are specific, I examined their respective intensity in TRF1-depleted HeLaII cells expressing vector, wild type TRF1, and T271A. Cell images were captured at various exposure time (50 to 2000ms), and Image J analysis of captured images suggested that images captured at 350ms lay well within the 95% confidence interval of the linear range (Figure 3.2). We reasoned that if the observed nuclear and midbody-like staining were specific to TRF1, then the staining intensity for T271A mutant, which is defective in phosphorylation at T271, would be similar to the vector control (i.e. TRF1-knockdown) since the antibody does not recognize the T271A mutant. On the other hand, the fluorescence intensity for both nuclear and midbody-like staining would be higher in the wild type TRF1 control, as wild type TRF1 should be recognized by the anti-(pT271)TRF1 antibody and thus rescue the knockdown vector control to a higher level. IF image analysis

on nuclear staining revealed that there was a significant difference between the vector and TRF1, the vector and T271A, but no difference between TRF1 and T271A (Figure 3.3A). Despite having significant difference, the average nuclei fluorescence intensity in TRF1 is lowered than the vector control, which is not expected. Since no difference was observed between TRF1 and T271A in the nuclear staining, it was concluded that the nuclear staining pattern observed on IF using anti-(pT271)TRF1 antibody is likely not to be TRF1-dependent. Conversely, IF analysis on the midbody-like staining revealed that the mean midbody-like fluorescence intensity was higher in the T271A mutant compared to wild type TRF1. Furthermore, the midbody-like staining in TRF1 was also significantly lowered than that of the vector control (Figure 3.3B). Taken together, results from IF analyses suggest that the observed IF staining pattern by the anti-(pT271)TRF1 antibody is not TRF1-dependent, and could potentially be an artifact. Therefore, it was determined that IF experiments using the anti-(pT271)TRF1 antibody should be ceased as it is not a reliable method to assess the effect of TRF1 phosphorylation on T271.

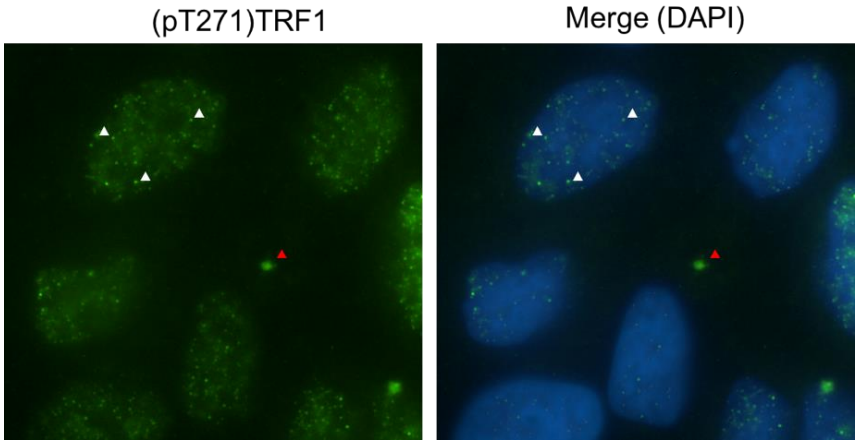

Figure 3.1 – Indirect immunofluorescence staining of anti-phosphorylated (pT271)TRF1. HeLaII cells fixed and stained for chromosomes (DAPI, blue), and (pT271)TRF1 (green). Punctate telomere-like (white arrows) and midbody-like (red arrow) staining of (pT271)TRF1 are indicated.

A

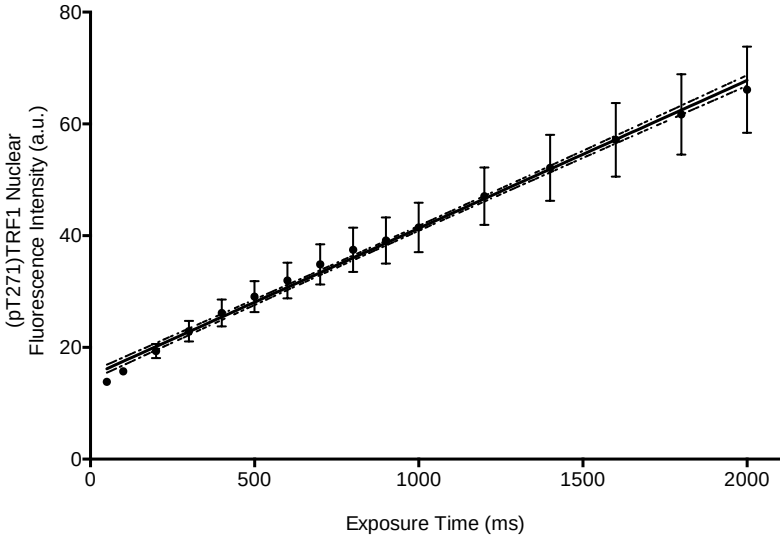

B

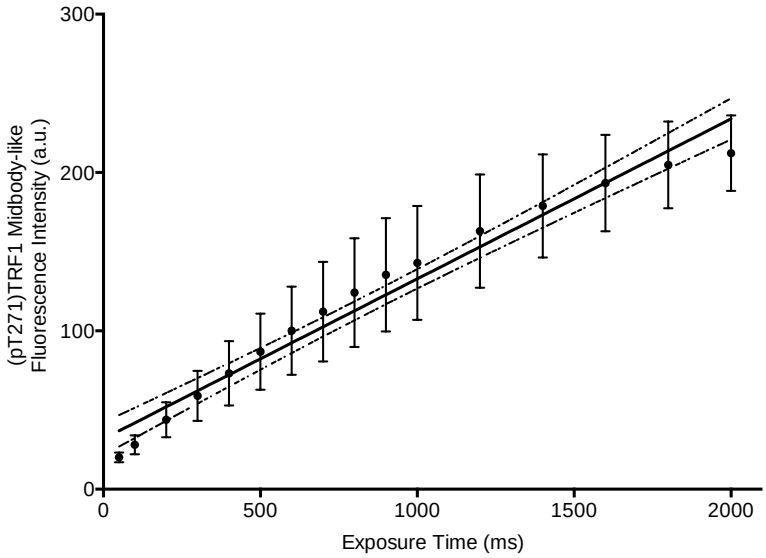

Figure 3.2 - Linear regression model of exposure time and staining intensity of (pT271)TRF1 under indirect immunofluorescence in HeLaII cells. Fluorescence intensity of **A)** nuclear staining and **B)** midbody-like staining of anti-(pT271)TRF1 are shown. Dotted lines represent the 95% confidence interval about the best-fit line (solid). Analysis of fluorescence intensity of captured images over a range of exposure time of 200ms to 500ms. Fluorescence intensity of images captured at 350ms is maintained well within the 95% confidence interval of the linear range. See Materials and Methods for details.

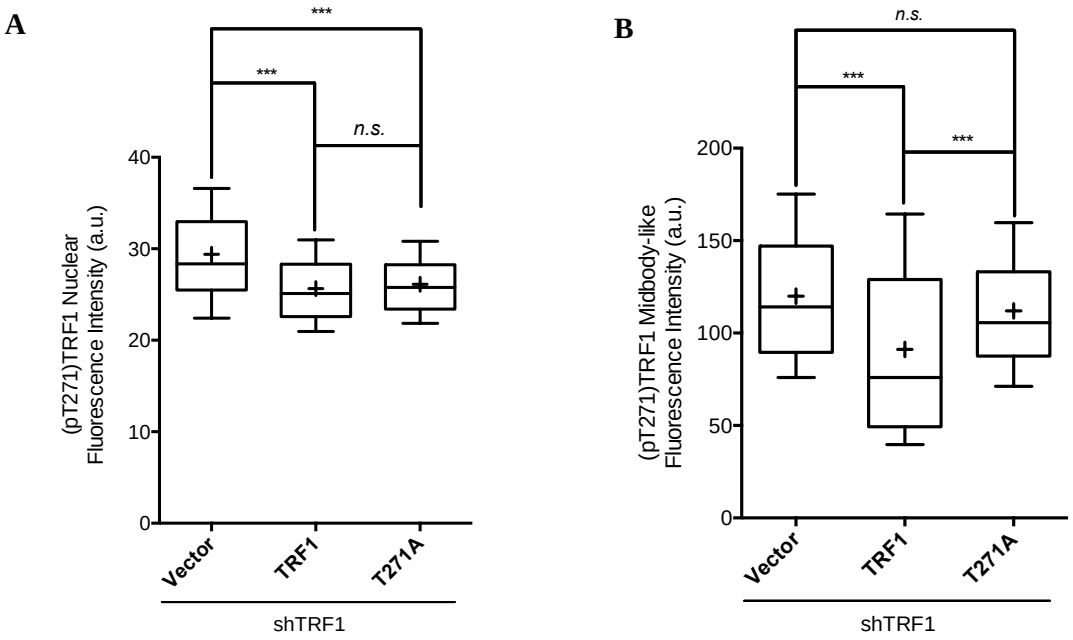

Figure 3.3 – Analysis on indirect immunofluorescence staining of anti-(pT271)TRF1. TRF1-depleted HeLaII cells stably expressing the vector, TRF1, and TRF1-T271A mutant were fixed and stained for (pT271)TRF1. **A)** Quantification of fluorescence intensity of nuclear staining. **B)** Quantification of fluorescence intensity of midbody-like staining. Fluorescence intensity is measured in arbitrary units (a.u.). Values were calculated using ImageJ to measure captured images of nuclear or midbody-like staining. All images were captured at 350ms of exposure (See Figure 3.2). *P*-values are calculated by Mann-Whitney Test.

3.2 TRF1 phosphorylation on T271 facilitates its association with telomeric DNA *in vivo*.

TRF1's association with telomeres has been demonstrated to be important for telomerase-dependent telomere elongation (A. Smogorzewska et al., 2000; van Steensel & de Lange, 1997). In order to elucidate how the site T271 may play a role in telomerase-dependent telomere elongation, the ability of TRF1, T271A, and T271D mutants to associate with chromatin, and presumably telomeres *in vivo* was tested. The first approach to evaluate whether TRF1 phosphorylation on T271 influences TRF1's association with telomeric DNA was by performing differential salt extraction of chromatin in TRF1-depleted HeLaII cells (HeLaII shTRF1) stably expressing Myc-TRF1, Myc-TRF1-T271A or Myc-TRF1-T271D. The decision to perform the experiment in a TRF1-depleted background was to minimize any possible influence by endogenous wild type TRF1 levels. Expression of various Myc-tagged TRF1 alleles was comparable across all cell lines (Figure 3.4). Unlike previous findings, in which TRF1 was found to predominately exist in the 420mM (chromatin) fraction and some in the pellet fraction, and very low levels in the soluble 150mM fraction (McKerlie & Zhu, 2011), all Myc-tagged TRF1 were found to exist in all three fractions (Figure 3.5). Moreover, it was also difficult to decipher whether there were truly differences between wild type TRF1 and the mutants. To this end, results from the differential salt extraction of chromatin analysis was inconclusive and unable to reveal any insights as to whether the T271A and T271D mutations could influence TRF1's association with telomeric DNA.

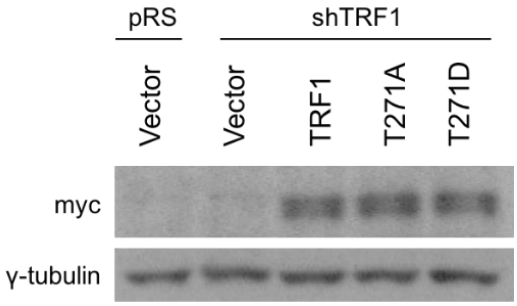

Figure 3.4 - Western analysis of TRF1-depleted HeLaII cells stably expressing the vector alone or various TRF1 alleles as indicated. Immunoblotting was carried out with anti-myc or anti-γ-tubulin. γ-tubulin was used as a loading control and subsequent figures.

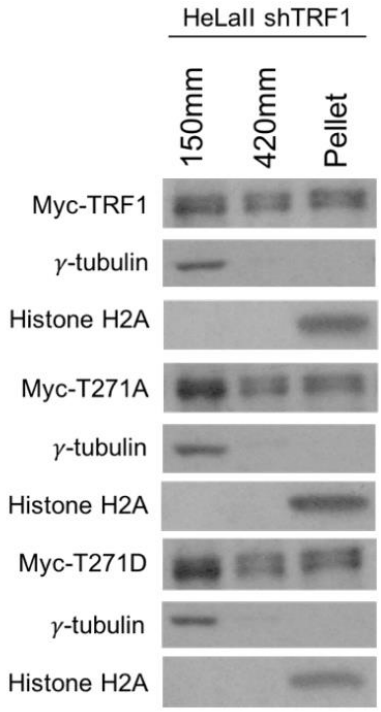

Figure 3.5 – Differential salt extraction of chromatin analysis on TRF1 association with telomeres in T271D phosphomimic and T271A unphosphorylatable mutants. Immunoblotting was carried out with anti-Myc, or anti-H2A, or anti-γ-tubulin antibody. The anti-H2A and anti-γ-tubulin blots were used as controls to assess the extraction of chromatin. 12% SDS-PAGE gels were used to separate total histones.

In order to evaluate whether phosphorylation on T271 can influence TRF1's association with telomeres, I next performed chromatin immunoprecipitation (ChIP) in TRF1-depleted HeLaII cells expressing various TRF1 alleles, followed by detection of pulled-down telomeric DNA. Myc-ChIP analyses revealed that upon TRF1-depletion, phosphomimic T271D mutant was able to rescue the levels of telomeric DNA similar to wild type TRF1, but the non-phosphorylatable T271A mutant failed to rescue TRF1's association with telomeric DNA (Figure 3.6). The results suggest that when TRF1 cannot be phosphorylated at T271, TRF1's association with telomeric DNA is impaired. Therefore, phosphorylation on T271 promotes TRF1's association with telomeric DNA.

It has been previously reported that when TRF1 is phosphorylated, this can render TRF1's stability to be reduced (McKerlie et al., 2012; Walker & Zhu, 2012). Thus, it was formally possible that the impaired telomeric association of the T271A mutant with telomeric DNA might be due to a reduced protein stability. To investigate whether TRF1 phosphorylation on T271 might influence protein stability, I performed a cycloheximide chase experiment in HT1080 cells stably expressing the vector, Myc-tagged TRF1, Myc-tagged TRF1-T271A, and Myc-tagged TRF1-T271D. Over the course of an 8 hours post release from cycloheximide treatments, no significant differences were observed in the stability of TRF1 (Figure 3.7), suggesting that TRF1 phosphorylation on T271 is unlikely to play a role in regulating TRF1's stability. Collectively, these results suggest that the impaired telomeric DNA association of Myc-tagged TRF1-T271A is unlikely due to the reduced stability of the protein. These results are also in support to the previous

observations that Myc-tagged TRF1-T271A fails to suppress telomerase-dependent telomere elongation (K. Jeyanthan, and F.R.W., unpublished data).

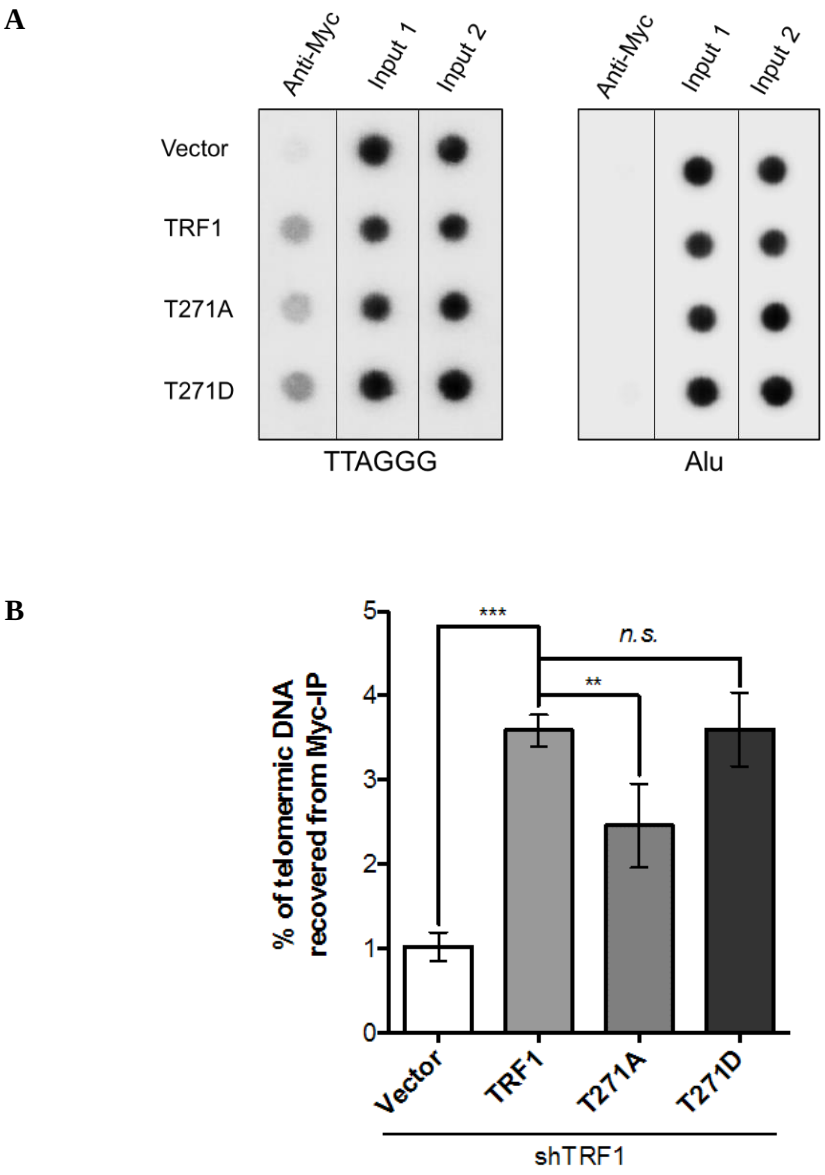

Figure 3.6 – A non-phosphorylatable mutation at T271 (T271A) impairs TRF1 interaction with telomeres. **A)** Dot blots of anti-Myc ChIPs from TRF1-depleted HeLaII cells expressing various TRF1 constructs as indicated on the left. **B)** Quantification of anti-Myc ChIPs from (A). Standard deviations from three independent experiments are indicated. *P*-values are calculated by Tukey's Multiple Comparison Test (Tukey HSD) with a significance level of $P<0.05$. Significance tests of all combinations of pairs are taken into account using with this method. Unless otherwise

stated, all P-values in subsequent figures are calculated using this method. Significant differences ($P<0.05$) are displayed on the graphs as asterisks as follow: 'ns' $P>0.05$, '*' $P\leq0.05$, '**' $P\leq0.01$, '***' $P\leq0.001$. See Chapter 2–Materials and Methods, Section 2.19 for details.

A

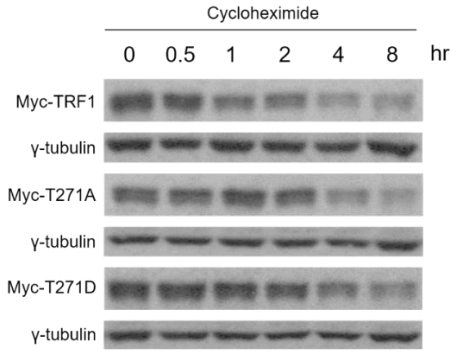

B

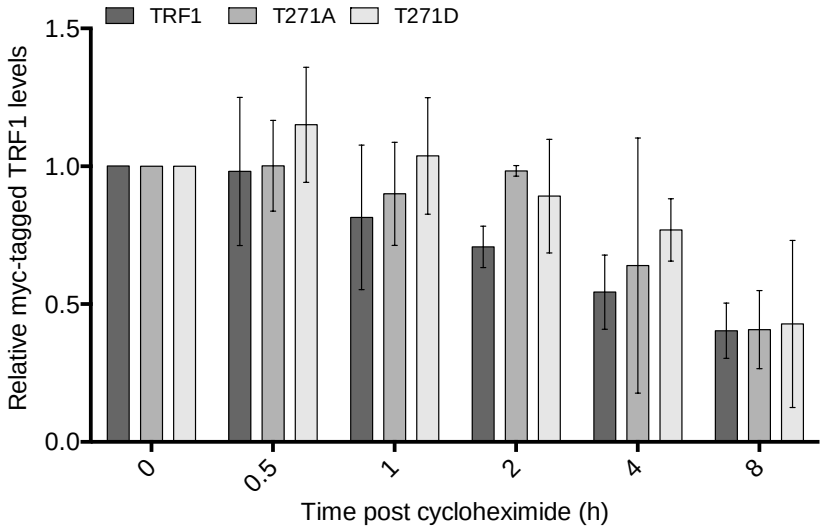

Figure 3.7 - Cycloheximide chase experiment. A) TRF1-depleted HeLaII cells stably expressing Myc-TRF1, Myc-TRF1-T271A or Myc-TRF1-T271D were treated with 100µg/ml cycloheximide for the indicated times, followed by immunoblotting of the lysates with anti-Myc or anti-γ-tubulin antibody. **B)** Quantification of cycloheximide chase experiments from HT1080 cells stably expressing Myc-tagged wild-type TRF1, Myc-tagged TRF1-T271A and Myc-tagged TRF1-T271D from (A). The signals from the western blots were quantified with densitometry. The level of Myc-tagged TRF1 proteins is represented in arbitrary units after their signals were normalized relative to those of γ-tubulin. One-way ANOVA test was performed between TRF1 and T271A, or T271D at each time point. Standard deviations from three independent experiments are indicated.

3.3 TRF1 Phosphorylation on T271 does not influence TRF2 or TIN2's association with telomeric DNA

It has been previously reported that binding of TRF2 or TIN2 at telomeres could also contribute to telomere length control in telomerase-positive cells (Sahn-ho H Kim et al., 1999; A. Smogorzewska et al., 2000). Thus, following Myc-ChIP analysis, I wanted to ask whether T271 phosphorylation might also have an impact on other shelterin subunits in telomeric DNA association, and perhaps potentially influencing telomere elongation.

TIN2 is an essential shelterin subunit that regulate telomere length in human cells and has been shown that it is an essential mediator of TRF1 function in regulating telomere length (Campisi, Kim, & Kaminker, 1999). To address whether TRF1 phosphorylation on T271 influences TIN2's association with telomeric DNA, TIN2-ChIP was performed in the TRF1-depleted HeLaII cell lines stably expressing the vector alone and various TRF1 alleles. TIN2-ChIP analyses revealed that there was no impairment in the association of TIN2 with telomeric DNA in various TRF1 alleles (Figure 3.8). Western analysis also confirms that TRF1-depletion and expression of various TRF1 alleles mutants did not alter the expression levels of TIN2 (Figure 3.10A). These results suggest that TRF1 phosphorylation on T271 is not involved in the regulation of telomeric association of TIN2.

TRF2, like TRF1, binds to telomeric DNA. Conceivably, it was possible that a reduction in the level of telomere-bound TRF1 might lead to a change in telomeric association of TRF2. To investigate if TRF1 phosphorylation on T271 might affect telomeric association of TRF2, I performed TRF2-ChIP analysis. Similar to TIN2-ChIP, no significant difference was observed in the level of recovered telomeric DNA following

TRF2-IP (Figure 3.9). The expression level of TRF2 remain unchanged across all cell lines (Figure 3.10B). Taken together, these results suggest that TRF1 phosphorylation on T271 is important for the binding of TRF1 on telomeres, which is important for the negative regulation of telomere elongation. Yet, the same phosphorylation does not play a role in regulating the association of TIN2 and TRF2's association with telomeric DNA.

A

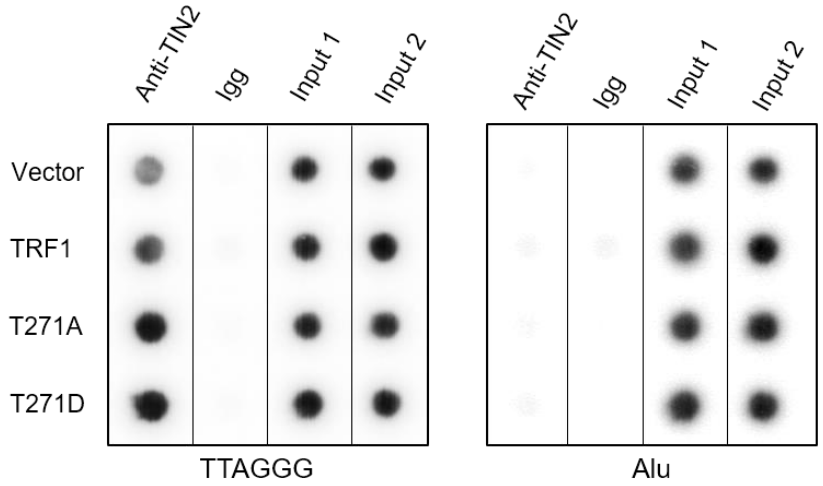

B

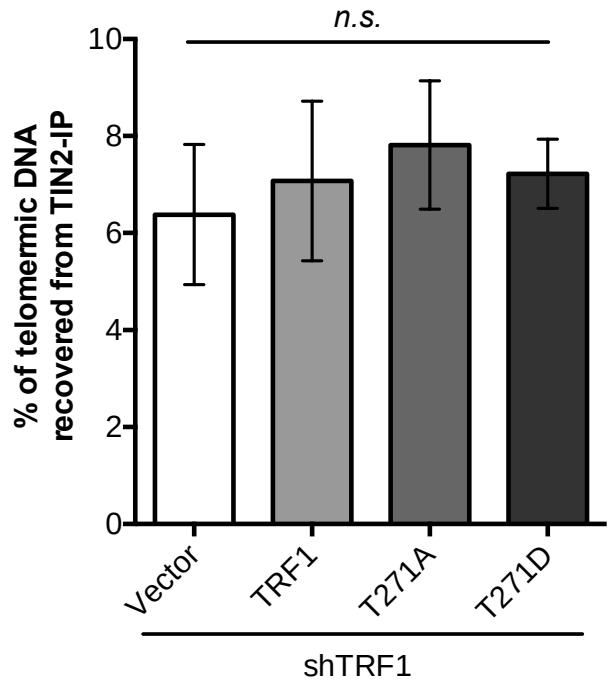

Figure 3.8 – TRF1 Phosphorylation on T271 does not affect TIN2's association with telomeric DNA. A) Dot blots of anti-TIN2 ChIPs from TRF1-depleted HeLaII cells expressing various constructs as indicated on the left. **B)** Quantification of anti-TIN2 ChIPs from (A). Standard deviations from three independent experiments are indicated.

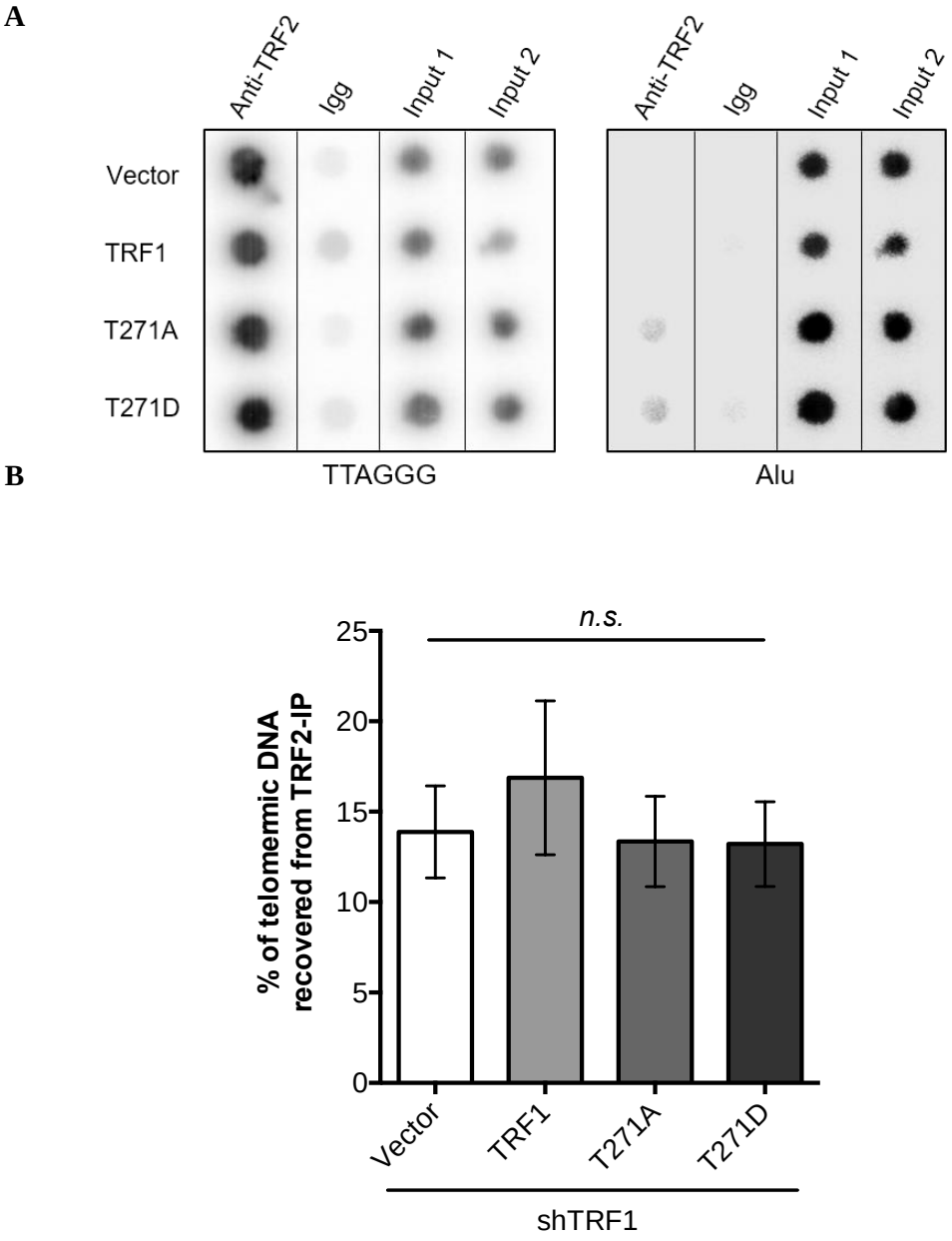

Figure 3.9 – TRF1 Phosphorylation on T271 does not affect TRF2's association with telomeric DNA. A) Dot blots of anti-TRF2 ChIPs from TRF1-depleted HeLaII cells expressing various constructs as indicated on the left. **B)** Quantification of anti-TRF2 ChIPs from (A). Standard deviations from three independent experiments are indicated.

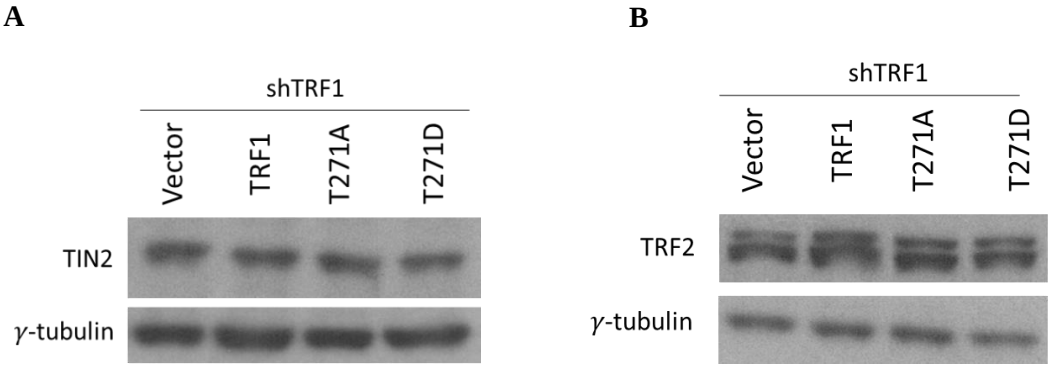

Figure 3.10 - Western analysis of shelterin subunits in TRF1-depleted HeLaII cells stably expressing the vector alone or various TRF1 alleles as indicated. A) Western analysis of TIN2 levels in TRF1-depleted HeLaII cells expressing various constructs as indicated. Immunoblotting was performed using anti-TIN2 and anti-γ-tubulin antibodies. **B)** Western analysis of TRF2 in TRF1-depleted HeLaII cells expressing various constructs as indicated. Immunoblotting was performed using anti-TRF2 and anti-γ-tubulin antibodies.

3.4 TRF1 Phosphorylation on T271 is needed to support APB formation.

In human cells, telomere length maintenance can also occur in a telomerase-independent fashion, also referred to as alternative lengthening of telomeres (ALT). In ALT cells, the production of C-circles and ALT-associated PML bodies (APBs) are key quantifiable hallmarks and an indirect measure of ALT activity in cells (Henson et al., 2002; Osterwald et al., 2015; Stagno D'Alcontres, Mendez-Bermudez, Foxon, Royle, & Salomoni, 2007). We have also recently reported that TRF1 is implicated in the production of C-circles and APB formation (Wilson et al., 2016) – see also CHAPTER 4. To this end, I wanted to assess whether TRF1 phosphorylation of T271 might be involved in regulating the formation of APBs by examining the colocalization of TRF2 and Rap1 with PML bodies in TRF1-depleted GM847 ALT cells expressing the vector alone and the various TRF1 alleles, which have been previously generated (Wilson, 2014).

Using indirect immunofluorescence, I observed that wild type TRF1 was able to rescue the formation of APBs as demonstrated by an approximately 10% increase in the number of GM847 cells exhibiting TRF2 or Rap1 colocalization with PML following TRF1-depletion (Figure 3.11 A-D). Conversely, overexpression of the TRF1-T271A mutant was unable to rescue APB formation. It has been reported that cells with APBs are predominately in S/G2/M phases of the cell cycle (Grobelny et al., 2000; G Wu et al., 2000). To this end, it was formally possible that the observed decrease in APB formation might arise from a dysregulated cell cycle profile in cells overexpressing the TRF1-T271A mutant. When cells positive for cyclin-A was

analyzed, the percentage of GM847 cells in S/G2 phase did not appear to be altered (Figure 3.11E), suggesting that overexpression of the TRF1-T271A mutant allele does not alter the cell cycle profile in GM847 cells. Interestingly, overexpression of the TRF1-T271D phosphomimic mutant was also unable to rescue APB formation (Figure 3.11 A-D), which indicates that the T271D mutation may not effectively mimic T271 phosphorylation. Moreover, overexpression of various TRF1 mutant alleles had little impact on the endogenous level of either TRF2 or hRap1, indicating that the changes observed in their localization to PML bodies could not be due to a variation in protein levels (Figure 3.11 F, G). Taken together, the impaired localization of TRF2 and Rap1 to PML suggests that TRF1 phosphorylation on T271 is needed and important to support the formation of APBs in ALT cells.

A

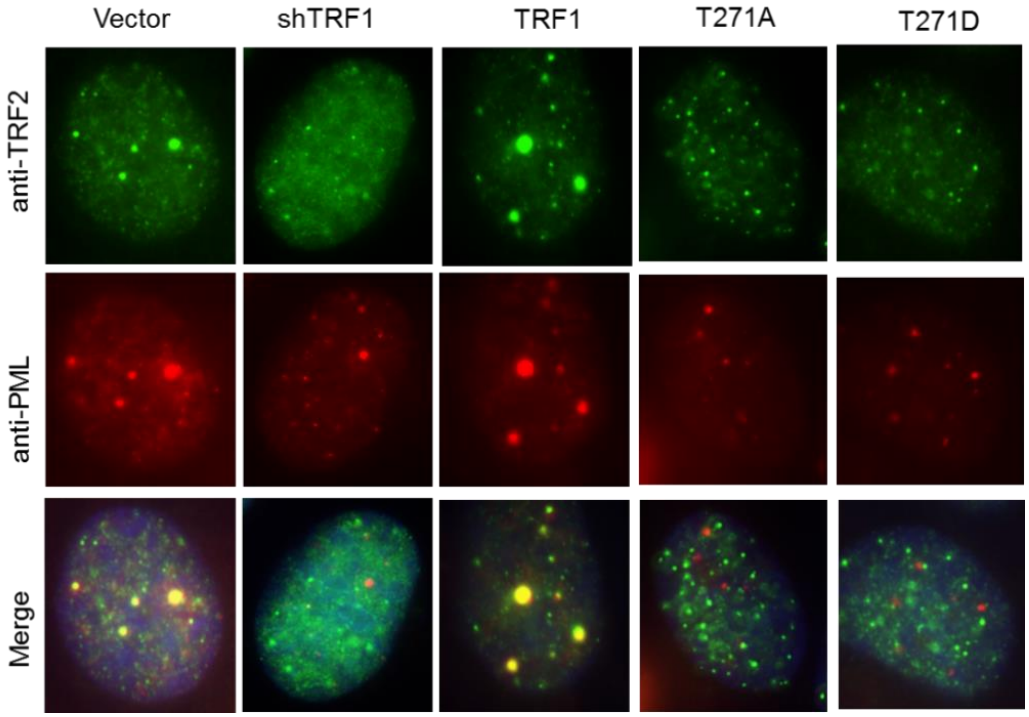
Vector
shTRF1
TRF1
T271A
T271D
anti-TRF2
anti-PML
Merge

B

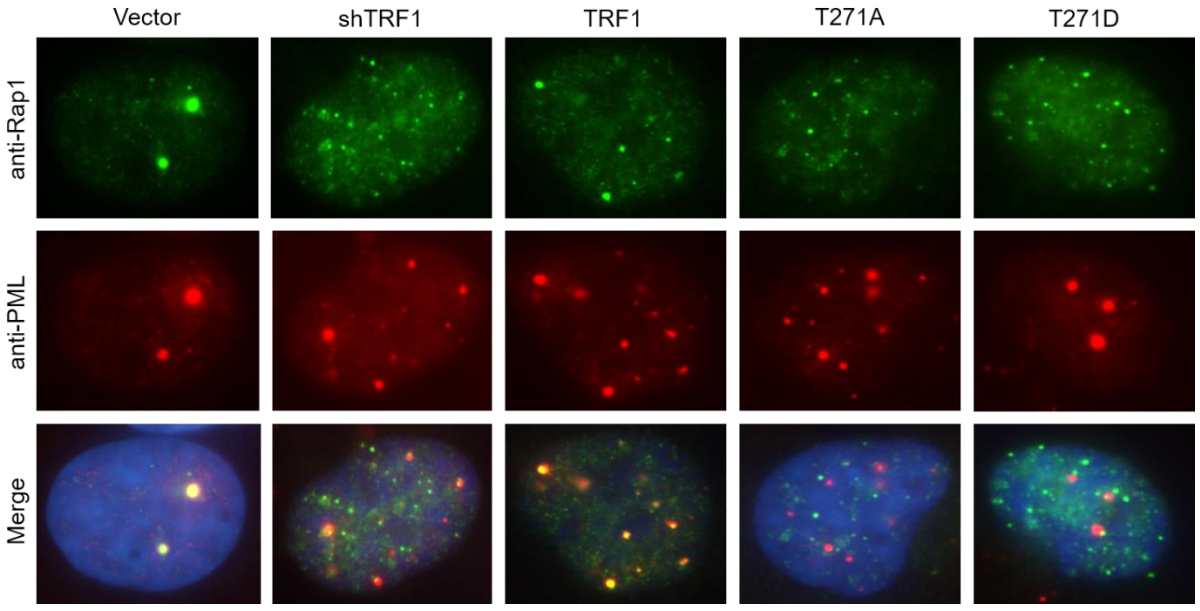
Vector
shTRF1
TRF1
T271A
T271D
anti-Rap1
anti-PML
Merge

C

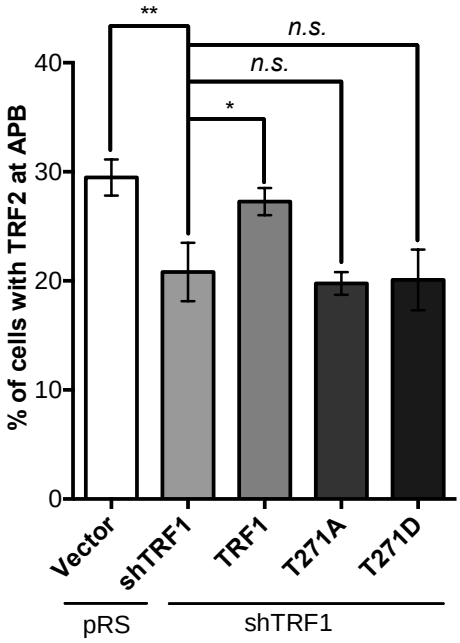
**
n.s.
n.s.
*
% of cells with TRF2 at APB
40
30
20
10
0
Vector
shTRF1
TRF1
T271A
T271D
pRS
shTRF1

D

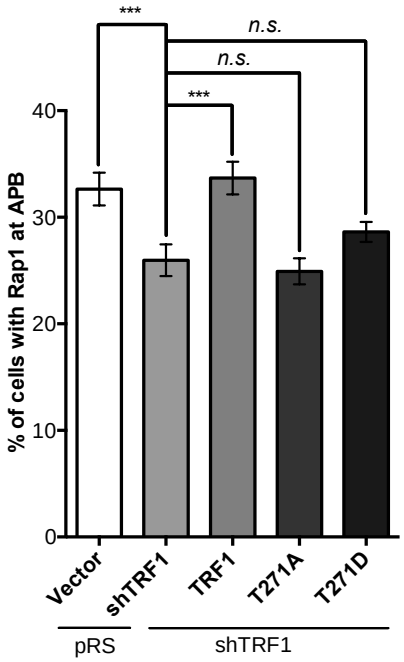
***
n.s.
n.s.
***
% of cells with Rap1 at APB
40
30
20
10
0
Vector
shTRF1
TRF1
T271A
T271D
pRS
shTRF1

E

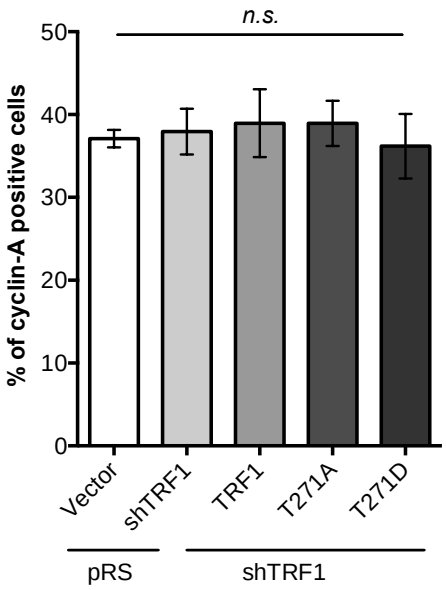
n.s.
% of cyclin-A positive cells
50
40
30
20
10
0
Vector
shTRF1
TRF1
T271A
T271D
pRS
shTRF1

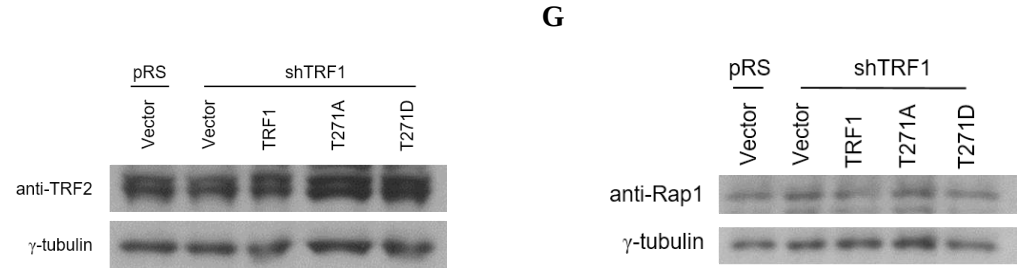

Figure 3.11 – TRF1 phosphorylation on T271 is important for APB formation in ALT cells

A) Indirect immunofluorescence analysis was performed with anti-TRF2 with anti-PML antibodies in GM847 cells expressing various constructs as indicated. Cell nuclei are stained with DAPI in blue as shown in Merge images. **B)** Indirect IF analysis with anti-Rap1 and anti-PML antibodies in GM847 cells expressing various constructs as indicated. **C)** Quantification of the percentage of cells with TRF2 at PML bodies from (A). **D)** Quantification of the percentage of cells with Rap1 at PML bodies from (B). A total of 500 cells from each independent experiment were scored for each cell line in blind. Standard deviations from three independent experiments are indicated. **E)** Quantification of the percentage of cells positive for cyclin-A. A total of 1000 cells from each independent experiment were scored for each cell line in blind. Standard deviations from three independent experiments are indicated. **F)** Western analysis of TRF2 levels in GM847 cells expressing various constructs as indicated. Immunoblotting was performed using anti-TRF2 and anti-γ-tubulin antibodies. **G)** Western analysis of Rap1 levels in GM847 cells expressing various constructs as indicated. Immunoblotting was performed using anti-Rap1 and anti-γ-tubulin antibodies.

3.5 TR1 phosphorylation at T271 is needed to support (pT371)TRF1's localization to PML bodies

Recently, we have reported that Cdk-dependent TRF1 phosphorylation on T371 can act as a molecular switch to create a pool of TRF1, referred to as (pT371)TRF1. We find that phosphorylation of T371 is essential for the formation of APBs, which are key hallmarks of ALT (Wilson et al., 2016). To this end, localization of (pT371)TRF1 at PML bodies can also serve as a marker for APB assembly in cells.

In order to validate whether the phosphorylation site T271 of TRF1 is important for APB formation, as suggested by TRF2/Rap1's localization to PML, I assessed the levels of (pT371)TRF1's localization to PML bodies in TRF1-depleted GM847 cells expressing the various TRF1 alleles. Upon TRF1 depletion, (pT371)TRF1's localization to PML bodies was impaired, and this defect was not rescued when cells were complemented with either the TRF1-T271A or T271D (Figure 3.12). Since the expression level and the staining of (pT371)TRF1 is cell-cycle dependent (McKerlie & Zhu, 2011; Wilson et al., 2016), it was also confirmed that the levels of cyclin-A positive cells did not alter among the various cell lines (Figure 3.11E). These results suggest TRF1 phosphorylation at T271 is needed to support (pT371)TRF1's localization to PML bodies. Collectively, results from analyzing APB formation may further imply that that TRF1 phosphorylation at T271 and T371 may be functionally linked and important for regulating ALT activity.

A

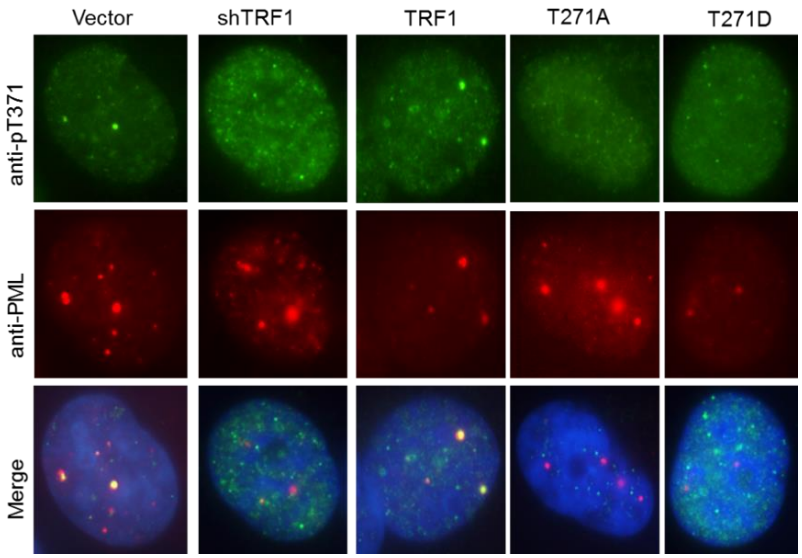

B

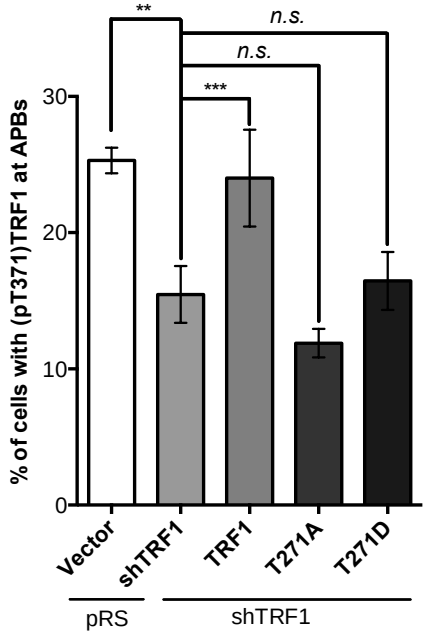

Figure 3.12 - Analysis of cells with (pT371)TRF1 at PML bodies. A) Indirect immunofluorescence analysis was performed with anti-(pT371)TRF1 and anti-PML antibodies. **B)** A total of 1000 cells from each independent experiment were scored for each cell line in blind. Standard deviations from three independent experiments are indicated.

3.6 TRF1 Phosphorylation on T271 is not required to regulate C-circle production in ALT cells.

In addition to APB formation, the production of C-circles is another quantifiable marker of ALT activity in cells (Henson et al., 2009). To investigate whether TRF1 phosphorylation on T271 may regulate the production of C-circles in ALT cells, the levels of C-circles in TRF1-depleted GM847 cells expressing various TRF1 alleles were analyzed. Results from the C-circle assays revealed that upon TRF1 depletion, the levels of C-circles in cells was reduced, which was consistent with an earlier finding that we have previously reported (Wilson et al., 2016). When Myc-tagged TRF1-T271A and TRF1–T271D mutants were overexpressed, both were able to rescue the level of C-circle production in GM847 cells just as well as wild type TRF1 (Figure 3.13). These results suggest that TRF1 phosphorylation on T271 is not involved in the regulation of C-circle productions. This further implies that there may be a separate regulatory function of phosphorylated TRF1 at T271 in APB formation, despite the fact that both APB and C-circles are quantifiable markers of ALT activity in cells.

A

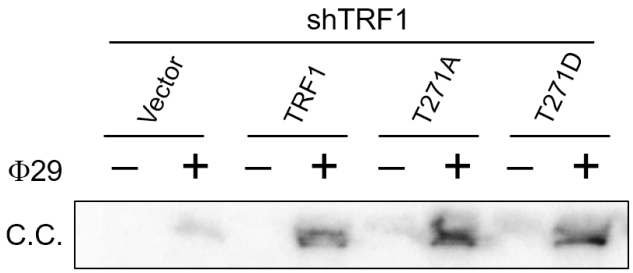

B

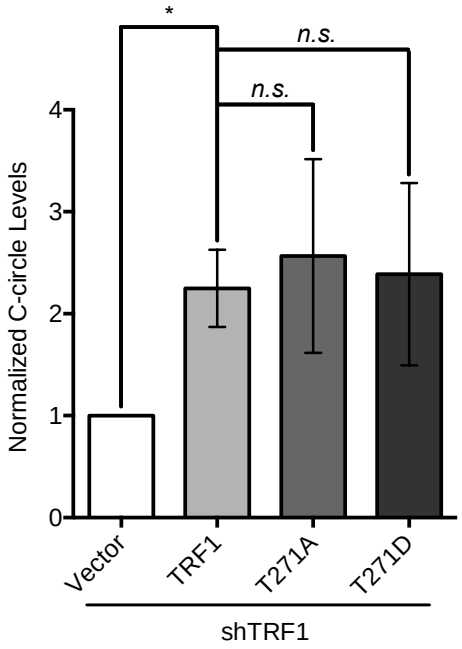

Figure 3.13 – TRF1 phosphorylation at T271 does not influence the production of C-circles. **A)** C-circle (C.C.) amplification assay was performed in TRF1-depleted GM847 cells expressing various TRF1 constructs as indicated. 50ng of DNA was used per amplification reaction. **B)** Quantification of the relative level of C-circles from (A). Signals were quantified using ImageQuantTL (G.E. Healthcare). The levels of C-circles for Myc-tagged TRF1, TRF1-T271A, and TRF-T271D were normalized relative to the levels of C-circles in TRF1-depleted GM847 cell lines. Since comparisons are made to a normalized value (i.e. Vector control), P-values are calculated by Student's t-test to account for the significance for each pair of individual comparison. Standard deviations from three independent experiments are indicated.

CHAPTER 4 TRF1 PHOSPHORYLATION ON T371 REGULATES APB FORMATION AND THE PRODUCTION OF C-CIRCLES IN ALT CELLS

Preface

The second part of this thesis discusses the study on the functional analysis of phosphorylation site threonine-371 (T371) of TRF1 in telomerase-independent telomere maintenance, or the ALT pathway, was a continuation of the work started by a former graduate student (Wilson, 2014). It has been the majority of the first half of my Masters' work. This work has resulted in a co-authorship publication. The work was published on pages 2559-2572 of Volume 129, No. 13, doi: 10.1242/jcs.186098. The complete citation is as follow:

Wilson, F. R., Ho, A., Walker, J. R., & Zhu, X.-D. (2016). **Cdk-dependent phosphorylation regulates TRF1 recruitment to PML bodies and promotes C-circle production in ALT cells.** *Journal of Cell Science*, 129(13), jcs.186098. http://doi.org/10.1242/jcs.186098

Briefly, previous work has demonstrated that phosphorylation of TRF1 at T371 causes TRF1 to preferentially associate with ALT telomeres in a cell-cycle dependent manner. In addition, it was also shown that the association of (pT371)TRF1's localization to APBs is dependent upon factors important for homologous-recombination (HR) activity. This observation strongly suggests a functional role of (pT371)TRF1 in regulating HR-mediated mechanism of the ALT pathway. Nevertheless, how TRF1 effects this regulation is poorly understood. My contribution to the work sets out to dissect the underlying

mechanism, and to provide functional insights as to how (pT371)TRF1 regulates telomere maintenance in ALT cells.

N.B. - Usage of figures (without obscuring the information or context of the data) from the original publication, and/or full paper (DOI: http://doi.org/10.1242/jcs.186098) is reproduced/adapted with permission of *Journal of Cell Science*, The Company of Biologists. Authors (Wilson, F. R., Ho, A., Walker, J. R., & Zhu, X.-D.) retain copyright of the article.

4.1 Phosphorylation of TRF1 on T371 peaks in S/G2 phases in ALT cells.

It has been reported that Cdk1 phosphorylates TRF1 on T371 (McKerlie & Zhu, 2011). In ALT cells, 80%-90% of cells that exhibit punctate (pT371)TRF1 staining were also positive for cyclin-A staining suggesting that the expression of (pT371)TRF1 may be cell-cycle regulated (Wilson et al., 2016). To investigate whether Cdk activity regulates the punctate staining of (pT371)TRF1 in ALT cells, a cell synchronization experiment using double-thymidine block was performed in GM847 cells. Western analysis using a phospho-specific anti-(pT371)TRF1 antibody revealed that the level of (pT371)TRF1 increased overtime and peaked at 10h post release of the thymidine block (Figure 4.1B). The level of total endogenous TRF1 was assessed, and no apparent change in expression level was observed following double-thymidine release, which argued against the possibility that the observed changes on the level of (pT371)TRF1 is due to a reduction in TRF1 level (Figure 4.1B). Moreover, when cells were analyzed for (pT371)TRF1 staining across the cell cycle using indirect immunofluorescence (IF), the percentage of cells positive for (pT371)TRF1 staining was also consistent with the dynamics of (pT371)TRF1 levels observed by western analysis (Fig 4.1A,D). Similar results were obtained when the same experiment was performed in U2OS cells (Fig 4.1A,C,E). These results suggest that the level of (pT371)TRF1 steadily increases as cells enter into S phase and finally peak upon mitotic entry, which is consistent with earlier findings (McKerlie & Zhu, 2011). Altogether, these results suggest that Cdk-mediated T371 phosphorylation is cell-cycle regulated, peaking in S/G2 phase and into early mitosis. This further implies that the lack of (pT371)TRF1

staining in G1 cells is likely due to a lack Cdk activity (McKerlie & Zhu, 2011; Wilson et al., 2016).

A

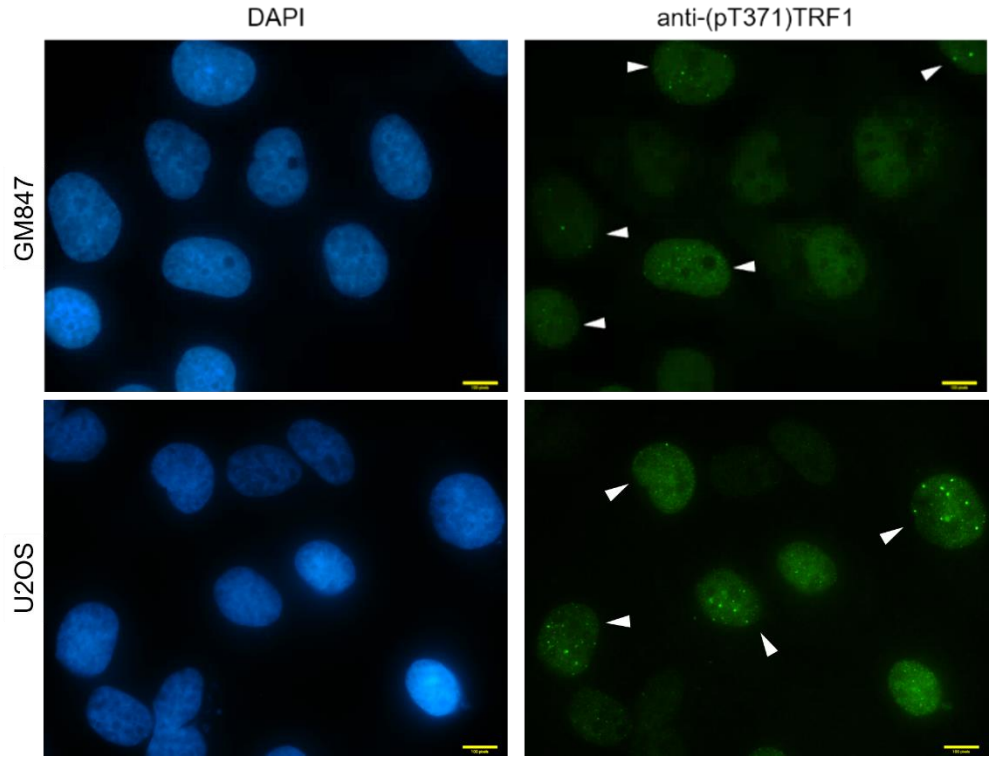
DAPI
anti-(pT371)TRF1
GM847
U2OS

B

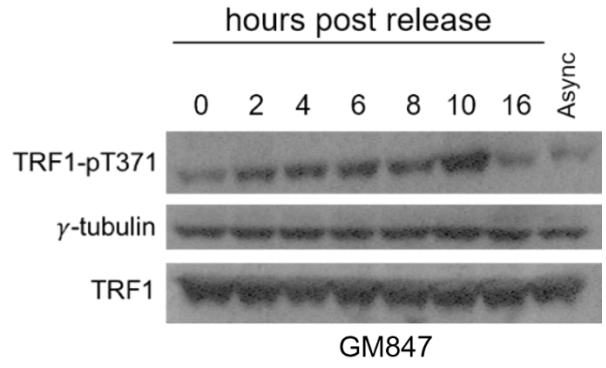
hours post release
0
2
4
6
8
10
16
Async
TRF1-pT371
γ-tubulin
TRF1
GM847

C

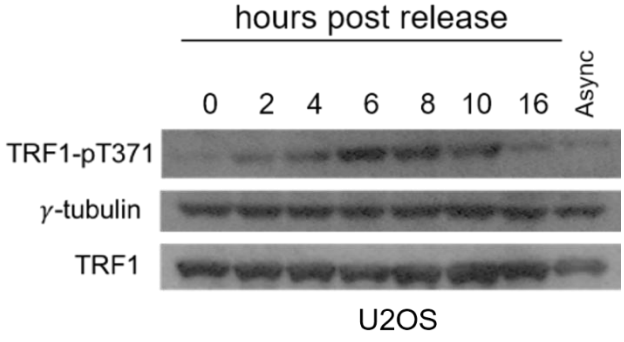
hours post release
0
2
4
6
8
10
16
Async
TRF1-pT371
γ-tubulin
TRF1
U2OS

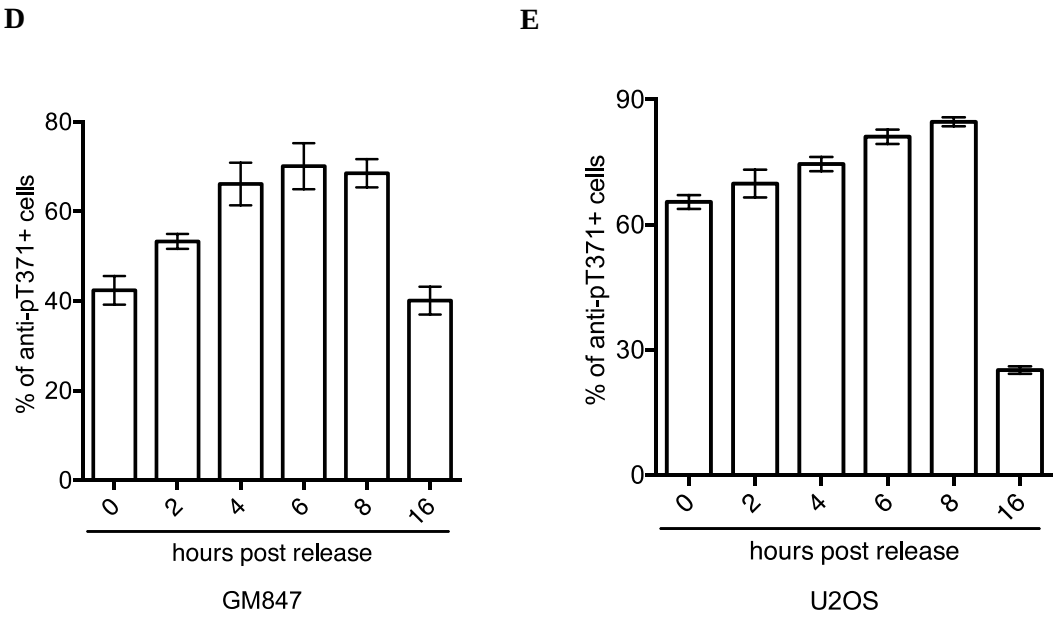

Figure 4.1 – Analysis on the level of phosphorylated (pT371)TRF1 across the cell cycle in ALT cells. **A)** Indirect immunofluorescence analysis of (pT371)TRF1 staining in GM847 and U2OS cells. Representative images are shown; cells are considered positive for (pT371)TRF1 staining if they contain bright, punctate and/or APB-like foci (i.e. cells indicated by white arrows). **B)** Western blot analysis for (pT371)TRF1 following double thymidine block release in GM847 cells. Immunoblotting was performed using anti-(pT371)TRF1, anti-TRF1, or anti-γ-tubulin antibodies. **C)** Western blot analysis for (pT371)TRF1 following double thymidine block release in U2OS cells. Immunoblotting was performed using anti-(pT371)TRF1, anti-TRF1, or anti-γ-tubulin antibodies. **D)** Quantification of the percentages of GM847 cells with (pT371)TRF1 staining following cell synchronization. Triplicates of at least 1000 cells were scored at indicated time points. Error bars represent standard deviations from three independent experiment. **E)** Quantification of the percentages of U2OS cells with (pT371)TRF1 staining following cell synchronization as described in (C).

4.2 Phosphorylated (pT371)TRF1 is preferentially associated with dysfunctional telomere ends in ALT cells

The observed punctate telomere-like staining of (pT371)TRF1 prompted us to ask whether (pT371)TRF1 may be associated with ALT telomeres. Using combined indirect immunofluorescence and fluorescence in-situ hybridization (IF-FISH), it was found that all punctate anti-pT371 foci seemed to colocalize well with telomeric DNA (detected by FITC-conjugated PNA probe), but not all telomere foci contained detectable (pT371)TRF1 staining (Wilson et al., 2016), which suggests that (pT371)TRF1 is associated with a subset of interphase ALT telomeres.

It has been previously reported that, in telomerase-positive cells, (pT371)TRF1 has been found to be recruited to sites of DNA damage to facilitate homologous-recombination (McKerlie et al., 2013). Interestingly, telomeres in ALT cells can be recognized as damaged DNA, and have also been reported to associate with DNA repair factors (Cho, Dilley, Lampson, & Greenberg, 2014; Dunham et al., 2000; Fasching et al., 2007; Marzec, Armenise, Roumelioti, Basyuk, & Gagos, 2015; Guikai Wu et al., 2003). To this end, I wanted to further investigate the nature of (pT371)TRF1's association with telomeres. In agreement with previous findings that ALT cells contain high levels of genome instability (Marzec et al., 2015), high levels of γH2AX staining was observed in GM847 cells (Figure 4.2A) with an estimation of at least 80% of GM847 cells containing γH2AX foci (Figure 4.2B). To this end, dual indirect IF analysis using anti-(pT371)TRF1 and anti-γH2AX antibodies revealed that the association of (pT371)TRF1 with γH2AX was cell-cycle regulated, with its highest level at 8 hours, and then to the lowest at 16 hours

post double thymidine block (Figure 4.2C). The highest level of colocalization between (pT371)TRF1 and γH2AX foci was observed in cells with more than 15 γH2AX foci. In addition, (pT371)TRF1 was often found to be associated with telomeres enriched for γH2AX on metaphase chromosome spreads (Wilson et al., 2016). Altogether, these results suggest that, in ALT cells, (pT371)TRF1 is preferentially associated with dysfunctional telomeres and that its localization to telomeres may be a response to DNA damage at the telomeric sites.

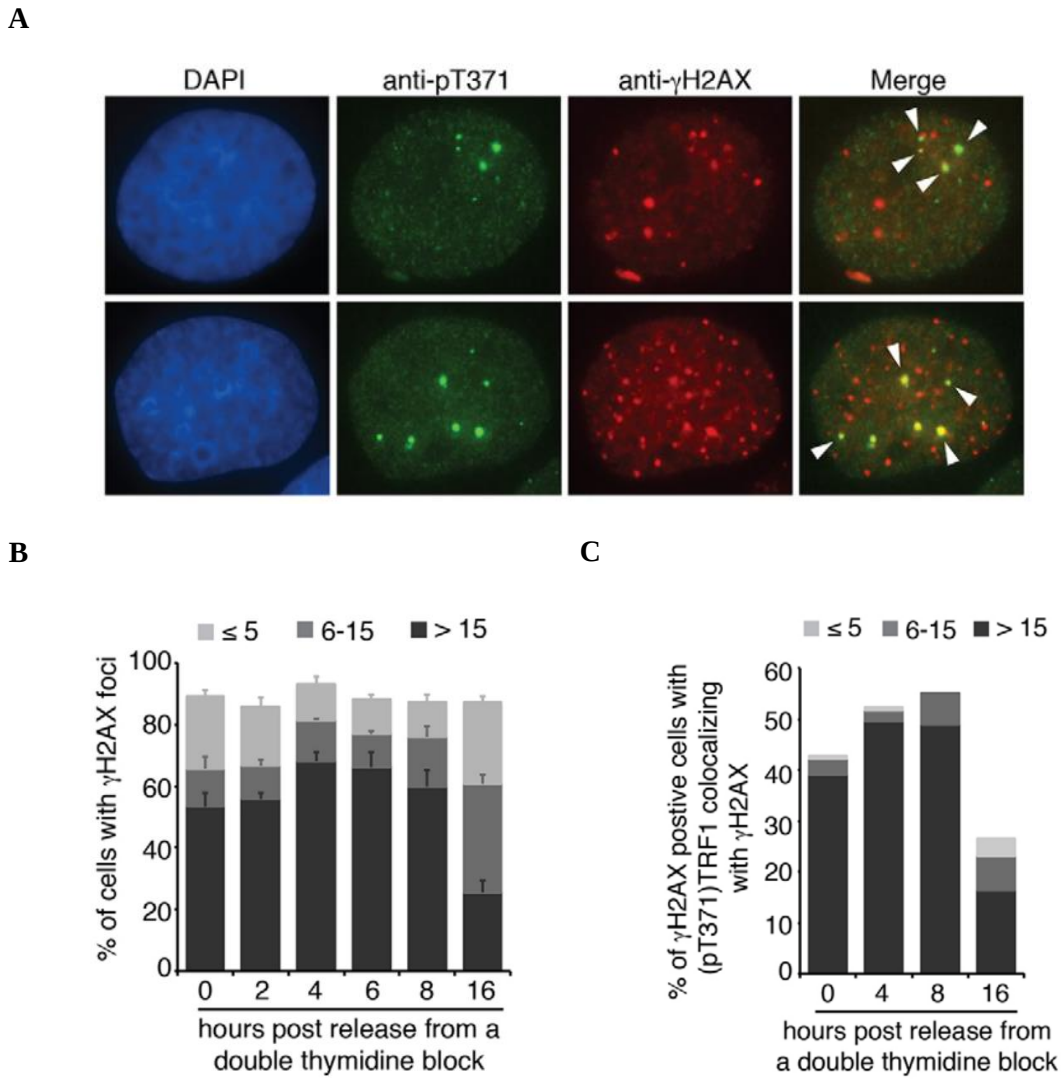

Figure 4.2 – Phosphorylated (pT371)TRF1 is associated with a subset of ALT telomeres that are predominantly dysfunctional. A) Immunofluorescence analysis of interphase GM847 cells with both anti-pT371 and anti-γH2AX antibodies. Arrowheads indicate colocalization of (pT371)TRF1 with γH2AX foci. **B)** Quantification of the percentage of synchronized GM847 cells exhibiting γH2AX foci as indicated. A total of 1000 cells from each independent experiment were scored in blind. Standard deviations from three independent experiments are indicated. Light grey bars, 1-5 γH2AX foci per cell; dark grey bars, 6-15 γH2AX foci per cell; black bars, >15 γH2AX foci per cell. **C)** Quantification of the percentage of γH2AX-positive GM847 cells exhibiting

(pT371)TRF1 colocalization with γH2AX foci as indicated. Scoring of colocalization was done in blind from captured cell images. The number of cells scored for each time point: 171 (0 h); 149 (4 h); 149 (8 h) and 208 (16 h). Light grey bars, 1-5 γH2AX foci per cell; dark grey bars, 6-15 γH2AX foci per cell; black bars, >15 γH2AX foci per cell. (Taken from Wilson et al., 2016)

4.3 Phosphorylated (pT371)TRF1 is needed to support the formation of ALT-associated PML bodies (APBs)

TRF1 is a component of APBs and is crucial for its assembly in ALT cells (Chung et al., 2011; Potts & Yu, 2007; Guikai Wu et al., 2003). One of the key hallmarks of ALT activity is the presence of APBs, which are nuclear bodies that contain components of the shelterin complex, and repair factors such as NBS1, all of which are crucial for the formation of APBs (Chung et al., 2011; Grobelny et al., 2000; Naka, Ikeda, & Motoyama, 2002; Z.-H. Zhong et al., 2007). In order to investigate whether phosphorylation of TRF1 at T371 could play a role in the assembly of APBs, we first asked the question whether (pT371)TRF1 might be a component of APBs. Using indirect IF and IF-FISH, we have shown that, in both U2OS and GM847 cells, (pT371)TRF1 colocalizes with PML foci, which also contains telomeric DNA (Wilson et al., 2016). Moreover, when TRF1 is depleted in GM847 cells, the localization of (pT371)TRF1, as well as the localization of TRF2, Rap1, TIN2, and NBS1 to PML bodies were impaired, which strongly suggests a role for TRF1 in regulating the functional assembly of APB in ALT cells (Wilson et al., 2016). Unlike Myc-tagged wild type TRF1, Myc-tagged-TRF1 carrying an unphosphorylatable T371A mutation failed to rescue the localization of (pT371)TRF1, TRF2, Rap1, TIN2, and NBS to PML bodies in TRF1-depleted GM847 cells (Wilson et al., 2016). These results demonstrate that (pT371)TRF1 is part of APB.

It is posited that APBs could serve as sites of homologous-recombination mediated telomere elongation in ALT cells (Fasching et al., 2007; Henson et al., 2002), and thus I wanted to asked whether DNA synthesis at APBs might be affected in GM847 cells

expressing the TRF1-T371A mutant. The generation of single stranded DNA (ssDNA) is a key intermediate of homologous recombination activity; as a result, I performed indirect immunofluorescence with an anti-BrdU antibody with an anti-PML antibody under denaturing condition (Figure 4.3A). IF analysis revealed that in GM847 cells expressing the vector alone, up to 9% of cells exhibited the presence of ssDNA at APBs. Depletion of TRF1 led to a significant decrease in the percentages of cells containing ssDNA at APBs, and this defect was rescued by a complementation of Myc-tagged wild type TRF1, but not by Myc-tagged TRF1 mutant carrying the T371A mutation (Figure 4.3B). Taken together, these results suggest that phosphorylation of TRF1 on T371 is necessary for the functional assembly of APBs by facilitating HR-mediated telomere synthesis at APBs.

A

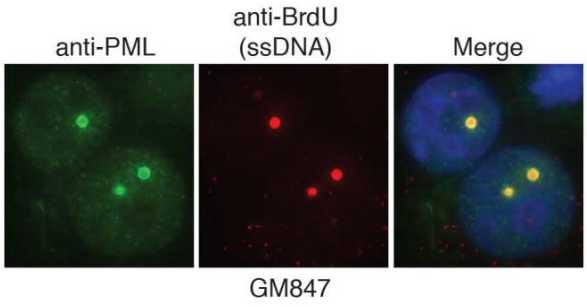

B

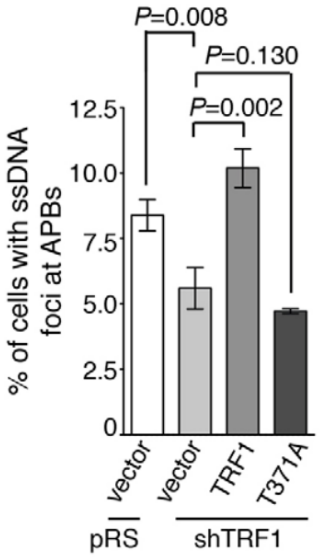

Figure 4.3 – Phosphorylation of TRF1 at T371 is necessary to support homologous-recombination activity at APB. A) Dual indirect immunofluorescence of GM847 cells with an anti-PML antibody in conjunction with an anti-BrdU antibody. **B)** Quantification of the percentage of cells with ssDNA foci at APBs. GM847 cells as indicated were incubated in the presence of 10 µM BrdU (Sigma) for 24h prior to immunofluorescence analysis with anti-BrdU and anti-PML antibodies. A total of 1000 cells from each independent experiment were scored for each cell line in blind. Standard deviations from three independent experiments are indicated. (Taken from Wilson et al., 2016)

4.4 The telomeric binding activity of TRF1 is crucial for the production of C-circles in ALT cells.

Another key indicator of ALT activity in cells is the generation of C-circles. Thus, to examine the role of T371 phosphorylation in the production of C-circles, C-circle assays were performed. Analysis of C-circle assays revealed that TRF1 depletion in GM847 cells resulted in a decrease in the level of C-circles. Although overexpression of Myc-tagged wild type TRF1 suppressed the reduction in the level of C-circles in TRF1-depleted cells, overexpression of Myc-tagged TRF1 carrying T371A mutation failed to do so (Wilson et al., 2016). In telomerase-positive cells, it has been shown that the DNA binding ability of TRF1 is crucial for the regulation of telomere length maintenance (Broccoli, Smogorzewska, et al., 1997; Chang, 2003; Hanaoka et al., 2005). Thus, I wanted to ask whether TRF1's DNA binding ability might play a role in facilitating ALT activity, such as the production of C-circles. C-circle assay revealed that when TRF1 was depleted, the level of C-circles was reduced. As expected, introduction of Myc-tagged wild type TRF1 rescued the level of C-circles in TRF1-depleted cells, but overexpression of Myc-tagged TRF1-ΔM (Myb-like DNA binding domain deletion mutant) failed to rescue the level of C-circles back to wild type levels (Figure 4.4). Taken together, these results indicate that T371 phosphorylation and the DNA binding activity of TRF1 plays a crucial role in facilitating the production in C-circles.

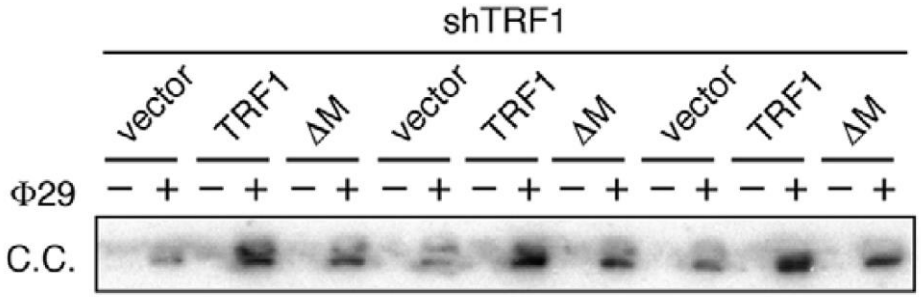

Figure 4.4 - The Myb-like DNA binding domain of TRF1 is required for C-circle production. Analysis of C-circle formation. 50ng of DNA was used for each reaction. The blot represents three pairs of C-circle assays from three independent experiments. C.C., C-circles. (Taken from Wilson et al., 2016)

4.5 Transcription-associated DNA damage at telomeres mediates the association of (pT371)TRF1 with APBs

Recently, it has been reported that transcription of telomeric DNA, and hence TERRA levels, are upregulated in ALT cells (Arora et al., 2014; Azzalin, Reichenbach, Khoriauli, Giulotto, & Lingner, 2007). Replication and transcription machinery can compete for the same DNA template and can therefore interfere with each other. Transcription can arrest DNA synthesis and compromise replication fork stability, thus causing replication stress. Upon fork arrest or collapse, DNA damage may result from collisions of replication and transcription machineries (Brambati, Colosio, Zardoni, Galanti, & Liberi, 2015; Olavarrieta, Martínez-Robles, Hernández, Krimer, & Schvartzman, 2002). We propose that enhanced transcription at ALT telomeres could give rise to a source of DNA damage, which might trigger the recruitment of (pT371)TRF1 to APBs. To investigate this hypothesis, GM847 cells were treated with transcription inhibitors, DRB and Actinomycin D. Analysis of indirect immunofluorescence with an anti-TRF2 antibody and anti-γH2AX, a marker for DNA damage, revealed that treatment with DRB impaired the colocalization of TRF2 and γH2AX (Figure 4.5A,B). This result suggests that ALT telomeres are associated with transcription-induced DNA damage.

Consistent with the notion of transcription-induced DNA damage being a source of DNA damage to stimulate the localization of (pT371)TRF1 at APBs, DRB and ActinomycinD treatments also significantly reduced the percentage of GM847 cells exhibiting (pT371)TRF1 association with APBs (Figure 4.5C-E). Similar results were also observed in U2OS cells (Figure 4.5F-H). As a control, PML foci were quantified to ensure

that the observed changes in the level of (pT371)TRF1 at APBs was not due to a change in the level of PML foci following DRB treatments (Figure 4.5G,H). Transcription inhibitor treatment did not affect the percentage of cells that were cyclin A-positive, suggesting that any changes observed on the level of (pT371)TRF1 foci is unlikely due to a change in cell cycle profile (Figure 4.5H), nor did it affect the percentage of cells with PML bodies (Figure 4.5I,J). Western analysis demonstrated that the level of (pT371)TRF1 and PML expressions remained unchanged after treatments with DRB or Actinomycin D (Figure 4.5K,L.). Collectively, these results suggest that the association of (pT371)TRF1 with APBs is dependent upon active transcription, and that this association may be triggered by transcription-induced DNA damage at telomeres.

ATM has been shown to be important for regulating (pT371)TRF1's recruitment to sites of DNA damage (McKerlie et al., 2013). Moreover, we have also shown that (pT371)TRF1's localization to APB is also mediated by ATM (Wilson et al., 2016). To this end, I wanted to further investigate whether there might exist an epistatic relationship between ATM and transcription in the regulation of (pT371)TRF1's association with APBs. GM847 cells were subjected to ATM inhibitor KU55933 and transcription inhibitor DRB treatments. Using indirect immunofluorescence with anti-(pT371)TRF1 and anti-PML antibodies, I observed that a combined treatment with both KU55933 and DRB did not lead to any further reduction in the localization of (pT371)TRF1 to APBs compared to the treatment with either KU55933 or DRB (Figure 4.5N). These results indicate that ATM and transcription act in the same epistatic pathway in regulating the recruitment of (pT371)TRF1 to APBs.

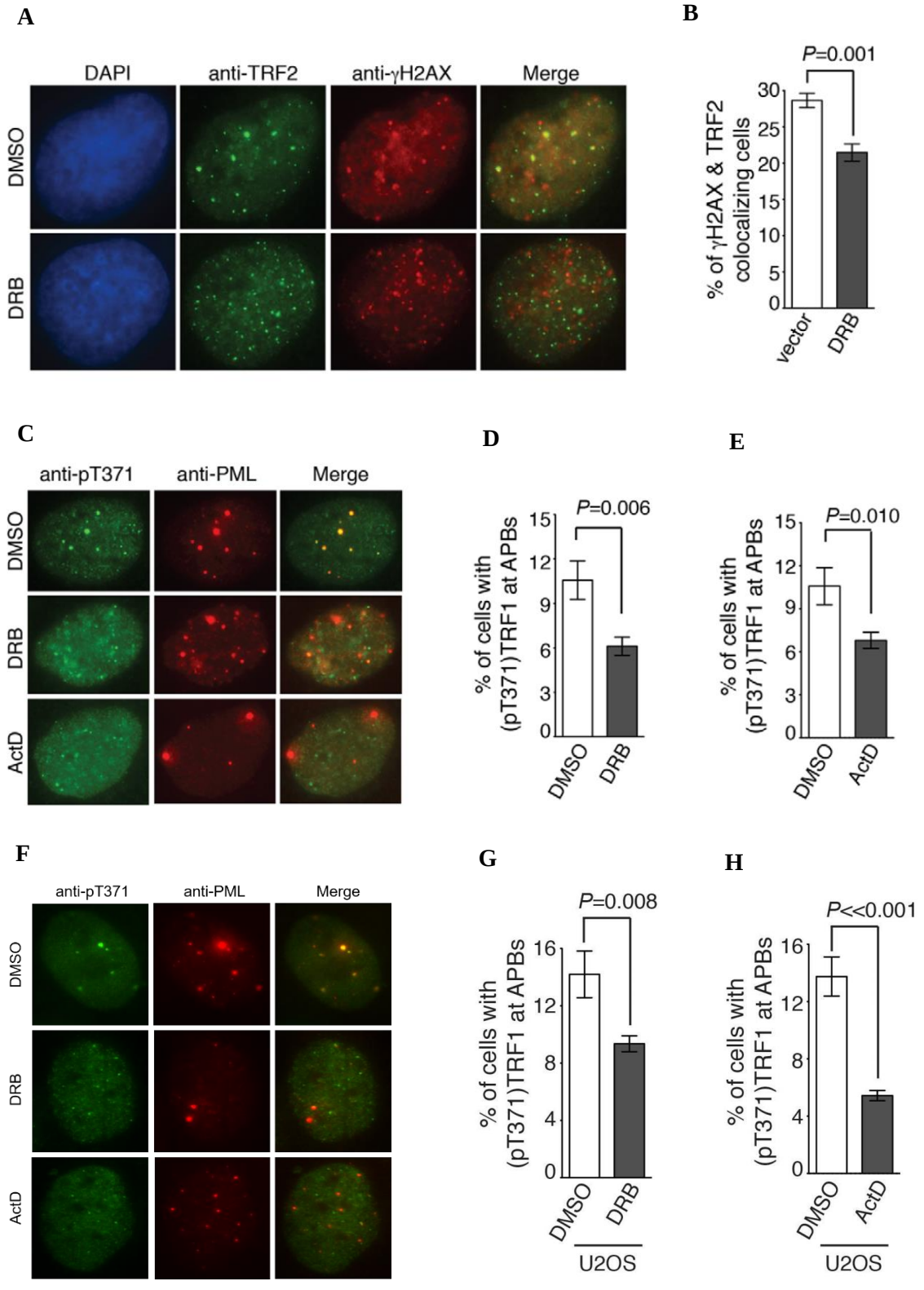
A
DAPI
anti-TRF2
anti-γH2AX
Merge
DMSO
DRB
B
P=0.001
% of γH2AX & TRF2 colocalizing cells
30
25
20
15
10
5
0
vector
DRB
C
anti-pT371
anti-PML
Merge
DMSO
DRB
ActD
D
P=0.006
% of cells with (pT371)TRF1 at APBs
15
12
9
6
3
0
DMSO
DRB
E
P=0.010
% of cells with (pT371)TRF1 at APBs
15
12
9
6
3
0
DMSO
ActD
F
anti-pT371
anti-PML
Merge
DMSO
DRB
ActD
G
P=0.008
% of cells with (pT371)TRF1 at APBs
16
12
8
4
0
DMSO
DRB
U2OS
H
P<<0.001
% of cells with (pT371)TRF1 at APBs
16
12
8
4
0
DMSO
ActD
U2OS

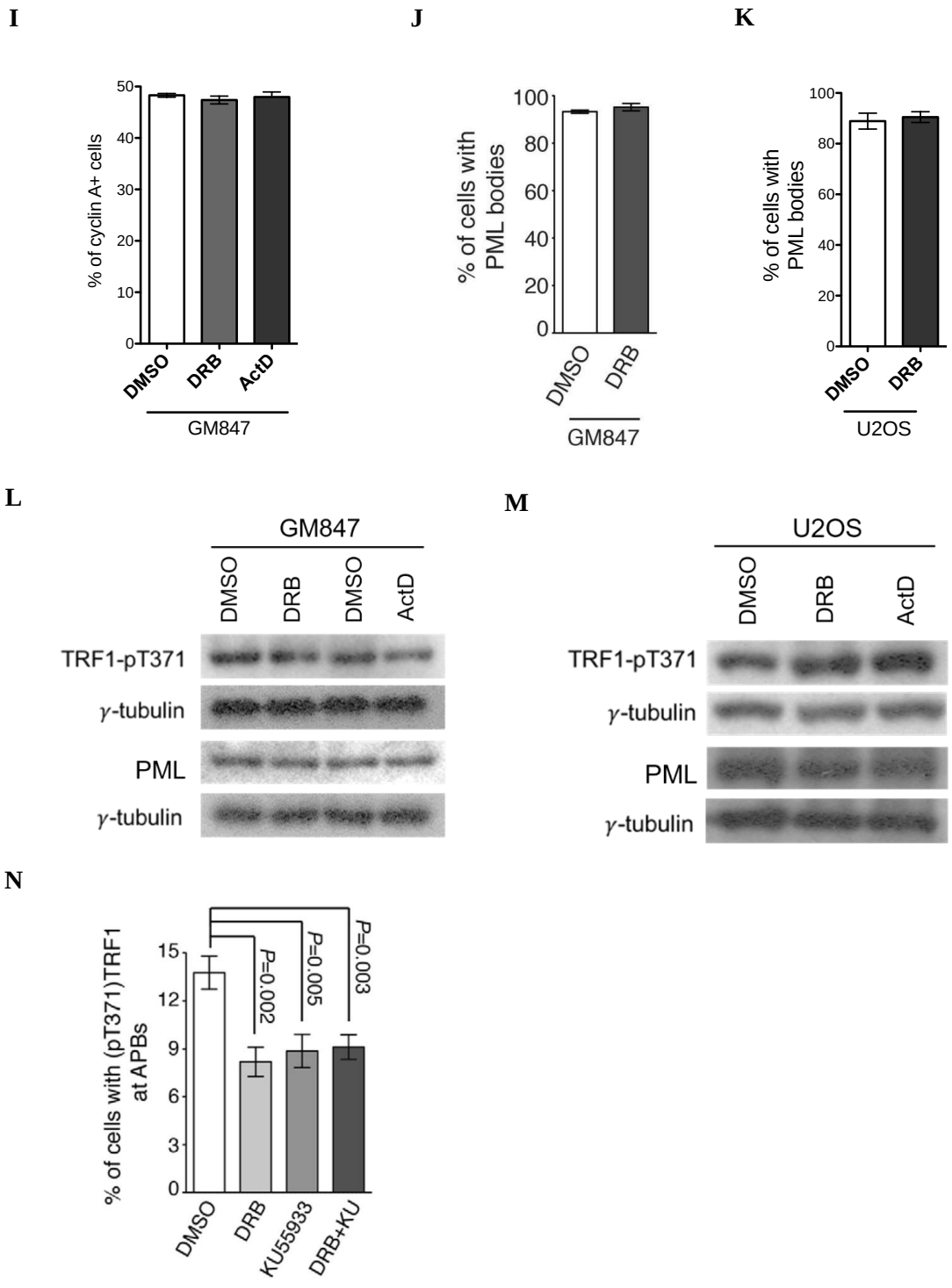

Figure 4.5 – Transcription inhibition reduces telomeric accumulation of γH2AX and impairs (pT371)TRF1 interaction with APBs in GM847 cells. A) Immunofluorescence analysis of

staining with anti-TRF2 or anti-γH2AX antibodies in GM847 cells treated with either DMSO or DRB for 3 h prior to fixation. **B)** Quantification of the percentage of DMSO- and DRB-treated GM847 cells exhibiting TRF2 colocalization with γH2AX. A total of 1000 cells from each independent experiment were scored in blind. Standard deviations from three independent experiments are indicated. **C)** Immunofluorescence analysis of staining with anti-pT371 and anti-PML antibodies in GM847 cells treated with DMSO, DRB or actinomycin D (ActD). Treatment with ActD was done for 2 h whereas treatment with DRB was carried out for 3 h. **D)** Quantification of the percentage of DMSO- and DRB-treated GM847 cells exhibiting (pT371)TRF1 at APBs. Scoring was done as described in B. Standard deviations from three independent experiments are indicated. **E)** Quantification of the percentage of DMSO- and actinomycin-D (ActD)-treated GM847 cel**ls** exhibiting (pT371)TRF1 at APBs. Scoring was done as described in B. Standard deviations from three independent experiments are indicated. **F)** Immunofluorescence analysis of staining with anti-pT371 and anti-PML antibodies in U2OS cells treated with DMSO, DRB or actinomycin D (ActD). Treatment with ActD was done for 2 h whereas treatment with DRB was carried out for 3 h. **G)** Quantification of the percentage of DMSO- and DRB-treated U2OS cells exhibiting (pT371)TRF1 at APBs. Scoring was done as described in B. Standard deviations from three independent experiments are indicated. **H)** Quantification of the percentage of DMSO- and actinomycin-D (ActD)-treated U2OS cells exhibiting (pT371)TRF1 at APBs. Scoring was done as described in B. Standard deviations from three independent experiments are indicated. **I)** Quantification of the percentage of DMSO-, DRB-, and ActD-treated GM847 cells staining positive for cyclin A. Scoring was done as described in B. Standard deviations from three independent experiments are indicated. **J-K)** Quantification of the percentage of DMSO- and DRB-treated GM847 or U2OS cells, as indicated, staining positive for PML bodies. Scoring was done as described in B. Standard deviations from three independent experiments are indicated. **L-M)**

Western analysis of DMSO-, DRB-, and ActD-treated GM847 or U2OS cells as indicated. Immunoblotting was performed with anti-pT371, anti-PML and anti-γ-tubulin antibodies. (Figures 4.4 A-E, G-H, J, and N were taken from Wilson et al., 2016).

4.6 RNA-DNA hybrids modulate the association of (pT371)TRF1 with APBs

A consequence of replication–transcription collisions is the formation of stable RNA-DNA hybrids in molecular structures called R-loops (Skourti-Stathaki & Proudfoot, 2014). R-loops are generated when nascent elongating RNA transcripts hybridize with the DNA template to form RNA-DNA hybrid, and in so doing displaces the non-template ssDNA strand; this three-stranded structure forms the R-loop (Thomas, White, & Davis, 1976). The exposed ssDNA in R-loops can become susceptible to damaging processes such as deamination of cytosine to uracil and can induce DNA double-stranded breaks (DSBs), which could then trigger recombination events (Arora et al., 2014; Thomas et al., 1976). In ALT cells, transcription of telomeric DNA is upregulated, and as such generates a high level of TERRA molecules (Arora et al., 2014; Azzalin et al., 2007). Thus, at the telomeres, DNA-RNA hybrid structures such as TERRA-telomere hybrids are examples of R-loop structures that can be formed. To address whether the localization of (pT371)TRF1 to APBs might be dependent on RNA-DNA hybrids, U2OS cell lines stably expressing the vector alone or Myc-tagged RNaseH1 were generated (Figure 4.6A) (Wilson et al., 2016). The overexpression of RNaseH1 did not result in any significant changes to the percentage of cells with (pT371)TRF1 at APBs (Figure 4.6B). Little change in the level of TERRA was detected in RNaseH1 overexpressing cells (Figure 4.6C), which was inconsistent with a previous finding that overexpression of RNaseH1 led to a decrease in TERRA levels (Arora et al., 2014). It was posited that the disparity in TERRA levels between the two studies may be due to differences in the expression levels of RNaseH1 in our cell lines even though expression was readily detectable (Fig. 4.6A).

It is possible that RNA-DNA hybrids at telomeres might exist transiently and thus fail to elicit a large enough effect to allow changes in (pT371)TRF1's localization at APBs to be detected using indirect IF. We needed a different approach to address the role of RNA-DNA hybrids in regulating (pT371)TRF1 to APBs. Interestingly, it has been previously reported that R-loop structures can be induced by Top1 (DNA Topoisomerase I) inhibition by CPT (Marinello et al., 2016; Marinello, Chillemi, Bueno, Manzo, & Capranico, 2013). Previous studies have also shown that overexpression of RNaseH1 decreases the induction of γH2AX following CPT treatment in post mitotic primary neurons and noncycling HeLa cells, which suggests that CPT is capable of generating R-loops and induces DNA DSBs (Sordet et al., 2009). Moreover, when cells are depleted of splicing factors or subjected to CPT treatments, R-loops accumulate and can result in genome instability (Schoeftner & Blasco, 2008; Sollier et al., 2014). To this end, RNaseH1-expressing cells were treated with camptothecin (CPT) and then the localization of (pT371)TRF1 at APBs was evaluated. Upon CPT treatment, a significant reduction in (pT371)TRF1 association with APBs in RNaseH1-expressing U2OS cells was observed (Figure 4.6D). As a control, CPT treatment did not alter the percentage of cells positive for cyclin A nor the expression levels of (pT371)TRF1 (Figure 4.6D,E). Collectively, these results indicate that (pT371)TRF1 association with APBs may potentially be regulated by DNA damage that might result from the formation of RNA-DNA hybrids at APBs.

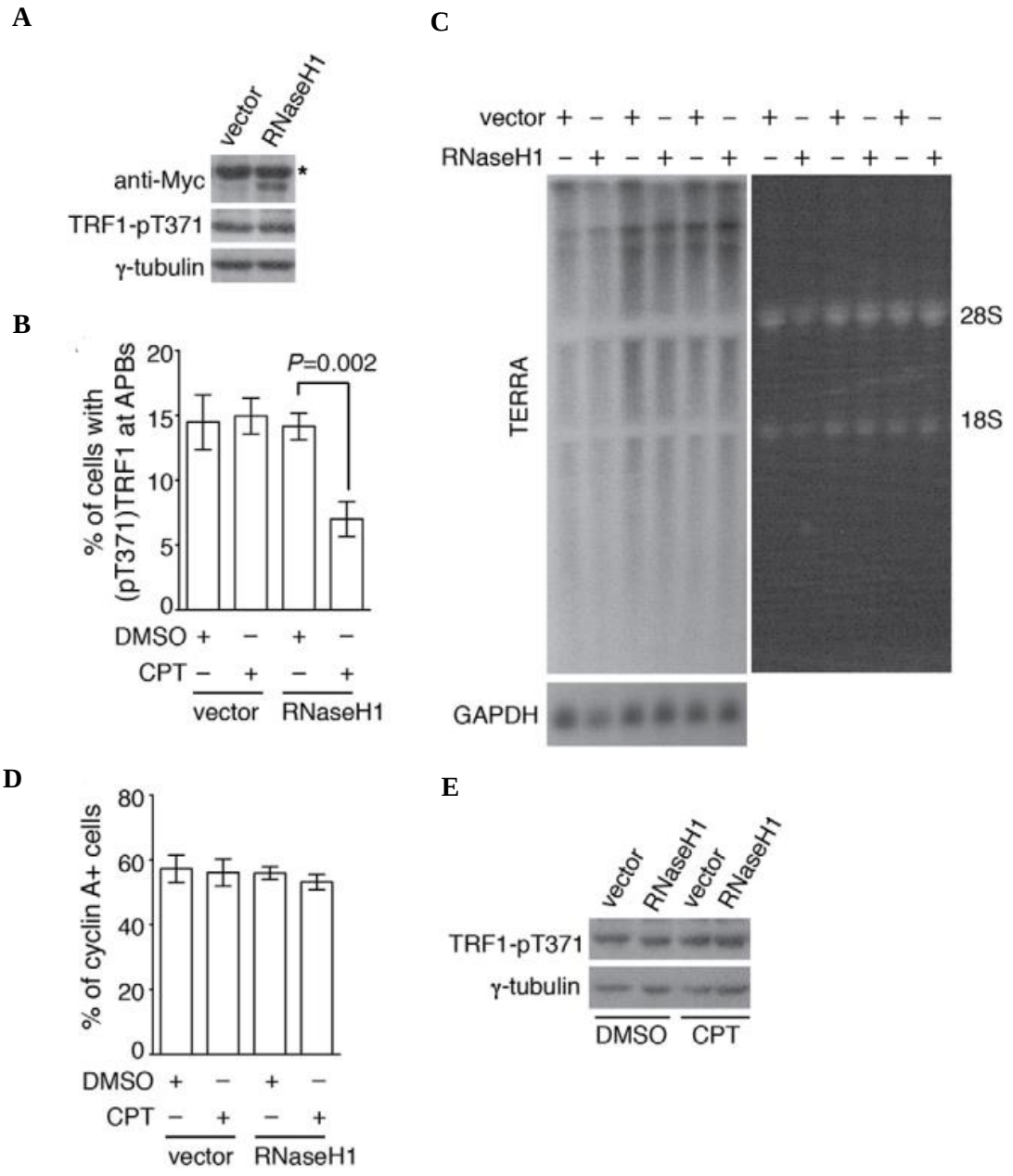

Figure 4.6 – Overexpression of RNaseH1 impairs (pT371) TRF1 recruitment to APBs in the presence of camptothecin (CPT). A) Western analysis of U2OS cells stably expressing the vector alone or Myc-tagged RNaseH1. Immunoblotting was performed with anti-Myc, anti-pT371 and anti-γ-tubulin antibodies. Asterisk represents a nonspecific band. **B)** Quantification of the percentage of cells exhibiting (pT371)TRF1 at APBs. U2OS cells stably expressing the vector

alone or Myc-tagged RNaseH1 were treated with DMSO or 5 μM CPT for 2 h prior to immunofluorescence analysis. A total of 1000 cells from each independent experiment were scored in blind. Standard deviations from three independent experiments are indicated. **C)** Analysis of TERRA expression from U2OS cells stably expressing the vector alone or Myc-tagged RNaseH1. Three pairs of total RNA isolated from three independent experiments were subjected to TERRA analysis. Northern blotting was performed with a ^{32}P-labeled telomeric DNA-containing probe, as shown in the left main panel. The northern blot of GAPDH shown on the left bottom panel was used as a loading control. The right panel was taken from the ethidium-bromide-stained agarose gel. The position of 28S and 18S ribosomal RNA is indicated. **D)** Quantification of cyclin-A-positive cells. U2OS cells stably expressing the vector alone or Myc-tagged RNaseH1 were treated with DMSO or 5 μM CPT for 2 h prior to immunofluorescence analysis. Immunofluorescence analysis was performed with an anti-cyclin-A antibody. Scoring was done as described in B. Standard deviations from three independent experiments are indicated. **E)** Western analysis of DMSO- and CPT-treated U2OS cells stably expressing the vector alone or Myc-tagged RNaseH1. Immunoblotting was performed with anti-pT371 and anti-γ-tubulin antibodies. (Taken from Wilson et al., 2016)

CHAPTER 5 CONCLUSION

5.1 DISCUSSION

5.1.1 The role of phosphorylated (pT271)TRF1 in telomerase-dependent telomere elongation

Phosphorylation of TRF1 has been shown to be important for regulating TRF1's nuclear localization in cells. It has been reported that upon phosphorylation at S367, TRF1 becomes free of telomeres and is targeted to nuclear proteolytic sites for degradation (McKerlie et al., 2012). Phosphorylation of T371 also renders TRF1 free of telomeric DNA in S/G2 phases and prevents TRF1 from being targeted for degradation (McKerlie & Zhu, 2011). In this thesis, an extensive analysis of an antibody that was raised to supposedly recognize endogenous phosphorylated TRF1 at T271 reveals that the anti-pT271 antibody is unusable for indirect immunofluorescence. To this end, whether phosphorylation of TRF1 on T271 might influence TRF1's nuclear localization would require further investigation in the future.

TRF1 contains an acidic N-terminal domain, a dimerization domain, a linker/hinge domain, and a C-terminal Myb-like DNA binding domain (Bianchi et al., 1999; Hanaoka et al., 2005). TRF1 binds to telomeric DNA as a homodimer, and its Myb-like DNA binding domain makes direct contacts with telomeric DNA (Hanaoka et al., 2005; Konig, Fairall, & Rhodes, 1998). The linker region of TRF1 is thought to provide its structural flexibility to bind to telomeric sites. It has been reported that TRF1 phosphorylation on serines or threonines of the linker region can modulate TRF1's association with telomeric

DNA. TRF1 phosphorylation on S367 impairs its ability to bind telomeric DNA, resulting in its inability to inhibit telomerase-dependent telomere lengthening in cells (McKerlie et al., 2012; McKerlie & Zhu, 2011). In this thesis, we have uncovered that TRF1 phosphorylation on T271 in the linker region enhances the binding of TRF1 with telomeric DNA *in-vivo*. My finding presented here suggests that phosphorylation in the linker region can also positively regulate TRF1 interaction with telomeric DNA. Indeed, overexpression of a unphosphorylatable T271A mutant in telomerase-positive cells was unable to suppress telomerase-dependent telomere elongation (K.J, F.R.W., and X.-D.Z., unpublished data). These results are consistent with the protein counting model whereby TRF1 binding to telomeres functions as a negative mediator of telomerase-dependent telomere elongation (Marcand et al., 1997; A. Smogorzewska et al., 2000).

The linker region of TRF1 has also been reported to physically interact with the ubiquitin ligase RLIM, which modulates the ubiquitin-mediated proteolysis of TRF1 (Her & Chung, 2009). Consistent with the notion that the linker region is involved in the modulation of the protein stability of TRF1, a recent study also demonstrates that TRF1 linker phosphorylation by ATM on S367 also promotes the ubiquitination and degradation of TRF1 (McKerlie et al., 2012). However, the lack of differences in protein degradation associated with T271 phosphorylation seems to suggest that TRF1 linker phosphorylation at T271 is not likely to be involved in regulating ubiquitination and degradation of TRF1. Collectively, the work presented in this thesis further supports the notion that TRF1 phosphorylation regulates its telomeric binding activity and telomerase-dependent telomere elongation.

TRF1 has previously been implicated in interacting with POT1, and it has been reported that removal of TRF1/TIN2 complex from telomeres results in a diminished amount of POT1 on telomeres (Loayza & Lange, 2003). It is believed that POT1 functions as a signal transducer by relaying telomere length information from TRF1 complex to the single-stranded part of the telomere where telomerase is regulated (Colgin et al., 2003; Loayza & Lange, 2003). Results from Chapter 3 indicate that T271 phosphorylation promotes TRF1 binding to telomeres and inhibits telomere elongation. Whether TRF1 phosphorylation on T271 might be involved in relaying telomere length information between TRF1 and POT1 require further investigation.

In this thesis, identification of a candidate kinase responsible for T271 phosphorylation has not been addressed. However, using the prediction software, GPS 3.0 (Group-based Prediction System; http://gps.biocuckoo.org/), approximately 45% of the potential kinases identified were found to be part of the AGC kinase group (Appendix I). The AGC kinases have been implicated to be important for contributing to the pathogenesis of many human diseases, including cancer (Pearce, Komander, & Alessi, 2010). Interestingly, T273, which is a few amino acid away from T271, has been reported to become phosphorylated by the AGC kinase Akt *in-vitro*, and is implicated in inducing telomere shortening *in-vivo* (Y.-C. Chen et al., 2009). To this end, whether AGC kinases might phosphorylate T271 to modulate TRF1 binding and telomerase-dependent elongation remains to be determined.

5.1.2 The role of phosphorylated (pT271)TRF1 in the ALT pathway

In this thesis, it has been demonstrated that phosphorylation of TRF1 on T271 is important for the assembly of APBs in ALT cells, a key indicator of ALT activity (Fasching et al., 2007; Guikai Wu et al., 2003). The phosphomimic T271D mutant was unable to support TRF2 or RAP1's localization to APBs, suggesting that the phosphomimic mutant may be impaired in the interaction or recruitment of protein factors to APBs. Several groups have published findings that phosphomimic mutants do not necessarily mimic phosphorylation *in vivo* (Durocher et al., 1999; Zisch et al., 2000). In the context of biochemical analysis, the negative charge carried by aspartic acid substitution (-1) does not match a true phosphorylated residue (approximately -2.0) *in vivo* at physiological pH (7.4) (Pearlman et al., 2011; Strickfaden et al., 2007). Furthermore, the molecular size and the ionic property of a phosphate group are also different from those of a charged amino acid, and thus the overall chemical environment created by a negatively charged amino acid is very different from a phosphorylation (Hunter et al., 2012). Therefore, if natural phosphorylation is critical for recruiting other factors to APBs, perhaps through protein-protein interaction, then analysis of APB formation must be critically evaluated since phosphomimic mutants might not provide the proper biochemical environment to facilitate the localization of other factors at APBs.

In ALT cells, the associations of telomere binding proteins and telomeric DNA can occur at telomeres or with ECTR DNA (Henson et al., 2002). The presence of ECTR within the nuclei of ALT cells has been reported to reside either inside or outside of APBs (Cesare & Griffith, 2004; Fasching et al., 2007; Yeager et al., 1999). Moreover, it has been reported

that when TRF1 is phosphorylated on T371, TRF1 becomes preferentially associated with a subset of ALT telomeres that are dysfunctional (Wilson et al., 2016). In this study, we have demonstrated that T271 phosphorylation promotes TRF1's association with telomeric DNA. However, it is unclear whether there is a preferential association of (pT271)TRF1 with dysfunctional ALT telomeres that are inside or outside of APBs.

Phosphorylation of amino acid sites adjacent to canonical SUMO consensus motifs can have a positive effect on SUMO conjugation of protein targets. For instance, it has been reported that ERK2-mediated phosphorylation of the nuclear receptor TR2 promotes its SUMOylation and its subsequent association with PML bodies in cells (Gupta et al., 2008). Enhanced SUMOylation of PML protein has also been reported to occur following phosphorylation by ERK1/2 or HIPK2 under genotoxic stress in cells. More importantly, these phosphorylations do not occur within canonical PDSMs (phosphorylation-dependent SUMO motifs) or phospho-SIMs (SUMO interacting motifs) (Gresko et al., 2009; Hayakawa & Privalsky, 2004; Müller, Matunis, & Dejean, 1998). In ALT cells, SUMOylation of telomeric proteins, PML and SP100 proteins is crucial for the assembly APBs, as well as the subsequent recruitment of telomeres to APBs (Chung et al., 2011; Naka et al., 2002; Potts & Yu, 2007). TRF1 has also been reported to contain SUMOylation sites in the linker region (Potts & Yu, 2007). Since the T271 site also resides in the linker region, whether T271 phosphorylation might be involved in the regulation of SUMOylation of TRF1 remains to be determined.

5.1.3 The role of phosphorylated (pT371)TRF1 in the ALT pathway

ALT cells are believed to employ a homologous-recombination based mechanism to maintain telomere length. It has also been suggested that DNA damage may serve as an initiation event for telomeric recombination in ALT cells. It has been reported that induction of DNA DSBs at telomeres in ALT cells by Fok1-TRF1 expression led to the recruitment of HR repair factors to sites of DNA damage, which also reside at PML bodies (Cho et al., 2014). TRF1 has been demonstrated to be a critical factor for the formation of APBs in ALT cells (G Wu et al., 2000). Furthermore, a phosphorylated form of TRF1, (pT371)TRF1 has also been implicated to be involved in HR activity in facilitating the repair of DNA DSB (McKerlie et al., 2013). It has been suggested that ALT activity may be initiated by DNA damage events at APBs to trigger telomeric recombination events to facilitate telomere lengthening. Consistent with this view, the data presented in Chapter 4 suggest that TRF1 is involved in C-circle production and APB formation, which are indicators of ALT activity (Wilson et al., 2016). The results from Chapter 4 have demonstrated that phosphorylated (pT371)TRF1 is associated with a subset of dysfunctional ALT telomeres, and that association of (pT371)TRF1 with APBs is dependent on active transcription. TERRA transcription in ALT cells has been reported to be deregulated and remains at high levels in S/G2 phases, which is also concomitant when APBs are enriched (Arora et al., 2014; Flynn et al., 2015; Guikai Wu et al., 2003). The results from Chapter 4 also demonstrate that the association of (pT371)TRF1 with APBs is sensitive to RNaseH1 following treatment with CPT. These results suggest that TRF1 phosphorylation on T371 is essential to support APB formation, and that localization of

(pT371)TRF1 to APBs may serve as a functional marker for ALT activity in cells. Collectively, we are proposing that telomeric RNA–DNA hybrids as a result of transcription and replication collision at telomeres might serve as a natural source of DNA damage that triggers ALT (Wilson et al., 2016).

5.1.4 APB formation and C-circle productions may be mechanistically separate processes in ALT cells

I have shown that TRF1 phosphorylation on T271 is not required to regulate C-circle production but is essential for APB formation in ALT cells. On the other hand, phosphorylation of T371 is essential for the regulation of both APBs and the production of C-circles (Wilson et al., 2016). These findings suggest that APB formation and C-circle production may be two mechanistically separate processes, both of which serve as independent markers of ALT activity. In support of this hypothesis, it has been previously reported that an immortal human ALT cell line, C3-cl6, is capable of maintaining telomere length in the absence of telomerase and ALT markers (Cerone et al., 2005). This cell line lacked all typical features of ALT cells including long heterogeneous telomeres, APBs, and the presence of extra-chromosomal telomeric circles (Cerone et al., 2005). However, this cell line bears a high rate of T-SCE events suggesting that it utilizes a recombination-based mechanism of telomere length maintenance, which is consistent with the ALT pathway (Bailey et al., 2004). Consistent with the notion that one ALT phenotype may not be a consistent marker to identify ALT status of cells, conflicting results of the presence of APBs have been reported in subtypes of gastric carcinomas (Heaphy et al., 2011; Omori et al., 2009). Collectively, these results highlight the significance when assessing ALT

activity in cells, one must avoid dismissing negative results since the absence of one or more particular ALT phenotypes does not necessarily correlate with the absence of other ALT features, and therefore the ALT status of a cell. To this end, further studies are warranted to assess the potential prognostic significance of APBs and C-circle productions in the unique biology of ALT-positive tumors.

5.2 FUTURE DIRECTIONS

5.2.1 Identifying candidate kinase responsible for the phosphorylation of T271 of TRF1

To gain a mechanistic understanding of the role of TRF1 phosphorylation at T271 in telomere length maintenance, an important experiment to perform is to identify a candidate kinase responsible for T271 phosphorylation. Using the prediction software, GPS 3.0, numerous potential kinases were identified (Appendix I). Approximately 45% of the predicted candidate kinases belonged to the AGC kinase family, and as such may serve as a good starting point for the search of a candidate kinase. Since an antibody specifically against a TRF1 peptide containing phosphorylated T271 has been raised, we can take advantage of this antibody by performing western blot analysis following treatment of cells with various kinase inhibitors to narrow down the search. A first-in-class multi-AGC kinase inhibitor, AT13148, has recently been identified to be a potent inhibitor to block substrate phosphorylation of multiple AGC kinases, including AKT, p70S6K, PKA, ROCK, and SGK *in vitro* and *in vivo* (Xi et al., 2016; Yap et al., 2012), all of which have been identified in the bioinformatics analysis. Should T271 be found to be phosphorylated by AGC kinases, then we would expect a loss of the anti-pT271 antibody band signal for

drug-treated samples in western blot analysis. Subsequently, once potential kinases have been narrowed down, a systematic approach in knocking down individual kinases may be performed in cells to identify the candidate kinase. In conjunction, *in vitro* kinase assays may also be performed by incubating tagged wild-type or mutant TRF1 (i.e. T271A), and the candidate kinase in the presence of γ-^{32}P-ATP as previously described (McKerlie & Zhu, 2011).

5.2.2 The potential role of phosphorylated (pT271)TRF1 in regulating telomeric recombination in ALT cells

In ALT cells, evidence of telomeric recombination is evident from experimental observation demonstrating direct replication of a telomere integrated "tag" from one telomere to another on different chromosome (Dunham et al., 2000). Telomeric recombination activities are also evident from the analysis of T-SCE events visualized in metaphase spreads (Jung et al., 2013). The work presented in this thesis has demonstrated that TRF1 phosphorylation on T271 is critical for the formation of APBs, indicative of a potential role for regulating ALT activity. Therefore, to better understand the mechanistic role of (pT271)TRF1 in the ALT pathway, it is necessary to further investigate whether TRF1 phosphorylation on T271 might be involved in T-SCE events and in the regulation telomere length heterogeneity. It has been suggested that TRF1 depletion did not result in any significant change in telomere length heterogeneity and T-SCE. Though, it is hypothesized that incomplete depletion of TRF1 in ALT cells might have contributed to the lack of change (Wilson et al., 2016). A different approach to address the role of TRF1 in T-SCE and telomere length heterogeneity might involve the use of a mouse model.

While embryonic lethality has been reported to be a consequence in *Trf1* nulls mice (J. Karlseder et al., 2003), successful murine TRF1 conditional knockout model has been previously reported to be an effective way to study telomere biology as a result of TRF1 deficiency (Martínez et al., 2009). Recently, there has been a successful report of the generation of an ALT mouse model of glioma (Jeitany et al., 2015). Therefore, it will be a potential avenue to explore whether TRF1 conditional knockout in ALT mice may provide additional insights into the role of TRF1 in regulating T-SCE and telomere length heterogeneity.

Our recent study has demonstrated that interaction of (pT371)TRF1 with APBs is dependent upon ATM and homologous-recombination-promoting factors Mre11 and BRCA1. Furthermore, the localization of the DNA repair factor NBS1 to APBs was also dependent on T371 phosphorylation (Wilson et al., 2016). Since the phosphorylation site T271 also resides in the linker region, it will be important to investigate whether this site is also involved in the recruitment of DNA repair factors and HR promoting factors to APBs. Understanding how TRF1 phosphorylation might regulate the recruitment of protein factors will provide valuable insights into the functional role of TRF1 phosphorylation in the ALT pathway.

5.2.3 Exploring the role of (pT271)TRF1 in DNA damage response

In this thesis, experimental evidence demonstrates that TRF1 phosphorylation on T271 is important for regulating the recruitment of TRF2 and Rap1 to APBs, which are nuclear sites known to be associated with damaged telomeres in ALT cells (Wilson et al.,

2016). Consistent with this view, (pT271)TRF1 has also been found to regulate the activity of (pT371)TRF1, which has been shown to associate with sites of DNA damage in both telomerase-positive and ALT cells (McKerlie et al., 2013; Wilson et al., 2016). Therefore, the work presented in this thesis raises the possibility that (pT271)TRF1 might be involved in recruiting TRF2, Rap1, and (pT371)TRF1 to sites of DNA damage in telomerase-positive cells. In support of this hypothesis, a recent study reported that Rap1 is indispensable to TRF2-mediated etoposide resistance in gastric cancer cells by inhibiting ATM signaling in early DDR (X Li et al., 2015). Moreover, TRF2 has been shown to become rapidly phosphorylated in response to DNA damage resulting from ionizing radiation, and to localize to sites of DNA damage (Tanaka et al., 2005). Whether (pT271)TRF1 might play a role in DNA damage response remains to be determined.

5.3 IMPLICATION AND SIGNIFICANCE

In human cells, TRF1 is implicated in both telomeric and non-telomeric roles. These roles include telomere protection, telomere length maintenance, resolution of sister telomeres during mitosis, and homologous-recombination-mediated DNA double strand break repair (McKerlie et al., 2012, 2013; McKerlie & Zhu, 2011; van Steensel & de Lange, 1997). These functions of TRF1 are also tightly regulated by post-translational modification such as phosphorylation (Walker & Zhu, 2012). In the context of cancer development, telomere length maintenance is crucial for the proliferative ability of cancer cells. While much is known about the role of TRF1 in telomerase-positive cancer cells, the role of TRF1 in the ALT pathway has yet to be fully characterized.

This thesis has investigated the functional and regulatory mechanisms of two TRF1 phosphorylation sites in the linker domain, T271 and T371, in telomerase-dependent telomere elongation and in ALT pathway. In Chapter 3, the results presented suggest that TRF1 phosphorylation on T271 is needed to facilitate TRF1's association with telomeric DNA *in-vivo* and this function may explain, at least in part, the requirement of T271 phosphorylation to modulate telomere length maintenance in telomerase-positive cells. In addition to regulating telomerase-dependent telomere lengthening, the results from Chapter 3 also suggest a role for (pT271)TRF1 in supporting the formation of APBs in ALT cells. In Chapter 4, the results presented are part of a recent publication in which we proposed that transcription-associated DNA damage triggers (pT371)TRF1 recruitment to APBs to facilitate ALT activity. Taken together, the results presented in this thesis propose that TRF1 phosphorylation at T271 and T371 may be functionally linked to regulate telomere length maintenance in cells.

In conclusion, the work presented here provides new insights into the regulatory role of TRF1 phosphorylation in both telomerase-dependent telomere length maintenance and in ALT. Given the intricate mechanisms behind telomere length maintenance in telomerase-positive and ALT cells, our knowledge of how post-translational modifications on TRF1 may be linked to telomere homeostasis will be crucial for our understanding in cancer cell biology. A clear mechanistic understanding of telomere maintenance will be conducive to the future development of drug therapeutics against cancer.

REFERENCES

Abreu, E., Aritonovska, E., Reichenbach, P., Cristofari, G., Culp, B., Terns, R. M., … Terns, M. P. (2010). TIN2-tethered TPP1 recruits human telomerase to telomeres in vivo. *Molecular and Cellular Biology*, *30*(12), 2971–82. http://doi.org/10.1128/MCB.00240-10

Ahnesorg, P., Smith, P., & Jackson, S. P. (2006). XLF interacts with the XRCC4-DNA ligase IV complex to promote DNA nonhomologous end-joining. *Cell*, *124*(2), 301–13. http://doi.org/10.1016/j.cell.2005.12.031

Ambrus, A., Chen, D., Dai, J., Bialis, T., Jones, R. A., & Yang, D. (2006). Human telomeric sequence forms a hybrid-type intramolecular G-quadruplex structure with mixed parallel/antiparallel strands in potassium solution. *Nucleic Acids Research*, *34*(9), 2723–35. http://doi.org/10.1093/nar/gkl348

Arnoult, N., & Karlseder, J. (2015). Complex interactions between the DNA-damage response and mammalian telomeres. *Nature Structural & Molecular Biology*, *22*(11), 859–866. http://doi.org/10.1038/nsmb.3092

Arnoult, N., Van Beneden, A., & Decottignies, A. (2012). Telomere length regulates TERRA levels through increased trimethylation of telomeric H3K9 and HP1α. *Nature Structural & Molecular Biology*, *19*(9), 948–56. http://doi.org/10.1038/nsmb.2364

Arora, R., Lee, Y., Wischnewski, H., Brun, C. M., Schwarz, T., & Azzalin, C. M. (2014). RNaseH1 regulates TERRA-telomeric DNA hybrids and telomere maintenance in ALT tumour cells. *Nature Communications*, *5*, 5220. http://doi.org/10.1038/ncomms6220

Azzalin, C. M., Reichenbach, P., Khoriauli, L., Giulotto, E., & Lingner, J. (2007). Telomeric repeat containing RNA and RNA surveillance factors at mammalian chromosome ends. *Science (New York, N.Y.)*, *318*(5851), 798–801. http://doi.org/10.1126/science.1147182

Bailey, S. M., Brenneman, M. A., & Goodwin, E. H. (2004). Frequent recombination in telomeric DNA may extend the proliferative life of telomerase-negative cells. *Nucleic Acids Research*, *32*(12), 3743–51. http://doi.org/10.1093/nar/gkh691

Balk, B., Maicher, A., Dees, M., Klermund, J., Luke-Glaser, S., Bender, K., & Luke, B. (2013). Telomeric RNA-DNA hybrids affect telomere-length dynamics and senescence. *Nature Structural & Molecular Biology*, *20*(10), 1199–205. http://doi.org/10.1038/nsmb.2662

Batenburg, N. L., Mitchell, T. R. H., Leach, D. M., Rainbow, A. J., & Zhu, X.-D. (2012). Cockayne Syndrome group B protein interacts with TRF2 and regulates telomere length and stability. *Nucleic Acids Research*, *40*(19), 9661–74. http://doi.org/10.1093/nar/gks745

Baumann, P., & Cech, T. R. (2001). Pot1, the putative telomere end-binding protein in fission yeast and humans. *Science (New York, N.Y.)*, *292*(5519), 1171–5. http://doi.org/10.1126/science.1060036

Baumann, P., Podell, E., & Cech, T. R. (2002). Human Pot1 (protection of telomeres) protein: cytolocalization, gene structure, and alternative splicing. *Molecular and Cellular Biology*, *22*(22), 8079–87.

Benetti, R., García-Cao, M., & Blasco, M. A. (2007). Telomere length regulates the epigenetic status of mammalian telomeres and subtelomeres. *Nature Genetics*, *39*(2), 243–250. http://doi.org/10.1038/ng1952

Bianchi, A., Stansel, R. M., Fairall, L., Griffith, J. D., Rhodes, D., & De Lange, T. (1999). TRF1 binds a bipartite telomeric site with extreme spatial flexibility. *The EMBO Journal*, *18*(20), 5735–5744.

Blackburn, E. H., Greider, C. W., & Szostak, J. W. (2006). Telomeres and telomerase: the path from maize, Tetrahymena and yeast to human cancer and aging. *Nature Medicine*, *12*(10), 1133–8. http://doi.org/10.1038/nm1006-1133

Blagoev, K. B., Goodwin, E. H., & Bailey, S. M. (2010). Telomere sister chromatid exchange and the process of aging. *Aging*, *2*(10), 727–30. http://doi.org/10.18632/aging.100206

Brambati, A., Colosio, A., Zardoni, L., Galanti, L., & Liberi, G. (2015). Replication and transcription on a collision course: eukaryotic regulation mechanisms and implications for DNA stability. *Frontiers in Genetics*, *6*, 166. http://doi.org/10.3389/fgene.2015.00166

Brandsma, I., & Gent, D. C. (2012). Pathway choice in DNA double strand break repair: observations of a balancing act. *Genome Integrity*, *3*(1), 9. http://doi.org/10.1186/2041-9414-3-9

Broccoli, D., Chong, L., Oelmann, S., Fernald, A. A., Marziliano, N., van Steensel, B., … de Lange, T. (1997). Comparison of the human and mouse genes encoding the telomeric protein, TRF1: chromosomal localization, expression and conserved protein domains. *Human Molecular Genetics*, *6*(1), 69–76. http://doi.org/10.1093/hmg/6.1.69

Broccoli, D., Smogorzewska, A., Chong, L., & de Lange, T. (1997). Human telomeres contain two distinct Myb-related proteins, TRF1 and TRF2. *Nature Genetics*, *17*(2), 231–5. http://doi.org/10.1038/ng1097-231

Brouwer, A. K., Schimmel, J., Wiegant, J. C. A. G., Vertegaal, A. C. O., Tanke, H. J., & Dirks, R. W. (2009). Telomeric DNA Mediates De Novo PML Body Formation. *Molecular Biology of the Cell*, *20*(22), 4804–4815. http://doi.org/10.1091/mbc.E09-04-0309

Bryan, T. M., Englezou, A., Gupta, J., Bacchetti, S., & Reddel, R. R. (1995). Telomere elongation in immortal human cells without detectable telomerase activity. *The EMBO Journal*, *14*(17), 4240–8. http://doi.org/papers3://publication/uuid/E553EAC0-7D77-471F-A996-D41412778FFB

Bryan, T. M., Marusic, L., Bacchetti, S., Namba, M., & Reddel, R. R. (1997). The telomere lengthening mechanism in telomerase-negative immortal human cells does not involve the telomerase RNA subunit. *Human Molecular Genetics*, *6*(6), 921–6. http://doi.org/10.1093/hmg/6.6.921

Callen, E., Di Virgilio, M., Kruhlak, M. J., Nieto-Soler, M., Wong, N., Chen, H.-T., … Nussenzweig, A. (2013). 53BP1 mediates productive and mutagenic DNA repair through distinct phosphoprotein interactions. *Cell*, *153*(6), 1266–80. http://doi.org/10.1016/j.cell.2013.05.023

Castellano-Pozo, M., Santos-Pereira, J. M. M., Rondón, A. G. A. G. G., Barroso, S., Andújar, E., Pérez-Alegre, M., … Dent, S. Y. (2013). R Loops Are Linked to Histone H3 S10 Phosphorylation and Chromatin Condensation. *Molecular Cell*, *52*(4), 583–590. http://doi.org/10.1016/j.molcel.2013.10.006

Cerone, M. A., Autexier, C., Londoño-Vallejo, J. A., & Bacchetti, S. (2005). A human cell line that maintains telomeres in the absence of telomerase and of key markers of ALT. *Oncogene*, *24*(53), 7893–901. http://doi.org/10.1038/sj.onc.1208934

Cesare, A. J., & Griffith, J. D. (2004). Telomeric DNA in ALT cells is characterized by free telomeric circles and heterogeneous t-loops. *Molecular and Cellular Biology*, *24*(22), 9948–57. http://doi.org/10.1128/MCB.24.22.9948-9957.2004

Cesare, A. J., Kaul, Z., Cohen, S. B., Napier, C. E., Pickett, H. A., Neumann, A. A., & Reddel, R. R. (2009). Spontaneous occurrence of telomeric DNA damage response in the absence of chromosome fusions. *Nature Structural & Molecular Biology*, *16*(12), 1244–1251. http://doi.org/10.1038/nsmb.1725

Cesare, A. J., & Reddel, R. R. (2010). Alternative lengthening of telomeres: models, mechanisms and implications. *Nature Reviews. Genetics*, *11*(5), 319–330. http://doi.org/10.1038/nrg2763

Chang, W. (2003). TRF1 is degraded by ubiquitin-mediated proteolysis after release from telomeres. *Genes & Development*, *17*(>11), 1328–1333. http://doi.org/10.1101/gad.1077103

Chapman, J. R., Barral, P., Vannier, J.-B., Borel, V., Steger, M., Tomas-Loba, A., … Boulton, S. J. (2013). RIF1 is essential for 53BP1-dependent nonhomologous end joining and suppression of DNA double-strand break resection. *Molecular Cell*, *49*(5), 858–71. http://doi.org/10.1016/j.molcel.2013.01.002

Chen, L.-Y., Liu, D., & Songyang, Z. (2007). Telomere Maintenance through Spatial Control of Telomeric Proteins. *Molecular and Cellular Biology*, *27*(16), 5898–5909. http://doi.org/10.1128/MCB.00603-07

Chen, Y., Yang, Y., van Overbeek, M., Donigian, J. R., Baciu, P., de Lange, T., & Lei, M. (2008). A shared docking motif in TRF1 and TRF2 used for differential recruitment of telomeric proteins. *Science (New York, N.Y.)*, *319*(5866), 1092–6. http://doi.org/10.1126/science.1151804

Chen, Y.-C., Teng, S.-C., & Wu, K.-J. (2009). Phosphorylation of telomeric repeat binding factor 1 (TRF1) by Akt causes telomere shortening. *Cancer Investigation*, *27*(1), 24–8. http://doi.org/10.1080/07357900802027081

Cho, N. W., Dilley, R. L., Lampson, M. A., & Greenberg, R. A. (2014). Interchromosomal Homology Searches Drive Directional ALT Telomere Movement and Synapsis. *Cell*, *159*(1), 108–121. http://doi.org/10.1016/j.cell.2014.08.030

Chong, L., van Steensel, B., Broccoli, D., Erdjument-Bromage, H., Hanish, J., Tempst, P., & de Lange, T. (1995). A human telomeric protein. *Science (New York, N.Y.)*, *270*(5242), 1663–7.

Chung, I., Leonhardt, H., & Rippe, K. (2011). De novo assembly of a PML nuclear subcompartment occurs through multiple pathways and induces telomere elongation. *Journal of Cell Science*, *124*(21), 3603–3618. http://doi.org/10.1242/jcs.084681

Chung, I., Osterwald, S., Deeg, K. I., & Rippe, K. (2012). PML body meets telomere: the beginning of an ALTernate ending? *Nucleus (Austin, Tex.)*, *3*(3), 263–75. http://doi.org/10.4161/nucl.20326

Colgin, L. M. L. M., Baran, K., Baumann, P., Cech, T. R. T. R., Reddel, R. R. R., Cervantes, R. B., … Piatyszek, M. A. (2003). Human POT1 Facilitates Telomere Elongation by Telomerase. *Current Biology*, *13*(11), 942–946. http://doi.org/10.1016/S0960-9822(03)00339-7

Conomos, D., Pickett, H. a, & Reddel, R. R. (2013). Alternative lengthening of telomeres: remodeling the telomere architecture. *Frontiers in Oncology*, *3*(February), 27. http://doi.org/10.3389/fonc.2013.00027

Conomos, D., Reddel, R. R., & Pickett, H. a. (2014). NuRD-ZNF827 recruitment to telomeres creates a molecular scaffold for homologous recombination. *Nature Structural & Molecular Biology*, (August). http://doi.org/10.1038/nsmb.2877

Conomos, D., Stutz, M. D., Hills, M., Neumann, A. A., Bryan, T. M., Reddel, R. R., & Pickett, H. A. (2012). Variant repeats are interspersed throughout the telomeres and recruit nuclear receptors in ALT cells. *The Journal of Cell Biology*, *199*(6), 893–906. http://doi.org/10.1083/jcb.201207189

Corriveau, M., Mullins, M. R., Baus, D., Harris, M. E., & Taylor, D. J. (2013). Coordinated interactions of multiple POT1-TPP1 proteins with telomere DNA. *The Journal of Biological Chemistry*, *288*(23), 16361–70. http://doi.org/10.1074/jbc.M113.471896

Cruz-García, A., López-Saavedra, A., & Huertas, P. (2014). BRCA1 Accelerates CtIP-Mediated DNA-End Resection. *Cell Reports*, *9*(2), 451–9. http://doi.org/10.1016/j.celrep.2014.08.076

d'Adda di Fagagna, F., Reaper, P. M., Clay-Farrace, L., Fiegler, H., Carr, P., Von Zglinicki, T., … Jackson, S. P. (2003). A DNA damage checkpoint response in telomere-initiated senescence. *Nature*, *426*(6963), 194–8. http://doi.org/10.1038/nature02118

Daley, J. M., & Sung, P. (2014). 53BP1, BRCA1, and the choice between recombination and end joining at DNA double-strand breaks. *Molecular and Cellular Biology*, *34*(8), 1380–8. http://doi.org/10.1128/MCB.01639-13

de Lange, T. (2005). Shelterin: The protein complex that shapes and safeguards human telomeres. *Genes and Development*, *19*(18), 2100–2110. http://doi.org/10.1101/gad.1346005

Denchi, E. L., & de Lange, T. (2007). Protection of telomeres through independent control of ATM and ATR by TRF2 and POT1. *Nature*, *448*(7157), 1068–1071. http://doi.org/10.1038/nature06065

Draskovic, I., Arnoult, N., Steiner, V., Bacchetti, S., Lomonte, P., & Londoño-Vallejo, A. (2009). Probing PML body function in ALT cells reveals spatiotemporal requirements for telomere recombination. *Proceedings of the National Academy of Sciences of the United States of America*, *106*(37), 15726–31. http://doi.org/10.1073/pnas.0907689106

Dunham, M. A., Neumann, A. A., Fasching, C. L., & Reddel, R. R. (2000). Telomere maintenance by recombination in human cells. *Nature Genetics*, *26*(4), 447–50. http://doi.org/10.1038/82586

Durocher, D., Henckel, J., Fersht, A. R., Jackson, S. P., Blasina, A., Weyer, I. Van de, … Zakian, V. A. (1999). The FHA domain is a modular phosphopeptide recognition motif. *Molecular Cell*, *4*(3), 387–94. http://doi.org/10.1016/s1097-2765(00)80340-8

Episkopou, H., Draskovic, I., Van Beneden, A., Tilman, G., Mattiussi, M., Gobin, M., … Decottignies, A. (2014). Alternative Lengthening of Telomeres is characterized by reduced compaction of telomeric chromatin. *Nucleic Acids Research*, *42*(7), 4391–4405. http://doi.org/10.1093/nar/gku114

Everett, R. D., Lomonte, P., Sternsdorf, T., van Driel, R., & Orr, A. (1999). Cell cycle regulation of PML modification and ND10 composition. *Journal of Cell Science*, *112 (Pt 2*, 4581–8.

Fairall, L., Chapman, L., Moss, H., de Lange, T., & Rhodes, D. (2001). Structure of the TRFH dimerization domain of the human telomeric proteins TRF1 and TRF2. *Molecular Cell*, *8*(2), 351–61. http://doi.org/10.1016/S1097-2765(01)00321-5

Fasching, C. L., Bower, K., & Reddel, R. R. (2005). Telomerase-independent telomere length maintenance in the absence of alternative lengthening of telomeres-associated promyelocytic leukemia bodies. *Cancer Research*, *65*(7), 2722–9. http://doi.org/10.1158/0008-5472.CAN-04-2881

Fasching, C. L., Neumann, A. A., Muntoni, A., Yeager, T. R., & Reddel, R. R. (2007). DNA Damage Induces Alternative Lengthening of Telomeres (ALT) Associated Promyelocytic Leukemia Bodies that Preferentially Associate with Linear Telomeric DNA. *Cancer Research*, *67*(15), 7072–7077. http://doi.org/10.1158/0008-5472.CAN-07-1556

Feng, L., Li, N., Li, Y., Wang, J., Gao, M., Wang, W., & Chen, J. (2015). Cell cycle-dependent inhibition of 53BP1 signaling by BRCA1. *Cell Discovery*, *1*, 15019. http://doi.org/10.1038/celldisc.2015.19

Flynn, R. L., Cox, K. E., Jeitany, M., Wakimoto, H., Bryll, A. R., Ganem, N. J., … Zou, L. (2015). Alternative lengthening of telomeres renders cancer cells hypersensitive to ATR inhibitors. *Science*, *347*(6219), 273–277. http://doi.org/10.1126/science.1257216

Frescas, D., & de Lange, T. (2014). Binding of TPP1 protein to TIN2 protein is required for POT1a,b protein-mediated telomere protection. *The Journal of Biological Chemistry*, *289*(35), 24180–7. http://doi.org/10.1074/jbc.M114.592592

Galati, A., Micheli, E., & Cacchione, S. (2013). Chromatin structure in telomere dynamics. *Frontiers in Oncology*, *3*, 46. http://doi.org/10.3389/fonc.2013.00046

Gonzalo, S., Jaco, I., Fraga, M. F., Chen, T., Li, E., Esteller, M., & Blasco, M. A. (2006). DNA methyltransferases control telomere length and telomere recombination in mammalian cells. *Nature Cell Biology*, *8*(4), 416–24. http://doi.org/10.1038/ncb1386

Gottlieb, T. M., Jackson, S. P., Allaway, G. P., Vivino, A. A., Kohn, L. D., Notkins, A. L., … Yaneva, M. (1993). The DNA-dependent protein kinase: requirement for DNA ends and association with Ku antigen. *Cell*, *72*(1), 131–42. http://doi.org/10.1016/0092-8674(93)90057-w

Greenberg, R. A. (2005). Telomeres, crisis and cancer. *Current Molecular Medicine*, *5*(2), 213–8.

Gresko, E., Ritterhoff, S., Sevilla-Perez, J., Roscic, A., Fröbius, K., Kotevic, I., … Schmitz, M. L. (2009). PML tumor suppressor is regulated by HIPK2-mediated phosphorylation in response to DNA damage. *Oncogene*, *28*(5), 698–708. http://doi.org/10.1038/onc.2008.420

Griffith, J. D., Comeau, L., Rosenfield, S., Stansel, R. M., Bianchi, A., Moss, H., & de Lange, T. (1999). Mammalian telomeres end in a large duplex loop. *Cell*, *97*(4), 503–14.

Grobelny, J. V, Godwin, A. K., Broccoli, D., Auersperg, N., Maines-Bndiera, S., Lynch, J. H., … Robinson, M. (2000). ALT-associated PML bodies are present in viable cells and are enriched in cells in the G(2)/M phase of the cell cycle. *Journal of Cell Science*, *113 Pt 24*(24), 4577–85. http://doi.org/10.1016/0002-9378(95)90282-1

Groth, A., Corpet, A., Cook, A. J. L., Roche, D., Bartek, J., Lukas, J., & Almouzni, G. (2007). Regulation of replication fork progression through histone supply and demand. *Science (New York, N.Y.)*, *318*(5858), 1928–31. http://doi.org/10.1126/science.1148992

Gupta, P., Ho, P.-C., Huq, M. M., Ha, S. G., Park, S. W., Khan, A. A., … Wei, L.-N. (2008). Retinoic acid-stimulated sequential phosphorylation, PML recruitment, and SUMOylation of nuclear receptor TR2 to suppress Oct4 expression. *Proceedings of the National Academy of Sciences of the United States of America*, *105*(32), 11424–9. http://doi.org/10.1073/pnas.0710561105

Hanaoka, S., Nagadoi, A., & Nishimura, Y. (2005). Comparison between TRF2 and TRF1 of their telomeric DNA-bound structures and DNA-binding activities. *Protein Science : A Publication of the Protein Society*, *14*(1), 119–30. http://doi.org/10.1110/ps.04983705

Hayakawa, F., & Privalsky, M. L. (2004). Phosphorylation of PML by mitogen-activated protein kinases plays a key role in arsenic trioxide-mediated apoptosis. *Cancer Cell*, *5*(4), 389–401.

Hayflick, L., & Moorhead, P. S. (1961). The serial cultivation of human diploid cell strains. *Experimental Cell Research*, *25*(3), 585–621. http://doi.org/10.1016/0014-4827(61)90192-6

Heaphy, C. M., Subhawong, A. P., Hong, S.-M., Goggins, M. G., Montgomery, E. A., Gabrielson, E., … Meeker, A. K. (2011). Prevalence of the alternative lengthening of telomeres telomere maintenance mechanism in human cancer subtypes. *The American Journal of Pathology*, *179*(4), 1608–15. http://doi.org/10.1016/j.ajpath.2011.06.018

Hecker, C.-M., Rabiller, M., Haglund, K., Bayer, P., & Dikic, I. (2006). Specification of SUMO1- and SUMO2-interacting motifs. *The Journal of Biological Chemistry*, *281*(23), 16117–27. http://doi.org/10.1074/jbc.M512757200

Hemann, M. T., Strong, M. A., Hao, L. Y., & Greider, C. W. (2001). The shortest telomere, not average telomere length, is critical for cell viability and chromosome stability. *Cell*, *107*(1), 67–77. http://doi.org/10.1016/s0092-8674(01)00504-9

Henson, J. D., Cao, Y., Huschtscha, L. I., Chang, A. C., Au, A. Y. M., Pickett, H. A., & Reddel, R. R. (2009). DNA C-circles are specific and quantifiable markers of alternative-lengthening-of-telomeres activity. *Nature Biotechnology*, *27*(12), 1181–1185. http://doi.org/10.1038/nbt.1587

Henson, J. D., Neumann, A. A., Yeager, T. R., & Reddel, R. R. (2002). Alternative lengthening of telomeres in mammalian cells. *Oncogene*, *21*(4), 598–610. http://doi.org/10.1038/sj.onc.1205058

Her, Y. R., & Chung, I. K. (2009). Ubiquitin Ligase RLIM Modulates Telomere Length Homeostasis through a Proteolysis of TRF1. *The Journal of Biological Chemistry*, *284*(13), 8557–66. http://doi.org/10.1074/jbc.M806702200

Hockemeyer, D., Palm, W., Else, T., Daniels, J.-P., Takai, K. K., Ye, J. Z.-S., … Hammer, G. D. (2007). Telomere protection by mammalian Pot1 requires interaction with Tpp1. *Nature Structural & Molecular Biology*, *14*(8), 754–61. http://doi.org/10.1038/nsmb1270

Holt, L. J., Tuch, B. B., Villén, J., Johnson, A. D., Gygi, S. P., & Morgan, D. O. (2009). Global analysis of Cdk1 substrate phosphorylation sites provides insights into evolution. *Science (New York, N.Y.)*, *325*(5948), 1682–6. http://doi.org/10.1126/science.1172867

Houghtaling, B. R., Cuttonaro, L., Chang, W., Smith, S., Granger, M. P., Wright, W. E., … Smith, S. (2004). A Dynamic Molecular Link between the Telomere Length Regulator TRF1 and the Chromosome End Protector TRF2. *Current Biology*, *14*(18), 1621–1631. http://doi.org/10.1016/j.cub.2004.08.052

Hu, C.-K., Coughlin, M., & Mitchison, T. J. (2012). Midbody assembly and its regulation during cytokinesis. *Molecular Biology of the Cell*, *23*(6), 1024–1034. http://doi.org/10.1091/mbc.E11-08-0721

Hunter, T., Lad, C., Williams, N. H., Wolfenden, R., Rosen, O. M., Erlichman, J., … Wolfe-Simon, F. (2012). Why nature chose phosphate to modify proteins. *Philosophical Transactions of the Royal Society of London. Series B, Biological Sciences*, *367*(1602), 2513–6. http://doi.org/10.1098/rstb.2012.0013

Jackson, S. P. (2002). Sensing and repairing DNA double-strand breaks. *Carcinogenesis*, *23*(5), 687–696. http://doi.org/10.1093/carcin/23.5.687

Janou kova, E., Ne asova, I., Pavlou kova, J., Zimmermann, M., Hluchy, M., Marini, V., … Hofr, C. (2015). Human Rap1 modulates TRF2 attraction to telomeric DNA. *Nucleic Acids Research*, *43*(5), 2691–2700. http://doi.org/10.1093/nar/gkv097

Jeitany, M., Pineda, J. R., Liu, Q., Porreca, R. M., Hoffschir, F., Desmaze, C., … Boussin, F. D. (2015). A preclinical mouse model of glioma with an alternative mechanism of telomere maintenance (ALT). *International Journal of Cancer*, *136*(7), 1546–58. http://doi.org/10.1002/ijc.29171

Jiang, W.-Q., Zhong, Z.-H., Henson, J. D., & Reddel, R. R. (2007). Identification of candidate alternative lengthening of telomeres genes by methionine restriction and RNA interference. *Oncogene*, *26*(32), 4635–4647. http://doi.org/10.1038/sj.onc.1210260

Jung, A. R., Yoo, J. E., Shim, Y.-H., Choi, Y.-N., Jeung, H.-C., Chung, H. C., … Oh, B.-K. (2013). Increased alternative lengthening of telomere phenotypes of telomerase-negative immortal cells upon trichostatin--a treatment. *Anticancer Research*, *33*(3), 821–9.

Karlseder, J., Hoke, K., Mirzoeva, O. K., Bakkenist, C., Kastan, M. B., Petrini, J. H. J., & de Lange, T. (2004). The telomeric protein TRF2 binds the ATM kinase and can inhibit the ATM-dependent DNA damage response. *PLoS Biology*, *2*(8), E240. http://doi.org/10.1371/journal.pbio.0020240

Karlseder, J., Kachatrian, L., Takai, H., Mercer, K., Hingorani, S., Jacks, T., & de Lange, T. (2003). Targeted Deletion Reveals an Essential Function for the Telomere Length Regulator Trf1. *Molecular and Cellular Biology*, *23*(18), 6533–6541. http://doi.org/10.1128/MCB.23.18.6533-6541.2003

Karlseder, J., Smogorzewska, A., & de Lange, T. (2002). Senescence induced by altered telomere state, not telomere loss. *Science (New York, N.Y.)*, *295*(5564), 2446–9. http://doi.org/10.1126/science.1069523

Kelleher, C., Kurth, I., & Lingner, J. (2005). Human protection of telomeres 1 (POT1) is a negative regulator of telomerase activity in vitro. *Molecular and Cellular Biology*, *25*(2), 808–18. http://doi.org/10.1128/MCB.25.2.808-818.2005

Kim, M. K., Kang, M. R., Nam, H. W., Bae, Y.-S., Kim, Y. S., & Chung, I. K. (2008). Regulation of telomeric repeat binding factor 1 binding to telomeres by casein kinase 2-mediated phosphorylation. *The Journal of Biological Chemistry*, *283*(20), 14144–52. http://doi.org/10.1074/jbc.M710065200

Kim, S. H., Beausejour, C., Davalos, A. R., Kaminker, P., Heo, S. J., & Campisi, J. (2004). TIN2 mediates functions of TRF2 at human telomeres. *Journal of Biological Chemistry*, *279*(42), 43799–43804. http://doi.org/10.1074/jbc.M408650200

Kim, S. H., Kaminker, P., Campisi, J., Kim, S. H., Kaminker, P., & Campisi, J. (1999). TIN2, a new regulator of telomere length in human cells. *Nature Genetics*, *23*(4), 405–412. http://doi.org/10.1038/70508

Kim, S.-T., Lim, D.-S., Canman, C. E., & Kastan, M. B. (1999). Substrate Specificities and Identification of Putative Substrates of ATM Kinase Family Members. *Journal of Biological Chemistry*, *274*(53), 37538–37543. http://doi.org/10.1074/jbc.274.53.37538

Kinner, A., Wu, W., Staudt, C., & Iliakis, G. (2008). Gamma-H2AX in recognition and signaling of DNA double-strand breaks in the context of chromatin. *Nucleic Acids Research*, *36*(17), 5678–94. http://doi.org/10.1093/nar/gkn550

Kishi, S., & Lu, K. P. (2002). A Critical Role for Pin2/TRF1 in ATM-dependent Regulation: INHIBITION OF Pin2/TRF1 FUNCTION COMPLEMENTS TELOMERE SHORTENING, RADIOSENSITIVITY, AND THE G2/M CHECKPOINT DEFECT OF ATAXIA-TELANGIECTASIA CELLS. *Journal of Biological Chemistry*, *277*(9), 7420–7429. http://doi.org/10.1074/jbc.M111365200

Kishi, S., Zhou, X. Z., Ziv, Y., Khoo, C., Hill, D. E., Shiloh, Y., & Lu, K. P. (2001). Telomeric Protein Pin2/TRF1 as an Important ATM Target in Response to Double Strand DNA Breaks. *Journal of Biological Chemistry*, *276*(31), 29282–29291. http://doi.org/10.1074/jbc.M011534200

Konig, P., Fairall, L., & Rhodes, D. (1998). Sequence-specific DNA recognition by the Myb-like domain of the human telomere binding protein TRF1: A model for the protein-DNA complex. *Nucleic Acids Research*, *26*(7), 1731–1740. http://doi.org/10.1093/nar/26.7.1731

Kuo, L. J., & Yang, L.-X. Gamma-H2AX - a novel biomarker for DNA double-strand breaks. *In Vivo (Athens, Greece)*, *22*(3), 305–9.

Lallemand-Breitenbach, V., & de The, H. (2010). PML Nuclear Bodies. *Cold Spring Harbor Perspectives in Biology*, *2*(5), a000661–a000661. http://doi.org/10.1101/cshperspect.a000661

Lang, M., Jegou, T., Chung, I., Richter, K., Münch, S., Udvarhelyi, A., … Rippe, K. (2010). Three-dimensional organization of promyelocytic leukemia nuclear bodies. *Journal of Cell Science*, *123*(Pt 3), 392–400. http://doi.org/10.1242/jcs.053496

Latrick, C. M., & Cech, T. R. (2010). POT1–TPP1 enhances telomerase processivity by slowing primer dissociation and aiding translocation. *The EMBO Journal*, *29*, 924–933. http://doi.org/10.1038/emboj.2009.409

Lee, J., & Gollahon, L. (2013). Mitotic perturbations induced by Nek2 overexpression require interaction with TRF1 in breast cancer cells. *Cell Cycle (Georgetown, Tex.)*, *12*(23), 3599–614. http://doi.org/10.4161/cc.26589

Lee, M., Hills, M., Conomos, D., Stutz, M. D., Dagg, R. a., Lau, L. M. S., … Pickett, H. a. (2014). Telomere extension by telomerase and ALT generates variant repeats by mechanistically distinct processes. *Nucleic Acids Research*, *42*(3), 1733–46. http://doi.org/10.1093/nar/gkt1117

Lee, T. H., Tun-Kyi, A., Shi, R., Lim, J., Soohoo, C., Finn, G., … Lu, K. P. (2009). Essential role of Pin1 in the regulation of TRF1 stability and telomere maintenance. *Nature Cell Biology*, *11*(1), 97–105. http://doi.org/10.1038/ncb1818

Lei, M., Zaug, A. J., Podell, E. R., & Cech, T. R. (2005). Switching Human Telomerase On and Off with hPOT1 Protein in Vitro. *Journal of Biological Chemistry*, *280*(21), 20449–20456. http://doi.org/10.1074/jbc.M502212200

Li, B., & de Lange, T. (2003). Rap1 affects the length and heterogeneity of human telomeres. *Molecular Biology of the Cell*, *14*(12), 5060–8. http://doi.org/10.1091/mbc.E03-06-0403

Li, B., Oestreich, S., & de Lange, T. (2000). Identification of human Rap1: implications for telomere evolution. *Cell*, *101*(5), 471–83. http://doi.org/10.1016/S0092-8674(00)80858-2

Li, X., & Heyer, W.-D. (2008). Homologous recombination in DNA repair and DNA damage tolerance. *Cell Research*, *18*(1), 99–113. http://doi.org/10.1038/cr.2008.1

Li, X., Liu, W., Wang, H., Yang, L., Li, Y., Wen, H., … Fan, D. (2015). Rap1 is indispensable for TRF2 function in etoposide-induced DNA damage response in gastric cancer cell line. *Oncogenesis*, *4*(3), e144. http://doi.org/10.1038/oncsis.2015.1

Li, X., Stith, C. M., Burgers, P. M., & Heyer, W.-D. (2009). PCNA is required for initiation of recombination-associated DNA synthesis by DNA polymerase delta. *Molecular Cell*, *36*(4), 704–13. http://doi.org/10.1016/j.molcel.2009.09.036

Liang, F., & Jasin, M. (1996). Ku80-deficient cells exhibit excess degradation of extrachromosomal DNA. *The Journal of Biological Chemistry*, *271*(24), 14405–11.

Lieber, M. R. (2010). The mechanism of double-strand DNA break repair by the nonhomologous DNA end-joining pathway. *Annual Review of Biochemistry*, *79*, 181–211. http://doi.org/10.1146/annurev.biochem.052308.093131

Limbo, O., Chahwan, C., Yamada, Y., de Bruin, R. A. M., Wittenberg, C., & Russell, P. (2007). Ctp1 is a cell-cycle-regulated protein that functions with Mre11 complex to control double-strand break repair by homologous recombination. *Molecular Cell*, *28*(1), 134–46. http://doi.org/10.1016/j.molcel.2007.09.009

Liu, D., Safari, A., O'Connor, M. S., Chan, D. W., Laegeler, A., Qin, J., & Songyang, Z. (2004). PTOP interacts with POT1 and regulates its localization to telomeres. *Nature Cell Biology*, *6*(7), 673–80. http://doi.org/10.1038/ncb1142

Loayza, D., & Lange, T. De. (2003). POT1 as a terminal transducer of TRF1 telomere length control, *75*, 1013–1018. http://doi.org/10.1038/nature01720.1.

Londoño-vallejo, J. A., Der-sarkissian, H., Cazes, L., & London, J. A. (2004). Alternative Lengthening of Telomeres Is Characterized by High Rates of Telomeric Exchange Advances in Brief Alternative Lengthening of Telomeres Is Characterized by High Rates of Telomeric Exchange, 2324–2327.

Lovejoy, C. A., Li, W., Reisenweber, S., Thongthip, S., Bruno, J., de Lange, T., … ALT Starr Cancer Consortium. (2012). Loss of ATRX, genome instability, and an altered DNA damage response are hallmarks of the alternative lengthening of telomeres pathway. *PLoS Genetics*, *8*(7), e1002772. http://doi.org/10.1371/journal.pgen.1002772

Lu, K. P., Hanes, S. D., & Hunter, T. (1996). A human peptidyl-prolyl isomerase essential for regulation of mitosis. *Nature*, *380*(6574), 544–7. http://doi.org/10.1038/380544a0

Luo, J., Manning, B. D., & Cantley, L. C. (2003). Targeting the PI3K-Akt pathway in human cancer: rationale and promise. *Cancer Cell*, *4*(4), 257–62.

Maher, R. L., Branagan, A. M., & Morrical, S. W. (2011). Coordination of DNA replication and recombination activities in the maintenance of genome stability. *Journal of Cellular Biochemistry*, *112*(10), 2672–82. http://doi.org/10.1002/jcb.23211

Makarov, V. L., Hirose, Y., & Langmore, J. P. (1997). Long G tails at both ends of human chromosomes suggest a C strand degradation mechanism for telomere shortening. *Cell*, *88*(5), 657–66.

Malligarjunan Rajavel, M. R. M. D. J. T. (2014). Multiple facets of TPP1 in telomere maintenance. *Biochimica et Biophysica Acta*, *1844*(9), 1550.

Marcand, S., Gilson, E., & Shore, D. (1997). A protein-counting mechanism for telomere length regulation in yeast. *Science (New York, N.Y.)*, *275*(5302), 986–90.

Marinello, J., Bertoncini, S., Aloisi, I., Cristini, A., Malagoli Tagliazucchi, G., Forcato, M., … Capranico, G. (2016). Dynamic Effects of Topoisomerase I Inhibition on R-Loops and Short Transcripts at Active Promoters. *PloS One*, *11*(1), e0147053. http://doi.org/10.1371/journal.pone.0147053

Marinello, J., Chillemi, G., Bueno, S., Manzo, S. G., & Capranico, G. (2013). Antisense transcripts enhanced by camptothecin at divergent CpG-island promoters associated with bursts of topoisomerase I-DNA cleavage complex and R-loop formation. *Nucleic Acids Research*, *41*(22), 10110–23. http://doi.org/10.1093/nar/gkt778

Martínez, P., Thanasoula, M., Muñoz, P., Liao, C., Tejera, A., McNees, C., … Blasco, M. A. (2009). Increased telomere fragility and fusions resulting from TRF1 deficiency lead to degenerative pathologies and increased cancer in mice. *Genes & Development*, *23*(17), 2060–75. http://doi.org/10.1101/gad.543509

Marzec, P., Armenise, C., Roumelioti, F., Basyuk, E., & Gagos, S. (2015). Nuclear-Receptor-Mediated Telomere Insertion Leads to Genome Instability in ALT Cancers Article Nuclear-Receptor-Mediated Telomere Insertion Leads to Genome Instability in ALT Cancers, 913–927. http://doi.org/10.1016/j.cell.2015.01.044

McKerlie, M., Lin, S., & Zhu, X. D. (2012). ATM regulates proteasome-dependent subnuclear localization of TRF1, which is important for telomere maintenance. *Nucleic Acids ResearcMcKerlie M, Lin S, Zhu XD (2012) ATM Regulates Proteasome-Dependent Subnuclear Localization of TRF1, Which Is Important for Telomere Maintenance. Nucleic Acids Res 40: 3975–3989h*, *40*(9), 3975–3989. http://doi.org/10.1093/nar/gks035

McKerlie, M., Walker, J. R., Mitchell, T. R. H., Wilson, F. R., & Zhu, X.-D. (2013). Phosphorylated (pT371)TRF1 is recruited to sites of DNA damage to facilitate homologous recombination and checkpoint activation. *Nucleic Acids Research*, *41*(22), 10268–82. http://doi.org/10.1093/nar/gkt775

McKerlie, M., & Zhu, X.-D. (2011). Cyclin B-dependent kinase 1 regulates human TRF1 to modulate the resolution of sister telomeres. *Nature Communications*, *2*, 371. http://doi.org/10.1038/ncomms1372

Meselson, M., & Stahl, F. W. (1958). Vulgaris. 1. *Proceedings of the National Academy of Sciences*, *44*, 671–682. http://doi.org/10.1073/pnas.44.7.671

Mitchell, T. R. H., Glenfield, K., Jeyanthan, K., & Zhu, X.-D. (2009). Arginine methylation regulates telomere length and stability. *Molecular and Cellular Biology*, *29*(18), 4918–34. http://doi.org/10.1128/MCB.00009-09

Molenaar, C., Wiesmeijer, K., Verwoerd, N. P., Khazen, S., Eils, R., Tanke, H. J., & Dirks, R. W. (2003). Visualizing telomere dynamics in living mammalian cells using PNA probes. *The EMBO Journal*, *22*(24), 6631–41. http://doi.org/10.1093/emboj/cdg633

Morin, G. B. (1989). The human telomere terminal transferase enzyme is a ribonucleoprotein that synthesizes TTAGGG repeats. *Cell*, *59*(3), 521–9.

Müller, S., Matunis, M. J., & Dejean, A. (1998). Conjugation with the ubiquitin-related modifier SUMO-1 regulates the partitioning of PML within the nucleus. *The EMBO Journal*, *17*(1), 61–70. http://doi.org/10.1093/emboj/17.1.61

Muñoz, P., Blanco, R., de Carcer, G., Schoeftner, S., Benetti, R., Flores, J. M., … Blasco, M. A. (2009). TRF1 controls telomere length and mitotic fidelity in epithelial homeostasis. *Molecular and Cellular Biology*, *29*(6), 1608–25. http://doi.org/10.1128/MCB.01339-08

Muntoni, A., Neumann, A. A., Hills, M., & Reddel, R. R. (2009). Telomere elongation involves intra-molecular DNA replication in cells utilizing alternative lengthening of telomeres. *Human Molecular Genetics*, *18*(6), 1017–27. http://doi.org/10.1093/hmg/ddn436

Nabetani, A., Yokoyama, O., & Ishikawa, F. (2004). Localization of hRad9, hHus1, hRad1, and hRad17 and caffeine-sensitive DNA replication at the alternative lengthening of telomeres-associated promyelocytic leukemia body. *Journal of Biological Chemistry*, *279*(24), 25849–25857. http://doi.org/10.1074/jbc.M312652200

Naka, K., Ikeda, K., & Motoyama, N. (2002). Recruitment of NBS1 into PML oncogenic domains via interaction with SP100 protein. *Biochemical and Biophysical Research Communications*, *299*(5), 863–71.

Nandakumar, J., Bell, C. F., Weidenfeld, I., Zaug, A. J., Leinwand, L. A., & Cech, T. R. (2012). The TEL patch of telomere protein TPP1 mediates telomerase recruitment and processivity. *Nature*, *492*(7428), 285–289. http://doi.org/10.1038/nature11648

Natarajan, S., & McEachern, M. J. (2002). Recombinational Telomere Elongation Promoted by DNA Circles. *Molecular and Cellular Biology*, *22*(13), 4512–4521. http://doi.org/10.1128/MCB.22.13.4512-4521.2002

Ng, L. J., Cropley, J. E., Pickett, H. A., Reddel, R. R., & Suter, C. M. (2009). Telomerase activity is associated with an increase in DNA methylation at the proximal subtelomere and a reduction in telomeric transcription. *Nucleic Acids Research*, *37*(4), 1152–9. http://doi.org/10.1093/nar/gkn1030

O'Sullivan, R. J., & Almouzni, G. (2014). Assembly of telomeric chromatin to create ALTernative endings. *Trends in Cell Biology*. http://doi.org/10.1016/j.tcb.2014.07.007

O'Sullivan, R. J., Arnoult, N., Lackner, D. H., Oganesian, L., Haggblom, C., Corpet, A., … Karlseder, J. (2014). Rapid induction of alternative lengthening of telomeres by depletion of the histone chaperone ASF1. *Nature Structural & Molecular Biology*, *21*(2), 167–74. http://doi.org/10.1038/nsmb.2754

Ohishi, T., Hirota, T., Tsuruo, T., & Seimiya, H. (2010). TRF1 mediates mitotic abnormalities induced by Aurora-A overexpression. *Cancer Research*, *70*(5), 2041–52. http://doi.org/10.1158/0008-5472.CAN-09-2008

Ohishi, T., Muramatsu, Y., Yoshida, H., & Seimiya, H. (2014). TRF1 ensures the centromeric function of Aurora-B and proper chromosome segregation. *Molecular and Cellular Biology*, *34*(13), 2464–78. http://doi.org/10.1128/MCB.00161-14

Okazaki, R., Okazaki, T., Sakabe, K., Sugimoto, K., Kainuma, R., Sugino, A., & Iwatsuki, N. (1968). In Vivo Mechanism of DNA Chain Growth. *Cold Spring Harbor Symposia on Quantitative Biology*, *33*(0), 129–143. http://doi.org/10.1101/SQB.1968.033.01.017

Olavarrieta, L., Martínez-Robles, M. L., Hernández, P., Krimer, D. B., & Schvartzman, J. B. (2002). Knotting dynamics during DNA replication. *Molecular Microbiology*, *46*(3), 699–707. http://doi.org/10.1046/j.1365-2958.2002.03217.x

Olovnikov, a M. (1996). Telomeres, telomerase, and aging: origin of the theory. *Experimental Gerontology*, *31*(4), 443–448. http://doi.org/10.1016/0531-5565(96)00005-8

Omori, Y., Nakayama, F., Li, D., Kanemitsu, K., Semba, S., Ito, A., & Yokozaki, H. (2009). Alternative lengthening of telomeres frequently occurs in mismatch repair system-deficient gastric carcinoma. *Cancer Science*, *100*(3), 413–418. http://doi.org/10.1111/j.1349-7006.2008.01063.x

Osterwald, S., Deeg, K. I., Chung, I., Parisotto, D., Wörz, S., Rohr, K., … Rippe, K. (2015). PML induces compaction , TRF2 depletion and DNA damage signaling at telomeres and promotes their alternative lengthening Journal of Cell Science Accepted manuscript. *Journal of Cell Science*, (April), 1887–1900. http://doi.org/10.1242/jcs.148296

Palm, W., & de Lange, T. (2008). How Shelterin Protects Mammalian Telomeres. *Annual Review of Genetics*, *42*(1), 301–334. http://doi.org/10.1146/annurev.genet.41.110306.130350

Pearce, L. R., Komander, D., & Alessi, D. R. (2010). The nuts and bolts of AGC protein kinases. *Nature Reviews. Molecular Cell Biology*, *11*(1), 9–22. http://doi.org/10.1038/nrm2822

Pearlman, S. M., Serber, Z., Ferrell, J. E., Abascal, F., Zardoya, R., Posada, D., … Hart, G. W. (2011). A mechanism for the evolution of phosphorylation sites. *Cell*, *147*(4), 934–46. http://doi.org/10.1016/j.cell.2011.08.052

Pellegrini, L., Yu, D. S., Lo, T., Anand, S., Lee, M., Blundell, T. L., & Venkitaraman, A. R. (2002). Insights into DNA recombination from the structure of a RAD51-BRCA2 complex. *Nature*, *420*(6913), 287–93. http://doi.org/10.1038/nature01230

Plantinga, M. J., Pascarelli, K. M., Merkel, A. S., Lazar, A. J., von Mehren, M., Lev, D., & Broccoli, D. (2013). Telomerase suppresses formation of ALT-associated single-stranded telomeric C-circles. *Molecular Cancer Research : MCR*, *11*(6), 557–67. http://doi.org/10.1158/1541-7786.MCR-13-0013

Potts, P. R., & Yu, H. (2007). The SMC5/6 complex maintains telomere length in ALT cancer cells through SUMOylation of telomere-binding proteins. *Nature Structural & Molecular Biology*, *14*(7), 581–90. http://doi.org/10.1038/nsmb1259

Poulet, A., Pisano, S., Faivre-Moskalenko, C., Pei, B., Tauran, Y., Haftek-Terreau, Z., … Giraud-Panis, M.-J. (2012). The N-terminal domains of TRF1 and TRF2 regulate their ability to condense telomeric DNA. *Nucleic Acids Research*, *40*(6), 2566–76. http://doi.org/10.1093/nar/gkr1116

Redon, S., Reichenbach, P., & Lingner, J. (2010). The non-coding RNA TERRA is a natural ligand and direct inhibitor of human telomerase. *Nucleic Acids Research*, *38*(17), 5797–806. http://doi.org/10.1093/nar/gkq296

Riballo, E., Kühne, M., Rief, N., Doherty, A., Smith, G. C. M., Recio, M.-J., … Löbrich, M. (2004). A pathway of double-strand break rejoining dependent upon ATM, Artemis, and proteins locating to gamma-H2AX foci. *Molecular Cell*, *16*(5), 715–24. http://doi.org/10.1016/j.molcel.2004.10.029

Rogakou, E. P., Pilch, D. R., Orr, A. H., Ivanova, V. S., & Bonner, W. M. (1998). DNA double-stranded breaks induce histone H2AX phosphorylation on serine 139. *The Journal of Biological Chemistry*, *273*(10), 5858–68.

Sartori, A. A., Lukas, C., Coates, J., Mistrik, M., Fu, S., Bartek, J., … Jackson, S. P. (2007). Human CtIP promotes DNA end resection. *Nature*, *450*(7169), 509–14. http://doi.org/10.1038/nature06337

Schoeftner, S., & Blasco, M. A. (2008). Developmentally regulated transcription of mammalian telomeres by DNA-dependent RNA polymerase II. *Nature Cell Biology*, *10*(2), 228–36. http://doi.org/10.1038/ncb1685

Sebesta, M., Burkovics, P., Juhasz, S., Zhang, S., Szabo, J. E., Lee, M. Y. W. T., … Krejci, L. (2013). Role of PCNA and TLS polymerases in D-loop extension during homologous recombination in humans. *DNA Repair*, *12*(9), 691–8. http://doi.org/10.1016/j.dnarep.2013.05.001

Sekhri, K. (2014). Telomeres and telomerase: Understanding basic structure and potential new therapeutic strategies targeting it in the treatment of cancer. *Journal of Postgraduate Medicine*, *60*(3), 303. http://doi.org/10.4103/0022-3859.138797

Shen, M., Haggblom, C., Vogt, M., Hunter, T., & Lu, K. P. (1997). Characterization and cell cycle regulation of the related human telomeric proteins Pin2 and TRF1 suggest a role in mitosis. *Proceedings of the National Academy of Sciences of the United States of America*, *94*(25), 13618–23.

Shen, T. H., Lin, H.-K., Scaglioni, P. P., Yung, T. M., & Pandolfi, P. P. (2006). The mechanisms of PML-nuclear body formation. *Molecular Cell*, *24*(3), 331–9. http://doi.org/10.1016/j.molcel.2006.09.013

Shiloh, Y. (2003). ATM and related protein kinases: safeguarding genome integrity. *Nature Reviews. Cancer*, *3*(3), 155–68. http://doi.org/10.1038/nrc1011

Shiotani, B., & Zou, L. (2009). Single-stranded DNA orchestrates an ATM-to-ATR switch at DNA breaks. *Molecular Cell*, *33*(5), 547–58. http://doi.org/10.1016/j.molcel.2009.01.024

Shrivastav, M., Miller, C. A., De Haro, L. P., Durant, S. T., Chen, B. P. C., Chen, D. J., & Nickoloff, J. A. (2009). DNA-PKcs and ATM co-regulate DNA double-strand break repair. *DNA Repair*, *8*(8), 920–9. http://doi.org/10.1016/j.dnarep.2009.05.006

Skourti-Stathaki, K., & Proudfoot, N. J. (2014). A double-edged sword: R loops as threats to genome integrity and powerful regulators of gene expression. *Genes and Development*, *28*(13), 1384–1396. http://doi.org/10.1101/gad.242990.114

Smogorzewska, A., & de Lange, T. (2004). Regulation of telomerase by telomeric proteins. *Annual Review of Biochemistry*, *73*, 177–208. http://doi.org/10.1146/annurev.biochem.73.071403.160049

Smogorzewska, A., van Steensel, B., Bianchi, A., Oelmann, S., Schaefer, M. R., Schnapp, G., & de Lange, T. (2000). Control of human telomere length by TRF1 and TRF2. *Molecular and Cellular Biology*, *20*(5), 1659–68. http://doi.org/10.1128/MCB.20.5.1659-1668.2000

Sollier, J., Stork, C. T. T., García-Rubio, M. L., Paulsen, R. D. D., Aguilera, A., Cimprich, K. A. A., … Cimprich, K. A. A. (2014). Transcription-Coupled Nucleotide Excision Repair Factors Promote R-Loop-Induced Genome Instability. *Molecular Cell*, *56*(6), 777–785. http://doi.org/10.1016/j.molcel.2014.10.020

Soohoo, C. Y., Shi, R., Lee, T. H., Huang, P., Lu, K. P., & Zhou, X. Z. (2011). Telomerase inhibitor PinX1 provides a link between TRF1 and telomerase to prevent telomere elongation. *The Journal of Biological Chemistry*, *286*(5), 3894–906. http://doi.org/10.1074/jbc.M110.180174

Sordet, O., Redon, C. E., Guirouilh-Barbat, J., Smith, S., Solier, S., Douarre, C., … Pommier, Y. (2009). Ataxia telangiectasia mutated activation by transcription- and topoisomerase I-induced DNA double-strand breaks. *EMBO Reports*, *10*(8), 887–93. http://doi.org/10.1038/embor.2009.97

Stagno D'Alcontres, M., Mendez-Bermudez, A., Foxon, J. L., Royle, N. J., & Salomoni, P. (2007). Lack of TRF2 in ALT cells causes PML-dependent p53 activation and loss of telomeric DNA. *The Journal of Cell Biology*, *179*(5), 855–67. http://doi.org/10.1083/jcb.200703020

Stracker, T. H., & Petrini, J. H. J. (2011). The MRE11 complex: starting from the ends. *Nature Reviews. Molecular Cell Biology*, *12*(2), 90–103. http://doi.org/10.1038/nrm3047

Strickfaden, S. C., Winters, M. J., Ben-Ari, G., Lamson, R. E., Tyers, M., Pryciak, P. M., … Whiteway, M. (2007). A mechanism for cell-cycle regulation of MAP kinase signaling in a yeast differentiation pathway. *Cell*, *128*(3), 519–31. http://doi.org/10.1016/j.cell.2006.12.032

Sugiyama, T., Zaitseva, E. M., & Kowalczykowski, S. C. (1997). A single-stranded DNA-binding protein is needed for efficient presynaptic complex formation by the Saccharomyces cerevisiae Rad51 protein. *The Journal of Biological Chemistry*, *272*(12), 7940–5.

Symington, L. S., & Gautier, J. (2011). Double-strand break end resection and repair pathway choice. *Annual Review of Genetics*, *45*, 247–71. http://doi.org/10.1146/annurev-genet-110410-132435

Tanaka, H., Mendonca, M. S., Bradshaw, P. S., Hoelz, D. J., Malkas, L. H., Meyn, M. S., & Gilley, D. (2005). DNA damage-induced phosphorylation of the human telomere-associated protein TRF2. *Proceedings of the National Academy of Sciences of the United States of America*, *102*(43), 15539–44. http://doi.org/10.1073/pnas.0507915102

Tang, J., Cho, N. W., Cui, G., Manion, E. M., Shanbhag, N. M., Botuyan, M. V., … Greenberg, R. A. (2013). Acetylation limits 53BP1 association with damaged chromatin to promote homologous recombination. *Nature Structural & Molecular Biology*, *20*(3), 317–25. http://doi.org/10.1038/nsmb.2499

Testa, J. R., & Bellacosa, A. (2001). AKT plays a central role in tumorigenesis. *Proceedings of the National Academy of Sciences of the United States of America*, *98*(20), 10983–5. http://doi.org/10.1073/pnas.211430998

Theimer, C. A., & Feigon, J. (2006). Structure and function of telomerase RNA. *Current Opinion in Structural Biology*, *16*(3), 307–18. http://doi.org/10.1016/j.sbi.2006.05.005

Thomas, M., White, R. L., & Davis, R. W. (1976). Hybridization of RNA to double-stranded DNA: formation of R-loops. *Proceedings of the National Academy of Sciences of the United States of America*, *73*(7), 2294–8.

Tokutake, Y., Matsumoto, T., Watanabe, T., Maeda, S., Tahara, H., Sakamoto, S., … Furuichi, Y. (1998). Extra-chromosomal telomere repeat DNA in telomerase-negative immortalized cell lines. *Biochemical and Biophysical Research Communications*, *247*(3), 765–72. http://doi.org/10.1006/bbrc.1998.8876

van Steensel, B., & de Lange, T. (1997). Control of telomere length by the human telomeric protein TRF1. *Nature*, *385*(6618), 740–3. http://doi.org/10.1038/385740a0

Veldman, T., Etheridge, K. T., & Counter, C. M. (2004). Loss of hPot1 function leads to telomere instability and a cut-like phenotype. *Current Biology : CB*, *14*(24), 2264–70. http://doi.org/10.1016/j.cub.2004.12.031

Walker, J. R., & Zhu, X.-D. (2012). Post-translational modifications of TRF1 and TRF2 and their roles in telomere maintenance. *Mechanisms of Ageing and Development*, *133*(6), 421–434. http://doi.org/10.1016/j.mad.2012.05.002

Wang, C., Zhao, L., & Lu, S. (2015). Role of TERRA in the regulation of telomere length. *International Journal of Biological Sciences*, *11*(3), 316–23. http://doi.org/10.7150/ijbs.10528

Wang, F., Podell, E. R., Zaug, A. J., Yang, Y., Baciu, P., Cech, T. R., & Lei, M. (2007). The POT1–TPP1 telomere complex is a telomerase processivity factor. *Nature*, *445*(7127), 506–510. http://doi.org/10.1038/nature05454

Wang, R. C., Smogorzewska, A., & de Lange, T. (2004). Homologous Recombination Generates T-Loop-Sized Deletions at Human Telomeres. *Cell*, *119*(3), 355–368. http://doi.org/10.1016/j.cell.2004.10.011

Wilson, F. R. (2014). *Analysis of trf1 function in alternative lengthening of telomeres activity*. *Masters Thesis*. McMaster University.

Wilson, F. R., Ho, A., Walker, J. R., & Zhu, X.-D. (2016). Cdk-dependent phosphorylation regulates TRF1 recruitment to PML bodies and promotes C-circle production in ALT cells. *Journal of Cell Science*, *129*(13), jcs.186098. http://doi.org/10.1242/jcs.186098

Wu, G., Jiang, X., Lee, W. W.-H., & Chen, P. P.-L. (2003). Assembly of functional ALT-associated promyelocytic leukemia bodies requires Nijmegen Breakage Syndrome 1. *Cancer Research*, *63*(10), 2589–95.

Wu, G., Lee, W. H., & Chen, P. L. (2000). NBS1 and TRF1 colocalize at promyelocytic leukemia bodies during late S/G2 phases in immortalized telomerase-negative cells. Implication of NBS1 in alternative lengthening of telomeres. *The Journal of Biological Chemistry*, *275*(39), 30618–22. http://doi.org/10.1074/jbc.C000390200

Wu, Y., Zacal, N. J., Rainbow, A. J., & Zhu, X.-D. (2007). XPF with mutations in its conserved nuclease domain is defective in DNA repair but functions in TRF2-mediated telomere shortening. *DNA Repair*, *6*(2), 157–66. http://doi.org/10.1016/j.dnarep.2006.09.005

Wu, Z.-Q., Yang, X., Weber, G., & Liu, X. (2008). Plk1 phosphorylation of TRF1 is essential for its binding to telomeres. *The Journal of Biological Chemistry*, *283*(37), 25503–13. http://doi.org/10.1074/jbc.M803304200

Xi, Y., Niu, J., Shen, Y., Li, D., Peng, X., & Wu, X. (2016). AT13148, a first-in-class multi-AGC kinase inhibitor, potently inhibits gastric cancer cells both in vitro and in vivo. *Biochemical and Biophysical Research Communications*, *478*(1), 330–6. http://doi.org/10.1016/j.bbrc.2016.01.167

Yap, T. A., Walton, M. I., Grimshaw, K. M., Te Poele, R. H., Eve, P. D., Valenti, M. R., … Garrett, M. D. (2012). AT13148 is a novel, oral multi-AGC kinase inhibitor with potent pharmacodynamic and antitumor activity. *Clinical Cancer Research : An Official Journal of the American Association for Cancer Research*, *18*(14), 3912–23. http://doi.org/10.1158/1078-0432.CCR-11-3313

Ye, J. Z. S., Donigian, J. R., Van Overbeek, M., Loayza, D., Luo, Y., Krutchinsky, A. N., … De Lange, T. (2004). TIN2 binds TRF1 and TRF2 simultaneously and stabilizes the TRF2 complex on telomeres. *Journal of Biological Chemistry*, *279*(45), 47264–47271. http://doi.org/10.1074/jbc.M409047200

Ye, J. Z.-S., Hockemeyer, D., Krutchinsky, A. N., Loayza, D., Hooper, S. M., Chait, B. T., & de Lange, T. (2004). POT1-interacting protein PIP1: a telomere length regulator that recruits POT1 to the TIN2/TRF1 complex. *Genes & Development*, *18*(14), 1649–54. http://doi.org/10.1101/gad.1215404

Yeager, T. T. R., Neumann, A. A. A., Englezou, A., Huschtscha, L. I., Noble, J. R., & Reddel, R. R. (1999). Telomerase-negative immortalized human cells contain a novel type of promyelocytic leukemia (PML) body. *Cancer Research*, *59*(17), 4175–4179.

Zaug, A. J., Podell, E. R., Nandakumar, J., & Cech, T. R. (2010). Functional interaction between telomere protein TPP1 and telomerase. *Genes & Development*, *24*(6), 613–622. http://doi.org/10.1101/gad.1881810

Zhong, F. L., Batista, L. F. Z., Freund, A., Pech, M. F., Venteicher, A. S., & Artandi, S. E. (2012). TPP1 OB-Fold Domain Controls Telomere Maintenance by Recruiting Telomerase to Chromosome Ends, 481–494. http://doi.org/10.1016/j.cell.2012.07.012

Zhong, Z., Shiue, L., Kaplan, S., & de Lange, T. (1992). A mammalian factor that binds telomeric TTAGGG repeats in vitro. *Molecular and Cellular Biology*, *12*(11), 4834–4843. http://doi.org/10.1128/MCB.12.11.4834.Updated

Zhong, Z.-H., Jiang, W.-Q., Cesare, A. J., Neumann, A. a, Wadhwa, R., & Reddel, R. R. (2007). Disruption of telomere maintenance by depletion of the MRE11/RAD50/NBS1 complex in cells that use alternative lengthening of telomeres. *The Journal of Biological Chemistry*, *282*(40), 29314–22. http://doi.org/10.1074/jbc.M701413200

Zhu, X.-D., Niedernhofer, L., Kuster, B., Mann, M., Hoeijmakers, J. H. J., & De Lange, T. (2003). ERCC1/XPF Removes the 3˜Overhang from Uncapped Telomeres and Represses Formation of Telomeric DNA-Containing Double Minute Chromosomes. *Molecular Cell*, *12*, 1489–1498.

Zisch, A. H., Pazzagli, C., Freeman, A. L., Schneller, M., Hadman, M., Smith, J. W., … Pasquale, E. B. (2000). Replacing two conserved tyrosines of the EphB2 receptor with glutamic acid prevents binding of SH2 domains without abrogating kinase activity and biological responses. *Oncogene*, *19*(2), 177–87. http://doi.org/10.1038/sj.onc.1203304

APPENDIX I POTENTIAL KINASES FOR THE PHOSPHORYLATION SITE T271 OF TRF1

Computational prediction of potential kinases responsible for the phosphorylation of T271 of TRF1 was performed using the stand-alone prediction software GPS 3.0 (Group-based Prediction System, ver 3.0; available at http://gps.biocuckoo.org/online.php). Presented below are the results from the prediction list, with results of other amino acid positions omitted. Threshold setting was set to 'High'. The following TRF1 sequence in FASTA format was used as input:

```
>sp|P54274|TERF1_HUMAN Telomeric repeat-binding factor 1 OS=Homo
sapiens GN=TERF1 PE=1 SV=3
MAEDVSSAAPSPRGCADGRDADPTEEQMAETERNDEEQFECQELLECQVQVGAPEEEEEE
EEDAGLVAEAEAVAAGWMLDFLCLSLCRAFRDGRSEDFRRTRNSAEAIIHGLSSLTACQL
RTIYICQFLTRIAAGKTLDAQFENDERITPLESALMIWGSIEKEHDKLHEEIQNLIKIQA
IAVCMENGNFKEAEEVFERIFGDPNSHMPFKSKLLMIISQKDTFHSFFQHFSYNHMMEKI
KSYVNYVLSEKSSTFLMKAAAKVVESKRTRTITSQDKPSGNDVEMETEANLDTRKSVSDK
QSAVTESSEGTVSLLRSHKNLFLSKLQHGTQQQDLNKKERRVGTPQSTKKKKESRRATES
RIPVSKSQPVTPEKHRARKRQAWLWEEDKNLRSGVRKYGEGNWSKILLHYKFNNRTSVML
KDRWRTMKKLKLISSDSED
```

Position	Code	Kinase	Peptide	Score	Cutoff
271	T	AGC/AKT	VESKRTRTITSQDKP	9.514	6.459
271	T	AGC/GRK	VESKRTRTITSQDKP	10.129	7.991
271	T	AGC/PKC	VESKRTRTITSQDKP	1.587	1.416
271	T	AGC/RSK	VESKRTRTITSQDKP	3.106	3.035
271	T	AGC/SGK	VESKRTRTITSQDKP	5.246	4.813
271	T	CAMK/CAMK1	VESKRTRTITSQDKP	3.593	3.507
271	T	CAMK/CAMKL	VESKRTRTITSQDKP	12.097	8.942
271	T	CAMK/MAPKAPK	VESKRTRTITSQDKP	11.922	8.972
271	T	Other/Wnk	VESKRTRTITSQDKP	4.917	3.514
271	T	AGC/AKT/AKT1	VESKRTRTITSQDKP	6.74	2.98
271	T	AGC/DMPK/ROCK	VESKRTRTITSQDKP	9.516	9.266
271	T	AGC/PKC/PKCa	VESKRTRTITSQDKP	5.143	4.803
271	T	AGC/RSK/RSKp70	VESKRTRTITSQDKP	8.816	5.594
271	T	AGC/SGK/SGK1	VESKRTRTITSQDKP	5.725	5.723
271	T	AGC/SGK/SGK3	VESKRTRTITSQDKP	6.286	5.871
271	T	CAMK/CAMK2/CAMK2D	VESKRTRTITSQDKP	5.167	4.204
271	T	CAMK/CAMKL/PASK	VESKRTRTITSQDKP	9.5	5.767
271	T	CMGC/DYRK/DYRK2	VESKRTRTITSQDKP	11.944	11.395

Position	Code	Kinase	Peptide	Score	Cutoff
271	T	Other/PLK/SAK	VESKRTRTITSQDKP	12.667	4.9
271	T	Other/Wnk/Wnk1	VESKRTRTITSQDKP	4.917	3.514
271	T	STE/STE20/SLK	VESKRTRTITSQDKP	9.667	7.9
271	T	AGC/DMPK/ROCK/ROCK2	VESKRTRTITSQDKP	5.148	4.403
271	T	AGC/RSK/RSKp90/RPS6KA1	VESKRTRTITSQDKP	2.708	2.462
271	T	CAMK/CAMKL/CHK1/CHEK1	VESKRTRTITSQDKP	3.379	2.783
271	T	CAMK/CAMKL/MARK/MARK3	VESKRTRTITSQDKP	8.667	7.5
271	T	CK1/CK1/CK1-D/CK1e	VESKRTRTITSQDKP	6.529	6.526
271	T	Other/IKK/IKKb/IKBKB	VESKRTRTITSQDKP	10.677	8.506
271	T	Other/PLK/SAK/PLK4	VESKRTRTITSQDKP	12.667	4.9
271	T	STE/STE20/SLK/LOK	VESKRTRTITSQDKP	9.667	7.9

APPENDIX II STATISTICAL RESULTS

One-way ANOVA and Tukey HSD (multiple comparison test of means with 95% confidence interval), Student's *t*-test, and Mann-Whitney test were performed using the statistical software GraphPad Prism 5.0a. Presented hereafter are results from these tests for indicated figures. Significant differences ($P<0.05$) are displayed on the graphs as asterisks as follow: 'ns' $P>0.05$, '*' $P\leq0.05$, '**' $P\leq0.01$, '***' $P\leq0.001$.

For statistical methods used for figures presented in Chapter 4 that were taken from original publication (http://doi.org/10.1242/jcs.186098), please refer to the original article (APPENDIX III).

Figure 3.3A					
One-way analysis of variance					
P value	< 0.0001				
P value summary	***				
Are means signif. different? (P < 0.05)	Yes				
Number of groups	3				
F	41.02				
R squared	0.1172				
Bartlett's test for equal variances					
Bartlett's statistic (corrected)	73.37				
P value	< 0.0001				
P value summary	***				
Do the variances differ signif. (P < 0.05)	Yes				
ANOVA Table	SS	df	MS		
Treatment (between columns)	1764	2	882		
Residual (within columns)	13290	618	21.5		
Total	15050	620			
Tukey's Multiple Comparison Test	Mean Diff.	q	Significant? P < 0.05?	Summary	95% CI of diff
shTRF1/pWZL vs shTRF1/TRF1	3.753	11.49	Yes	***	2.659 to 4.847
shTRF1/pWZL vs shTRF1/T271A	3.279	10.44	Yes	***	2.227 to 4.330
shTRF1/TRF1 vs shTRF1/T271A	-0.4743	1.443	No	ns	-1.575 to 0.6267
Figure 3.3B					
One-way analysis of variance					
P value	< 0.0001				
P value summary	***				
Are means signif. different? (P < 0.05)	Yes				
Number of groups	3				
F	13.68				

R squared	0.08111				
Bartlett's test for equal variances					
Bartlett's statistic (corrected)	14.02				
P value	0.0009				
P value summary	***				
Do the variances differ signif. (P < 0.05)	Yes				
ANOVA Table	SS	df	MS		
Treatment (between columns)	44620	2	22310		
Residual (within columns)	505500	310	1630		
Total	550100	312			
Tukey's Multiple Comparison Test	Mean Diff.	q	Significant? P < 0.05?	Summary	95% CI of diff
shTRF1/pWZL vs shTRF1/TRF1	28.76	7.1	Yes	***	15.18 to 42.34
shTRF1/pWZL vs shTRF1/T271A	7.923	2.003	No	ns	-5.340 to 21.19
shTRF1/TRF1 vs shTRF1/T271A	-20.84	5.368	Yes	***	-33.85 to -7.822
Figure 3.6B					
One-way analysis of variance					
P value	< 0.0001				
P value summary	***				
Are means signif. different? (P < 0.05)	Yes				
Number of groups	4				
F	49.59				
R squared	0.914				
ANOVA Table	SS	df	MS		
Treatment (between columns)	20.44	3	6.815		
Residual (within columns)	1.924	14	0.1374		
Total	22.37	17			

Tukey's Multiple Comparison Test	Mean Diff.	q	Significant? P < 0.05?	Summary	95% CI of diff
Vector vs TRF1	-2.565	13.4	Yes	***	-3.352 to -1.778
Vector vs T271A	-1.438	8.673	Yes	***	-2.119 to -0.7563
Vector vs T271D	-2.578	15.55	Yes	***	-3.259 to -1.896
TRF1 vs T271A	1.127	5.886	Yes	**	0.3399 to 1.914
TRF1 vs T271D	-0.01303	0.06809	No	ns	-0.8000 to 0.7739
T271A vs T271D	-1.14	6.876	Yes	**	-1.821 to -0.4583
Figure 3.7B					
One-way analysis of variance					
P value	0.6305				
P value summary	ns				
Are means signif. different? (P < 0.05)	No				
Number of groups	3				
F	0.4758				
R squared	0.05966				
Bartlett's test for equal variances					
Bartlett's statistic (corrected)	0.02483				
P value	0.9877				
P value summary	ns				
Do the variances differ signif. (P < 0.05)	No				
ANOVA Table	SS	df	MS		
Treatment (between columns)	0.05806	2	0.02903		
Residual (within columns)	0.9152	15	0.06101		
Total	0.9732	17			
Tukey's Multiple Comparison Test	Mean Diff.	q	Significant? P < 0.05?	Summary	95% CI of diff
TRF1 vs T271A	-0.08096	0.8029	No	ns	-0.4514 to 0.2895

TRF1 vs T271D	-0.1385	1.373	No	ns	-0.5089 to 0.2320
T271A vs T271D	-0.05749	0.5701	No	ns	-0.4280 to 0.3130
Figure 3.8B					
One-way analysis of variance					
P value	0.6373				
P value summary	ns				
Are means signif. different? (P < 0.05)	No				
Number of groups	4				
F	0.5923				
R squared	0.1817				
ANOVA Table	SS	df	MS		
Treatment (between columns)	3.133	3	1.044		
Residual (within columns)	14.11	8	1.763		
Total	17.24	11			
Tukey's Multiple Comparison Test	Mean Diff.	q	Significant? P < 0.05?	Summary	95% CI of diff
Vector vs TRF1	-0.6939	0.9051	No	ns	-4.166 to 2.778
Vector vs T271A	-1.436	1.873	No	ns	-4.908 to 2.036
Vector vs T271D	-0.8408	1.097	No	ns	-4.313 to 2.632
TRF1 vs T271A	-0.7422	0.9681	No	ns	-4.215 to 2.730
TRF1 vs T271D	-0.1468	0.1915	No	ns	-3.619 to 3.325
T271A vs T271D	0.5954	0.7765	No	ns	-2.877 to 4.068
Figure 3.9B					
One-way analysis of variance					
P value	0.45				
P value summary	ns				
Are means signif. different? (P < 0.05)	No				

Number of groups	4				
F	0.9776				
R squared	0.2683				
ANOVA Table	SS	df	MS		
Treatment (between columns)	26.67	3	8.89		
Residual (within columns)	72.75	8	9.094		
Total	99.42	11			
Tukey's Multiple Comparison Test	Mean Diff.	q	Significant? P < 0.05?	Summary	95% CI of diff
Vector vs TRF1	-2.994	1.719	No	ns	-10.88 to 4.892
Vector vs T271A	0.5284	0.3035	No	ns	-7.357 to 8.414
Vector vs T271D	0.6727	0.3864	No	ns	-7.212 to 8.558
TRF1 vs T271A	3.522	2.023	No	ns	-4.363 to 11.41
TRF1 vs T271D	3.666	2.106	No	ns	-4.219 to 11.55
T271A vs T271D	0.1442	0.08284	No	ns	-7.741 to 8.029
Figure 3.11C					
One-way analysis of variance					
P value	0.0003				
P value summary	***				
Are means signif. different? (P < 0.05)	Yes				
Number of groups	5				
F	15.25				
R squared	0.8591				
ANOVA Table	SS	df	MS		
Treatment (between columns)	248	4	62.01		
Residual (within columns)	40.67	10	4.067		
Total	288.7	14			

Tukey's Multiple Comparison Test	Mean Diff.	q	Significant? P < 0.05?	Summary	95% CI of diff
Vector vs shTRF1	8.663	7.44	Yes	**	3.244 to 14.08
Vector vs TRF1	2.214	1.902	No	ns	-3.204 to 7.633
Vector vs T271A	9.712	8.342	Yes	**	4.294 to 15.13
Vector vs T271D	9.388	8.063	Yes	**	3.969 to 14.81
shTRF1 vs TRF1	-6.448	5.538	Yes	*	-11.87 to -1.030
shTRF1 vs T271A	1.05	0.9015	No	ns	-4.369 to 6.468
shTRF1 vs T271D	0.7247	0.6224	No	ns	-4.694 to 6.143
TRF1 vs T271A	7.498	6.44	Yes	**	2.079 to 12.92
TRF1 vs T271D	7.173	6.161	Yes	**	1.754 to 12.59
T271A vs T271D	-0.3249	0.2791	No	ns	-5.744 to 5.094
Figure 3.11D					
One-way analysis of variance					
P value	< 0.0001				
P value summary	***				
Are means signif. different? (P < 0.05)	Yes				
Number of groups	5				
F	24.55				
R squared	0.9076				
ANOVA Table	SS	df	MS		
Treatment (between columns)	183	4	45.74		
Residual (within columns)	18.63	10	1.863		
Total	201.6	14			
Tukey's Multiple Comparison Test	Mean Diff.	q	Significant? P < 0.05?	Summary	95% CI of diff
Vector vs shTRF1	6.681	8.478	Yes	***	3.014 to 10.35
Vector vs TRF1	-1.031	1.309	No	ns	-4.699 to 2.636

Vector vs T271A	7.721	9.798	Yes	***	4.053 to 11.39
Vector vs T271D	4.022	5.104	Yes	*	0.3544 to 7.689
shTRF1 vs TRF1	-7.712	9.787	Yes	***	-11.38 to -4.045
shTRF1 vs T271A	1.04	1.32	No	ns	-2.627 to 4.707
shTRF1 vs T271D	-2.659	3.375	No	ns	-6.326 to 1.008
TRF1 vs T271A	8.752	11.11	Yes	***	5.085 to 12.42
TRF1 vs T271D	5.053	6.413	Yes	**	1.386 to 8.720
T271A vs T271D	-3.699	4.694	Yes	*	-7.366 to -0.03179
Figure 3.11E					
One-way analysis of variance					
P value	0.7696				
P value summary	ns				
Are means signif. different? (P < 0.05)	No				
Number of groups	5				
F	0.4513				
R squared	0.1529				
ANOVA Table	SS	df	MS		
Treatment (between columns)	17.36	4	4.341		
Residual (within columns)	96.2	10	9.62		
Total	113.6	14			
Tukey's Multiple Comparison Test	Mean Diff.	q	Significant? P < 0.05?	Summary	95% CI of diff
Vector vs shTRF1	-0.8565	0.4783	No	ns	-9.190 to 7.477
Vector vs TRF1	-1.874	1.047	No	ns	-10.21 to 6.460
Vector vs T271A	-1.853	1.035	No	ns	-10.19 to 6.481
Vector vs T271D	0.9034	0.5045	No	ns	-7.431 to 9.237
shTRF1 vs TRF1	-1.018	0.5684	No	ns	-9.352 to 7.316

shTRF1 vs T271A	-0.9969	0.5567	No	ns	-9.331 to 7.337
shTRF1 vs T271D	1.76	0.9828	No	ns	-6.574 to 10.09
TRF1 vs T271A	0.02096	0.01171	No	ns	-8.313 to 8.355
TRF1 vs T271D	2.778	1.551	No	ns	-5.556 to 11.11
T271A vs T271D	2.757	1.539	No	ns	-5.577 to 11.09
Figure 3.12B					
One-way analysis of variance					
P value	< 0.0001				
P value summary	***				
Are means signif. different? (P < 0.05)	Yes				
Number of groups	5				
F	42.82				
R squared	0.8726				
Bartlett's test for equal variances					
Bartlett's statistic (corrected)	10.46				
P value	0.0334				
P value summary	*				
Do the variances differ signif. (P < 0.05)	Yes				
ANOVA Table	SS	df	MS		
Treatment (between columns)	802.3	4	200.6		
Residual (within columns)	117.1	25	4.684		
Total	919.5	29			
Tukey's Multiple Comparison Test	Mean Diff.	q	Significant? P < 0.05?	Summary	95% CI of diff
Vector vs shTRF1	9.838	11.13	Yes	***	6.166 to 13.51
Vector vs TRF1	1.296	1.466	No	ns	-2.376 to 4.967
Vector vs T271A	13.42	15.18	Yes	***	9.746 to 17.09

Vector vs T271D	8.859	10.03	Yes	***	5.187 to 12.53
shTRF1 vs TRF1	-8.542	9.668	Yes	***	-12.21 to -4.871
shTRF1 vs T271A	3.579	4.051	No	ns	-0.09251 to 7.251
shTRF1 vs T271D	-0.979	1.108	No	ns	-4.651 to 2.693
TRF1 vs T271A	12.12	13.72	Yes	***	8.450 to 15.79
TRF1 vs T271D	7.563	8.56	Yes	***	3.892 to 11.23
T271A vs T271D	-4.558	5.159	Yes	**	-8.230 to -0.8865
Figure 3.13B					
Column A	Vector				
vs	vs				
Column B	TRF1				
Paired t test					
P value	0.0292				
P value summary	*				
Are means signif. different? (P < 0.05)	Yes				
One- or two-tailed P value?	Two-tailed				
t, df	t=5.723 df=2				
Number of pairs	3				
How big is the difference?					
Mean of differences	-1.249				
95% confidence interval	-2.188 to -0.3099				
R squared	0.9425				
Column B	TRF1				
vs	vs				
Column C	T271A				
Unpaired t test					
P value	0.618				

P value summary	ns				
Are means signif. different? (P < 0.05)	No				
One- or two-tailed P value?	Two-tailed				
t, df	t=0.5398 df=4				
How big is the difference?					
Mean ± SEM of column B	2.249 ± 0.2182 N=3				
Mean ± SEM of column C	2.567 ± 0.5481 N=3				
Difference between means	-0.3185 ± 0.5899				
95% confidence interval	-1.956 to 1.319				
R squared	0.06791				
F test to compare variances					
F,DFn, Dfd	6.307, 2, 2				
P value	0.2737				
P value summary	ns				
Are variances significantly different?	No				
Column B	TRF1				
vs	vs				
Column D	T271D				
Unpaired t test					
P value	0.8162				
P value summary	ns				
Are means signif. different? (P < 0.05)	No				
One- or two-tailed P value?	Two-tailed				
t, df	t=0.2481 df=4				
How big is the difference?					
Mean ± SEM of column B	2.249 ± 0.2182 N=3				
Mean ± SEM of column D	2.388 ± 0.5161 N=3				
Difference between means	-0.1391 ± 0.5604				
95% confidence interval	-1.695 to 1.416				
R squared	0.01516				

F test to compare variances					
F,DFn, Dfd	5.593, 2, 2				
P value	0.3034				
P value summary	ns				
Are variances significantly different?	No				
Figure 4.1E					
One-way analysis of variance					
P value	< 0.0001				
P value summary	***				
Are means signif. different? (P < 0.05)	Yes				
Number of groups	6				
F	385.8				
R squared	0.9938				
ANOVA Table	SS	df	MS		
Treatment (between columns)	6996	5	1399		
Residual (within columns)	43.52	12	3.626		
Total	7039	17			
Tukey's Multiple Comparison Test	Mean Diff.	q	Significant? P < 0.05?	Summary	95% CI of diff
0 vs 2	-4.381	3.985	No	ns	-9.605 to 0.8421
0 vs 4	-9.071	8.251	Yes	***	-14.29 to -3.848
0 vs 6	-15.63	14.22	Yes	***	-20.86 to -10.41
0 vs 8	-19.21	17.48	Yes	***	-24.44 to -13.99
0 vs 16	40.34	36.69	Yes	***	35.12 to 45.57
2 vs 4	-4.69	4.266	No	ns	-9.913 to 0.5337
2 vs 6	-11.25	10.23	Yes	***	-16.48 to -6.028
2 vs 8	-14.83	13.49	Yes	***	-20.06 to -9.610

2 vs 16	44.72	40.68	Yes	***	39.50 to 49.95
4 vs 6	-6.562	5.969	Yes	*	-11.79 to -1.339
4 vs 8	-10.14	9.226	Yes	***	-15.37 to -4.920
4 vs 16	49.41	44.94	Yes	***	44.19 to 54.64
6 vs 8	-3.581	3.257	No	ns	-8.805 to 1.642
6 vs 16	55.98	50.91	Yes	***	50.75 to 61.20
8 vs 16	59.56	54.17	Yes	***	54.33 to 64.78
Figure 4.1D					
One-way analysis of variance					
P value	< 0.0001				
P value summary	***				
Are means signif. different? (P < 0.05)	Yes				
Number of groups	6				
F	39.8				
R squared	0.9431				
ANOVA Table	SS	df	MS		
Treatment (between columns)	2696	5	539.1		
Residual (within columns)	162.6	12	13.55		
Total	2858	17			
Tukey's Multiple Comparison Test	Mean Diff.	q	Significant? P < 0.05?	Summary	95% CI of diff
0 vs 2	-10.9	5.13	Yes	*	-21.00 to -0.8048
0 vs 4	-23.73	11.17	Yes	***	-33.83 to -13.64
0 vs 6	-27.64	13.01	Yes	***	-37.74 to -17.55
0 vs 8	-26.1	12.28	Yes	***	-36.20 to -16.01
0 vs 16	2.316	1.09	No	ns	-7.779 to 12.41
2 vs 4	-12.83	6.039	Yes	*	-22.93 to -2.738

2 vs 6	-16.74	7.879	Yes	**	-26.84 to -6.647
2 vs 8	-15.2	7.155	Yes	**	-25.30 to -5.109
2 vs 16	13.22	6.22	Yes	**	3.121 to 23.31
4 vs 6	-3.909	1.84	No	ns	-14.00 to 6.187
4 vs 8	-2.371	1.116	No	ns	-12.47 to 7.724
4 vs 16	26.05	12.26	Yes	***	15.95 to 36.15
6 vs 8	1.538	0.7236	No	ns	-8.558 to 11.63
6 vs 16	29.96	14.1	Yes	***	19.86 to 40.05
8 vs 16	28.42	13.37	Yes	***	18.33 to 38.52
Figure 4.4I					
One-way analysis of variance					
P value	0.3774				
P value summary	ns				
Are means signif. different? (P < 0.05)	No				
Number of groups	3				
F	1.151				
R squared	0.2773				
ANOVA Table	SS	df	MS		
Treatment (between columns)	1.303	2	0.6515		
Residual (within columns)	3.396	6	0.5659		
Total	4.699	8			
Tukey's Multiple Comparison Test	Mean Diff.	q	Significant? P < 0.05?	Summary	95% CI of diff
DMSO vs DRB	0.9207	2.12	No	ns	-0.9639 to 2.805
DMSO vs ActD	0.3349	0.7711	No	ns	-1.550 to 2.220
DRB vs ActD	-0.5858	1.349	No	ns	-2.470 to 1.299

Figure 4.4K					
Column A	DMSO				
vs	vs				
Column B	DRB				
Unpaired t test					
P value	0.5121				
P value summary	ns				
Are means signif. different? (P < 0.05)	No				
One- or two-tailed P value?	Two-tailed				
t, df	t=0.7186 df=4				
How big is the difference?					
Mean ± SEM of column A	88.93 ± 1.812 N=3				
Mean ± SEM of column B	90.50 ± 1.230 N=3				
Difference between means	-1.574 ± 2.190				
95% confidence interval	-7.654 to 4.506				
R squared	0.1143				
F test to compare variances					
F,DFn, Dfd	2.171, 2, 2				
P value	0.6307				
P value summary	ns				
Are variances significantly different?	No				

APPENDIX III PUBLICATION

Results presented in Chapter 4 were part of the work published in *Journal of Cell Science*, on May 16, 2016. The work was published in Volume 129, Issue 13, pages 2259-2572 (DOI: http://dx.doi.org/10.1242/jcs.186098). The authors listed were as follows: Florence R. Wilson*, Angus Ho*, John R. Walker, and Xu-Dong Zhu. * These authors contributed equally to the work.

Presented hereafter is the original publication.

© 2016. Published by The Company of Biologists Ltd | Journal of Cell Science (2016) 129, 2559-2572 doi:10.1242/jcs.186098

RESEARCH ARTICLE

Cdk-dependent phosphorylation regulates TRF1 recruitment to PML bodies and promotes C-circle production in ALT cells

Florence R. Wilson*, Angus Ho*, John R. Walker and Xu-Dong Zhu‡

ABSTRACT

TRF1, a duplex telomeric DNA binding protein, is implicated in homologous-recombination-based alternative lengthening of telomeres, known as ALT. However, how TRF1 promotes ALT activity has yet to be fully characterized. Here we report that Cdk-dependent TRF1 phosphorylation on T371 acts as a switch to create a pool of TRF1, referred to as (pT371)TRF1, which is recruited to ALT-associated PML bodies (APBs) in S and G2 phases independently of its binding to telomeric DNA. We find that phosphorylation of T371 is essential for APB formation and C-circle production, both of which are hallmarks of ALT. We show that the interaction of (pT371)TRF1 with APBs is dependent upon ATM and homologous-recombination-promoting factors Mre11 and BRCA1. In addition, (pT371)TRF1 interaction with APBs is sensitive to transcription inhibition, which also reduces DNA damage at telomeres. Furthermore, overexpression of RNaseH1 impairs (pT371)TRF1 recruitment to APBs in the presence of campothecin, an inhibitor that prevents topoisomerase I from resolving RNA–DNA hybrids. These results suggest that transcription-associated DNA damage, perhaps arising from processing RNA–DNA hybrids at telomeres, triggers (pT371)TRF1 recruitment to APBs to facilitate ALT activity.

KEY WORDS: Cdk, TRF1, PML bodies, ALT

INTRODUCTION

In most human somatic cells, telomeres shorten with each round of DNA replication, in part because of an inability of DNA polymerases to fill in the gap left from removal of the last RNA primer (Levy et al., 1992). When the length of telomeric DNA becomes critically short, the DNA damage response is activated, triggering the induction of replicative senescence (d'Adda di Fagagna et al., 2003). About 85-90% of human cancers avoid replicative senescence and gain unlimited growth potential by activating telomerase (Shay and Bacchetti, 1997). The remaining 10-15% of human cancers do not activate telomerase but instead maintain their telomere length through a homologous-recombination-based mechanism, referred to as alternative lengthening of telomeres (ALT) (Cesare and Reddel, 2010). ALT tends to be associated with aggressive cancers including osteosarcomas, soft tissue sarcomas, gastric carcinomas, astrocytomas and neuroblastomas, as well as a subset of *in vitro* transformed cell lines (Henson and Reddel, 2010).

Department of Biology, McMaster University, Hamilton, Ontario, Canada L8S 4K1.
*These authors contributed equally to this work

‡Author for correspondence (zhuxu@mcmaster.ca)

X.-D.Z., 0000-0003-1859-3134

Received 14 January 2016; Accepted 6 May 2016

ALT cells carry several hallmarks (Cesare and Reddel, 2010), which include telomere length heterogeneity, a high level of extra-chromosome telomeric DNA such as C-circles, as well as PML bodies containing telomeric chromatin, referred to as ALT-associated PML bodies (APBs) (Henson and Reddel, 2010). APBs contain many proteins involved in DNA replication, recombination and repair (Chung et al., 2011), including the Mre11–Rad50–Nbs1 complex (Nbs1 is also known as NBN) (Wu et al., 2003, 2000), BRCA1, Rad51, Rad52 and RPA (Yeager et al., 1999). It has been reported that APB formation requires Nbs1, which mediates the recruitment of Mre11, Rad50 and BRCA1 to APBs (Wu et al., 2003). DNA synthesis has been shown to occur at APBs (Grobelny et al., 2000; Wu et al., 2000) and has been found to be dependent upon ATM and ATR (Nabetani et al., 2004). It has been suggested that APBs might be sites where homologous-recombination-mediated telomere maintenance takes place (Draskovic et al., 2009; Wu et al., 2000). Disruption in the formation of APBs leads to telomere shortening in ALT cells (Zhong et al., 2007), suggesting that APBs are involved in ALT activity.

TRF1, a subunit of the shelterin (also known as telosome) complex that also includes TRF2 (also known as TERF2), TIN2 (also known as TINF2), hRap1 (also known as TERF2IP), TPP1 and POT1 (de Lange, 2005; Liu et al., 2004), is a multifunctional protein that is implicated in telomere length maintenance (Ancelin et al., 2002; van Steensel and de Lange, 1997), cell cycle progression (Shen et al., 1997; Zhou et al., 2003), resolution of sister telomeres (Canudas et al., 2007; McKerlie and Zhu, 2011) as well as DNA double-strand break repair (Kishi et al., 2001; McKerlie et al., 2013). In telomerase-expressing cells, TRF1 acts as a negative regulator of telomere length maintenance (Ancelin et al., 2002; van Steensel and de Lange, 1997) whereas in ALT cells, TRF1 is implicated as a positive mediator of homologous-recombination-based telomere maintenance (Jiang et al., 2007). Depletion of TRF1 impairs the formation of APBs (Jiang et al., 2007). TRF1 is reported to be SUMOylated and SUMOylation has been suggested to promote APB formation (Potts and Yu, 2007). However, whether other types of post-translational modifications such as phosphorylation might regulate ALT activity has remained largely uncharacterized.

TRF1 undergoes extensive phosphorylation (Walker and Zhu, 2012). It has been reported that Cdk1 phosphorylates TRF1 on T371 and that this phosphorylation regulates sister telomere resolution and DNA double-strand break repair in telomerase-expressing cells (McKerlie et al., 2013; McKerlie and Zhu, 2011); however, the role of this phosphorylation in ALT cells has yet to be characterized. Here, we report that Cdk-dependent phosphorylation of TRF1 on T371 promotes TRF1 interaction with APBs in S and G2 phases independently of its binding to telomeric DNA. Loss of TRF1 phosphorylation on T371 impairs APB formation and C-circle production, indicative of its important role in promoting ALT

Journal of Cell Science (2016) 129, 2559-2572 doi:10.1242/jcs.186098

activity. We demonstrate that (pT371)TRF1 is associated with a subset of ALT telomeres that are predominantly dysfunctional as evidenced by their accumulation of γH2AX. The interaction of (pT371)TRF1 with APBs is dependent upon ATM and homologous-recombination-promoting factors Mre11 and BRCA1. We show that transcription inhibition not only impairs (pT371)TRF1 interaction with APBs but also reduces telomeric accumulation of γH2AX. Furthermore, overexpression of RNaseH1 impairs (pT371)TRF1 interaction with APBs in the presence of camptothecin, an inhibitor of topoisomerase I. Taken together, these results suggest that Cdk activity in S and G2 phases controls TRF1 interaction with APBs and that this interaction is triggered by transcription-associated DNA damage, perhaps arising from processing RNA–DNA hybrids at telomeres.

RESULTS

Cdk-dependent punctate nuclear staining of phosphorylated (pT371)TRF1

Cdk1 phosphorylates TRF1 on T371 and this phosphorylation creates a stable pool of TRF1, referred to as (pT371)TRF1, which exists largely free of telomere chromatin (McKerlie and Zhu, 2011). To investigate if (pT371)TRF1 might play a role in the regulation of ALT activity, we first examined the nuclear staining of (pT371)TRF1 in several ALT cell lines (GM847, U2OS and WI38VA13/2RA) through analysis of indirect immunofluorescence with a phospho-specific anti-TRF1-pT371 antibody. In all ALT cell lines examined, (pT371)TRF1 was found to exhibit punctate nuclear staining in about 50% of interphase cells whereas its nuclear staining in the remaining population of interphase cells was diffuse and barely detectable (Fig. 1A; Fig. S1A). This staining was in sharp contrast to anti-TRF1 staining, which predominantly detects telomere-bound TRF1 and was observed in all interphase cells (Fig. S1B). These results suggest that the punctate nuclear staining of (pT371)TRF1 might be cell-cycle regulated.

To investigate the nature of cell-cycle-dependent staining of (pT371)TRF1, we performed dual indirect immunofluorescence with an anti-pT371 antibody in conjunction with an antibody against cyclin A, a marker for S and G2 cells. The punctate nuclear staining of (pT371)TRF1 was overwhelmingly seen in cells staining positive for cyclin A (Fig. 1B). Over 80% and 90% of GM847 and U2OS cells, respectively, exhibiting punctate nuclear staining of (pT371)TRF1 were positive for cyclin A (Fig. 1C), suggesting that the punctate nuclear staining of (pT371)TRF1 occurs predominantly in the S and G2 phases of the cell cycle.

T371 of TRF1 is reported to be a target of Cdk1 (McKerlie and Zhu, 2011). To investigate if Cdk activity might regulate the punctate nuclear staining of (pT371)TRF1 in S and G2 cells, we subjected GM847 cells to a double thymidine block. Western analysis revealed that TRF1 phosphorylation on T371 started to increase as cells progressed through S and G2 phases, peaking 10 h post-release and falling sharply 16 h post-release from a double thymidine block (Fig. 1D), in agreement with previous finding (McKerlie and Zhu, 2011). We observed that the majority of GM847 cells at 10 h post-release were in mitosis and therefore we did not include them for examination of interphase nuclear staining of (pT371)TRF1. The number of GM847 cells exhibiting punctate nuclear staining of (pT371)TRF1 increased as cells progressed through S and G2 phases and then dropped sharply as cells entered G1 phase at 16 h post-release from a double thymidine block (Fig. 1E). In addition, we found that treatment with Cdk inhibitor roscovitine for one hour led to a significant reduction in the number of GM847 cells exhibiting the punctate nuclear staining of (pT371)TRF1 (Fig. 1F). Taken together, these results suggest that Cdk activity regulates the punctate nuclear staining of (pT371)TRF1, and further imply that the lack of detectable nuclear staining of (pT371)TRF1 in cyclin-A-negative cells probably results from a lack of Cdk-dependent T371 phosphorylation in G1 cells.

Phosphorylated (pT371)TRF1 is preferentially associated with dysfunctional telomere ends

Our finding of punctate nuclear staining of (pT371)TRF1 prompted us to investigate if (pT371)TRF1 might be associated with ALT telomeres. Immunofluorescence combined with fluorescence *in situ* hybridization (IF-FISH) analysis by using an anti-pT371 antibody (red) in conjunction with a FITC-conjugated PNA probe against telomeric DNA (green) revealed that the number of punctate anti-pT371 foci (red) in a given interphase cell was always less than that of punctate telomere foci (green) (Fig. 2A). Whereas all punctate anti-pT371 foci seemed to colocalize well with telomeric DNA, not all telomere foci contained detectable (pT371)TRF1 staining (Fig. 2A), suggesting that (pT371)TRF1 is associated with a subset of interphase ALT telomeres.

Telomeres in ALT cells are known to elicit a DNA damage response (Cesare et al., 2009; Cho et al., 2014; Dunham et al., 2000; Wu et al., 2000). In agreement with previous findings, we found that GM847 cells exhibited a high level of genomic instability as evidenced by their accumulation of γH2AX staining (Fig. 2B). We estimated that at least 80% of GM847 cells exhibited the formation of γH2AX foci (Fig. 2C). The number of γH2AX foci per GM847 cell ranged from less than 5 to greater than 15 foci (Fig. 2C). Although the total number of cells exhibiting γH2AX foci did not change significantly throughout the cell cycle (Fig. 2C), the number of cells exhibiting greater than 15 γH2AX foci dropped sharply 16 h post-release from a double thymidine block (Fig. 2C), suggesting that the amount of DNA damage per cell is higher in S/G2 cells than in G1 cells.

Analysis of dual indirect immunofluorescence with an anti-pT371 antibody in conjunction with an anti-γH2AX antibody revealed very good colocalization between punctate anti-pT371 foci and a subset of γH2AX foci in GM847 interphase cells (Fig. 2B), suggesting that (pT371)TRF1 is associated with dysfunctional telomeres. Further analysis of (pT371)TRF1 colocalization with γH2AX in synchronized GM847 cells revealed that the level of (pT371)TRF1 colocalization with γH2AX was cell-cycle regulated, dipping to the lowest level 16 h post-release from a double thymidine block (Fig. 2D). The colocalization of (pT371)TRF1 with γH2AX was predominantly seen in GM847 cells exhibiting greater than 15 γH2AX foci (Fig. 2D). Taken together, these results suggest that (pT371)TRF1 might be recruited to telomeres in response to DNA damage.

We also investigated the association of (pT371)TRF1 with telomeres on metaphase chromosome spreads from GM847 cells. Analysis of indirect immunofluorescence revealed that (pT371)TRF1 was also associated with only a subset of metaphase chromosome ends (Fig. 2E). In addition, (pT371)TRF1 was found to be almost always associated with telomere ends that were also enriched for γH2AX (Fig. 2E). These results suggest that (pT371)TRF1 is preferentially recruited to dysfunctional telomere ends.

Phosphorylated (pT371)TRF1 is a component of ALT-associated PML bodies (APBs)

Analysis of dual indirect immunofluorescence with an anti-pT371 antibody in conjunction with an anti-PML antibody in

Journal of Cell Science (2016) 129, 2559-2572 doi:10.1242/jcs.186098

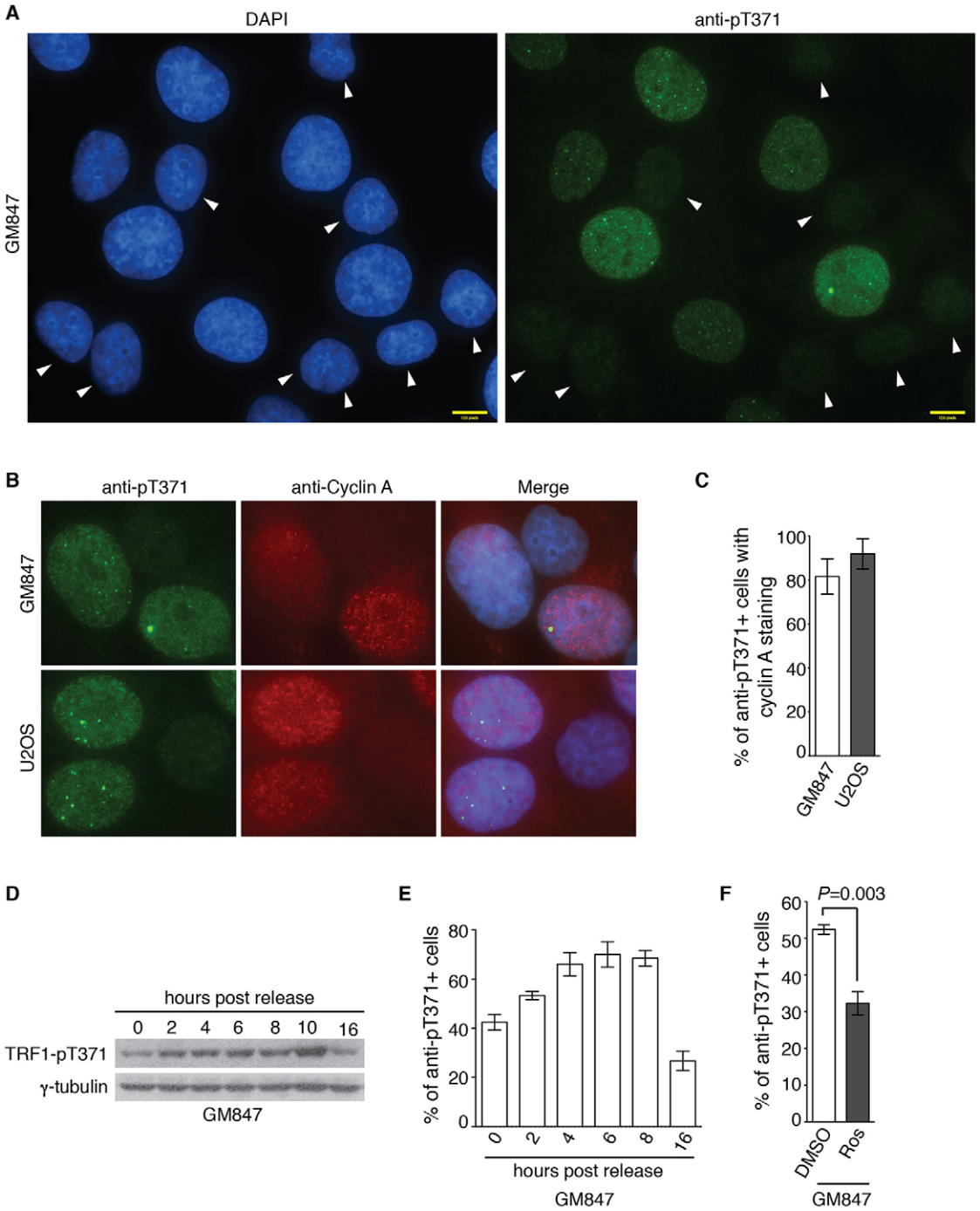

Fig. 1. Cell cycle-dependent association of (pT371)TRF1 with ALT telomeres. (A) Indirect immunofluorescence with rabbit anti-pT371 antibody. Cell nuclei were stained with DAPI in blue in this and subsequent figures. Arrowheads indicate nuclei with barely detectable anti-pT371 staining. (B) Immunofluorescence analysis with both anti-pT371 and anti-cyclin-A antibodies. (C) Quantification of the percentage of cells staining positive for both (pT371)TRF1 and cyclin A. A total of 500 cells from each independent experiment were scored in blind for each cell line. Standard deviations from three independent experiments are indicated. (D) Western analysis of GM847 cells post-release from a double thymidine block as indicated. Immunoblotting was carried out with an anti-pT371 antibody. The γ-tubulin blot was used as a loading control in this and subsequent figures. (E) Quantification of the percentage of synchronized GM847 cells staining positive for (pT371)TRF1. A total of 1000 cells from each independent experiment were scored in blind. Standard deviations from three independent experiments are indicated. (F) Quantification of the percentage of cells staining positive for (pT371)TRF1. GM847 cells were treated with either DMSO or roscovitine (20 μM), a Cdk inhibitor, for 1 h prior to IF analysis. Scoring was done as described in E. Standard deviations from three independent experiments are indicated.

ALT cell lines GM847 and U2OS revealed consistent and reproducible colocalization of labeled pT371 foci with PML foci (Fig. 3A), suggesting that (pT371)TRF1 is a component of APBs. This notion was further supported by IF-FISH analysis involving triple staining with an anti-pT371 antibody, an anti-PML antibody and a FITC-conjugated PNA probe against telomeric DNA, which demonstrated colocalization of (pT371)TRF1 foci with both telomeric DNA and PML (Fig. 3B).

Journal of Cell Science (2016) 129, 2559-2572 doi:10.1242/jcs.186098

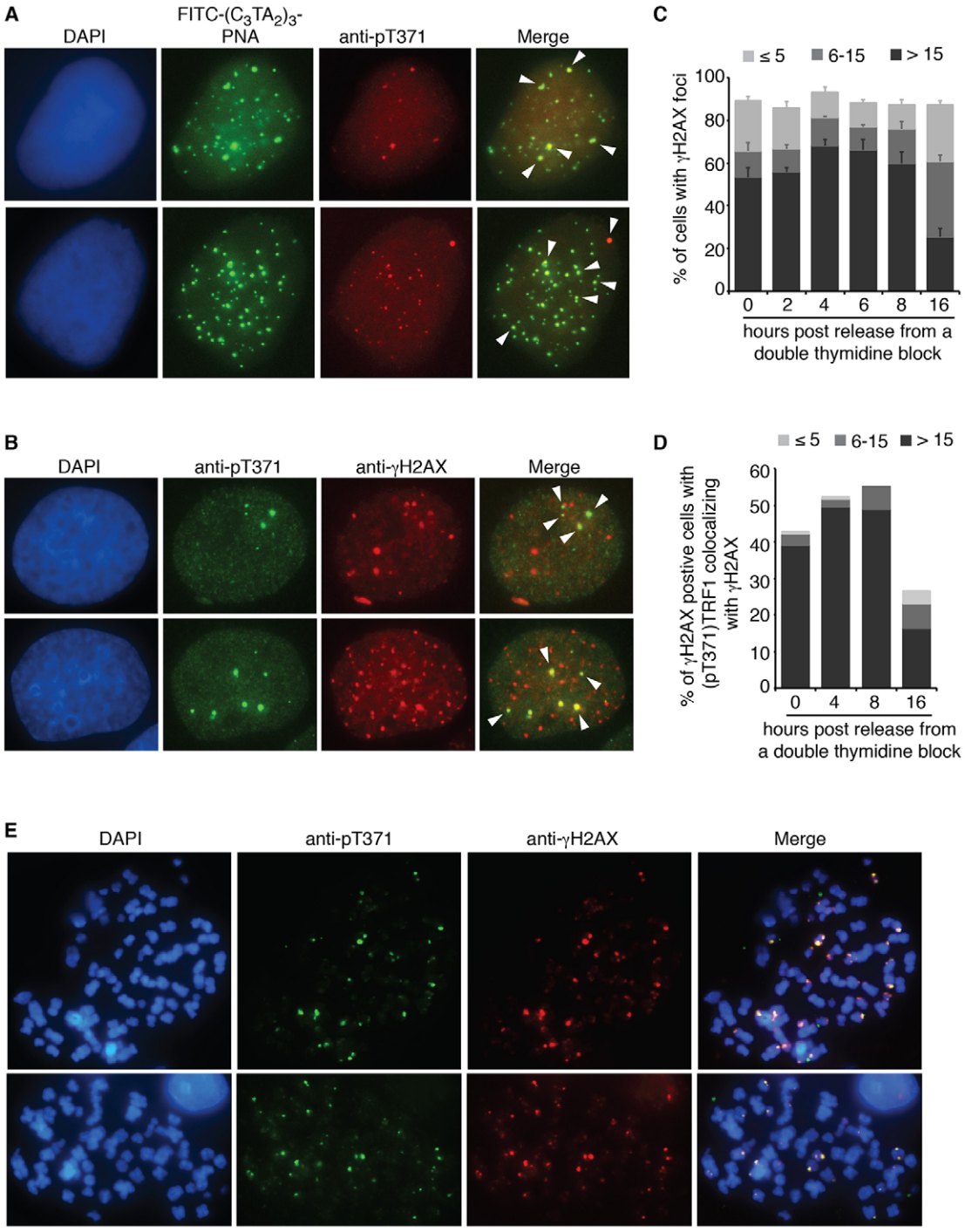

Fig. 2. Phosphorylated (pT371)TRF1 is associated with a subset of ALT telomeres that are predominantly dysfunctional. (A) IF-FISH analysis of interphase GM847 cells with a FITC-conjugated telomere-containing PNA probe (green) in conjunction with an anti-pT371 antibody (red). Arrowheads indicate colocalization of (pT371)TRF1 with telomeres. (B) Immunofluorescence analysis of interphase GM847 cells with both anti-pT371 and anti-γH2AX antibodies. Arrowheads indicate colocalization of (pT371)TRF1 with γH2AX foci. (C) Quantification of the percentage of synchronized GM847 cells exhibiting γH2AX foci as indicated. A total of 1000 cells from each independent experiment were scored in blind. Standard deviations from three independent experiments are indicated. Light grey bars, 1-5 γH2AX foci per cell; dark grey bars, 6-15 γH2AX foci per cell; black bars, >15 γH2AX foci per cell. (D) Quantification of the percentage of γH2AX-positive GM847 cells exhibiting (pT371)TRF1 colocalization with γH2AX foci as indicated. Scoring of colocalization was done in blind from captured cell images. The number of cells scored for each time point: 171 (0 h); 149 (4 h); 149 (8 h) and 208 (16 h). Light grey bars, 1-5 γH2AX foci per cell; dark grey bars, 6-15 γH2AX foci per cell; black bars, >15 γH2AX foci per cell. (E) Immunofluorescence analysis of metaphase GM847 cells with both anti-pT371 antibody and anti-γH2AX antibodies.

TRF1 phosphorylation on T371 is needed to support APB formation and C-circle production

TRF1 is crucial for the formation of APBs (Jiang et al., 2007; Potts and Yu, 2007), which are hallmarks of ALT cells and are composed of shelterin proteins and repair factors such as Nbs1, a component of the Mre11 complex essential for APB formation (Jiang et al., 2007; Wu et al., 2003; Zhong et al., 2007). We observed the colocalization of TRF2, hRap1, TIN2 and Nbs1 with

Journal of Cell Science (2016) 129, 2559-2572 doi:10.1242/jcs.186098

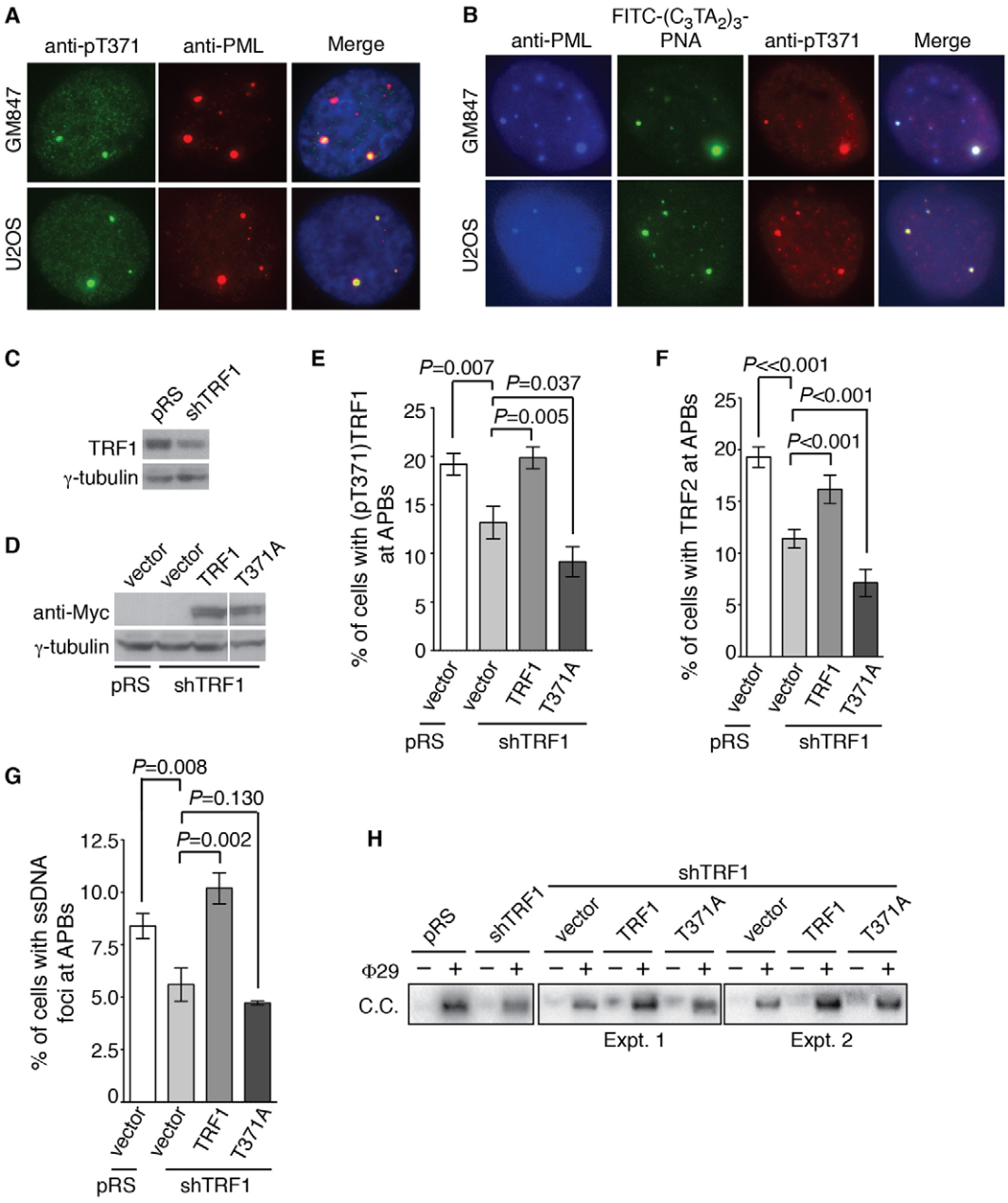

Fig. 3. TRF1 phosphorylation at T371 is needed to support APB formation and C-circle production. (A) Immunofluorescence analysis of GM847 and U2OS cells with both anti-pT371 and anti-PML antibodies. (B) IF-FISH analysis of GM847 and U2OS cells with a FITC-conjugated telomere-containing PNA probe in conjunction with anti-pT371 and anti-PML antibodies. (C) Western analysis of GM847 cells expressing the vector alone (pRS) or shRNA against TRF1 (shTRF1) as indicated. Immunoblotting was performed with anti-TRF1 and anti-γ-tubulin antibodies. (D) Western analysis of pRS- and shTRF1-expressing GM847 cells complemented with either the vector alone or various Myc-tagged TRF1 alleles as indicated. Immunoblotting was performed with anti-Myc and anti-γ-tubulin antibodies. (E) Quantification of the percentage of GM847 cells as indicated with (pT371)TRF1 at APBs. A total of 500 cells from each experiment were scored for each cell line as indicated in blind. Standard deviations from three independent experiments are indicated. (F) Quantification of the percentage of GM847 cells as indicated with TRF2 at APBs. Scoring was done as described in E. Standard deviations from six independent experiments are indicated. (G) Quantification of the percentage of cells with ssDNA foci at APBs. GM847 cells as indicated were incubated in the presence of 10 μM BrdU (Sigma) for 24 h prior to immunofluorescence analysis with anti-BrdU and anti-PML antibodies. A total of 1000 cells from each independent experiment were scored for each cell line in blind. Standard deviations from three independent experiments are indicated. (H) Analysis of C-circle formation. C.C., C-circles.

PML at APBs in GM847 cells (Fig. S2A), in agreement with previous findings (Jiang et al., 2007; Wu et al., 2003; Zhong et al., 2007). To investigate if phosphorylation of TRF1 on T371 might be involved in APB formation, we depleted endogenous TRF1 in GM847 cells (Fig. 3C) and then complemented TRF1-depleted GM847 cells with Myc-tagged shTRF1-resistant wild-type TRF1 or TRF1 carrying an amino acid substitution of T371A. The expression of Myc-tagged TRF1-T371A was comparable with that of Myc-tagged wild-type TRF1 (Fig. 3D). Depletion of TRF1 not only impaired the localization of (pT371)TRF1 to APBs (Fig. 3E) but also resulted in a significant decrease in the number of GM847 cells exhibiting colocalization of PML with TRF2 (Fig. 3F), hRap1 (Fig. S2B), TIN2 (Fig. S2C) and Nbs1 (Fig. S2D). Overexpression of Myc-tagged wild-type TRF1

Journal of Cell Science (2016) 129, 2559-2572 doi:10.1242/jcs.186098

suppressed the impaired association of (pT371)TRF1, TRF2, hRap1, TIN2 and Nbs1 with PML bodies in TRF1-depleted GM8487 cells (Fig. 3E,F; Fig. S2B-D), whereas introduction of Myc-tagged TRF1 carrying a T371 mutation failed to do so (Fig. 3E,F; Fig. S2B-D). Taken together, these results suggest that phosphorylation of TRF1 on T371 is necessary for the assembly of APBs. Furthermore, our finding that Myc-tagged TRF1-T371A fails to rescue (pT371)TRF1 association with APBs confirms that the observed staining of pT371 at APBs is specific.

APBs are thought to be sites of homologous-recombination-mediated telomere synthesis and therefore, we asked if T371 phosphorylation might play a role in the generation of single-stranded DNA (ssDNA), a key intermediate of homologous recombination, within APBs. To visualize the presence of ssDNA within APBs, we performed dual indirect immunofluorescence with an anti-PML antibody in conjunction with an anti-BrdU antibody under non-denaturing conditions (Fig. S2E). We observed the presence of ssDNA within APBs in about 8-9% of GM847 cells expressing the vector alone (Fig. 3G). Depletion of TRF1 led to a significant decrease in the number of cells containing ssDNA within APBs (Fig. 3G). This decrease was suppressed by Myc-tagged wild-type TRF1 but not by Myc-tagged TRF1 carrying a T371A mutation (Fig. 3G), indicating that T371 phosphorylation is necessary for the generation of ssDNA within APBs. These results suggest that T371 phosphorylation is needed to facilitate homologous-recombination-mediated telomere synthesis.

We also examined the role of T371 phosphorylation in the production of C-circles, another key feature of ALT activity. Analysis of C-circle assays revealed that depletion of TRF1 resulted in a decrease in the level of C-circles in GM847 cells (Fig. 3H). Introduction of Myc-tagged wild-type TRF1 reproducibly rescued the level of C-circles in TRF1-depleted cells, whereas overexpression of Myc-tagged TRF1 carrying a T371A mutation failed to do so (Fig. 3H), indicating that T371 phosphorylation plays an important role in C-circle production in ALT cells.

ATM and homologous-recombination-promoting factors Mre11 and BRCA1 mediate the association of (pT371)TRF1 with APBs

We have shown that (pT371)TRF1 is preferentially associated with dysfunctional telomere ends at APBs. To investigate how (pT371)TRF1 might be recruited to APBs, we asked if ATM, a master regulator of DNA damage response, might play a role in the regulation of (pT371)TRF1 association with APBs. To address this question, we performed indirect immunofluorescence with an anti-pT371 antibody in GM847 cells stably expressing the vector alone or shRNA against ATM. Depletion of ATM impaired the recruitment of (pT371)TRF1 to APBs (Fig. 4A,B). The impaired recruitment of (pT371)TRF1 to APBs was also observed in GM847 cells treated with KU55933, a specific inhibitor of ATM (Fig. 4C,D). Conversely, treatment with NU7026, a specific inhibitor of DNA-PKcs, had little impact on the association of (pT371)TRF1 with APBs (Fig. 4C,D). Knockdown or inhibition of ATM as well as inhibition of DNA-PKcs had little effect on the percentage of GM847 cells staining positive for cyclin A (Fig. 4E,F), indicating that the impaired recruitment of (pT371)TRF1 to APBs in ATM-depleted or -inhibited cells is unlikely to result from a change in the number of cyclin A-positive cells. Furthermore, knockdown of ATM did not alter the level of (pT371)TRF1 (Fig. 4G). Taken together, these results suggest that ATM mediates the association of (pT371)TRF1 with APBs.

APBs are thought to be sites of homologous-recombination-mediated telomere synthesis and therefore we examined if homologous-recombination-promoting factors such as Mre11 and BRCA1 might mediate the association of (pT371)TRF1 with APBs. Treatment with Mirin, a specific inhibitor of Mre11 (Dupre et al., 2008), led to a significant reduction in the number of GM847 cells with (pT371)TRF1 localized at APBs (Fig. 4C,D). Depletion of BRCA1 also impaired the association of (pT371)TRF1 with APBs (Fig. 4A,H). Conversely, depletion of 53BP1, a non-homologous-end-joining (NHEJ)-promoting factor, had little effect on (pT371)TRF1 association with APBs (Fig. 4A,H). Depletion of either BRCA1 or 53BP1 had little impact on the level of (pT371)TRF1 (Fig. 4I,J). Futhermore, no significant change in the number of cyclin-A-positive cells was detected as a result of Mirin treatment or depletion of either BRCA1 or 53BP1 (Fig. 4F,K). Collectively, these results suggest that the association of (pT371)TRF1 with APBs is dependent upon homologous-recombination-promoting factors but not NHEJ-promoting factors.

Transcription-associated DNA damage at telomeres mediates the association of (pT371)TRF1 with APBs

It has been reported that transcription of telomeric DNA is upregulated in ALT cells (Arora et al., 2014; Azzalin et al., 2007). Collision between the transcription and DNA replication machineries is known to give rise to DNA double-strand breaks (DSBs) (Helmrich et al., 2013). Therefore we reasoned that enhanced transcription at ALT telomeres might be a source of DNA damage that triggers the recruitment of (pT371)TRF1 to APBs. To investigate this hypothesis, we treated GM847 cells with transcription inhibitor DRB. Analysis of indirect immunofluorescence with an anti-TRF2 antibody in conjunction with an antibody against γH2AX, a marker for DNA damage, revealed that treatment with DRB led to a significant reduction in the number of cells exhibiting γH2AX colocalization with TRF2 (Fig. 5A,B), suggesting that ALT telomeres are associated with transcription-induced DNA damage. Treatment with DRB also significantly reduced the number of cells exhibiting (pT371)TRF1 association with APBs (Fig. 5C,D). The impaired association of (pT371)TRF1 with APBs was also observed in GM847 cells treated with another transcription inhibitor, actinomycin D (Fig. 5C,E), as well as in U2OS cells treated with either DRB or actinomycin D (Fig. S3A,B). By contrast, treatment with DRB did not affect the number of cyclin-A-positive GM847 cells (Fig. S3C), nor did it affect the number of GM847 cells with PML bodies (Fig. S3D). DRB treatment also had little impact on the level of (pT371)TRF1 and PML proteins in GM847 cells (Fig. S3E). Taken together, these results suggest that (pT371)TRF1 association with APBs is dependent upon active transcription, and further imply that transcription-associated DNA damage at telomeres mediates (pT371)TRF1 association with APBs.

Earlier, we showed that ATM regulates (pT371)TRF1 association with APBs. To investigate the epistatic relationship between ATM and transcription, we treated GM847 cells with both ATM inhibitor KU55933 and transcription inhibitor DRB. The combined treatment with both KU55933 and DRB did not lead to any further reduction in the localization of (pT371)TRF1 to APBs compared with treatment with either KU55933 or DRB alone (Fig. 5F), suggesting that ATM and transcription act in the same epistatic pathway in regulating the recruitment of (pT371)TRF1 to APBs.

Journal of Cell Science

Journal of Cell Science (2016) 129, 2559-2572 doi:10.1242/jcs.186098

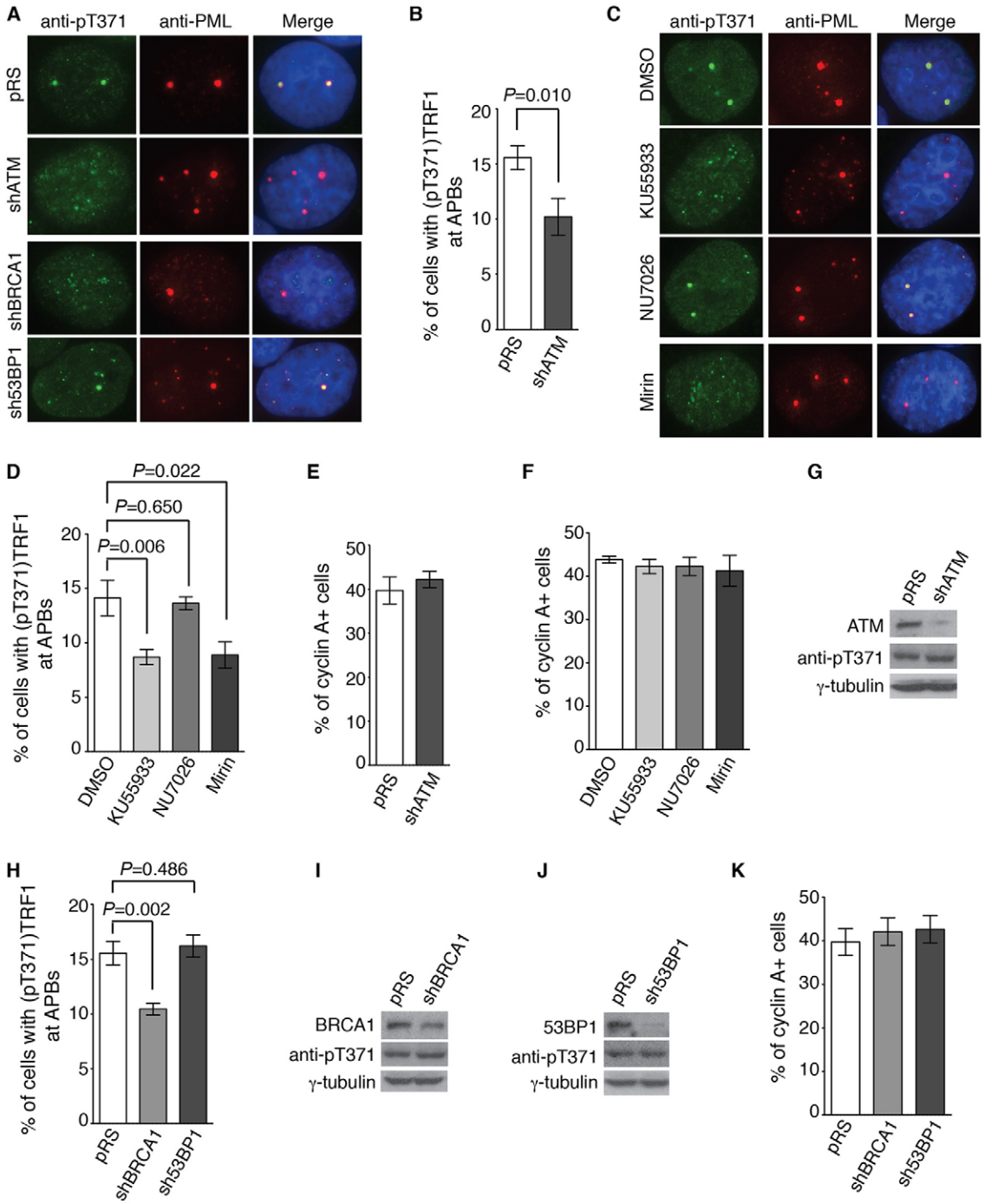

Fig. 4. Association of (pT371)TRF1 with APBs is dependent upon ATM, Mre11 and BRCA1 but not DNA-PKcs and 53BP1. (A) Immunofluorescence analysis of staining with anti-pT371 and anti-PML antibodies in GM847 cells expressing the vector alone or shRNA against ATM, BRCA1 or 53BP1 as indicated. (B) Quantification of the percentage of pRS- and shATM- expressing cells with (pT371)TRF1 at APBs. A total of 1000 cells from each independent experiment were scored for each cell line in blind. Standard deviations from three independent experiments are indicated. (C) Immunofluorescence analysis of staining with anti-pT371 and anti-PML antibodies in GM847 cells treated with either DMSO, KU55933 or NU7026 for 1 h prior to fixation. (D) Quantification of the percentage of GM847 cells with (pT371)TRF1 at APBs from C. Scoring was done as described in B. Standard deviations from three independent experiments are indicated. (E) Quantification of the percentage of pRS- and shATM-expressing GM847 cells staining positive for cyclin A. Scoring was done as described in B. Standard deviations from three independent experiments are indicated. (F) Quantification of the percentage of DMSO-, KU55933-, NU7026- and Mirin-treated GM847 cells staining positive for cyclin A. Scoring was done as described in B. Standard deviations from three independent experiments are indicated. (G) Western analysis of GM847 stably expressing the vector alone (pRS) or shRNA against ATM (shATM). Immunoblotting was performed with anti-ATM, anti-pT371 and anti-γ-tubulin antibodies. (H) Quantification of the percentage of pRS-, shBRCA1- and sh53BP1-expressing GM847 cells with (pT371)TRF1 at APBs. Scoring was done as described in B. Standard deviations from three independent experiments are indicated. (I) Western analysis of GM847 cells stably expressing the vector alone (pRS) or shRNA against BRCA1 (shBRCA1). Immunoblotting was performed with anti-BRCA1, anti-pT371 and anti-γ-tubulin antibodies. (J) Western analysis of GM847 cells stably expressing the vector alone (pRS) or shRNA against 53BP1 (sh53BP1). Immunoblotting was performed with anti-53BP1, anti-pT371 and anti-γ-tubulin antibodies. (K) Quantification of the percentage of pRS-, shBRCA1- and sh53BP1-expressing GM847 cells staining positive for cyclin A. Scoring was done as described in B. Standard deviations from three independent experiments are indicated.

Journal of Cell Science (2016) 129, 2559-2572 doi:10.1242/jcs.186098

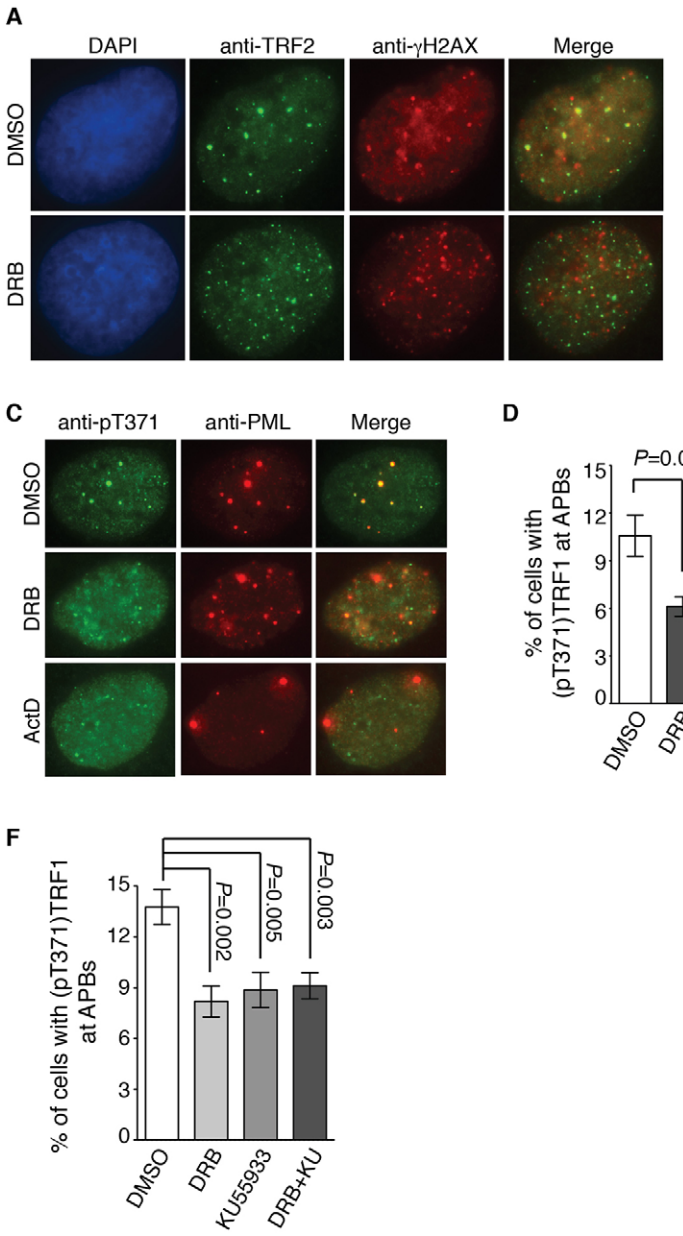

Fig. 5. Transcription inhibition reduces telomeric accumulation of γH2AX and impairs (pT371)TRF1 interaction with APBs. (A) Immunofluorescence analysis of staining with anti-TRF2 or anti-γH2AX antibodies in GM847 cells treated with either DMSO or DRB for 3 h prior to fixation. (B) Quantification of the percentage of DMSO- and DRB-treated GM847 cells exhibiting TRF2 colocalization with γH2AX. A total of 1000 cells from each independent experiment were scored in blind. Standard deviations from three independent experiments are indicated. (C) Immunofluorescence analysis of staining with anti-pT371 and anti-PML antibodies in GM847 cells treated with DMSO, DRB or actinomycin D (ActD). Treatment with ActD was done for 2 h whereas treatment with DRB was carried out for 3 h. (D) Quantification of the percentage of DMSO- and DRB-treated GM847 cells exhibiting (pT371)TRF1 at APBs. Scoring was done as described in B. Standard deviations from three independent experiments are indicated. (E) Quantification of the percentage of DMSO- and actinomycin-D (ActD)-treated GM847 cells exhibiting (pT371)TRF1 at APBs. Scoring was done as described in B. Standard deviations from three independent experiments are indicated. (F) Quantification of the percentage of cells with (pT371)TRF1 at APBs. GM847 cells were treated with DMSO, DRB, KU55933 or a combination of DRB and KU55933 prior to fixation. Scoring was done as described in B. Standard deviations from three independent experiments are indicated.

RNA-DNA hybrids modulate the association of (pT371)TRF1 with APBs

Telomeric DNA is known to be transcribed into a large non-coding RNA (Azzalin et al., 2007), referred to as TERRA, which can form RNA–DNA hybrids with telomeric DNA. RNA–DNA hybrids, also known as R loops, can be processed to give rise to DNA double-strand breaks (Hamperl and Cimprich, 2014; Sollier et al., 2014). To investigate if RNA–DNA hybrids might regulate (pT371)TRF1 recruitment to APBs, we generated U2OS cell lines stably expressing the vector alone or Myc-tagged RNaseH1 (Fig. 6A). Overexpression of Myc-tagged RNaseH1 did not result in any significant change in (pT371)TRF1 recruitment to APBs (Fig. 6B and data not shown). At the same time, we also did not detect any change in the level of TERRA in our Myc-RNaseH1-overexpressing U2OS cells (Fig. 6C), which was inconsistent with a previous report that overexpression of RNaseH1 decreases the TERRA level (Arora et al., 2014). We reasoned that this discrepancy in the level of TERRA might result from a difference in the level of RNaseH1 expression between the two studies although RNaseH1 expression was readily detectable in our cell line (Fig. 6A). Alternatively, it was possible that RNA–DNA hybrids at telomeres might exist transiently and that they might be sensitive to experimental conditions. To further investigate the role of RNA–DNA hybrids in regulating (pT371)TRF1 association with APBs, we turned to campothecin (CPT), which has been reported to induce the formation of RNA–DNA hybrids (Sollier et al., 2014; Sordet et al., 2009). CPT is an inhibitor of topoisomerase I, which prevents the formation of RNA–DNA hybrids and resolves conflicts between transcription and replication (Hamperl and Cimprich, 2014; Tuduri et al., 2009). CPT can also block DNA re-ligation and promotes the induction of single-strand breaks, which can be converted into DNA double-strand breaks during S phase. We found that treatment with CPT led to a significant reduction in (pT371)TRF1 association with APBs in RNaseH1-expressing U2OS cells, whereas it had little effect on (pT371)TRF1 association with APBs in vector-expressing U2OS cells (Fig. 6B). The latter suggests that (pT371)TRF1

Journal of Cell Science (2016) 129, 2559-2572 doi:10.1242/jcs.186098

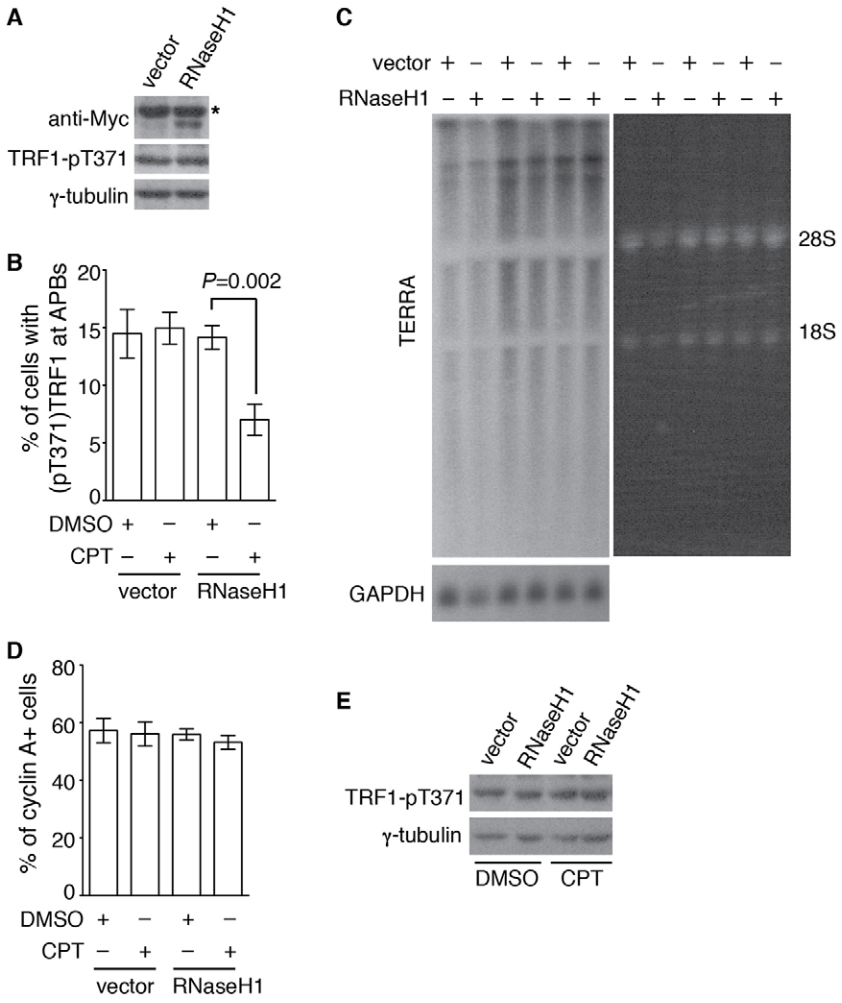

Fig. 6. Overexpression of RNaseH1 impairs (pT371) TRF1 recruitment to APBs in the presence of camptothecin (CPT). (A) Western analysis of U2OS cells stably expressing vector alone or Myc-tagged RNaseH1. Immunoblotting was performed with anti-Myc, anti-pT371 and anti-γ-tubulin antibodies. Asterisk represents a non-specific band. (B) Quantification of the percentage of cells exhibiting (pT371)TRF1 at APBs. U2OS cells stably expressing the vector alone or Myc-tagged RNaseH1 were treated with DMSO or 5 μM CPT for 2 h prior to immunofluorescence analysis. A total of 1000 cells from each independent experiment were scored in blind. Standard deviations from three independent experiments are indicated. (C) Analysis of TERRA expression from U2OS cells stably expressing the vector alone or Myc-tagged RNaseH1. Three pairs of total RNA isolated from three independent experiments were subjected to TERRA analysis. Northern blotting was performed with a ^{32}P-labeled telomeric DNA-containing probe, as shown in the left main panel. The northern blot of GAPDH shown on the left bottom panel was used as a loading control. The right panel was taken from the ethidium-bromide-stained agarose gel. The position of 28S and 18S ribosomal RNA is indicated. (D) Quantification of cyclin-A-positive cells. U2OS cells stably expressing the vector alone or Myc-tagged RNaseH1 were treated with DMSO or 5 μM CPT for 2 h prior to immunofluorescence analysis. Immunofluorescence analysis was performed with an anti-cyclin-A antibody. Scoring was done as described in B. Standard deviations from three independent experiments are indicated. (E) Western analysis of DMSO- and CPT-treated U2OS cells stably expressing the vector alone or Myc-tagged RNaseH1. Immunoblotting was performed with anti-pT371 and anti-γ-tubulin antibodies.

association with APBs is unlikely promoted by CPT-induced DNA breaks alone. In addition, CPT treatment did not significantly alter the number of cyclin-A-positive cells (Fig. 6D), nor did it affect the level of (pT371)TRF1 (Fig. 6E). These results altogether suggest that (pT371)TRF1 association with APBs might be regulated by RNA–DNA hybrids.

The telomeric DNA binding activity of TRF1 is dispensable for its interaction with PML bodies but is crucial for both the production of C-circles and the assembly of APBs

Our earlier finding that (pT371)TRF1 is preferentially associated with dysfunctional telomeres at APBs suggests that TRF1 might interact with APBs independently of its binding to telomeric DNA per se. To address this hypothesis, we generated a Myc-tagged TRF1 deletion allele lacking the C-terminal Myb-like DNA binding domain (TRF1-ΔM). Myc-tagged TRF1-ΔM co-migrated with a non-specific protein band observed in the lane containing Myc-tagged wild-type TRF1 (Fig. 7A). Extracting the density of the non-specific protein band, we estimated that the expression of Myc-tagged TRF1-ΔM in TRF1-depleted GM847 cells was similar to wild-type TRF1 (Fig. 7A). Analysis of dual indirect immunofluorescence with an anti-Myc antibody in conjunction with an anti-PML antibody revealed that Myc-tagged TRF1-ΔM was competent in interacting with PML bodies (Fig. S4A). The number of cells containing Myc-tagged TRF1-ΔM at PML bodies was indistinguishable from that of cells containing Myc-tagged wild-type TRF1 (Fig. 7B). By contrast, unlike Myc-tagged wild-type TRF1, Myc-tagged TRF1-ΔM was predominantly free of chromatin (Fig. 7C), indicating that the observed association of Myc-tagged TRF1-ΔM to PML bodies is unlikely to result from its interaction with telomeric DNA. These results suggest that the Myb-like DNA binding domain of TRF1 is dispensable for its association with PML bodies.

It has been reported that R425 in the Myb-like DNA binding domain of TRF1 makes direct base contacts with telomeric DNA (Court et al., 2005). To gain further evidence about the role of the telomeric DNA binding activity in TRF1 association with PML bodies, we also generated Myc-tagged TRF1 carrying a R425V mutation. Myc-tagged TRF1-R425V was expressed at a level similar to Myc-tagged wild-type TRF1 (Fig. S4B) and was found to be largely soluble (Fig. S4C), in agreement with previous findings that the R425V mutation abrogates TRF1 binding to telomeric DNA both *in vivo* and *in vitro* (Fairall et al., 2001; McKerlie and Zhu, 2011). Analysis of indirect immunofluorescence revealed that Myc-tagged TRF1-R425V was able to localize to PML bodies indistinguishably from Myc-tagged wild-type TRF1 (Fig. S4D,E), further supporting the notion that TRF1 might interact with PML bodies in ALT cells independently of its telomeric DNA activity.

We also examined the role of the telomeric DNA binding activity of TRF1 in supporting both C-circle production and APB assembly. Unlike Myc-tagged wild-type TRF1, overexpression of Myc-tagged

Journal of Cell Science (2016) 129, 2559-2572 doi:10.1242/jcs.186098

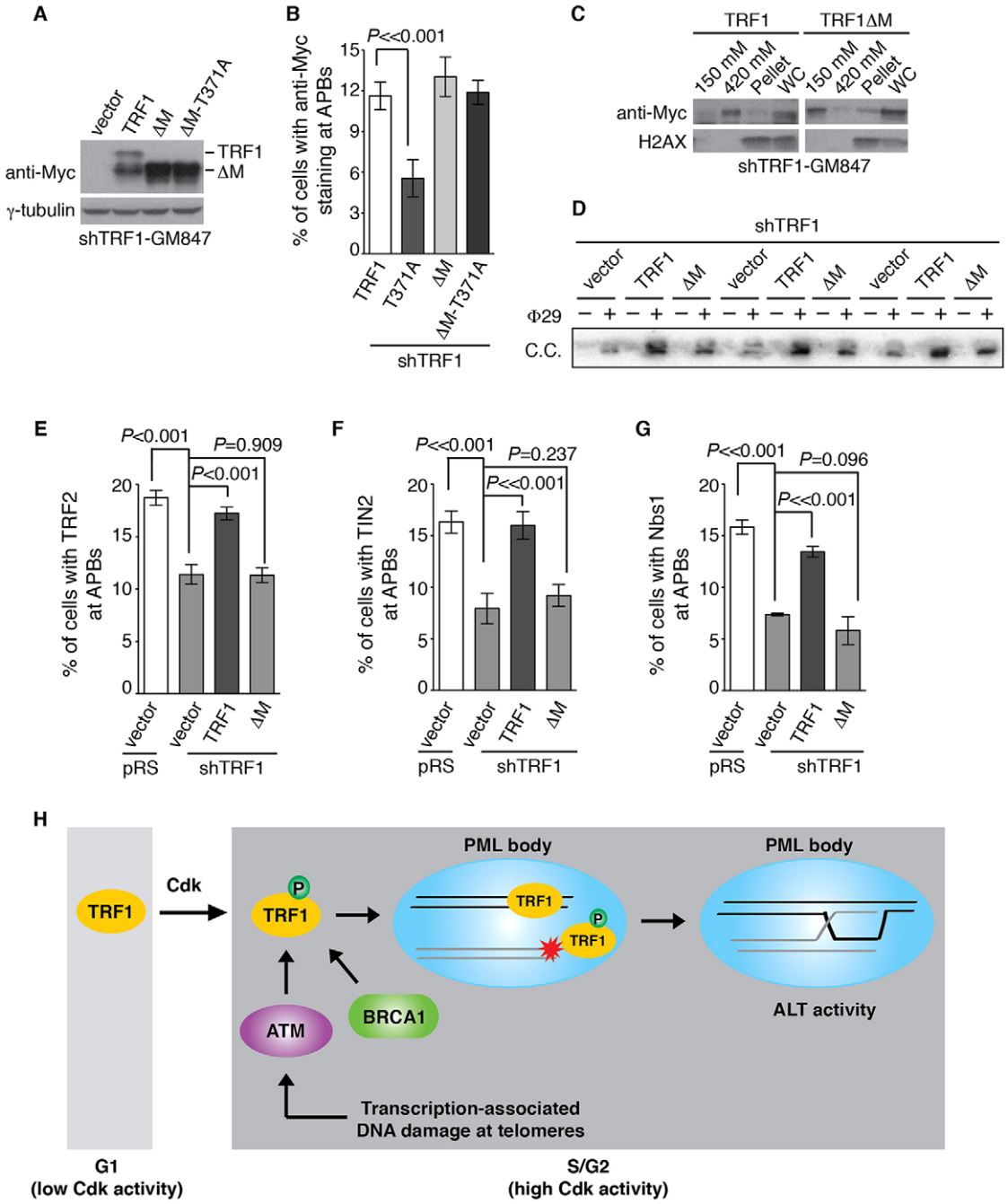

Fig. 7. The Myb-like DNA binding domain of TRF1 is dispensable for its association with APBs but is required for the recruitment of other shelterin proteins and Nbs1 to APBs. (A) Western analysis of TRF1-depleted GM847 cells overexpressing the vector alone and various Myc-tagged TRF1 alleles as indicated. Immunoblotting was performed with anti-Myc and anti-γ-tubulin antibodies. (B) Quantification of the percentage of cells with Myc staining at APBs. Immunofluorescence analysis was performed with anti-Myc and anti-PML antibodies. A total of 1000 cells from each independent experiment were scored for each cell line in blind. Standard deviations from three independent experiments are indicated. (C) Analysis of differential salt extraction of chromatin of TRF1-depleted GM847 cells overexpressing various Myc-tagged TRF1 alleles. Immunoblotting was performed with anti-Myc and anti-H2AX antibodies. The H2AX blot was used as a control for differential salt extraction of chromatin. WC, whole cell lysate. (D) Analysis of C-circle formation. The blot represents three pairs of C-circle assays from three independent experiments. C.C., C-circles. (E) Quantification of the percentage of cells with TRF2 at APBs. Immunofluorescence analysis was performed with anti-TRF2 and anti-PML antibodies. Scoring was done as described in B. Standard deviations from three independent experiments are indicated. (F) Quantification of the percentage of cells with TIN2 at APBs. Immunofluorescence analysis was performed with anti-TIN2 and anti-PML antibodies. Scoring was done as described in B. Standard deviations from three independent experiments are indicated. (G) Quantification of the percentage of cells with Nbs1 at APBs. Immunofluorescence analysis was performed with anti-Nbs1 and anti-PML antibodies. Scoring was done as described in B. Standard deviations from three independent experiments are indicated. (H) Model for Cdk-dependent control of TRF1 interaction with APBs. See the text for details.

TRF1-ΔM failed to rescue the level of C-circles in TRF1-depleted GM847 cells (Fig. 7D). Overexpression of Myc-tagged TRF1-ΔM also failed to rescue the association of TRF2, TIN2 and Nbs1 with PML bodies in TRF1-depleted GM847 cells (Fig. 7E-G). The failure to rescue the association of TRF2, TIN2 and Nbs1 with PML bodies in TRF1-depleted GM847 cells was also observed with

Journal of Cell Science (2016) 129, 2559-2572 doi:10.1242/jcs.186098

Myc-tagged mutant TRF1-R425V (Fig. S4F-H). These results suggest that the telomeric DNA binding activity of TRF1 is crucial for both the production of C-circles and the assembly of other shelterin and repair proteins at PML bodies.

Deletion of the Myb-like DNA binding domain voids the need for T371 phosphorylation in regulating TRF1 interaction with PML bodies

Earlier, we showed that Myc-tagged TRF1 carrying a T371A mutation fails to rescue (pT371)TRF1 association with APBs in TRF1-depleted GM847 cells (Fig. 3E), prompting us to investigate the ability of Myc-tagged TRF1-T371A to localize to PML bodies. Analysis of dual indirect immunofluorescence with an anti-Myc antibody in conjunction with an anti-PML antibody revealed that the T371A mutation significantly impaired the colocalization of Myc-tagged TRF1 with PML bodies (Fig. 7B; Fig. S4A), suggesting that TRF1 interaction with PML bodies requires its phosphorylation on T371.

To investigate if T371 phosphorylation might be needed for the association of Myc-tagged TRF1-ΔM with PML bodies, we introduced the T371A mutation into Myc-tagged TRF1-ΔM. The expression of Myc-tagged TRF1-ΔM-T371A was indistinguishable from that of Myc-tagged TRF1-ΔM (Fig. 7A). Analysis of indirect immunofluorescence with an anti-Myc antibody revealed that the mutation of T371A had little effect on the association of Myc-tagged TRF1-ΔM with PML bodies (Fig. 7B; Fig. S4A). These results suggest that T371 phosphorylation becomes dispensable for TRF1 association with PML bodies in the absence of the Myb-like DNA binding domain. These results further imply that T371 phosphorylation acts as a switch to create a pool of TRF1 to be recruited to PML bodies independently of its binding to telomeric DNA.

DISCUSSION

In this report, we have uncovered that Cdk-dependent phosphorylation of TRF1 on threonine 371 promotes TRF1 to interact with APBs in S and G2 phases independently of its binding to telomeric DNA. We have shown that TRF1 phosphorylation on T371 is essential for the formation of APBs and the production of C-circles, both of which are hallmarks of ALT cells. We have demonstrated that the interaction of (pT371)TRF1 with APBs is dependent upon ATM and homologous-recombination-promoting factors such as Mre11 and BRCA1. Furthermore, we have shown that the interaction of (pT371)TRF1 with APBs is sensitive to transcription inhibition, which reduces the accumulation of γH2AX at telomeres. These results suggest that transcription-associated DNA damage might act as a trigger to recruit (pT371)TRF1 to dysfunctional telomeres to facilitate homologous-recombination-mediated ALT activity (Fig. 7H). It is possible that this process might occur both within and outside of PML bodies in ALT cells.

We have shown that (pT371)TRF1 is preferentially associated with dysfunctional telomere ends in response to DNA damage rather than binding to telomeric DNA per se, in agreement with previous finding that (pT371)TRF1 can be recruited to sites of DNA damage independently of telomeric DNA (McKerlie et al., 2013). It has been reported that (pT371)TRF1 facilitates DNA end resection to promote homologous-recombination-mediated repair of DNA double-strand breaks (McKerlie et al., 2013). Perhaps, (pT371)TRF1 might help process dysfunctional telomere ends for homologous-recombination-mediated events in ALT cells.

TRF1 binds to duplex telomeric DNA and it is also found to interact directly with PML (Hsu et al., 2012; Yu et al., 2010) and PML-associated proteins such as Nbs1 at APBs (Wu et al., 2000). In addition, TRF1 is reported to be SUMOylated and that its SUMOylation promotes APB formation (Potts and Yu, 2007). SUMOylated TRF1 is found to interact with PML-IV (Hsu et al., 2012), and it has been suggested that noncovalent binding of PML to SUMOylated TRF1 and other shelterin proteins might promote the recruitment of telomere heterochromatin to PML bodies (Potts and Yu, 2007). Alternatively, SUMOylation of TRF1 and other shelterin proteins might take place within PML bodies to facilitate the maintenance of APBs (Potts and Yu, 2007). However, whether TRF1 binding to telomeric DNA is important for its interaction with PML bodies has yet to be characterized. In this report, we have shown that deletion of the Myb-like DNA binding domain of TRF1 does not affect its interaction with PML bodies although it abrogates TRF1 binding to telomere chromatin. These results suggest that TRF1 interaction with PML bodies in ALT cells can occur independently of its binding to telomeric DNA. It would be of interest to investigate if deletion of the Myb-like DNA binding domain might affect SUMOylation of TRF1.

We have shown that deletion of the Myb-like DNA binding domain suppresses the deficiency in localizing to PML bodies demonstrated by TRF1 carrying a T371A mutation, suggesting that Cdk-dependent TRF1 phosphorylation on T371 acts as a switch to create a pool of TRF1 that can be recruited to PML bodies independently of its binding to telomeric DNA. Although the Myb-like DNA binding domain is dispensable for TRF1 localization to PML bodies, it is necessary to support the recruitment of other shelterin and repair factors to PML bodies as well as the production of C-circles. These results suggest that TRF1 interaction with PML bodies is a separable process from the recruitment of telomere heterochromatin to PML bodies, both of which are necessary for APB formation and C-circle production. These results further imply that Cdk activity in S and G2 cells controls the function of TRF1 in these two processes to facilitate ALT activity (Fig. 7H).

It has been reported that depletion of TRF1 impairs APB formation (Jiang et al., 2007), however little is known about the role of TRF1 in other features of ALT cells such as C-circle prodution, telomere length heterogeneity and telomere sister chromatin exchange (T-SCE). We have shown that depletion of TRF1 impairs not only APB formation but also C-circle production. However, we did not detect any significant change in telomere length heterogeneity and T-SCE in our TRF1-depleted ALT cells (F.R.W., A.H. and X.-D.Z., unpublished data). It is possible that an incomplete depletion of TRF1 in ALT cells might have contributed to this lack of change in telomere length heterogeneity and T-SCE. Future studies would be needed to investigate the role of TRF1 in telomere length heterogeneity and T-SCE in ALT cells.

We have shown that the formation of APBs is sensitive to transcription inhibition, which also reduces the accumulation of γH2AX at ALT telomeres, suggesting that transcription-associated DNA damage at telomeres might act as a trigger to induce ALT. Telomeric DNA is transcribed into a large non-coding telomeric DNA-containing RNA, referred to as TERRA (Azzalin et al., 2007). In telomerase-positive cancer cells, TERRA expression is cell cycle regulated, plunging to its lowest level as cells progress from S to G2 phase, which is thought to prevent deleterious interference with DNA replication of telomeric tracts (Flynn et al., 2015; Porro et al., 2010). Conversely, ALT cells are found to be defective in regulating TERRA expression (Flynn et al., 2015). Not only are TERRA levels increased in ALT cells (Arora et al., 2014; Azzalin et al., 2007) but

Journal of Cell Science (2016) 129, 2559-2572 doi:10.1242/jcs.186098

also they remain highly elevated in S and G2 phases (Flynn et al., 2015). We have shown that association of (pT371)TRF1 with APBs is sensitive to RNaseH1 in the presence of camptothecin, an inhibitor of topoisomerase I, an enzyme known to prevent the formation of RNA–DNA hybrids and to resolve conflicts between transcription and replication (Hamperl and Cimprich, 2014; Tuduri et al., 2009). RNA–DNA hybrids can be processed into DNA double-strand breaks (DSBs) (Sollier et al., 2014), and recently, it has been reported that DNA DSBs at ALT telomeres induce telomere clustering, APB formation as well as other homologous-recombination-based ALT activities (Cho et al., 2014). Perhaps, telomeric RNA–DNA hybrids arising from transcription and replication collision might be a natural source of DNA damage that triggers ALT.

MATERIALS AND METHODS

DNA constructs and inhibitor treatment

Retroviral expression constructs for shTRF1, shATM, shBRCA1, sh53BP1 as well as various full-length TRF1 alleles (wild-type TRF1, and TRF1 mutant alleles T371A and R425V) have been previously described (McKerlie et al., 2013; McKerlie and Zhu, 2011). The retroviral construct for TRF1 lacking the entire Myb-like DNA binding domain (missing the last 60 amino acids from 379 to 439) (TRF1-ΔM) was generated through PCR using shTRF1-resistant wild-type TRF1 as a template. The sequence of primers for cloning TRF1-ΔM will be made available upon request. The QuickChange site-directed mutagenesis kit (Strategene) was used to create a T371A mutation in the TRF1-ΔM allele.

Inhibitors used include: KU55933 (Sigma), a specific inhibitor for ATM; NU7026 (Sigma), a specific inhibitor for DNA-PKcs; Mirin (Sigma), a specific inhibitor for Mre11 (Dupre et al., 2008); roscovitine (Sigma), a Cdk inhibitor; camptothecin (Sigma); DRB (Cayman Chemical) and actinomycin D (Sigma), transcription inhibitors. KU55933, NU7026 and roscovitine were each used at 20 μM. Mirin and DRB were each used at 100 μM. Actinomycin D was used at 2 μg/ml.

Cell culture and synchronization

Cells were grown in DMEM medium with 5% fetal bovine serum (FBS) for GM847 (a gift from Titia de Lange, Rockefeller University), U2OS (ATCC), WI38VA13/2RA (Zhu et al., 2003) and Phoenix cells (Zhu et al., 2003), supplemented with non-essential amino acids, L-glutamine, 100 U/ml penicillin and 0.1 mg/ml streptomycin. Cell lines were tested to be free of mycoplasma contamination. Retroviral gene delivery was carried out as described (Mitchell et al., 2009) to generate stable cell lines. TRF1-depleted GM847 cells stably expressing various TRF1 alleles were maintained in the selection medium containing either puromycin (2 μg/ml) or hygromycin (90 μg/ml), alternating every 2 weeks for the entirety of the experiments. For analysis of APB formation and C-circle production, we used cell lines that were kept in culture for less than a month following their generation. For analysis of telomere length heterogeneity, cell lines were cultured continuously for up to 2 months.

Cell synchronization at the G1/S boundary was carried out essentially as described with some modifications (Zhu et al., 2000). GM847 and U2OS cells were first arrested with thymidine (2.5 mM) for 17 h, followed by washing in PBS for three times and then released into fresh media for 14 h. Subsequently, cells were arrested again with 2.5 mM thymidine for 17 h and washed in PBS for three times before their release into fresh media for 0-16 h.

Protein extracts, differential salt extraction of chromatin and immunoblotting

Protein extracts, differential salt extraction of chromatin and immunoblotting were performed as described (McKerlie et al., 2013; McKerlie and Zhu, 2011). Phospho-specific anti-pT371-TRF1 antibody has been previously described (McKerlie and Zhu, 2011). Mouse anti-TRF1 antibody and rabbit antibodies against total TRF1 (van Steensel and de Lange, 1997), TRF2 (Zhu et al., 2000), hRap1 (Li et al., 2000) and TIN2 (Ye et al., 2004) were generous gifts from Titia de Lange, Rockefeller University. Other antibodies include: Nbs1 (a kind gift from John Petrini, Memorial Sloan-Kettering Cancer Center); PML (sc-966, Santa Cruz); PML (ab53773, Abcam); anti-BrdU (NB200-569, Novus Biologicals); BRCA1 (MS110, Abcam); BRCA1 (07-434, Millipore); Cyclin A (6E6, Abcam); γ-H2AX (05-636, Milipore); 53BP1 (612522, BD Biosciences) and γ-tubulin (GTU88, Sigma).

IF-FISH

Immunofluorescence combined with fluorescence *in situ* hybridization (IF-FISH) was carried out as follows. Immunofluorescence was performed as described (Mitchell and Zhu, 2014; Zhu et al., 2003). FISH analysis was carried out essentially as described (McKerlie et al., 2012). For triple staining, blocked coverslips were incubated with both rabbit anti-pT371 (at 1:500) and mouse anti-PML (at 1:200) antibodies in blocking buffer (1 mg/ml BSA, 3% goat serum, 0.1% Triton X-100 and 1 mM EDTA in PBS) at room temperature for 2 h. After three washes in PBS, coverslips were incubated with both TRITC-conjugated donkey anti-rabbit (1:250; Cat. no. 715-025-152, Jackson Laboartories) and AMCA-conjugated donkey anti-mouse (1:250; Cat. no. 715-156-150, Jackson Laboratories) at room temperature for 30 min. Subsequently, coverslips were processed as described (McKerlie et al., 2012). Cell images were then recorded on a Zeiss Axioplan 2 microscope with a Hammamatsu C4742-95 camera and processed in Open Lab.

Metaphase chromosome spreads

Metaphase chromosome spreads were essentially prepared as described (Batenburg et al., 2012; Zhu et al., 2003). Cells were arrested in nocodazole (0.1 μg/ml) for 120 min. Following arrest, cells were collected by shake-off, spun down and incubated at 37°C for 10 min in RSB buffer [10 mM Tris-HCl (pH 7.4), 10 mM NaCl, 5 mM $MgCl_2$]. Cell droplets were spun onto glass coverslips, fixed in PBS-buffered 2% paraformaldehyde and followed by standard immunofluorescence as described above.

Northern analysis of TERRA and C-circle amplification assays

Northern analysis of TERRA was carried out as described (Batenburg et al., 2012). C-circle amplification assays were performed essentially as described (Henson et al., 2009). Briefly, each DNA sample (10 μl or 50 ng) was incubated with or without 7.5 U ϕ29 DNA polymerase (NEB) in a 20 μl reaction containing 9.25 μl of premix (0.2 mg/ml BSA, 0.1% Tween 20, 1 mM ATP, 1 mM dTTP, 1 mM dGTP, 1× ϕ29 buffer) at 30°C for 8 h. Following heat inactivation of ϕ29 at 65°C for 20 min, samples were separated on a 0.6% agarose gel in 0.5× Tris-borate-EDTA (TBE) at 1.75 V/cm for 12-16 h. Gels were dried at 50°C and then hybridized with a ^{32}P-end-labeled single-strand $(CCCTAA)_3$ probe under native conditions as described (Lackner et al., 2012). Gels were exposed to PhosphorImager screens and scanned using a Typhoon FLA9500 biomolecular imager (GE Healthcare).

Statistical analysis

A Student's two-tailed *t*-test was used to derive all *P*-values.

Acknowledgements

We are grateful to Titia de Lange for cell lines (GM847, WI38VA13/2RA and phoenix) as well as antibodies against TRF1, TRF2, hRap1 and TIN2. John Petrini is thanked for the anti-Nbs1 antibody. Nicole Batenburg is thanked for generating RNaseH1-expressing U2OS cells.

Competing interests

The authors declare no competing or financial interests.

Author contributions

F.R.W., A.H., and J.R.W. performed the experiments. J.R.W. and X.-D.Z. conceived hypotheses and designed the project. All authors contributed to data analysis and manuscript writing.

Funding
This work was supported by funding from Canadian Institutes of Health Research [MOP-285822 to X.-D.Z.]

Supplementary information
Supplementary information available online at
http://jcs.biologists.org/lookup/doi/10.1242/jcs.186098.supplemental

References

Ancelin, K., Brunori, M., Bauwens, S., Koering, C.-E., Brun, C., Ricoul, M., Pommier, J.-P., Sabatier, L. and Gilson, E. (2002). Targeting assay to study the cis functions of human telomeric proteins: evidence for inhibition of telomerase by TRF1 and for activation of telomere degradation by TRF2. *Mol. Cell. Biol.* **22**, 3474-3487.

Arora, R., Lee, Y., Wischnewski, H., Brun, C. M., Schwarz, T. and Azzalin, C. M. (2014). RNaseH1 regulates TERRA-telomeric DNA hybrids and telomere maintenance in ALT tumour cells. *Nat. Commun.* **5**, 5220.

Azzalin, C. M., Reichenbach, P., Khoriauli, L., Giulotto, E. and Lingner, J. (2007). Telomeric repeat containing RNA and RNA surveillance factors at mammalian chromosome ends. *Science* **318**, 798-801.

Batenburg, N. L., Mitchell, T. R. H., Leach, D. M., Rainbow, A. J. and Zhu, X.-D. (2012). Cockayne Syndrome group B protein interacts with TRF2 and regulates telomere length and stability. *Nucleic Acids Res.* **40**, 9661-9674.

Canudas, S., Houghtaling, B. R., Kim, J. Y., Dynek, J. N., Chang, W. G. and Smith, S. (2007). Protein requirements for sister telomere association in human cells. *EMBO J.* **26**, 4867-4878.

Cesare, A. J. and Reddel, R. R. (2010). Alternative lengthening of telomeres: models, mechanisms and implications. *Nat. Rev. Genet.* **11**, 319-330.

Cesare, A. J., Kaul, Z., Cohen, S. B., Napier, C. E., Pickett, H. A., Neumann, A. A. and Reddel, R. R. (2009). Spontaneous occurrence of telomeric DNA damage response in the absence of chromosome fusions. *Nat. Struct. Mol. Biol.* **16**, 1244-1251.

Cho, N. W., Dilley, R. L., Lampson, M. A. and Greenberg, R. A. (2014). Interchromosomal homology searches drive directional ALT telomere movement and synapsis. *Cell* **159**, 108-121.

Chung, I., Leonhardt, H. and Rippe, K. (2011). De novo assembly of a PML nuclear subcompartment occurs through multiple pathways and induces telomere elongation. *J. Cell Sci.* **124**, 3603-3618.

Court, R., Chapman, L., Fairall, L. and Rhodes, D. (2005). How the human telomeric proteins TRF1 and TRF2 recognize telomeric DNA: a view from high-resolution crystal structures. *EMBO Rep.* **6**, 39-45.

d'Adda di Fagagna, F., Reaper, P. M., Clay-Farrace, L., Fiegler, H., Carr, P., Von Zglinicki, T., Saretzki, G., Carter, N. P. and Jackson, S. P. (2003). A DNA damage checkpoint response in telomere-initiated senescence. *Nature* **426**, 194-198.

de Lange, T. (2005). Shelterin: the protein complex that shapes and safeguards human telomeres. *Genes Dev.* **19**, 2100-2110.

Draskovic, I., Arnoult, N., Steiner, V., Bacchetti, S., Lomonte, P. and Londono-Vallejo, A. (2009). Probing PML body function in ALT cells reveals spatiotemporal requirements for telomere recombination. *Proc. Natl. Acad. Sci. USA* **106**, 15726-15731.

Dunham, M. A., Neumann, A. A., Fasching, C. L. and Reddel, R. R. (2000). Telomere maintenance by recombination in human cells. *Nat. Genet.* **26**, 447-450.

Dupre, A., Boyer-Chatenet, L., Sattler, R. M., Modi, A. P., Lee, J.-H., Nicolette, M. L., Kopelovich, L., Jasin, M., Baer, R., Paull, T. T. et al. (2008). A forward chemical genetic screen reveals an inhibitor of the Mre11-Rad50-Nbs1 complex. *Nat. Chem. Biol.* **4**, 119-125.

Fairall, L., Chapman, L., Moss, H., de Lange, T. and Rhodes, D. (2001). Structure of the TRFH dimerization domain of the human telomeric proteins TRF1 and TRF2. *Mol. Cell* **8**, 351-361.

Flynn, R. L., Cox, K. E., Jeitany, M., Wakimoto, H., Bryll, A. R., Ganem, N. J., Bersani, F., Pineda, J. R., Suva, M. L., Benes, C. H. et al. (2015). Alternative lengthening of telomeres renders cancer cells hypersensitive to ATR inhibitors. *Science* **347**, 273-277.

Grobelny, J. V., Godwin, A. K. and Broccoli, D. (2000). ALT-associated PML bodies are present in viable cells and are enriched in cells in the G(2)/M phase of the cell cycle. *J. Cell Sci.* **113**, 4577-4585.

Hamperl, S. and Cimprich, K. A. (2014). The contribution of co-transcriptional RNA:DNA hybrid structures to DNA damage and genome instability. *DNA Repair* **19**, 84-94.

Helmrich, A., Ballarino, M., Nudler, E. and Tora, L. (2013). Transcription-replication encounters, consequences and genomic instability. *Nat. Struct. Mol. Biol.* **20**, 412-418.

Henson, J. D. and Reddel, R. R. (2010). Assaying and investigating Alternative Lengthening of Telomeres activity in human cells and cancers. *FEBS Lett.* **584**, 3800-3811.

Henson, J. D., Cao, Y., Huschtscha, L. I., Chang, A. C., Au, A. Y. M., Pickett, H. A. and Reddel, R. R. (2009). DNA C-circles are specific and quantifiable markers of alternative-lengthening-of-telomeres activity. *Nat. Biotechnol.* **27**, 1181-1185.

Hsu, J. K., Lin, T. and Tsai, R. Y. L. (2012). Nucleostemin prevents telomere damage by promoting PML-IV recruitment to SUMOylated TRF1. *J. Cell Biol.* **197**, 613-624.

Jiang, W.-Q., Zhong, Z.-H., Henson, J. D. and Reddel, R. R. (2007). Identification of candidate alternative lengthening of telomeres genes by methionine restriction and RNA interference. *Oncogene* **26**, 4635-4647.

Kishi, S., Zhou, X. Z., Ziv, Y., Khoo, C., Hill, D. E., Shiloh, Y. and Lu, K. P. (2001). Telomeric protein Pin2/TRF1 as an important ATM target in response to double strand DNA breaks. *J. Biol. Chem.* **276**, 29282-29291.

Lackner, D. H., Raices, M., Maruyama, H., Haggblom, C. and Karlseder, J. (2012). Organismal propagation in the absence of a functional telomerase pathway in Caenorhabditis elegans. *EMBO J.* **31**, 2024-2033.

Levy, M. Z., Allsopp, R. C., Futcher, A. B., Greider, C. W. and Harley, C. B. (1992). Telomere end-replication problem and cell aging. *J. Mol. Biol.* **225**, 951-960.

Li, B., Oestreich, S. and de Lange, T. (2000). Identification of human Rap1: implications for telomere evolution. *Cell* **101**, 471-483.

Liu, D., O'Connor, M. S., Qin, J. and Songyang, Z. (2004). Telosome, a mammalian telomere-associated complex formed by multiple telomeric proteins. *J. Biol. Chem.* **279**, 51338-51342.

McKerlie, M. and Zhu, X.-D. (2011). Cyclin B-dependent kinase 1 regulates human TRF1 to modulate the resolution of sister telomeres. *Nat. Commun.* **2**, 371.

McKerlie, M., Lin, S. and Zhu, X.-D. (2012). ATM regulates proteasome-dependent subnuclear localization of TRF1, which is important for telomere maintenance. *Nucleic Acids Res.* **40**, 3975-3989.

McKerlie, M., Walker, J. R., Mitchell, T. R. H., Wilson, F. R. and Zhu, X.-D. (2013). Phosphorylated (pT371)TRF1 is recruited to sites of DNA damage to facilitate homologous recombination and checkpoint activation. *Nucleic Acids Res.* **41**, 10268-10282.

Mitchell, T. R. H. and Zhu, X.-D. (2014). Methylated TRF2 associates with the nuclear matrix and serves as a potential biomarker for cellular senescence. *Aging* **6**, 248-263.

Mitchell, T. R. H., Glenfield, K., Jeyanthan, K. and Zhu, X.-D. (2009). Arginine methylation regulates telomere length and stability. *Mol. Cell. Biol.* **29**, 4918-4934.

Nabetani, A., Yokoyama, O. and Ishikawa, F. (2004). Localization of hRad9, hHus1, hRad1, and hRad17 and caffeine-sensitive DNA replication at the alternative lengthening of telomeres-associated promyelocytic leukemia body. *J. Biol. Chem.* **279**, 25849-25857.

Porro, A., Feuerhahn, S., Reichenbach, P. and Lingner, J. (2010). Molecular dissection of telomeric repeat-containing RNA biogenesis unveils the presence of distinct and multiple regulatory pathways. *Mol. Cell. Biol.* **30**, 4808-4817.

Potts, P. R. and Yu, H. (2007). The SMC5/6 complex maintains telomere length in ALT cancer cells through SUMOylation of telomere-binding proteins. *Nat. Struct. Mol. Biol.* **14**, 581-590.

Shay, J. W. and Bacchetti, S. (1997). A survey of telomerase activity in human cancer. *Eur. J. Cancer* **33**, 787-791.

Shen, M., Haggblom, C., Vogt, M., Hunter, T. and Lu, K. P. (1997). Characterization and cell cycle regulation of the related human telomeric proteins Pin2 and TRF1 suggest a role in mitosis. *Proc. Natl. Acad. Sci. USA* **94**, 13618-13623.

Sollier, J., Stork, C. T., Garcia-Rubio, M. L., Paulsen, R. D., Aguilera, A. and Cimprich, K. A. (2014). Transcription-coupled nucleotide excision repair factors promote R-loop-induced genome instability. *Mol. Cell* **56**, 777-785.

Sordet, O., Redon, C. E., Guirouilh-Barbat, J., Smith, S., Solier, S., Douarre, C., Conti, C., Nakamura, A. J., Das, B. B., Nicolas, E. et al. (2009). Ataxia telangiectasia mutated activation by transcription- and topoisomerase I-induced DNA double-strand breaks. *EMBO Rep.* **10**, 887-893.

Tuduri, S., Crabbe, L., Conti, C., Tourriere, H., Holtgreve-Grez, H., Jauch, A., Pantesco, V., De Vos, J., Thomas, A., Theillet, C. et al. (2009). Topoisomerase I suppresses genomic instability by preventing interference between replication and transcription. *Nat. Cell Biol.* **11**, 1315-1324.

van Steensel, B. and de Lange, T. (1997). Control of telomere length by the human telomeric protein TRF1 [see comments]. *Nature* **385**, 740-743.

Walker, J. R. and Zhu, X.-D. (2012). Post-translational modification of TRF1 and TRF2 and their roles in telomere maintenance. *Mech. Ageing Dev.* **133**, 421-434.

Wu, G., Lee, W.-H. and Chen, P.-L. (2000). NBS1 and TRF1 colocalize at Promyelocytic Leukemia bodies during late S/G2 phases in immortalized telomerase-negative cells: implication of NBS1 in alternative lengthening of telomeres. *J. Biol. Chem.* **275**, 30618-30622.

Wu, G., Jiang, X., Lee, W. H. and Chen, P. L. (2003). Assembly of functional ALT-associated promyelocytic leukemia bodies requires Nijmegen Breakage Syndrome 1. *Cancer Res.* **63**, 2589-2595.

Ye, J. Z.-S., Donigian, J. R., van Overbeek, M., Loayza, D., Luo, Y., Krutchinsky, A. N., Chait, B. T. and de Lange, T. (2004). TIN2 binds TRF1 and TRF2

simultaneously and stabilizes the TRF2 complex on telomeres. *J. Biol. Chem.* **279**, 47264-47271.

Yeager, T. R., Neumann, A. A., Englezou, A., Huschtscha, L. I., Noble, J. R. and Reddel, R. R. (1999). Telomerase-negative immortalized human cells contain a novel type of promyelocytic leukemia (PML) body. *Cancer Res.* **59**, 4175-4179.

Yu, J., Lan, J., Wang, C., Wu, Q., Zhu, Y., Lai, X., Sun, J., Jin, C. and Huang, H. (2010). PML3 interacts with TRF1 and is essential for ALT-associated PML bodies assembly in U2OS cells. *Cancer Lett.* **291**, 177-186.

Zhong, Z.-H., Jiang, W.-Q., Cesare, A. J., Neumann, A. A., Wadhwa, R. and Reddel, R. R. (2007). Disruption of telomere maintenance by depletion of the MRE11/RAD50/NBS1 complex in cells that use alternative lengthening of telomeres. *J. Biol. Chem.* **282**, 29314-29322.

Zhou, X. Z., Perrem, K. and Lu, K. P. (2003). Role of Pin2/TRF1 in telomere maintenance and cell cycle control. *J. Cell. Biochem.* **89**, 19-37.

Zhu, X.-D., Kuster, B., Mann, M., Petrini, J. H. J. and Lange, T. (2000). Cell-cycle-regulated association of RAD50/MRE11/NBS1 with TRF2 and human telomeres. *Nat. Genet.* **25**, 347-352.

Zhu, X.-D., Niedernhofer, L., Kuster, B., Mann, M., Hoeijmakers, J. H. J. and de Lange, T. (2003). ERCC1/XPF removes the 3′ overhang from uncapped telomeres and represses formation of telomeric DNA-containing double minute chromosomes. *Mol. Cell* **12**, 1489-1498.

SUPPLEMENTARY FIGURES

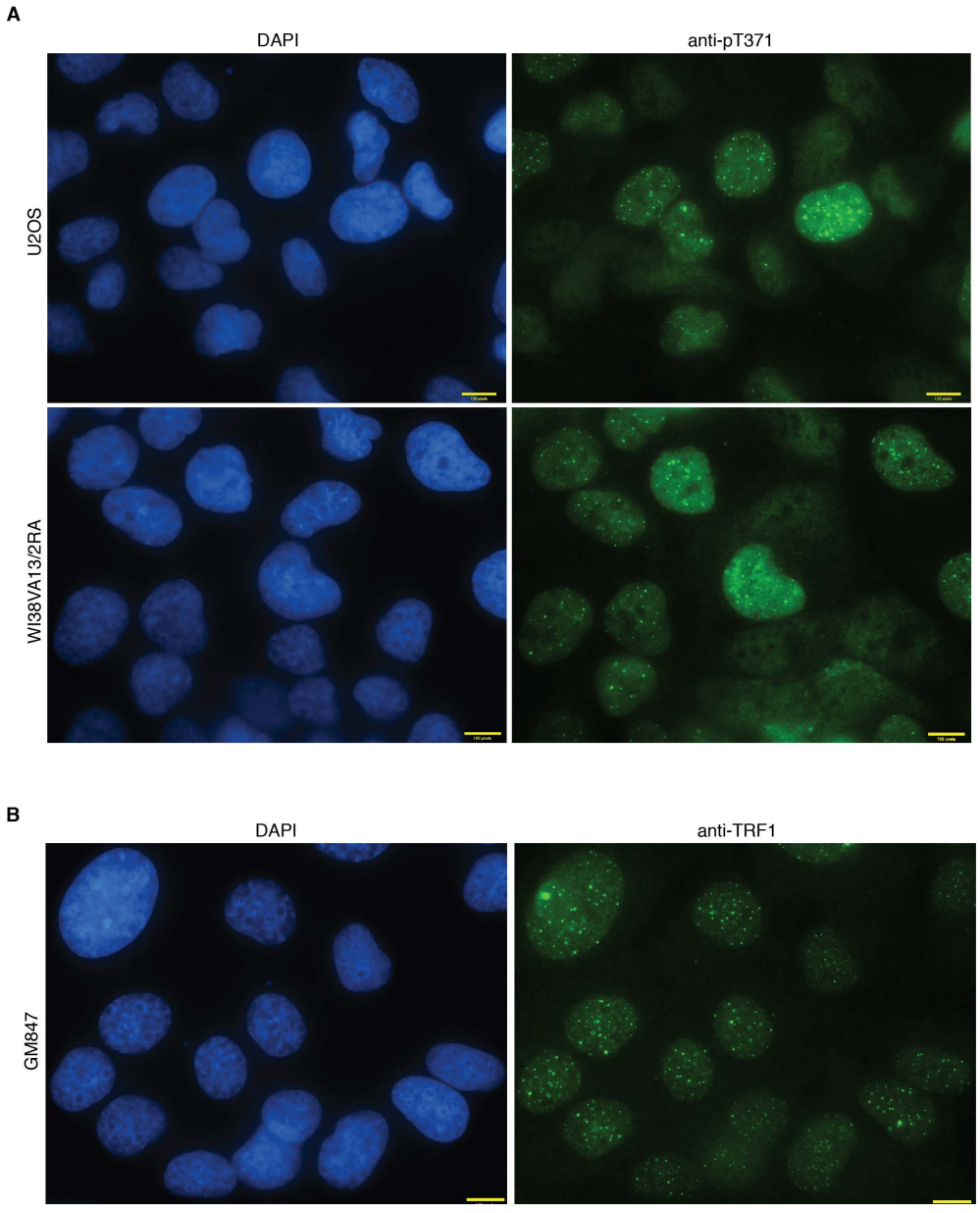

Figure 1. Phosphorylated (pT371)TRF1 exhibits distinct nuclear staining from telomere-bound TRF1. (**A**) Indirect immunofluorescence of interphase U2OS and WI38VA13/2RA cells with an anti-pT371 antibody. Cell nuclei were stained with DAPI in blue in this and subsequent figures. (**B**) Indirect immunofluorescence of interphase GM847 cells with an anti-TRF1 antibody.

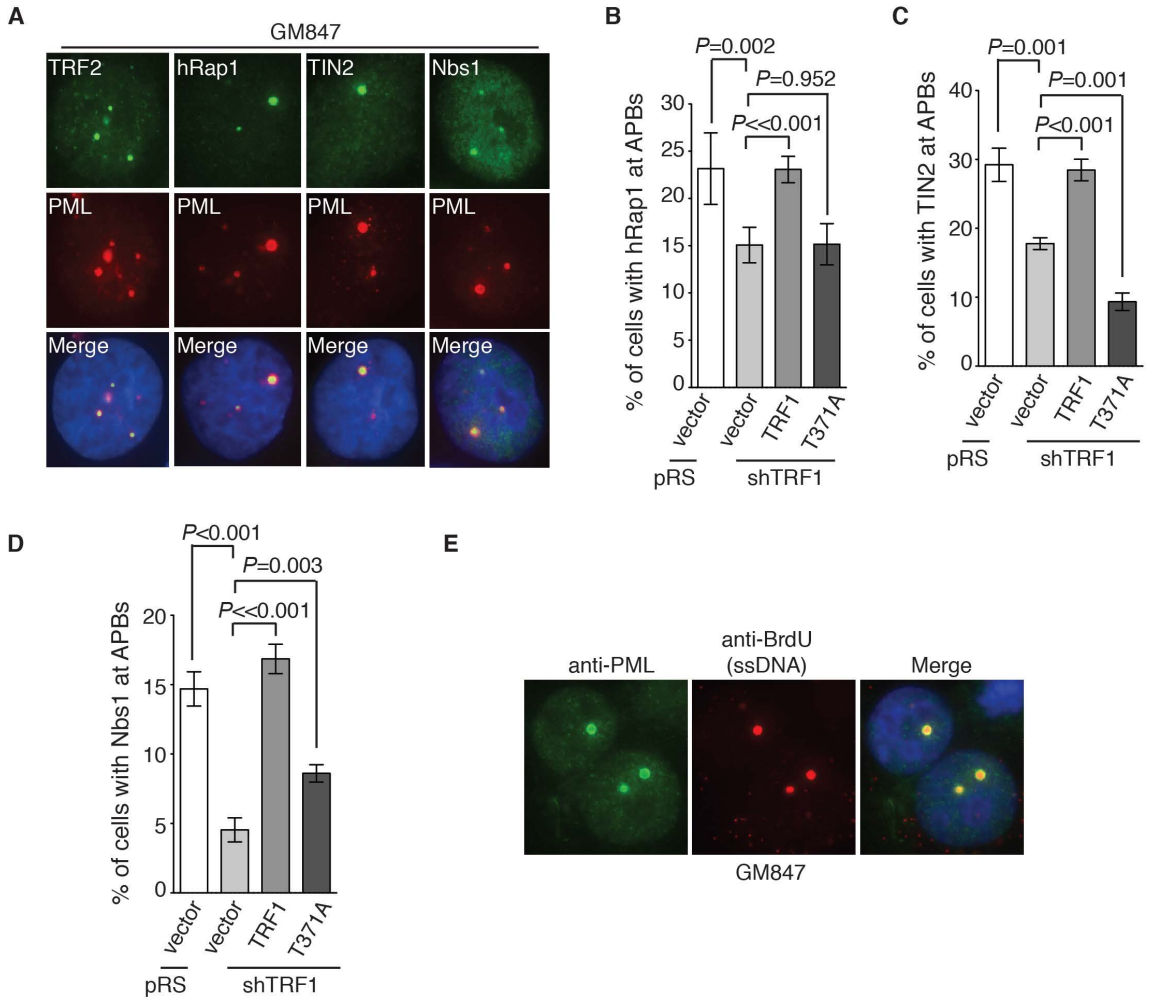

Figure 2. Phosphorylation of TRF1 at T371 is necessary to support APB formation. (**A**) Dual Indirect immunofluorescence of GM847 cells with an anti-PML antibody in conjunction with an antibody against TRF2, hRap1, TIN2 or Nbs1. (**B**) Quantification of the percentage of cells with hRap1 at APBs. pRS- and shTRF1-expressing GM847 cells were complemented with either the vector alone, Myc-tagged wild type TRF1 or Myc-tagged TRF1 carrying a T371A mutation as indicated. A total of 1000 cells from each independent experiments were scored for each cell line in blind. Standard deviations from six independent experiments are indicated. (**C**) Quantification of the percentage of cells with TIN2 at APBs. Scoring was done as described in (B). Standard deviations from three independent experiments are indicated. (**D**) Quantification of the percentage of GM847 cells with Nbs1 at APBs. Scoring was done as described in (B). Standard deviations from three independent experiments are indicated. (**E**) Dual indirect immunofluorescence of GM847 cells with an anti-PML antibody in conjunction with an anti-BrdU antibody.

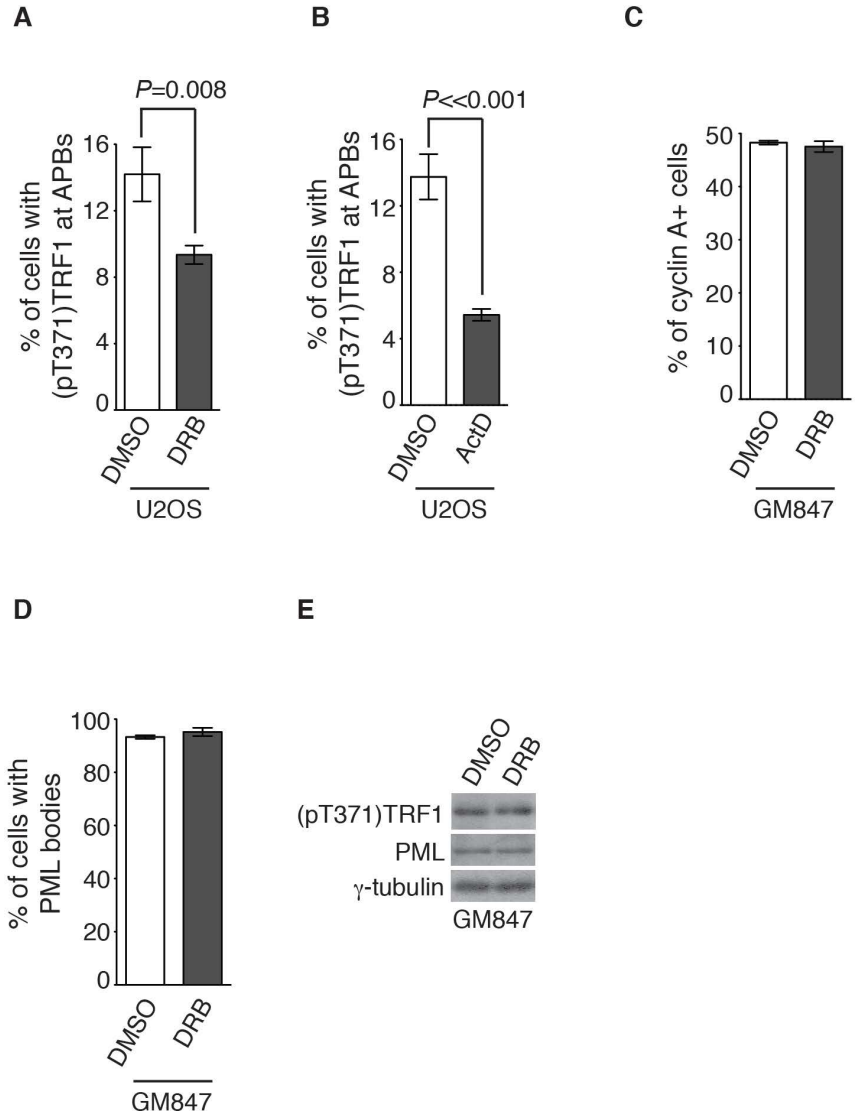

Figure 3. Transcription inhibition impairs (pT371)TRF1 association with APBs. (**A**) Quantification of the percentage of DMSO- and DRB-treated U2OS cells exhibiting (pT371)TRF1 at APBs. Analysis of dual indirect immunofluorecence was performed with anti-pT371 and anti-PML antibodies. A total of 1000 cells from each independent experiment were scored in blind. Standard deviations from three independent experiments are indicated. (**B**) Quantification of the percentage of DMSO- and actinomycin D (ActD)-

treated U2OS cells exhibiting (pT371)TRF1 at APBs. Scoring was done as described in (A). Standard deviations from three independent experiments are indicated. (**C**) Quantification of the percentage of DMSO- and DRB-treated GM847 cells staining positive for cyclin A. Scoring was done as described in (A). Standard deviations from three independent experiments are indicated. (**D**) Quantification of the percentage of DMSO- and DRB-treated GM847 cells staining positive for PML bodies. Scoring was done as described in (A). Standard deviations from three independent experiments are indicated. (**E**) Western analysis of DMSO- and DRB-treated GM847 cells. Immunoblotting was performed with anti-pT371, anti-PML and anti-γ-tubulin antibodies.

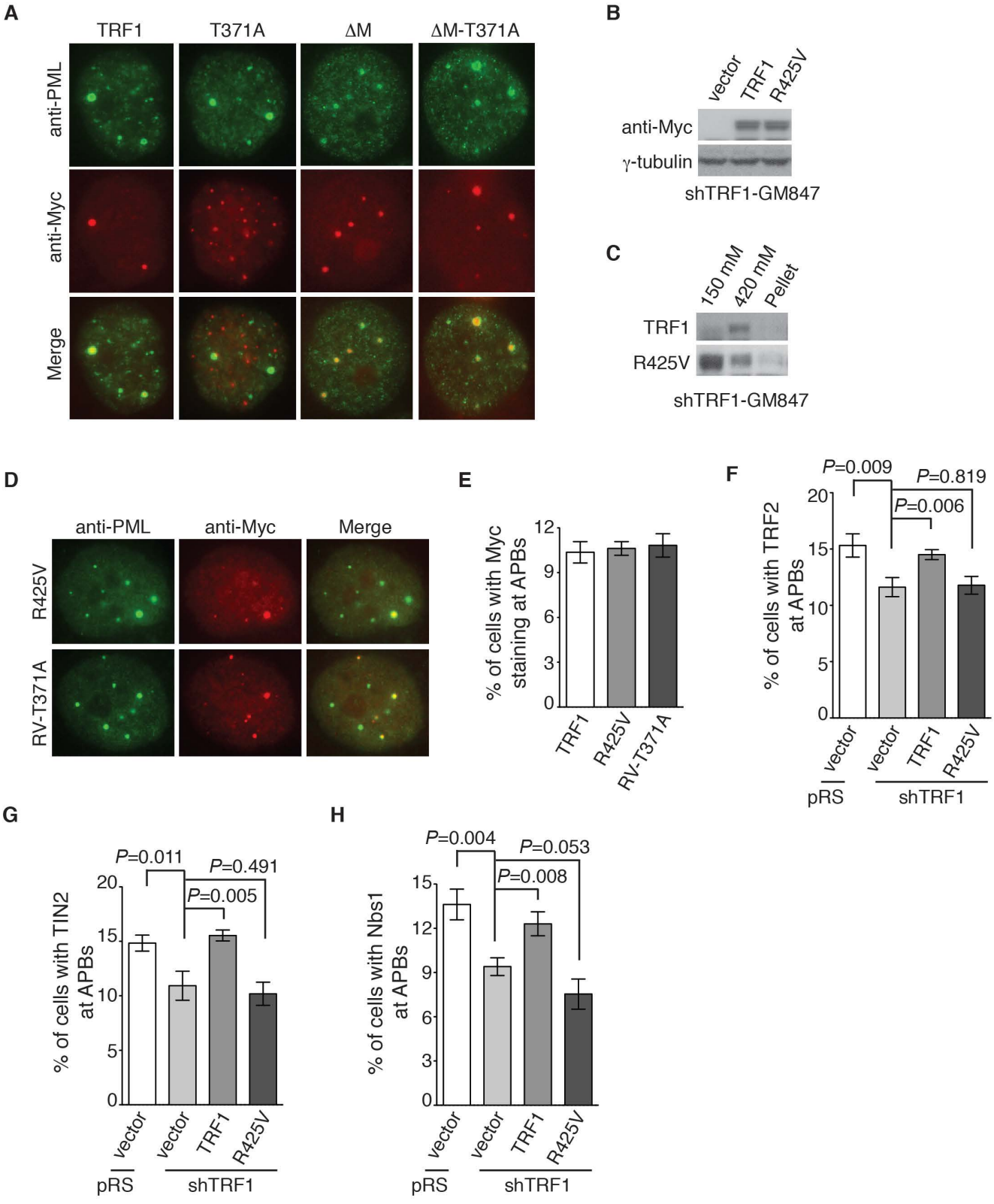

Figure 4. The telomeric DNA binding activity of TRF1 is dispensable for its association with PML bodies but is essential for the recruitment of Nbs1 and other shelterin proteins to PML bodies. (**A**) Dual indirect immunofluorescence with an anti-Myc antibody in conjunction with an anti-PML antibody. TRF1-depleted GM847 cells were complemented with Myc-tagged wild type TRF1, Myc-tagged TRF1 carrying a T371A mutation, Myc-tagged TRF1 lacking the Myb-like DNA binding domain (ΔM) or Myc-tagged TRF1-ΔM carrying a T371A mutation (ΔM-T371A) as indicated. (**B**) Western analysis of TRF1-depleted GM847 cells expressing the vector alone, Myc-tagged wild type TRF1 or Myc-tagged TRF1 carrying a R425V mutation. Immunoblotting was performed with anti-Myc and anti-γ-tubulin antibodies. (**C**) Analysis of differential salt extraction of chromatin of TRF1-depleted GM847 cells overexpressing Myc-tagged wild type TRF1 or Myc-tagged TRF1 carrying a R425V mutation. Immunoblotting was performed with an anti-Myc antibody. (**D**) Dual indirect immunofluorescence with both anti-PML antibody and anti-Myc antibodies. TRF1-depleted GM847 cells were complemented with either Myc-tagged TRF1 carrying a R425V mutation or Myc-tagged TRF1 carrying both R425V and T371A mutations (RV-T371A) as indicated. (**E**) Quantification of cells with Myc staining at APBs. TRF1-depleted GM847 cells complemented with various TRF1 alleles as indicated were co-immunostained with both anti-Myc and anti-PML antibodies. A total of 1000 cells from each independent experiment were scored for each cell line in blind. Standard deviations from three independent experiments are indicated. (**F**) Quantification of cells with TRF2 at APBs. Fixed pRS or shTRF1-expressing GM847 cells complemented with various TRF1 alleles as indicated were co-immunostained with both anti-TRF2 and anti-PML antibodies. Scoring was done as described in (E). Standard deviations from three independent experiments are indicated. (**G**) Quantification of cells with TIN2 at APBs. Fixed pRS or shTRF1-expressing GM847 cells complemented with various TRF1 alleles as indicated were co-immunostained with both anti-TIN2 and anti-PML antibodies. Scoring was done as described in (E). Standard deviations from three independent experiments are indicated. (**H**) Quantification of cells with Nbs1 at APBs. Fixed pRS or shTRF1-expressing GM847 cells complemented with various TRF1 alleles as indicated were co-immunostained with both anti-Nbs1 and anti-PML antibodies. Scoring was done as described in (E). Standard deviations from three independent experiments are indicated.